# PANTOTHENAMIDES AS ANTIBACTERIALS: MODE OF ACTION STUDIES AND IMPROVEMENT OF THEIR POTENCY BY STRUCTURAL MODIFICATION

**Leanne Barnard**

Dissertation presented for the degree of Doctor of Philosophy (Chemistry) in the Faculty of Natural Sciences at Stellenbosch University

**Supervisor: Prof. Erick Strauss**
Department of Biochemistry, Stellenbosch University

**Co-supervisor: Prof. Willem A. L. van Otterlo**
Department of Chemistry, Stellenbosch University

December 2015

## Declaration

By submitting this thesis/dissertation electronically, I declare that the entirety of the work contained therein is my own, original work, that I am the sole author thereof (save to the extent explicitly otherwise stated), that reproduction and publication thereof by Stellenbosch University will not infringe any third party rights and that I have not previously in its entirety or in part submitted it for obtaining any qualification.

December 2015

# Abstract

The emergence of multidrug-resistant organisms is one of the main driving forces for the continuous development of new antimicrobial chemotherapies. Previous research established that Coenzyme A (CoA), biosynthesized from pantothenic acid, promotes the growth of various disease-causing pathogens, including *Staphylococcus aureus* and *Plasmodium falciparum*. Selective inhibition of CoA biosynthesis in pathogens might be accomplished with selected small molecule inhibitors due to the high level of structural and mechanistic divergence between the prokaryotic and eukaryotic enzymes. Consequently, the CoA biosynthetic pathway is seen as a prospective target for such chemotherapies and therefore specific analogues of pantothenic acid have been used in the search for new antimicrobials in various studies.

One particular class of analogues, named *N*-substituted pantothenamides, has shown potential as inhibitors of CoA biosynthesis and utilization in *S. aureus*. However, our poor understanding of their mechanism of action has hampered their development as clinically relevant agents. Consequently, in this study we set out to elucidate the mode of action of pantothenamides by designing a compound that can only act as an inhibitor of *S. aureus* pantothenate kinase (*Sa*PanK-II) (the first enzyme in the CoA biosynthesis pathway) and not as a substrate. We were able to confirm that the mode of action of bacterial pantothenamide inhibition is determined by the PanK type of the targeted organism. Specifically, we show that in *S. aureus* growth inhibition is as a result of at least two factors working in combination: 1) by the formation of inactive acyl carrier proteins (ACPs) and CoA antimetabolites and 2) by the reduction of CoA levels through the inhibition of *Sa*PanK-II.

Although pantothenamides act as potent inhibitors of *S. aureus in vitro*, this promising antimicrobial activity is lost when such tests are performed *in vivo* due to enzymatic degradation of the pantothenamides by pantetheinase enzymes. This also translates to their inhibition of the malaria-causing parasite, *P. falciparum*, since pantetheinase enzymes are present in plasma and serum. Therefore, the second part of this study focused on the design and synthesis of new potent inhibitors that are resistant to pantetheinase-mediated degradation. *N*-Heptyl pantothenamide (N7-Pan) and *N*-phenethyl pantothenamide (*N*-PE-PanAm) were used as scaffolds, since these pantothenamides were previously shown to have excellent potential as inhibitors of *S. aureus* and *P. falciparum* proliferation, respectively. Structural modifications were made to the pantothenamides to protect the scissile amide bond from hydrolysis. Specifically, these modifications were chosen to increase the steric bulk around the amide bond, by replacing it with a bioisostere moiety that should withstand pantetheinase degradation, or by preventing the

compound from being recognized as a substrate. Ten N7-Pan analogues were successfully synthesized and fully characterized as inhibitors of *Sa*PanK-II and *S. aureus*, while nine *N*-PE-PanAm analogues were successfully synthesized and partially characterized as inhibitors of *P. falciparum*. Our results show that while modifications do result in imparting pantetheinase resistance, they also can impact negatively on target recognition.

# Opsomming

Die verskyning van weerstandbiedende organismes is een van die belangrikste dryfkragte vir die voordurende ontwikkeling van nuwe antimikrobiese middels. Vorige navorsing het vasgestel dat koënsiem A (KoA), wat gebiosintesitieer word vanaf pantoteensuur, die groei van verskeie siekte-veroorsakende patogene, insluitend *Staphylococcus aureus* en *Plasmodium falciparum*, bevorder. Weens die strukturele en meganistiese verskille tussen die prokariotiese en eukariotiese ensieme in die KoA-padweg is dit moontlik om die patogeniese ensieme selektief te inhibeer met spesifieke klein molekuul-inhibitore. Die KoA biosintese padweg word dus beskou as 'n voornemende teiken vir sulke inhibitore, en gevolglik was spesifieke analoë van pantoteensuur gebruik in die soektog na nuwe antimikrobiese middels in verskeie studies.

Een spesifieke klas van hierdie analoë, naamlik die *N*-gesubstitueerde pantoteenamiede, is potensieel goeie inhibitore van KoA biosintese en KoA gebruik in *S. aureus*. Ongelukkig, weens ons swak begrip van hul meganisme van aksie, word hul ontwikkeling as klienies relevante middels beperk. Die fokus van die eerste deel van hierdie studie was om die aksiemodus van werking van pantoteenamiede te bepaal deur ‘n verbinding te ontwerp wat slegs kan optree as 'n inhibitor van *S. aureus* pantoteensuurkinase (*Sa*PanK-II) (die eerste ensiem in die KoA biosintese padweg). Die resultate wys dat die meganisme van aksiemodus van die pantoteenamiede in bakterië bepaal word deur die tipe PanK wat die organisme van belang bevat. Ons toon spesifiek dat in *S. aureus* groei-inhibisie veroorsaak word deur ‘n kombinasie van twee faktore: 1) die vorming van onaktiewe asieldraerproteïene en KoA antimetaboliete en 2 ) die vermindering van die KoA vlakke deur die direkte inhibering van die *Sa*PanK-II ensiem.

Alhoewel pantoteenamiede optree as kragtige inhibitore van *S. aureus in vitro*, word hierdie belowende antimikrobiese aktiwiteit verloor *in vivo* weens ensiematiese afbraak deur pantetiënase ensieme teenwoordig in plasma en serum. Hierdie effek is ook waargeneem in studies met *P. falciparum*. Die tweede deel van hierdie studie het dus gefokus op die ontwerp en sintese van inhibitore wat bestand is teen hidrolise deur pantetiënase-ensieme. Die ontwerp van hierdie inhibitore is gebaseer op die *N*-heptiel pantoteenamied (N7-Pan) en *N*-fenetiel pantoteenamied (*N*-PE-PanAm) raamwerk, aangesien verskeie studies reeds bewys het dat hierdie pantoteenamiede uitstekende inhibitore van onderskeidelik *S. aureus* en *P. falciparum* is. Strukturele veranderinge was gemaak om die geteikende amiedbinding in die pantoteenamiede teen hidrolise te beskerm. Hierdie veranderinge sluit in: 1) toevoeging van steriese hindernis rondom die geteikende amiedbinding; 2) vervanging met 'n bioisosteer-groep wat hidrolise deur pantetiënase-ensieme sal weerstaan; of 3) strukturele veranderings wat verhoed dat die verbinding erken word as 'n

substraat vir pantetiënase-ensieme. Tien N7-Pan-analoë is suksesvol gesintetiseer en ten volle gekarakteriseer as inhibitore van *Sa*PanK-II en *S. aureus*, terwyl nege *N*-PE-PanAm-analoë suksesvol gesintetiseer en gedeeltelik gekarakteriseer is as inhibitore van *P. falciparum*. Ons resultate wys dat alhoewel die strukturele veranderinge tot toenemende weerstand teen pantetiënase-ensieme lei, hierdie veranderinge ook 'n negatiewe invloed op teiken-herkenning het.

The financial assistance of the National Research Foundation (NRF) towards this research is hereby acknowledged. Opinions expressed and conclusions arrived at, are those of the author and are not necessarily to be attributed to the NRF.

# Acknowledgements

I cannot believe that all the frustrations and hard work has finally come to an end; regardless of the long hours and many disappointments of lab work over the last four years, I've had lots of fun and laughter, and given the choice, I would do it all over again. However, if it weren't for my massive support structure I would not have been able to complete my PhD and I am grateful to one and all.

First and foremost I would like to thank my supervisor Prof. Erick Strauss for allowing me to stay on in his lab after my honours project and for letting me continue with my love for chemistry. I truly appreciate all your help and guidance as well as your infinite patience during these past four years. I thoroughly enjoyed our coffee time discussions regarding research and life, as well as many other interesting topics. I will definitely have to start training a new minion next year to take over the "koffie kaptein" responsibility.

Secondly, I would also like to thank my co-supervisor, Prof. Willem van Otterlo, for all his help and guidance throughout the course of this project and for making a bench available in his laboratory in order to conduct my research. How can I forget - thank you for the torturous problem sets at 8am on a Friday morning – it definitely made me a better organic chemist.

Then I would also like to thank all of the Strauss lab members who always supported and willingly helped me, specifically when it came to biologically related research and for the coffee time chats and lab outings. Lizbé and Ilse – who would've thought that we would become such great friends when Sporty Spice first walked into the lab. Thank you for always being there for me, whether it was to celebrate my success or drown my sorrows with cheese cake. Furthermore, I would like to thank Lizbé for all the help with my biological experiments, my upgrade proposal and for acting as a sounding board when I wasn't sure on how to do experiments. To the rest of the lab, Bertus, Sunette, René, Dirk, Albert, Ndivhu, Tanya, Cristiano, Riyad, Dave, Melisse, Gordon and Andrea, I am really thankful for all your contributions. To Marianne, it was nice to finally meet you after two and a half years – thank you for sharing first authorship in our article and for acting as the first line of editorial defence during the write up of this thesis. Additionally, I would also like to thank my extended lab family at chemistry. I am really thankful to Dewald, Lesotho, Jonny, Anton, Monica, Alet, Tanya and Ronel, for all of your help and thank you for letting me feel a part of the chemistry group.

Last but not least, I also wish to thank my family and friends for their constant love and support. Especially to my Mom and Dad, for giving me the opportunity to study at Maties and for your

unconditional love, encouragement and support, even though you don't always understand what I do. Hopefully one day I can repay your confidence in me. Thank you to oom Johan and tannie Judy for accompanying my parents during their visits, thereby making it extra special. From the moment I set foot in Stellenbosch Shelyn and Arno, you both have always been there for me. I am grateful for all that you have done, including sharing the Meerlust wine; you've definitely turned me into a wine snob. I would also like to thank oom Sakkie and tannie Poenie for making time to see their "hanskind" during their visits and for all the home cooked meals. Thank you Jade for all the crazy fun times and for trying to understand what I'm doing on a daily basis as well as explaining to your mom with enthusiasm what my research is about. Roelien, if it wasn't for you I would definitely not be where I am today – thank you for all the class notes and for all the fun times we've had over the years. On a final note Daniëlle, thank you for your friendship over the years – Stellenbosch is not the same without you.

In conclusion I would like to thank my latest addition of friends, Niël, Barry, Gail and Annie – I really enjoyed busting clays with you guys on a Saturday. It kept me grounded the past year and a half of my PhD. Thank you for taking pity on a student at drinks rounds.

## Additional Acknowledgements


- Stellenbosch University and Prof. Erick Strauss for the opportunity to study at this institution.
- Stellenbosch University, the National Research Foundation (NRF), and the H.B. Thom trust as well as Prof. Erick Strauss for financial support.
- The Department of Chemistry, specifically the GOMOC group, for accommodating me in the laboratory during my studies.
- Prof. Jacky Snoep from the Department of Biochemistry for all his help in establishing a working kinetic model.
- Dr. Marietjie Stander of the Central Analytical Facility of Stellenbosch University for HRMS analyses.
- Mrs. Elsa Malherbe and Dr. Jaco Brand of the Central Analytical Facility of Stellenbosch University for chiral NMR experiments and general assistance on NMR analyses.

***~ In loving memory of Ouma and Tannie Rita – I wish you were here to celebrate with me. I know that I have made you proud ~***

# Table of Contents

**Addendum**

# Outputs

The work reported in this thesis has contributed to the following outputs:

**Papers:**

1. De Villiers, M.,‡ Barnard, L.,‡ Koekemoer, L., Snoep, J. And Strauss, E. Variation in pantothenate kinase type determines the pantothenamide mode of action and impacts on coenzyme A salvage biosynthesis. *FEBS Journal* 2014, **281**, 4731-4753. doi:10.1111/febs.13013. [‡Denotes equal contribution].

2. Macuamule, C. J., Tjhin, E. T., Jana, C. E., Barnard, L., Koekemoer, L., de Villiers, M., Saliba, K. J. and Strauss, E. A pantetheinase-resistant pantothenamide with potent, on target, and selective antiplasmodial activity. *Antimicrobial Agents and Chemotherapy* 2015, **59**, 3666-3668. doi.org/10.1128/AAC.04970-14.

3. Macuamule, C. J., de Villiers, M., Wells, G., Barnard, L., Saliba, K. J. and Strauss, E. Pantothenate kinase as gateway to activate pantothenamides as potent antimalarials against *Plasmodium falciparum - Working title. Paper in preparation.*

Oral presentations:

1. “Validating *Staphylococcus aureus* pantothenate kinase a drug target”. MSc progress lecture presented at the Department of Biochemistry, Faculty of Science, Stellenbosch University. May 2013.

2. “Pantothenamides as antibacterials: mode of action studies and improvement of their potency by structural modifications”. MSc upgrade lecture presented at the Department of Biochemistry, Faculty of Science, Stellenbosch University. October 2013.

3. “Developing degradation-resistant antimicrobials”. Lecture presented at the Biochemistry 40 year symposium at the Department of Biochemistry, Faculty of Science, Stellenbosch University. January 2015.

Poster presentations:

1. De Villiers, M., Barnard, L., Koekemoer, L., Snoep, J. and Strauss, E. “Studies on the mode of action of the pantothenamide antibacterials reveals the importance of pantothenate kinase variation”. Poster presented by Dr. M. de Villiers at the Coenzyme A and its derivatives in cellular metabolism and disease conference, London. March 2014.

2. Barnard, L., van Otterlo, W.A.L. and Strauss, E. “Design and synthesis of antistaphylococcal pantetheinase-resistant inhibitors”. Poster presented at the SACI-ACS bi-national organic chemistry conference, Stellenbosch. December 2014.

3. De Villiers, M., Barnard, L., Koekemoer, L., Snoep, J. and Strauss, E. “Studies on the mode of action of the pantothenamide antibacterials reveals the importance of pantothenate kinase variation”. Poster presented by Dr. M. de Villiers at the SACI-ACS bi-national organic chemistry conference, Stellenbosch. December 2014.

# List of Abbreviations

| | |
|---|---|
| ACP | Acyl carrier protein |
| ADP | Adenosine 5’-diphosphate |
| Ala | Alanine |
| Arg | Arginine |
| ATP | Adenosine 5’-triphosphate |
| $BiCl_3$ | Bismuth (III) chloride |
| BSA | Bovine serum albumin |
| Cbz | Carbobenzoxy |
| CAF | Central Analytical Facility |
| CDC | Center for Disease Control and Prevention |
| $CH_3I$ | Methyliodide |
| CoA | Coenzyme A |
| CoADR | Coenzyme A disulphide reductase |
| CTAB | Cetyltrimethylammonium bromide |
| CSA | 10-Camphorsulfonic acid |
| CsOH | Cesium hydroxide |
| $Cs_2CO_3$ | Cesium carbonate |
| Cu | Copper |
| CuCl | Copper (I) chloride |
| Cys | Cysteine |
| DAST | (Diethylamino)sulphur trifluoride |
| DCE | 1,2-Dichloroethane |
| DCM | Dichloromethane |

| | |
|---|---|
| DCP | Dicumyl peroxide |
| DEPC | Diethyl cyanophosphonate |
| DIC | *N*, *N*-Diisopropyl carbodiimide |
| DIPEA | *N*, *N*-Diisopropylethylamine |
| DMAP | *N*, *N*-Dimethyl aminopyridine |
| $DMBNH_2$ | Dimethoxybenzyl protected amine |
| DMF | *N*, *N*-Dimethylformamide |
| DMSO | Dimethyl sulfoxide |
| DPPA | Diphenyl phosphorylazide |
| *E. coli* | *Escherichia coli* (also *Ec*) |
| *Ec*PanK | *Escherichia coli* pantothenate kinase |
| EDC | *N*-(3-Dimethylaminopropyl)-*N*′-ethylcarbodiimide hydrochloride |
| equiv. | Equivalents |
| ESBL | Extended-spectrum β-lactamase |
| EtOH | Ethanol |
| EtOAc | Ethyl acetate |
| FCC | Flash column chromatography |
| FDA | Food and Drug Administration |
| Fmoc | 9-Fluorenylmethyl carbamate |
| F$sp^3$ | Fraction of $sp^3$ carbons |
| Glu | Glutamic acid |
| h | Hours |
| H-bond | Hydrogen bond |
| $H_2O$ | Water |
| HBr | Hydrobromic acid |

| | |
|---|---|
| His | Histidine |
| HIV | Human Immunodeficiency Virus |
| HOBt | *N*-Hydroxybenzotriazole |
| HRMS | High Resolution Mass Spectroscopy |
| $IC_{50}$ | Concentration required for 50% inhibition |
| IMAC | Immobilized Metal Affinity Chromatography |
| IPM | Isopropenyl methyl ether |
| IPTG | Isopropyl β-D-1-thiogalactopyranoside |
| KCl | Potassium chloride |
| $K_2CO_3$ | Potassium carbonate |
| $k_{cat}$ | Turnover number |
| $K_i$ | Inhibition constant |
| $K_M$ | Michaelis-Menten constant |
| $KMnO_4$ | Potassium permanganate |
| *t*BuOK | Potassium *tert*-butoxide |
| LB | Luria Bertani |
| LDH | Lactate dehydrogenase |
| Log$D_{7.4}$ | Distribution coefficient at pH 7.4 |
| Log*P* | Partition coefficient |
| cLog*P* | Calculated partition coefficient |
| Lys | Lysine |
| $CH_3CN$ | Acetonitrile |
| MeOH | Methanol |
| $MgCl_2$ | Magnesium chloride |
| $MgSO_4$ | Magnesium sulphate |

| | |
|---|---|
| MIC | Minimum inhibitory concentration needed to kill the organism |
| $MIC_{80}$ | Minimum inhibitory concentration needed to kill 80% of the organism |
| min | Minute |
| MRSA | Multidrug-resistant *Staphylococcus aureus* |
| $NaBH_4$ | Sodium borohydride |
| $NaBH_3CN$ | Sodium cyanoborohydride |
| NaCl | Sodium chloride / salt / brine |
| NADH | Nicotinamide adenine dinucleotide (reduced) |
| $NaN_3$ | Sodium azide |
| $Na_2SO_4$ | Sodium sulphate |
| $NaHCO_3$ | Sodium bicarbonate |
| NaOH | Sodium hydroxide |
| $Et_3N$ | Triethylamine |
| $NH_3$ | Ammonia |
| $NH_4Cl$ | Ammonium chloride |
| $NH_4OAc$ | Ammonium acetate |
| $Ni^{2+}$ | Nickel |
| NMR | Nuclear Magnetic Resonance Spectroscopy |
| NPPs | New permeability pathways |
| NRotBs | Number of rotatable bonds |
| MsCl | Methylsulfonyl chloride |
| OD | Optical density |
| P | Partition |
| Pan/PanCOOH | Pantothenic acid |
| PanK/CoaA | Pantothenate kinase |

| | |
|---|---|
| PantSH | Pantetheine |
| Pd | Palladium |
| Pd/C | Palladium on activated carbon |
| PDB | Protein data bank |
| PEP | Phosphoenolpyruvate |
| PK | Pyruvate kinase |
| PMB | *p*-Methoxybenzylidene |
| *P*PAT/CoaD | Phosphopantetheine adenylytransferase |
| *P*PCS/CoaB | Phosphopantothenoylcysteine synthetase |
| *P*PCDC/CoaC | Phosphopantothenoylcysteine decarboxylase |
| PPTS | Pyridinium *p*-toluenesulfonate |
| PSA | Polar surface area |
| *p*-TsOH | *p*-Toluenesulfonic acid |
| RND | Tripartite resistance-nodulation-cell division |
| rt | Room temperature |
| *S. aureus* | *Staphylococcus aureus* (also *Sa*) |
| *Sa*PanK | *Staphylococcus aureus* pantothenate kinase |
| SEM | Standard error of the mean |
| Ser | Serine |
| SPE | Solid Phase Extraction |
| TBSCl | *tert*-Butyldimethylsilyl chloride |
| TFA | Trifluoroacetic acid |
| THF | Tetrahydrofuran |
| TIPBSCl | 2,4,6-Triisopropyl-benzenesulfonyl chloride |
| TLC | Thin Layer Chromatography |

| | |
|---|---|
| TRIS-HCl | Tris(hydroxymethyl)aminomethane-HCl |
| Trp | Tryptophan |
| TsCl | 4-Toluenesulfonyl chloride |
| Tyr | Tyrosine |
| U | Units (enzyme concentration) |
| $V_{max}$ | Maximal velocity |
| Vit. B5 | Vitamin B5 also known as pantothenate/pantothenic acid |
| VNN | Vanin |
| WDI | World Drug Index |
| XDR | Extensively drug resistant |

*Chapter 1*

# Coenzyme A: Biosynthesis, Potential Drug Targets and Small Molecule Inhibitors

## 1.1 Increase in drug resistance is a global health threat

Antibiotics are seen as the original wonder drugs since their first discovery in 1940; since then they have been regarded as one of the most valuable forms of therapy in medicine [1-4]. To this day antibiotics still underpin modern medicine and it is central to healthcare facilities where it is used for treatments such as cancer chemotherapy to prevent patients from developing an infection when their white blood cell count is low, for complex surgical procedures to prevent surgical site infections, and for dialysis for end-stage renal failure given that patients who undergo dialysis treatment are more likely to get bloodstream infections. Additionally, antibiotics also lead to a major increase in life expectancy and a decrease in child mortality [5-6]. However, there has been a dramatic increase in morbidity and mortality worldwide over the last decade due to bacteria becoming increasingly drug resistant [3-4, 7]. According to the World Health Organization (WHO) emerging microbial resistance is most evident in bacteria that cause human diseases. In 2013 a national threat assessment was released by the Center for Disease Control and Prevention (CDC) in which the potential of a fatal infection becoming a reality as a result of increasing multidrug resistant (MDR) bacteria worldwide was highlighted [1, 5, 8]. Consequently, this threat has also been identified as a core medical challenge in most healthcare facilities [9].

This global increase in drug-resistant pathogens is believed to be the result of repeated intensive and improper use of antibiotics in the agricultural sector and the human and veterinary medicinal sections [10], with the CDC estimating that at least 50% of all prescriptions for antibiotics are not necessary [11]. In fact, MDR bacteria is so prevalent, that the CDC and the European Center for Disease Control and Prevention (ECDC) standardized terminology to facilitate grading of various antimicrobial resistance profiles and reporting of comparable statistics internationally. Antibiotic resistance has been classified into three groups using this system, these being: 1) MDR, which is defined as “having acquired non-susceptibility to at least one agent in three or more antimicrobial categories”; 2) extensively drug-resistant (XDR), which is defined as “non-susceptibility to at least one agent in all but two or fewer antimicrobial categories”; 3) and pandrug-resistant (PDR), which is defined as “non-susceptibility to all agents in all antimicrobial categories” [9].

Drug-resistant pathogens include, but are not limited to, methicillin- and MDR *Staphylococcus aureus* (MRSA), extended-spectrum β-lactamase (ESBL)-producing *Escherichia coli*, vancomycin-resistant enterococci (VRE), MDR and XDR *Mycobacterium tuberculosis* and penicillin- and

macrolide-resistant pneumococci [12-13]. The current arsenal of available antibiotics is being rendered ineffective due to bacteria becoming increasingly insensitive to these compounds, leading to treatment failure [3, 14]. The majority of antibiotic classes that are currently being used to treat diseases were discovered during the 'Golden Age' of antibiotic discovery (from 1940-1960), which lead to the 'Golden Age' of antibiotic medicinal chemistry (from 1960 to present) (Figure 1.1) [15]. However, there has been a great innovation gap from 1960 to 2000 where no new antibiotic molecular entities were discovered. Moreover, none of the new antibiotic classes that were introduced from 2000 have made a noteworthy impact [15-16]. Consequently, we are losing the battle against the rapid emergence and spread of MDR bacteria, since we have not been successful at providing a continuous pipeline of novel antibiotics [9].

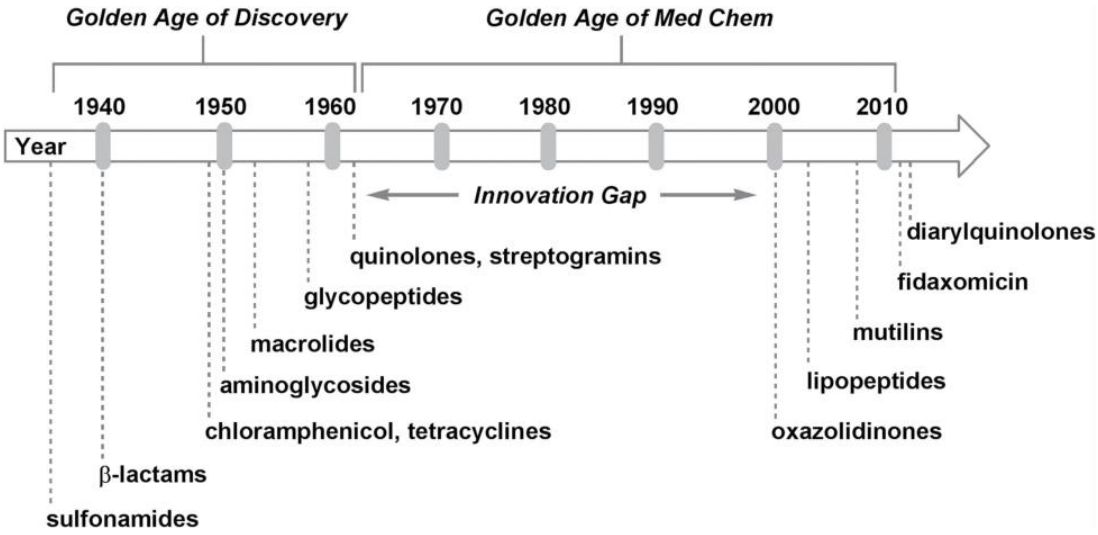


**Figure 1.1. Timeline illustrating the 'Golden Age' of antibiotic discovery from 1940 to 1960, the 'Golden Age' of medicinal chemistry from 1960 to present and the big Innovation Gap for antibiotic discovery from 1960 to 2000. Reproduced from Ref. [15].**

## 1.2 Antibiotic development is declining

In addition to bacteria becoming antibiotic-resistant, many pharmaceutical companies have cut down on their development of new antimicrobials [3]. Figure 1.2 shows the rapid decrease in the approval of new antimicrobial agents by the Food and Drug Administration (FDA) over the last 30 years, with only two new antibiotic molecular entities being introduced between 2008 and 2012, compared to the 16 that was introduced between 1983 and 1987 [3-4]. This is almost a 90% decrease in the number of new FDA approved antibiotics over the last 30 years [17].

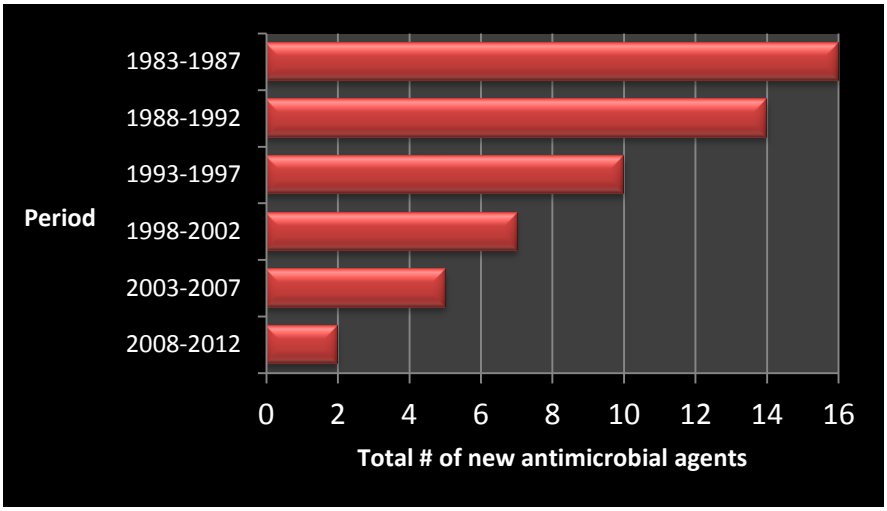


**Figure 1.2. Number of new antibiotic molecular entities approved by the FDA in five year periods from 1983 to 2012 [3-4].**

This decrease in the development of new antibiotic molecular entities is attributable to three main factors. First, the 'Golden Ages' of antibiotic discovery and antibiotic medicinal chemistry already provided us with more than 140 antibiotics globally. This limits the discovery and development of novel molecular entities due to the scientific challenge of identifying new targets and scaffolds that have not been utilized previously [17]. Second, and possibly the main reason, is the low return on investment in research and development. As is the case with all drugs, antibiotics are tremendously expensive and time-consuming to develop. However, when compared to chronic medicine (where a patient takes the medicine everyday for the rest of their lives) as well as lifestyle drugs (medicines that treat conditions associated with lifestyle such as drugs to treat smoking, weight loss and baldness to name but a few), antibiotics are normally used for short periods of time and the predominant market is patients from developing countries with a low income that cannot afford to pay inflated prices [4]. Figure 1.3 shows a typical drug discovery and development flowchart that illustrates that it takes a minimum of 12 years and a staggering $1.3 billion to develop a new antibiotic [4, 15, 17]. Additionally, sales of a new antibiotic can also be significantly hampered by antibiotic stewardship principles that demand that its use be limited. The London School of Economics used an advanced economic model to estimate the net present value of a new intravenous antibiotic to a company at the point of discovery; the prediction gave a value of minus $50 million [17].

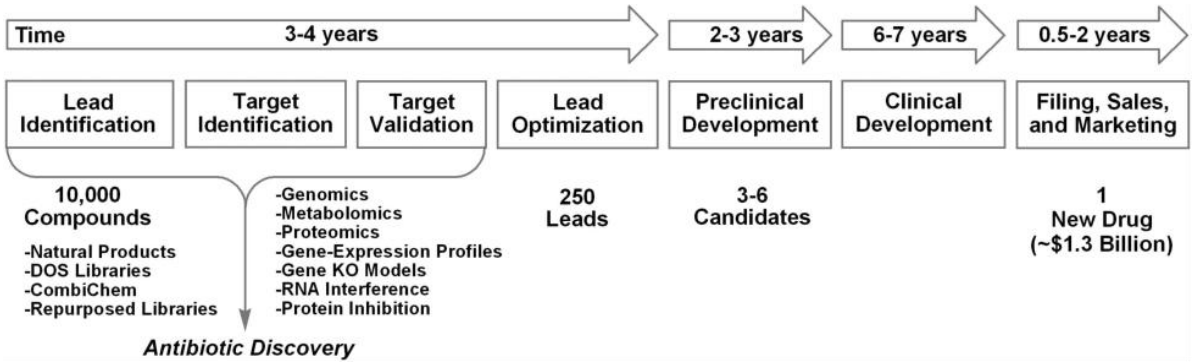


**Figure 1.3. Flowchart showing the timeline for the discovery and development of a new antibiotic. Reproduced from Ref. [15].**

The third and final factor is the re-evaluation of how clinical trials for a new antibiotic should be conducted by the Office of Antimicrobials from the FDA over the past decade. Originally, this re-evaluation was based on legitimate statistical and scientific concerns regarding conventional clinical trials; however, the concerns have been driven to irrational extremes based exclusively on statistical considerations, at the expense of feasibility trial conduct and clinical relevance of studies. Consequently, this re-evaluation has lead to a major increase in expenses, the clinical trials have become more time-consuming and the likelihood of a new antibiotic being approved decreased dramatically compared to previous years [17]. Therefore, it is not as profitable for pharmaceutical companies to invest in the research and development of new antimicrobial agents compared to chronic medicine and lifestyle drugs. However, with the rapid increase in drug-resistant and MDR pathogens globally, it has become a key medical challenge in most healthcare settings and extensive research worldwide will be crucial to reduce its consequences for patients and society [9, 18].

## 1.3 Bacteria use a variety of molecular mechanisms to become drug-resistant

To date, four molecular mechanisms for resistance have been described: 1) bypassing of the antibiotic targets, 2) preventing antibiotic access to the targets, 3) enzymatic inactivation of antibiotic structures, and 4) changes in antibiotic targets by mutation [2, 5, 19-20]. All of these molecular mechanisms are clinically important and the majority of antibiotics are subject to more than one mechanism [20]. Each of the four molecular mechanisms will be discussed in more detail below.

### 1.3.1 Bypassing of the antibiotic target

Bacteria have developed mechanisms by which they evade antibiotic action by bypassing their molecular targets, and by utilizing alternate pathways that are not susceptible to the action of the antibiotic in question [20]. An example of such a mechanism is resistance to glycopeptide antibiotics such as vancomycin, a fermentation product from Streptomycetes [19-20]. Vancomycin has a unique mode of action that inhibits peptidoglycan crosslinking by binding to the acyl-D-Alanyl-D-Alanine (acyl-D-Ala-D-Ala) terminus of the lipid-linked disaccharide pentapeptide, a precursor of cell wall peptidoglycan [5, 19-20]. Since vancomycin is an inhibitor of peptidoglycan crosslinking, it is mainly effective against Gram-positive bacteria by allowing vancomycin access to the lipid-linked disaccharide pentapeptide in the periplasm due to a lack of an outer membrane [5]. It was widely believed that antibiotic resistance would be impossible as a result of this unique mechanism; however, vancomycin resistance is now common among enterococci. Additionally, treatment of vancomycin-resistant enterococci is even more difficult, because they are naturally resistant to other antibiotics such as macrolides, aminoglycosides, tetracycline and β-lactams [19].

Vancomycin exhibits its antimicrobial action by binding to the acyl-D-Ala-D-Ala terminus of the lipid-linked disaccharide pentapeptide through five hydrogen bonds (H-bonds) to form a non-covalent complex (Figure 1.4). However, when vancomycin-resistance develops the acyl-D-Ala-D-Ala terminus is substituted with an isosteric depsipeptide acyl-D-Alanyl-D-Lactic acid (acyl-D-Ala-D-Lac). This substitution leads to the replacement of an amide bond with an ester bond (indicated in red in Figure 1.4), resulting in the loss of an H-bond donor, in addition to the acquisition of electronic repulsion. Consequently, these changes prevent efficient binding of vancomycin to the lipid-linked disaccharide pentapeptide, leading to antibiotic resistance. This resistance mechanism necessitates the participation of seven genes, namely *VanR*, *VanS*, *VanH*, *VanA*, *VanX*, *VanY* and *VanZ* [19-21].

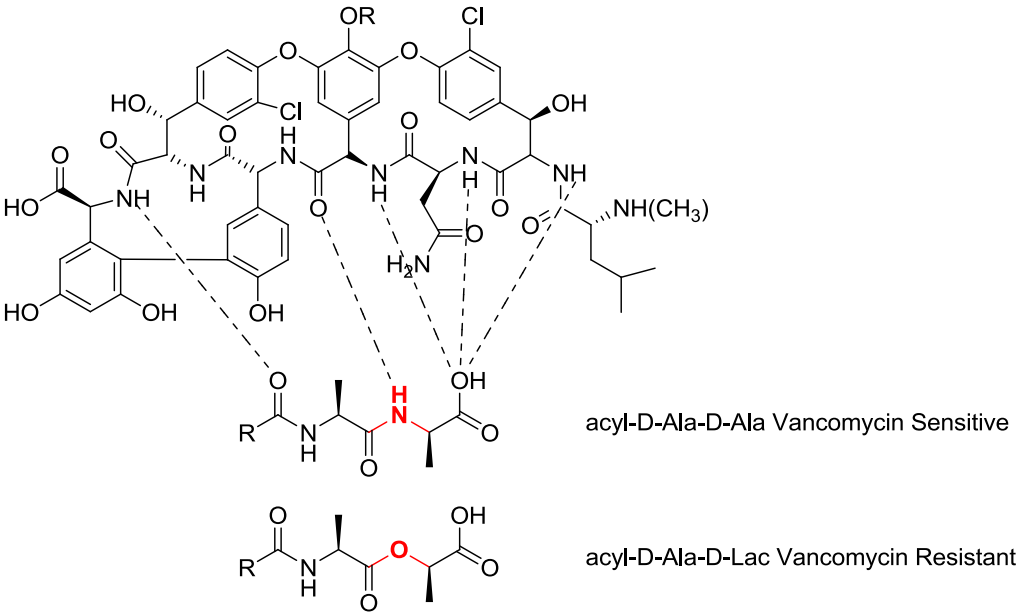


**Figure 1.4. Vancomycin binds to the acyl-D-Ala-D-Ala terminus of the lipid-linked disaccharide pentapeptide through five H-bonds to form a non-covalent complex. Resistance develops when the acyl-D-Ala-D-Ala terminus is substituted with an isosteric depsipeptide acyl-D-Ala-D-Lac, resulting in the loss of an H-bond and the acquisition of electronic repulsion (replacement of amide bond with an ester bond). Adapted from Ref. [20].**

## 1.3.2 Preventing antibiotic access to the targets

Bacteria have the ability to prevent antibiotic access to the targets through one of three methods: 1) drug access can be reduced locally, 2) access can be reduced by an active efflux process or 3) access can be reduced by decreasing the influx across an outer membrane barrier. The latter can only occur in Gram-negative bacteria.

### 1.3.2.1 Local inhibition of drug access

The access of antibiotics to their specific targets can be reduced locally in Gram-positive bacteria by ribosomal protection proteins such as Tet(M) or Tet(S) that are encoded by the *tet*(M) and *tet*(S) genes. [19]. These proteins affect the mode of action of tetracyclines, a broad-spectrum antibiotic that prevents protein synthesis by inhibiting the binding of aminoacyl-tRNA to the ribosomal acceptor (A) site [22]. Proteins Tet(M) and Tet(S) prevents the recognition of tetracyclines to ribosomes by binding with high affinity to the ribosomes, which subsequently triggers a conformational change [19, 22]. Another example of a class of broad-spectrum antibiotics that is effective against both Gram-positive and Gram-negative bacteria is the fluoroquinolones. Fluoroquinolones are the only known direct inhibitors of DNA synthesis; their mode of action entails either binding to the DNA-topoisomerases complex or the DNA-gyrase complex and in this manner they stabilize the DNA strand breaks created by DNA gyrase and topoisomerase IV [23]. It is

believed that DNA topoisomerases are protected from fluoroquinolones by plasmid-mediated quinolone resistance genes (Qnr) that encode Qnr proteins [19].

#### 1.3.2.2 Active drug-specific efflux pumps

Efflux pumps are also utilized by bacteria to actively remove antibiotics from within the cell. There are two groups of efflux pumps: 1) high substrate-specificity efflux pumps such as the Tet pumps that only transport a selective number of substrates and 2) MDR efflux pumps that transport a wide variety of substrates [2, 5, 20]. The best characterized of the clinically relevant MDR efflux transporters is the tripartite resistance-nodulation-cell division (RND) class found in Gram-negative bacteria. Some of the most studied RND class examples include the multidrug efflux pump AcrAB-TolC in *E. coli* and MexAB-OprM in *Pseudomonas aeruginosa*. Efflux pumps, such as AcrB, occurs as a homotrimer and is found in the inner membrane where it forms a tripartite complex with the outer-membrane channel (TolC or OprM) and the periplasmic adaptor protein (AcrA and MexA) [5, 20]. Additionally, *P. aeruginosa* also contains a MexXY multidrug efflux pump that is responsible for aminoglycoside resistance [2]. Furthermore, tetracycline is another antibiotic that is rendered ineffective by the efflux pumps – TetA, a well known tetracycline resistant protein, catalyzes the removal of a tetracycline-Magnesium ($Mg^{2+}$) complex via proton-motive-force-dependent pumping toward the outside of the cell [19].

#### 1.3.2.3 Decreasing membrane permeability

Additionally, antibiotic access can also be decreased by reducing the outer membrane permeability [2, 5, 19-20]. Gram-negative bacteria are inherently less permeable to antibiotics than Gram-positive bacteria due to the presence of an outer-membrane that forms a permeability barrier. Hydrophobic antibiotics utilize outer-membrane porin proteins to diffuse across the outer membrane; bacteria such as *E. coli* have OmpC and OmpF outer-membrane proteins that function as non-specific channels that can be targeted by such antibiotics. Bacteria have developed an antibiotic resistance mechanism by replacing the porins with more selective ones or by down regulating the porins which leads to a reduction in the outer-membrane permeability, thereby reducing antibiotic entry into the bacteria. For example *Pseudomonas* spp. and *Acinetobacter* spp. resistance to carbapenem and cephalosporin antibiotics were believed to be only as a result of enzymatic degradation; however, recent studies have shown that the reduction in porin expression also contributes extensively to the observed antibiotic resistance. Additionally, *Klebsiella pneumoniae* has also caused worldwide infections through clonal lineages that developed by means of expression of modified porins [5].

### 1.3.3 Enzymatic inactivation of antibiotic structures

The type of antibiotics that are most affected by enzyme-catalyzed inactivation are those that were developed from natural products such as the aminoglycosides (tobramycin, kanamycin and amikacin) and the β-lactams (penicillins, carbapenems, monobactams and cephalosporins) [19-20]. Aminoglycosides, a class of broad-spectrum antibiotics that inhibit protein synthesis by binding to the 30S ribosomal sub-unit leading to inaccurate mRNA translation, are inactivated by various enzymes that modify their structures in a variety of ways. These enzymes include aminoglycoside adenyltranferase or nucleotidyltransferase (inactivation through adenylation), aminoglycoside phosphoryl transferase (APH, inactivation through phosphorylation) and aminoglycoside acetyltransferase (AAC, inactivation through acetylation). The modifications inactivate the aminoglycosides by lowering the net positive charges on these polycationic antibiotics, resulting in their inactivation [19, 24].

β-lactams, a class of broad-spectrum antibiotics that inhibit the biosynthesis of cell walls [2], are inactivated in the periplasm by β-lactamases. These β-lactamases are among the most widespread and clinically important resistance enzymes. To date, two distinct chemical mechanisms of β-lactamases have been described: 1) those that use metal-activation to increase the nucleophilicity of the water molecule that leads to bond cleavage; or 2) the formation of a covalent enzyme-complex followed by hydrolysis (Figure 1.5). The first mechanism occurs through 1-2 active site zinc ($Zn^{2+}$) atoms that activate a water molecule for direct nucleophilic attack on the electrophilic carbonyl carbon of the β-lactam centre resulting in an inactive antibiotic. The second mechanism is functionally analogous to Serine (Ser) proteinases where Ser acts as the nucleophile – the hydroxyl group of Ser launches a nucleophilic attack on the electrophilic carbonyl carbon of the β-lactam ring to form a covalent enzyme-complex that is subsequently hydrolysed, leading to an inactive antibiotic. The covalent enzyme complex imitates the modification to the antibiotic targets, peptidoglycan transpeptidases [20].

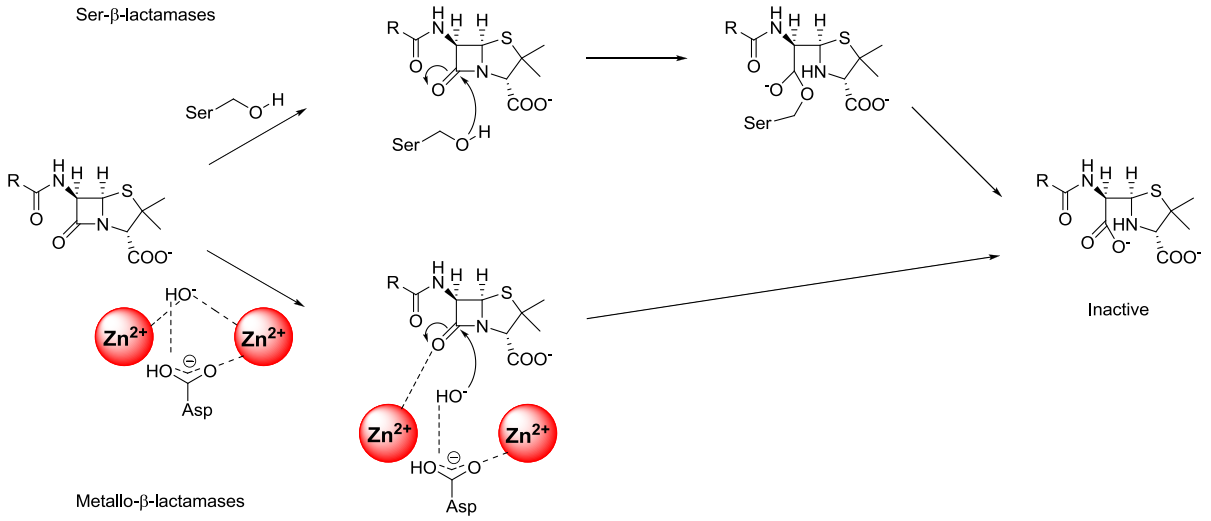


**Figure 1.5. General mechanism for Ser- and metallo-β-lactamases. In the Ser-β-lactamase mechanism the hydroxyl group of Ser makes a nucleophilic attack on the β-lactam ring followed by hydrolysis. In the metallo-β-lactamase mechanism water is first activated as a nucleophile by 1-2 active site $Zn^{2+}$ atoms, followed by a direct nucleophilic attack on the β-lactam ring. Adapted from Ref. [20].**

### 1.3.4 Changes in antibiotic targets by mutation

Additionally, bacteria also have the ability to develop antibiotic resistance either by obtaining new foreign genes or by mutating their own genes to modify their expression and function [5, 10, 19, 25-26]. To illustrate, *S. aureus* has the ability to use both of these mechanisms to develop antibiotic resistance. MRSA developed due to the acquisition of foreign DNA that encodes for the resistance *mec* regulon and by mutations in the *pbp* and *abc* genes. The *mec* regulon contains numerous genes of which the *mecA* gene—encoding the 76 kDa penicillin binding proteins (PBP 2' or PBP 2a) that has a low affinity for β-lactams—is a prerequisite for methicillin-resistance [5, 26]. Penicillin-resistant *S. aureus* strains have modified their gene expression to produce narrow spectrum β-lactamase, an enzyme that hydrolyzes penicillins, thus rendering them ineffective [25-26].

Another example of target mutation is against the fluoroquinolone antibiotics that bind to the DNA-enzyme complex resulting in the stabilization of DNA strand breaks created by DNA gyrase and topoisomerase IV. Even a single mutation to the *gyrA* gene, for example a mutation of Ser to a bulkier amino acid side chain such as isoleucine (Ile), tryptophan (Trp), leucine (Leu)) at position 83 or a mutation of aspartic acid (Asp) to asparagine (Asn), tyrosine (Tyr) or glycine (Gly) at position 87 leads to a high level of resistance. These minor alternations to the amino acid sequences change the protein's structure enough to inhibit antibiotic binding and action [19-20].

Since most bacteria make use of at least one mechanism to develop antibiotic resistance and most antibiotics are subject to several mechanisms, new antimicrobials with novel modes of action are needed as this will decrease the prospect of resistance across different classes of antibiotics (cross-resistance) [20].

## 1.4 Coenzyme A biosynthesis and CoA utilization as prospective drug targets

One set of potential novel targets that is currently being investigated for antimicrobial chemotherapy development is the coenzyme A (CoA) biosynthetic pathway, or the enzymes that subsequently utilize CoA. The value of this pathway as a drug target lies in CoA being an essential cofactor that needs to be synthesized *de novo* in all living organisms with an estimation that ~9% of all enzymes reported in the BRENDA database utilize CoA, or a CoA thioester as co-substrate in one way or another [12, 27]. This ubiquitous cofactor is involved in various reactions within the cell, for example ester-, thioester- and amide-bond formation reactions, in addition to Claisen condensation reactions. Furthermore, CoA also plays a major role in the biosynthesis of nonribosomal peptides and polyketides as well as fatty acid metabolism and the citric acid cycle (tricarboxylic acid cycle; TCA) [28-29].

The vital importance of the CoA biosynthetic pathway (which has been shown to be universal in all organisms) was further confirmed in various microorganisms given that attempts to disrupt genes encoding the enzymes of the CoA biosynthetic pathway consistently failed or resulted in lethal phenotypes [27]. It is important to note that even though the CoA biosynthetic pathway seems to be conserved across plants, microorganisms and mammals, there are several differences between the prokaryotic and eukaryotic pathways. For example, some of the prokaryotic enzymes show low sequence homology when compared to their human counterparts. They also show differences in regulation; these factors should allow for the selective targeting of the pathway in the pathogens without affecting the human host [30]. In *S. aureus*, CoA biosynthesis is an even more attractive target due to the accumulation of milimolar quantities of CoA in the organism. Moreover, CoA is involved in maintaining the redox balance in *S. aureus* through a unique CoA/CoA disulphide reductase (CoADR) redox system [12]. Taken together, these factors highlight the potential to develop high specificity inhibitors of bacterial CoA enzymes as new antimicrobial agents.

This study focussed on the CoA biosynthetic pathway as a prospective target for the development of new antibiotics in two pathogens that both have been shown to cause MDR, namely *S. aureus* and *Plasmodium falciparum*. CoA-based targets in *S. aureus* and *P. falciparum* have both been exploited through the use of pantothenic acid analogues as potential drug candidates.

Consequently, to put this study into perspective, the CoA metabolism in these two organisms is discussed below.

## 1.5 CoA metabolism in *S. aureus*

### 1.5.1 CoA biosynthesis from pantothenic acid

CoA is synthesized through a five-step universal pathway using pantothenic acid (also known as Vitamin $B_5$ or, when ionized, as pantothenate) as substrate (Scheme 1.1A). The first step entails the adenosine triphosphate (ATP)-dependent phosphorylation of pantothenic acid by pantothenate kinase (PanK; CoaA) to form 4'-phosphopantothenic acid. This is followed by the coupling of L-cysteine to 4'-phosphopantothenic acid by 4'-phosphopantothenoylcysteine synthetase (*P*PCS; CoaB) to form 4'-phosphopantothenoyl-cysteine. Subsequently, 4'-phosphopantothenoylcysteine is decarboxylated by 4'-phosphopantothenoylcysteine decarboxylase (*P*PCDC; CoaC) to yield 4'-phosphopantetheine. Dephospho-CoA is formed by phosphopantetheine adenylyltransferase (*P*PAT; CoaD), which couples an adenosine monophosphate (AMP) moiety from ATP to the phosphate of 4'-phosphopantetheine (step 4), with the concomitant formation of inorganic pyrophosphate. In the final step, the 3'-hydroxy group of the adenosine moiety is phosphorylated by dephospho-CoA kinase (DPCK; CoaE) to yield CoA.

Additionally, CoA can also be synthesized via the three step CoA salvage pathway using pantetheine (PantSH, a breakdown product of CoA) as an alternative substrate (Scheme1.1B). This pathway bypasses *P*PCS and *P*PCDC and only consists of three enzymes, i.e. PanK, *P*PAT and DPCK [12, 27, 31]. The universal five-step pathway and its shortened salvage route utilize four and three equivalents of ATP respectively, one of which provides the adenosine moiety of CoA during the *P*PAT-catalyzed reaction.

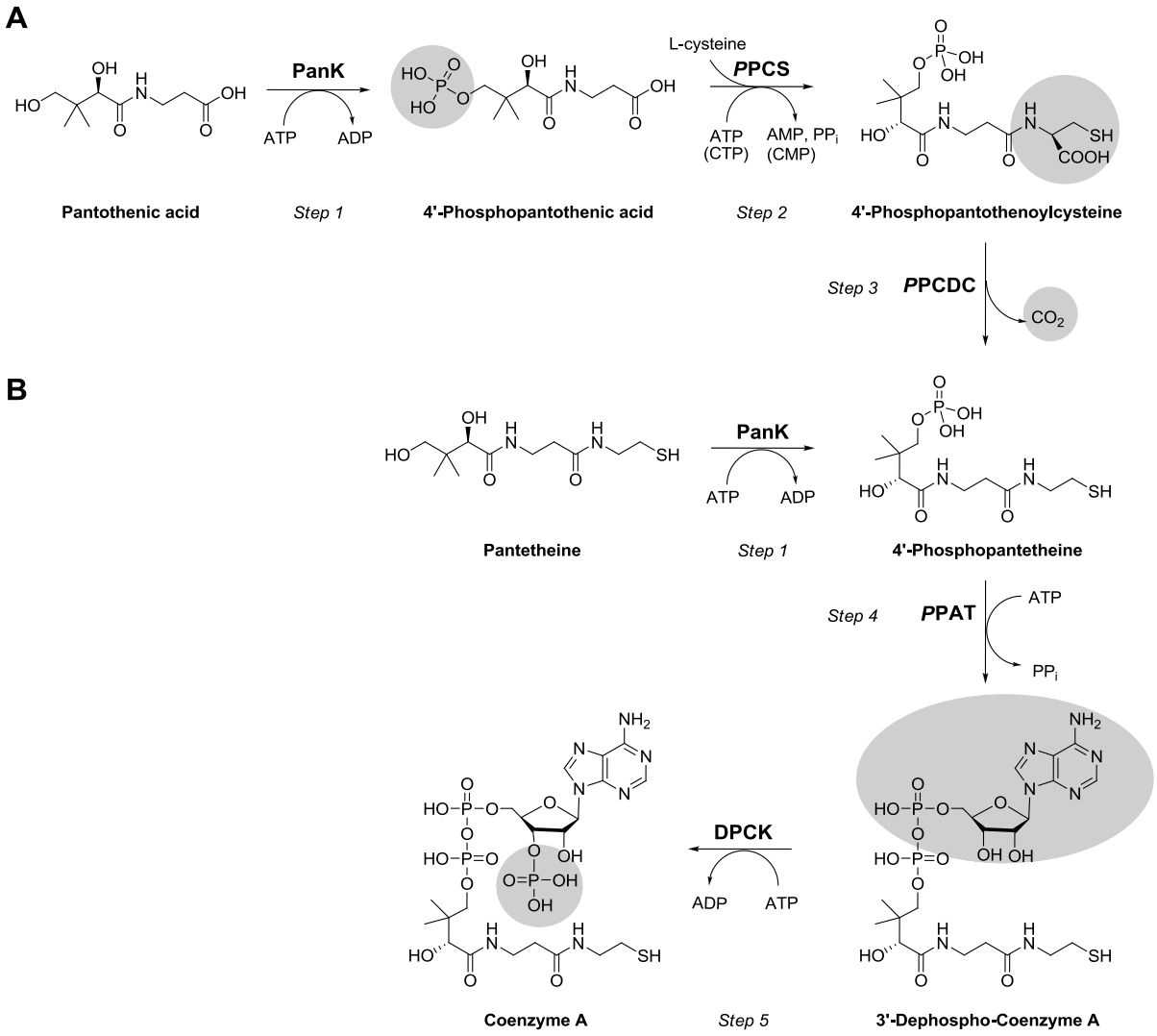


**Scheme 1.1. The CoA biosynthetic pathway. (A) Biosynthesis of CoA from pantothenic acid in the universal five-step pathway catalyzed by pantothenate kinase (PanK), phosphopantothenoylcysteine synthetase (*P*PCS), phosphopantothenoylcysteine decarboxylase (*P*PCDC), phosphopantetheine adenylyltransferase (*P*PAT) and dephospho-CoA kinase (DPCK). (B) Biosynthesis of CoA from pantetheine (PantSH) in the CoA salvage pathway catalyzed by PanK, *P*PAT and DPCK.**

### 1.5.1.1 Pantothenate kinase (PanK; CoaA)

The first enzyme in the pathway, PanK, can be distinguished as belonging to one of three distinct types based on sequence homology, enzyme structure, kinetic parameters and feedback inhibition. For ease of distinction they are labelled as type I (PanK-I), type II (PanK-II) and type III (PanK-III) [32-34]. Moreover, eukaryotic type II PanKs frequently occur as different isoforms within the same organism. To distinguish between PanK types and PanK isoforms, Roman numbers are used to denote PanK types while Latin numbers are used to denote PanK isoforms. The term “PanK isoforms” implies that the same protein is either expressed from different initiating exons (for

example human PanK1α and PanK1β) [35], or that the same enzyme is expressed in different tissues or is found in different cellular locations (for example human PanK2 and PanK3 are restricted to the mitochondria and the cytosol, respectively) [36].

Type I PanKs are classified as a P-loop kinase containing a Walker A motif, while both, the type II and type III PanKs have an actin-like fold and therefore belong to the ribonuclease H-like kinase group and are part of the acetate and sugar kinase/heat-shock protein 70/actin (ASKHA) superfamily [32-33, 37]. All known PanKs are homodimers with two identical subunits, each of which contains a single nucleotide binding site [38]. Although PanK-IIs and PanK-IIIs share the same conserved fold and key catalytic residues, they differ considerably in how the dimer interaction surface is formed, as well as in the architecture of substrate (ATP and pantothenic acid) binding sites [33]. PanK-IIs bind pantothenic acid in an open pocket, while the PanK-IIIs have a fully enclosed binding pocket. Conversely, ATP is tightly bound by PanK-II in a cavity that displays a classical P-loop architecture combined with very specific interactions to the adenine moiety, while structural analysis of the PanK-III from *Termotoga maritima* indicates a low binding affinity for ATP due to the enzyme making few contacts with any part of the ATP molecule apart from its phosphate groups [32].

*S. aureus* is the only bacterium that is known to have an active, albeit atypical, PanK-II enzyme, with most other PanK-IIs mainly being found in eukaryotes. Previous phylogenetic studies have shown that the primary sequence of *S. aureus*-like PanK proteins are distantly related to the eukaryotic PanK proteins, for example the cell division protein fumble from *Drosophila*. Even though these proteins are distantly related, there are numerous amino acid deletions and insertions that undoubtedly differentiate eukaryotic PanK-IIs from prokaryotic PanK-II [29-31]. Given that *S. aureus* is the only known bacterium with an active type II PanK enzyme, it is suggested that the staphylococcal *coaA* gene was horizontally transferred from eukaryotes to bacteria [30].

The kinetic mechanism of *S. aureus* PanK-II (*Sa*PanK-II) has been proposed as being an ordered bisubstrate (Bi-Bi) mechanism (two substrates and the formation of two products), which entails the formation of a ternary complex before the chemical step occurs [30, 39]. *Sa*PanK-II binds first to ATP in a highly cooperative manner, followed by the binding of pantothenic acid. After catalysis 4'-phosphopantothenic acid is released first, followed by adenosine diphosphate (ADP) [30]. Structural analysis of the *Sa*PanK-II structure with a non-hydrolyzable ATP analogue bound to the active site shows that it has two solvent exposed openings to the active site, indicating that it could also operate by a non-sequential mechanism, since ATP and pantothenic acid can enter from either side of the active site [32]. However, no kinetic data obtained to date provides any evidence of this.

The activity of the type I and type II PanKs are regulated via feedback inhibition by CoA and/or its thioesters which is responsible for the regulation of the flux through the pathway [29, 32, 37]. On the contrary, *Sa*PanK-II as well as prokaryotic PanK-IIIs is refractory to feedback inhibition by CoA and/or its thioesters. Metabolic labeling of *S. aureus* confirmed that CoA levels are not controlled by CoA or at steps downstream from CoA, due to the lack of pathway intermediates accumulating in either intra- or extracellular compartments [31-32, 40]. Furthermore, when the structure of *Sa*PanK-II was compared to human PanK3, a structural basis was found for this lack of feedback inhibition – two mutations (Ala to Tyr and Trp to arginine (Arg)) were found in the putative acetyl-CoA binding pocket [36]. This lack of regulation allows the accumulation of milimolar quantities of CoA in the organism which is the major intracellular thiol in *S. aureus* [32, 40]. This observation is consistent with the physiology of *S. aureus* which lacks the low molecular weight thiol glutathione, and consequently depends on the CoA/CoA disulfide reductase (CoADR) redox system (that reduces CoA-disulfides to CoA in a nicotinamide adenine dinucleotide (NADH)-dependent manner) for protection from oxidative damage [29, 34]. Furthermore, it is also suggested that the CoA levels in *S. aureus* is likely to be limited by the supply of pantothenic acid, which is synthesized by the biosynthetic pathway encoded by the *pan*B-E genes [29].

#### 1.5.1.2 Enzymes completing the CoA biosynthetic pathway (CoaBCDE)

Given that this study will primarily focus on PanK, the remainder of the enzymes in the CoA biosynthetic pathway will not be discussed in detail. However, CoaB (*P*PCS), CoaC (*P*PCDC), CoaD (*P*PAT) and CoaE (DPCK) have all been identified and fully characterized in various organisms and a full summary of these enzymes are available in reviews by Strauss [41] and Leonardi *et al*. [31].

### 1.5.2 CoA-dependent processes in metabolism

CoA serves as the primary acyl group carrier in metabolism, especially in processes involved in energy metabolism, such as fatty acid biosynthesis and degradation, as well as the citric acid cycle. These energy metabolism processes either utilize CoA independently or in combination with acyl carrier proteins (ACPs) which are small acidic proteins that interact with more than twelve other proteins to play a central role in fatty acid biosynthesis [42]. CoA functions as the source of the 4'-phosphopantetheine moiety of ACPs in a reaction catalyzed by phosphopantetheinyl transferase (PPTase) enzymes that transfer the moiety to *apo*-ACP (inactive) to convert it to its *holo*-ACP (active) form. The 4'-phosphopantetheine group is covalently bound to Ser-36 of the ACP, thereby activating it for the synthesis of growing acyl chains carried as thioesters of the terminal sulfhydryl group of the prosthetic group. Previous studies have characterized the PPTase in *E. coli* (ACP synthase; AcpS) and have shown it to be essential [27, 43]. Since the

characterization of AcpS, numerous other PPTases have been identified as *E. coli acpS* homologs in various prokaryotes. These PPTases have also been shown to be essential for survival, as a result of the essential role of ACPs in fatty acid biosynthesis and degradation [27, 42-43].

Since various processes involve the acyl functionality, many other enzymes depend on CoA as acyl carrier. These include HMG-CoA reductase (involved in cholesterol biosynthesis), 3-hydroxy-acyl-CoA dehydrogenase, 2-enoyl-CoA reductase, enoyl-CoA hydratase, 3-hydroxybutyryl-CoA epimerase, acyl-CoA oxidase, acyl-CoA dehydrogenases, and stearoyl-CoA desaturase (all involved in various fatty acid metabolic pathways), benzoyl-CoA reductase, and 4-chlorobenzoyl-CoA dehalogenase (involved in xenobiotic degradation), and methylmalonyl-CoA mutase (involved in several degradation pathways) [41].

### 1.5.3 The biosynthesis and utilization of CoA as an antimicrobial drug target

It has been hypothesized that selective inhibition of CoA biosynthesis in pathogens might be accomplished with selected small molecule inhibitors due to the high level of structural and mechanistic divergence between the prokaryotic and eukaryotic PanKs [12, 27]. There are four potential targets in the biosynthesis and utilization of CoA that these small molecule inhibitors can act upon, shown schematically in Figure 1.6. The first target (Figure 1.6, Target 1) entails the inhibition of pantothenic acid uptake. However, since *S. aureus* (as most prokaryotes) has the ability to synthesize pantothenic acid *de novo* and is able to transport pantothenic acid into the cell, this is not regarded a tractable target. The second target is CoA biosynthesis (Figure 1.6, Target 2), with the inhibition of the first enzyme (PanK) showing particular promise as PanK inhibition will decrease the amount of 4'-phosphopantothenic acid that forms and will consequently lead to a decrease in CoA levels, resulting in an overall decrease in the activity of CoA-dependent metabolic processes [44-46]. Coudhry *et al*. [30] have established that this is a viable drug target after they identified a series of low molecular weight compounds that inhibit *Sa*PanK-II activity [30].

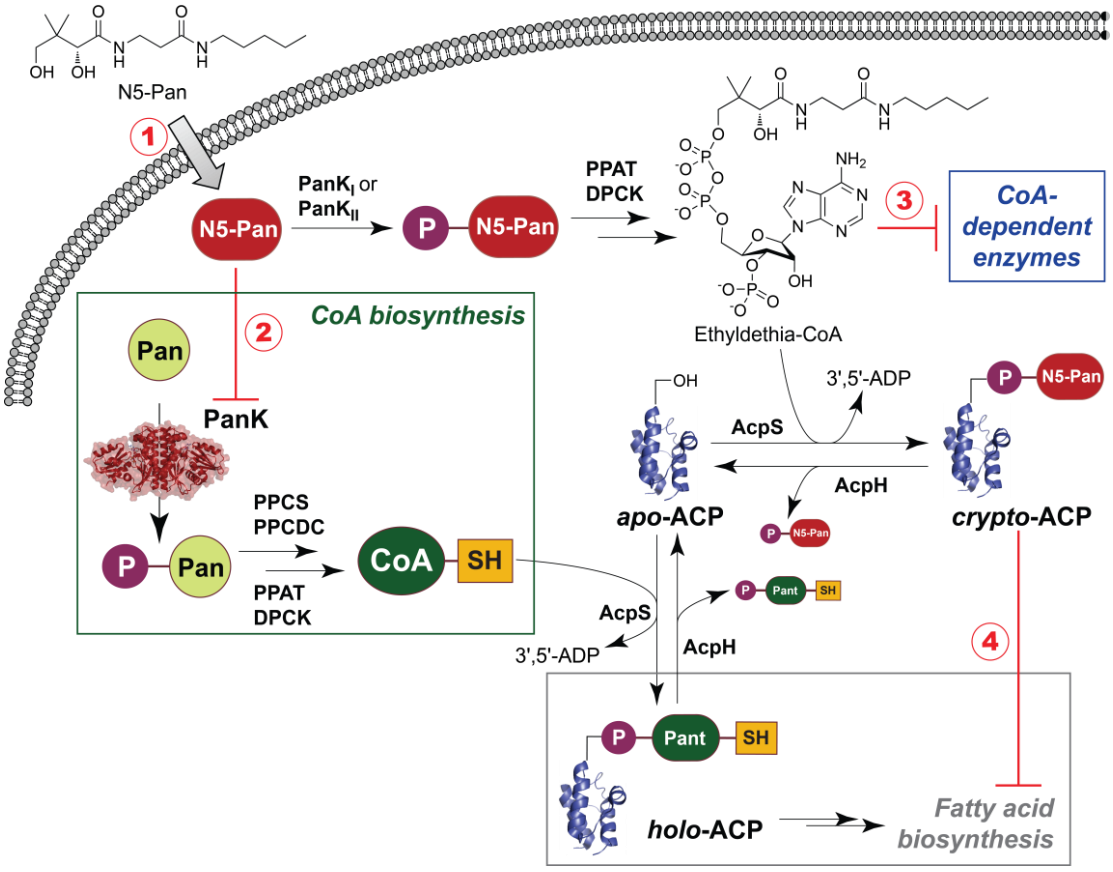


**Figure 1.6. The four major biological targets of pantothenic acid analogues such as *N*-pentyl pantothenamide (N5-Pan) used here as an example: 1) Pantothenic acid uptake 2) PanK, as the first CoA biosynthetic enzyme, 3) CoA-dependent enzymes, after transformation of the analogue into the corresponding CoA antimetabolite, and 4) fatty acid biosynthesis, when the CoA antimetabolite serves as substrate for AcpS to form a *crypto*-ACP instead of the catalytically active *holo*-ACP. *Holo*- and *crypto*-ACP are recycled back to *apo*-ACP by AcpH. Modified from Ref. [47].**

The third possible target is inhibition of CoA-dependent enzymes (Figure 1.6, Target 3). Compounds with this particular mode of action are usually pantothenic acid analogues that can be phosphorylated by PanK, and which are transformed by the remaining CoA biosynthetic machinery to the corresponding CoA antimetabolites. Since the essential terminal sulfhydryl group has been replaced by inactive moieties in these antimetabolites, this will adversely affect all CoA-dependent processes relying on this functional group. One specific process relying on CoA is fatty acid biosynthesis and is therefore seen as the fourth target of inhibition (Figure 1.6, Target 4). Fatty acid biosynthesis is dependent on ACPs to obtain the phosphopantetheine prosthetic group from the cofactor. If CoA is replaced by antimetabolites, it will lead to the synthesis of inactive ACPs due to the lack of the terminal sulfhydryl group needed for fatty acid biosynthesis [44-46]. This process has been validated as a potential drug target after Leonardi *et al*. discovered that low molecular weight compounds such as *N*-pentyl pantothenamide (N5-Pan) and *N*-heptyl pantothenamide (N7-

Pan) acts as substrates for *Sa*PanK-II and is subsequently converted to the inactive ethyldethia-CoA analogue (when N5-Pan is the substrate) or the inactive butyldethia-CoA analogue (when N7-Pan is the substrate), which is also incorporated into ACPs leading to the formation of *crypto*-ACP instead of the catalytically active *holo*-ACP [29]. These *crypto*-ACPs do not have the requisite thiol group and are therefore unable to act as acyl carriers.

However, it is important to note that previous studies have shown that some bacteria (especially some Gram-positives) have the ability to suppress fatty acid biosynthesis when exogenous fatty acids are present. This strict biochemical regulation of fatty acid biosynthesis by exogenous fatty acids means that these organisms are refractory to fatty acid biosynthesis inhibitors [48]. These implications will have to be considered for the development of antimicrobials that solely target fatty acid biosynthesis.

## 1.6 CoA metabolism in *Plasmodium falciparum*

### 1.6.1 Pantothenic acid and CoA biosynthesis in *P. falciparum*-infected erythrocytes

Pantothenic acid is one of only a handful of low molecular weight compounds and the only water soluble vitamin shown to be an absolute requirement for growth of the intracellular blood-stage *P. falciparum* parasites [27]. A study by Saliba *et al*. [49], demonstrated that pantothenic acid is rapidly taken up by *P. falciparum* infected erythrocytes and that this uptake is facilitated by “new permeability pathways” (NPPs) which is induced by the maturing parasite in the erythrocyte membranes [49]. These NPPs have a broad specificity and provide the host cell with an increased permeability to various low molecular weight compounds, including several nutrients, inorganic salts and metabolic wastes [27]. Pantothenic acid uptake occurs rapidly in *P. falciparum*-infected erythrocytes and this rapid uptake was also observed for intact isolated *P. falciparum* parasites (Scheme 1.2) [50].

It is believed that pantothenic acid enters the parasitophorous vacuole (a vacuole that forms when the parasite invades the erythrocyte via an endocytosis-like mechanism and in which the parasite remains enclosed) from the erythrocyte cytosol by diffusion through the vacuole membrane via low selectivity channels. Once it enters the vacuole, it is transported across the parasite’s membrane into the parasite where it gets phosphorylated by PanK [27]. The transporter (*Pf*PAT) responsible for the transport of pantothenic acid in *P. falciparum* was identified in 2013 and it is localized to the parasite plasma membrane [51]. Transport across the parasite’s membrane occurs via an $H^+$:pantothenic acid symport mechanism with a 1:1 stoichiometry (Scheme 1.2). This symport

mechanism couples the transport of one proton ($H^+$) to the transport of one pantothenic acid molecule down an electrochemical gradient. To date no candidate genes encoding the enzymes of the pantothenic acid biosynthetic pathway have been identified in the parasite's genome; this is consistent with studies on the *P. falciparum* parasite needing pantothenic acid for growth [27].

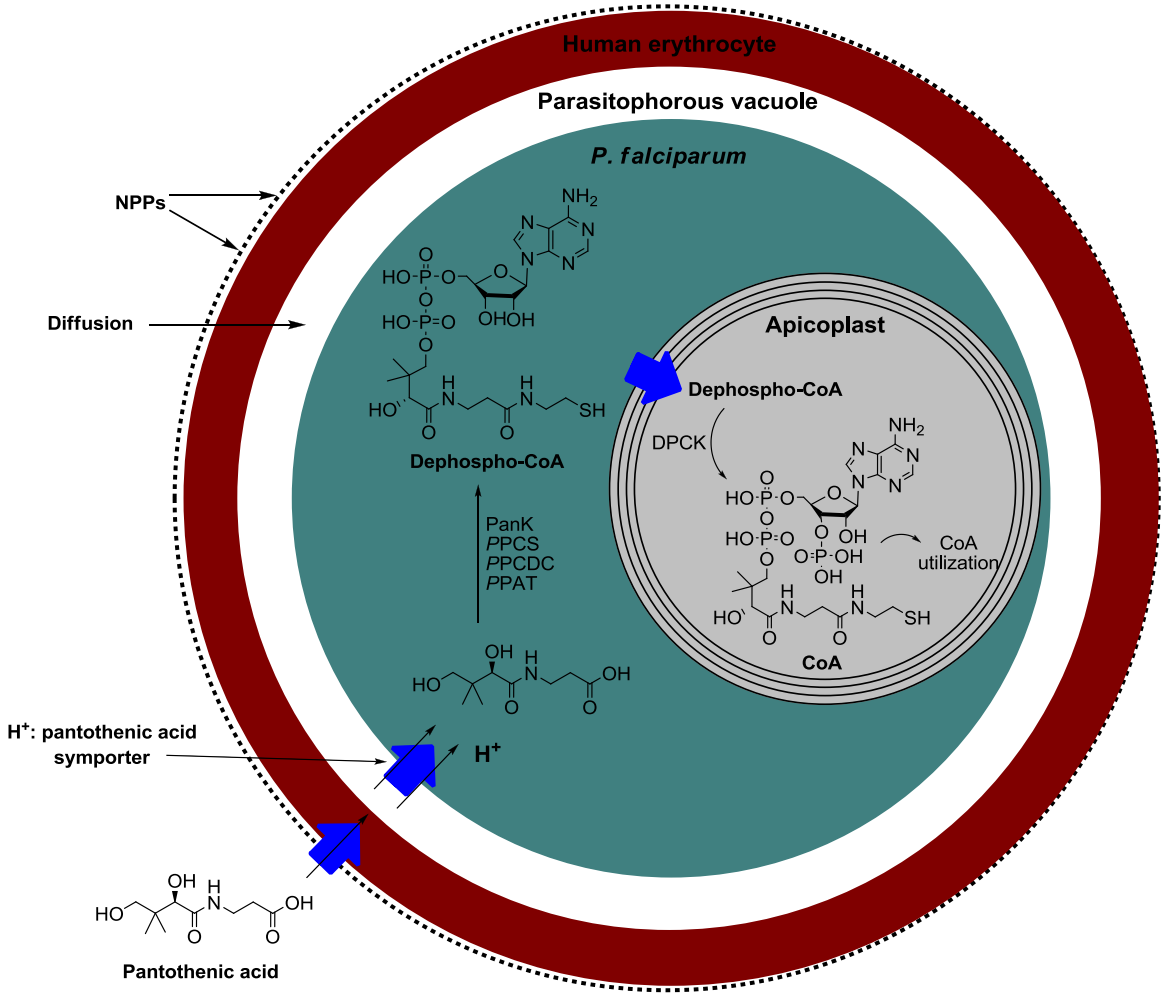


**Scheme 1.2. Pantothenic acid uptake and metabolism in *P. falciparum* infected erythrocytes. Pantothenic acid enters the erythrocyte through NPPs and is then believed to diffuse from the cytosol across the parasitophorous vacuole membrane into the parasitophorous vacuole. Subsequently, pantothenic acid is taken up by the parasite via an $H^+$:pantothenic acid symporter, after which it is converted to dephospho-CoA by the PanK, *P*PCS, *P*PCDC and *P*PAT enzymes located in the parasite cytosol. Dephospho-CoA enters the apicoplast via an unknown mechanism and the enzyme DPCK converts dephospho-CoA to CoA which is then used in CoA-dependent processes. Adapted from ref. [27, 46].**

There is a significant difference in pantothenic acid uptake between healthy erythrocytes and *P. falciparum*-infected erythrocytes. It was initially thought that pantothenic acid uptake in healthy erythrocytes is negligible due to the fact that they do not have NPPs in their membranes, in

addition to no scientific evidence supporting the existence of a functional transporter. However, in 2009 Spry *et al*. [50] showed that pantothenic acid uptake by healthy erythrocytes does indeed occur (albeit at a very slow rate) and these healthy erythrocytes do have the ability to metabolize pantothenic acid to form CoA. The mechanism by which healthy erythrocytes take up pantothenic acid remains to be established. Although pantothenic acid and CoA were detected in healthy erythrocytes, no other intermediates of the CoA pathway were detected. Conversely, CoA biosynthesis in *P. falciparum*-infected erythrocytes is considerably higher [50]. This is consistent with other published results on the increased permeability of *P. falciparum* infected erythrocytes to pantothenic acid [49]. These results suggest that CoA biosynthesis is regulated differently by *P. falciparum* and erythrocytes, and the rate of pantothenic acid phosphorylation by PanK does not determine the rate at which *P. falciparum* produces CoA [50].

#### 1.6.1.1 Pantothenate kinase (PanK; CoaA) as characterized from parasite lysates

PanK, expressed by *P. falciparum* (*Pf*PanK), is predicted to localize to the *P. falciparum* cytosol and has a significantly higher affinity for pantothenic acid compared to mammalian PanKs, with *Pf*PanK binding pantothenic acid with >10-fold higher affinity (based on $K_M$) compared to the mammalian PanKs described to date. This increase in affinity allows *Pf*PanK to trap pantothenic acid within the parasite cytosol in its phosphorylated form [27, 52]. Spry *et al*. [50] illustrated that although 4'-phoshopantothenic acid accumulates in *P. falciparum*-infected erythrocytes and isolated parasites, it does not accumulate in uninfected erythrocytes. This observation suggests 1) that the regulation of CoA biosynthesis by erythrocytes and *P. falciparum* is markedly different and 2) that unlike other organisms, the rate of pantothenic acid phosphorylation by *P. falciparum* does not determine the rate of CoA biosynthesis. However, PanK activity in *P. falciparum* lysates is inhibited by CoA with an $IC_{50}$ (the half maximal inhibitory concentration) of ~200 µM and is consequently not refractory to feedback inhibition (similar to what is shown for *Sa*PanK-II) [50].

Even though PanK activity has been observed in lysates for years, thus far no one has successfully overexpressed, purified and characterized the PanK enzyme from the organism or a heterologous expression system [27]. This lack of expression and purification could be attributable to the *P. falciparum* genome being adenine and thymine (AT)-rich, which requires the use of longer primers for polymerase chain reactions (PCR), while additionally exhibiting a codon bias with a heavy emphasis on AT-rich codons. Furthermore, *P. falciparum* proteins are often expressed in *E. coli* in insoluble inclusion bodies and it is not unusual for *P. falciparum* genes to contain start sites that are cryptic for *E. coli*, leading to the formation of numerous truncated products. Finally, there is also increasing evidence that *P. falciparum* proteins may bind the DNA and RNA which codes for them, thereby creating a regulatory mechanism which would impede attempts to overexpress the protein [53].

#### 1.6.1.2 Enzymes completing the CoA biosynthetic pathway (CoaBCDE)

Very limited information regarding the last four enzymes of the CoA biosynthetic pathway in *P. falciparum* is available. The genes predicted to code for the five enzymes share a sequence similarity with the genes coding for the human CoA biosynthetic enzymes; however, no soluble expression, purification and characterization has been achieved to date [27]. Spry *et al*. [50], however, have suggested that 4'-phosphopantothenoylcysteine synthetase (*P*PCS; CoaB), which catalyzes the condensation of L-cysteine to 4'-phosphopantothenic acid to form 4'-phospho-pantothenoylcysteine (Scheme 1.1, Step 2), is the rate-limiting step in *P. falciparum* CoA biosynthesis due to the accumulation of 4'-phosphopantothenic acid in the parasite. Previously, similar results were found in perfused rat hearts in which PanK was stimulated, but this was due to an insufficient supply of L-cysteine. Therefore, at this stage it still remains unclear whether the accumulation of 4'-phosphopantothenic acid in *P. falciparum* is due to a lack of available L-cysteine or whether it is due to regulation of *P*PCS [50].

From the predicted gene sequences phosphopantetheine adenylyltransferase (*P*PAT; CoaD) shows the lowest sequence similarity to its human counterpart. Interestingly, in *P. falciparum* it is predicted that separate genes code for *P*PAT and dephospho-CoA kinase (DPCK; CoaE) compared to the human genes that code for a bifunctional enzyme. It is predicted that enzymes two to four (i.e. *P*PCS, *P*PCDC and *P*PAT) are localized to the *P. falciparum* cytosol, while the fifth enzyme, DPCK, is localized to the apicoplast, a non-photosynthetic, relict plastid found in most apicomplexan parasites. The apicoplast is the site of fatty acid biosynthesis and the localization of DPCK to the apicoplast would allow for CoA biosynthesis to take place in the same organelle were the CoA-utilizing enzymes and ACPs are localized. This phenomenon has been reported previously for the human bifunctional *P*PAT/DPCK enzyme (also known as COASY or CoA synthase) that is localized to the mitochondrial outer membrane [27]. Furthermore, if DPCK is localized to the apicoplast, an uptake mechanism of dephospho-CoA by the apicoplast would be essential, since the other four enzymes are localized in the cytosol. Previous studies have hypothesized that intracellular pathogens such as *Chlamydia*, *Mycoplasma* and *Rickettsia*, which all appear to only possess a DPCK enzyme, also possess such a mechanism for dephospho-CoA uptake across the plasma membrane [27].

### 1.6.2 CoA utilization processes in metabolism

CoA serves as the primary acyl group carrier in metabolism, especially in processes involved in energy metabolism, such as fatty acid biosynthesis and degradation, as well as the citric acid cycle [42]. CoA metabolism in the *P. falciparum* parasite is greatly altered from CoA metabolism in their hosts. Generally, CoA is found as acetyl-CoA in organisms where it functions as a link between

glycolysis (which occurs in the cytosol) and the citric acid cycle (which occurs in the mitochondrion) by serving as the metabolite that initiates the citric acid cycle to produce ATP. However, current biochemical studies suggest that in *P. falciparum* glycolysis is the key pathway for ATP generation in intraerythrocytic parasites, even though the genes encoding the citric acid cycle enzymes and mitochondrial electron transport chain (ETC) complexes are present [54].

Furthermore, in most organisms succinyl-CoA (another vital CoA thioester) predominantly acts as a citric acid cycle intermediate; however, in *P. falciparum* it is also utilized for the *de novo* synthesis of heme (an important cofactor in parasite biology) and all the enzymes in the pathway have been characterized. In addition to *P. falciparum* having the ability to synthesize heme *de novo*, the intraerythrocytic parasites can also obtain heme from host hemoglobin if the heme biosynthetic pathway has been inactivated. However, for the survival of the mosquito as well as liver life stages of the parasite, *de novo* synthesis of heme (and thus the availability of succinyl-CoA) is an absolute necessity [55]. Additionally, *P. falciparum* parasites require a sufficient source of fatty acids for the synthesis of lipid species that are important for parasite membrane and lipid body biogenesis, as well as for glycosylphosphatidylinositol (GPI) moieties that serve to anchor parasite membrane proteins. Compared to uninfected erythrocytes, the fatty acid concentrations in infected erythrocytes are 6-fold higher [56]. Interestingly, Vaughan *et al*. [57] discovered that fatty acid biosynthesis is non-essential in blood stage parasites, since the deletion of *FabI* from *P. falciparum* has no apparent effect on blood stage replication when compared to wild type parasites. Consequently, *Plasmodium* fatty acid biosynthesis type II (FAS-II) takes place entirely during liver stage development, and fatty acid biosynthesis requires CoA to activate ACPs on which this process depends [56-57].

### 1.6.3 CoA biosynthesis and utilization as an antimalarial drug target

There are currently four potential drug targets in CoA metabolism in *P. falciparum* that are under investigation. The four potential targets in the CoA biosynthetic pathway that small molecule inhibitors can act upon are shown schematically in Figure 1.7. The first target entails the inhibition of pantothenic acid uptake (Figure 1.7, Target 1). *P. falciparum* acquires pantothenic acid using an $H^+$:pantothenic acid symport mechanism with a 1:1 stoichiometry as discussed earlier. Therefore, the transport of one $H^+$ is coupled to the transport of one pantothenic acid molecule down an electrochemical gradient. Since no candidate genes for the biosynthetic pathway of pantothenic acid have been identified in the parasite's genome thus far, this uptake mechanism is the only source of pantothenic acid available to the parasite [27]. Saliba *et al*. [58] have demonstrated that the provitamin pantothenol interferes with the uptake of pantothenic acid when they studied this uptake mechanism in *P. falciparum* infected erythrocytes and in parasites isolated from their host

cells. Although it remains unclear whether pantothenol gains access into infected erythrocytes via the NPPs in a similar fashion to that of pantothenic acid, or whether it gains access through an alternative mechanism, it is evident that pantothenic acid analogues have some potential to interfere with the uptake of pantothenic acid and therefore propose pantothenic acid uptake as a viable drug target [46, 58].

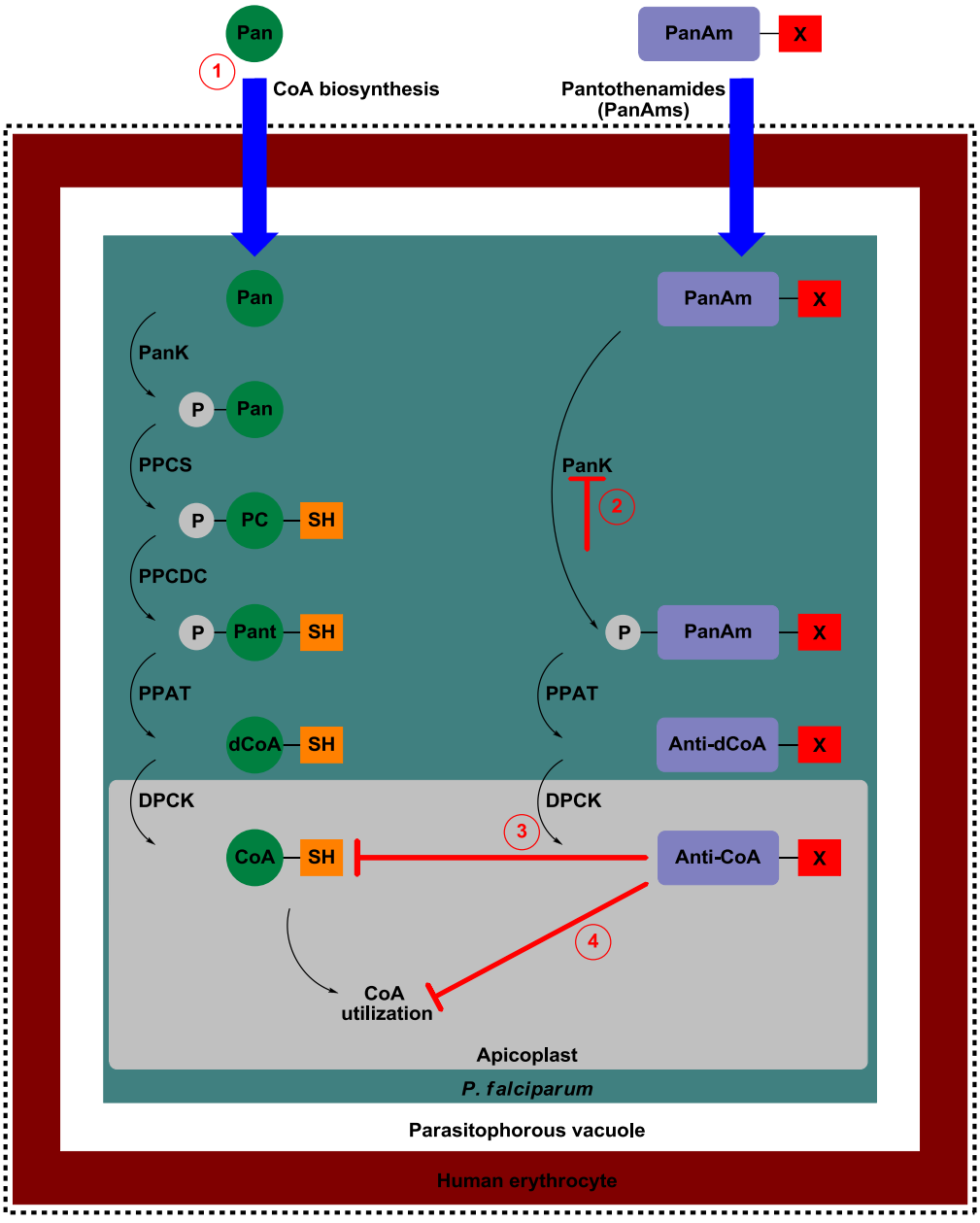


**Figure 1.7. The biosynthesis of CoA (left) proceeds via a universal five step pathway catalyzed by PanK, *P*PCS, *P*PCDC, *P*PAT and DPCK. There are four major biological targets for inhibitors in the CoA biosynthetic pathway of *P. falciparum*: 1) Pantothenic acid uptake 2) PanK, as the first CoA biosynthetic enzyme, 3) CoA-dependent enzymes, after its transformation into antimetabolites, and 4) fatty acid biosynthesis, when an anti-CoA serves as substrate for ACP synthase in its activation of *apo*-ACP.**

The second target identified is CoA biosynthesis, with the first step in the pathway (i.e. phosphorylation of pantothenic acid by PanK) as the specific target (Figure 1.7, Target 2). Previous studies have illustrated that *P. falciparum* has the ability to biosynthesize its own CoA, and it is therefore not dependent on the host for its CoA needs; this makes selective inhibition of *Pf*PanK a desirable target. Even though the *Pf*PanK enzyme has not been successfully overexpressed and purified from the organism or from a heterologous expression system, studies have investigated the catalytic effect of *Pf*PanK present in *P. falciparum* lysates [27]. These studies determined that *Pf*PanK has an extremely high affinity for pantothenic acid ($K_M$ = 0.3 µM) [52], compared to three human isoforms hPanK1β, hPanK2 and hPanK3 with $K_M$ values of 5.7 µM, 25.4 µM and 9.5 µM, respectively [59]. Additionally, Spry *et al*. [60] demonstrated that a group of pantothenic acid analogues inhibited the phosphorylation of pantothenic acid by *Pf*PanK in a competitive manner with $K_i$ values (the dissociation constant for the inhibitor) in the nanomolar range. Recently, a study showed that CoA biosynthesis can be targeted by a chemically diverse set of inhibitors that do not resemble pantothenic acid; these compounds' $IC_{50}$s ranged between 120 nM and 6 µM against blood-stage parasites [61]. Collectively, these facts suggest that *Pf*PanK might be an attractive antiplasmodial target.

The third possible target is CoA utilization (Figure 1.7, Target 3). Compounds with this mode of action are usually pantothenic acid analogues that act as substrates for PanK and can possibly be processed downstream in the pathway to the corresponding CoA antimetabolites. Since the terminal sulfhydryl group has been replaced by inactive moieties in these antimetabolites, this will adversely affect all CoA-dependent processes. One of these is fatty acid biosynthesis (the fourth possible target), which is dependent on ACPs for acquiring their phosphopantetheine prosthetic groups from CoA. If CoA is replaced by antimetabolites, it will lead to the synthesis of inactive ACPs, thereby blocking fatty acid biosynthesis (Figure 1.7, Target 4) [44-45]. According to Prigge *et al.* [62], the *P. falciparum* genome appears to encode an ACP synthase enzyme that has a 29% sequence homology with the ACP synthase found in *E. coli*. Although it is known that *E. coli* ACP synthase has the ability to transfer inactive moieties to ACP, the products of which then function as inhibitors of FAS-II, it remains to be determined whether *P. falciparum* ACP synthase also shows the same relaxed substrate specificity function. Given that there is a vast difference between human ACPs and *Plasmodium* ACPs, there might be definite selectivity for *Plasmodium* ACPs by pantothenic acid analogues. However, this hypothesis remains to be corroborated by experimental evidence.

Most malaria research thus far has focused on the blood-stage of the parasite, given that it is this stage that causes the characteristic symptoms of the disease [63]. As a result, most of the

antibiotic drugs that are currently being used to treat malaria target the blood-stage of the parasite [64]. However, a previous study has determined that fatty acid biosynthesis is non-essential in blood stage parasites and FAS-II takes place entirely during liver stage development [57]. Therefore, fatty acid biosynthesis is an attractive target for antimalarial drug design, given that this will target the liver stage of the parasite. Consequently, inhibition of progression through the liver stage of the parasite would prevent onset of the blood-stage of the disease, including the characteristic symptoms of the disease.

## 1.7 Pantothenic acid analogues as potential small molecule inhibitors

In recent years, many compounds based on the structure of pantothenic acid have been synthesized and tested for their antimicrobial activity against various organisms. A detailed review of the various compounds tested since 1940 was published by Spry *et al*. [27]. The antimicrobial activity of these pantothenic acid analogues varied considerably, with some analogues possessing growth-promoting activity for organisms that need an exogenous supply of pantothenic acid, some analogues not showing any antimicrobial activity, and finally, some that antagonized the growth promoting activity of pantothenic acid [27].

Consequently, pantothenic acid analogues can be used to influence all four CoA-based drug targets: 1) by either competing with or inhibiting pantothenic acid transport, 2) by either competing with pantothenic acid for PanK activity or by inhibiting the enzyme itself, 3) by acting as a substrate for PanK leading to the formation of downstream CoA antimetabolites or 4) by inhibiting fatty acid biosynthesis since CoA is replaced by antimetabolites which will lead to the synthesis of inactive ACPs due to the lack of the terminal sulfhydryl group needed for fatty acid biosynthesis. However, pantothenic acid uptake is not regarded as a feasible target, since many organisms can synthesize pantothenic acid *de novo*, in addition to being able to transport pantothenic acid into the cell [44-46].

Although CoA analogues have been widely used as inhibitors of enzymatic activity or as mechanistic probes, they cannot be transported across the cell membrane. As a result, inhibition can only occur if a pantothenic acid analogue with good cell permeability and PanK activity is applied [65]. This redirects the attention back to PanK as a drug target. Consequently, the development of pantothenic acid analogues that inhibit PanK activity completely or analogues that compete with pantothenic acid for PanK activity to have an effect downstream is vital. Given that this study will focus on *S. aureus* and *P. falciparum*, only pantothenic acid analogues that are relevant as antimicrobial agents in respect to these two organisms will be discussed.

## 1.7.1 Pantothenic acid analogues tested on *S. aureus*

### 1.7.1.1 Overview of pantothenic acid analogues tested on *S. aureus*

Various compounds based on pantothenic acid have been designed, synthesized and tested as inhibitors of the CoA biosynthetic pathway in several bacteria (including *S. aureus*) since 1940; these were summarized by Spry *et al*. in a review in 2008 [27]. Similar to the *de novo* biosynthesis of pantothenic acid by bacteria via the condensation of pantoic acid and β-alanine (Scheme 1.3, pathway on the left) [27], pantothenic acid can be synthesized chemically through the condensation of β-alanine with (*R*)-(-)-pantolactone instead of pantoic acid (Scheme 1.3, pathway on the right).

Since the structural determination of pantothenic acid in 1940 [27], various analogues of it have been synthesized. These include pantoyltaurine-related compounds, *N*-pantoyl-substituted amines, pantoylhydrazide- and pantothenone-related compounds, as well as analogues of pantothenic acid with a modified pantoyl moiety, all of which were prepared in an attempt to generate analogues with an activity similar to that of pantothenic acid [27, 66-67]. In general, the pantothenic acid analogues with the best antimicrobial activity were those in which the pantoyl moiety remained unmodified, while modifying the β-alanine moiety. Examples of these compounds include pantoyltauramide, pantoyltaurine (Scheme 1.6) and α-methyl pantothenic acid [66, 68]. However, most of these studies only reported antimicrobial action of these compounds on whole organisms, and therefore their mechanism of action still remains uncertain [27].

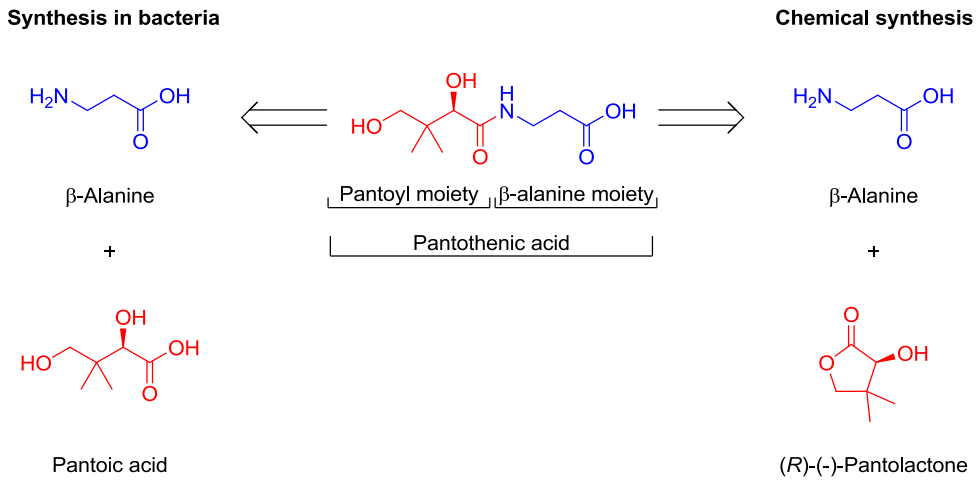


**Scheme 1.3. Synthesis of pantothenic acid using the two moieties, pantoyl (red) and β-alanine (blue). (Left) Pantothenic acid is synthesized *de novo* in bacteria by condensing β-alanine (blue) and pantoic acid (red). (Right) Chemical synthesis of pantothenic acid by condensing β-alanine (blue) with (*R*)-(-)-pantolactone (red).**

### 1.7.1.2 *N*-substituted pantothenamides tested on *S. aureus*.

Another group of potential small molecule inhibitors that have been investigated since 1970, with a similar backbone to pantothenic acid, is the *N*-substituted pantothenamides (referred to as pantothenamides from here on). These analogues are structurally different from pantothenic acid by having a secondary or tertiary amide instead of the carboxylic acid moiety (Scheme 1.4A). They are synthesized by condensing either a primary or secondary amine to the carboxylic acid of pantothenic acid to form a new secondary or tertiary amide bond (Scheme 1.4B) [27, 32]. Seeing as the carboxylic acid moiety has been replaced with a secondary or tertiary amide, these pantothenamides do not have the ability to accept L-cysteine in the condensation reaction catalyzed by *P*PCS to form a pantetheine analogue with a sulfhydryl moiety (Scheme 1.1, Step 2). Pantothenamides have been shown to act as inhibitors of *E. coli*, *S. aureus*, *Lactobacillus arabinosus* and *Lactobacillus casei* to name but a few [27, 69]. Furthermore, pantothenamides act as inhibitors (or alternative substrates) of type I and type II PanKs; however, type III PanKs are refractory to inhibition by pantothenamides due to the fully enclosed pantothenic acid binding pocket of PanK-III. In addition, the pantothenic acid binding pocket is situated above the ATP-binding cleft and is only accessible by passing through the ATP binding site [59].

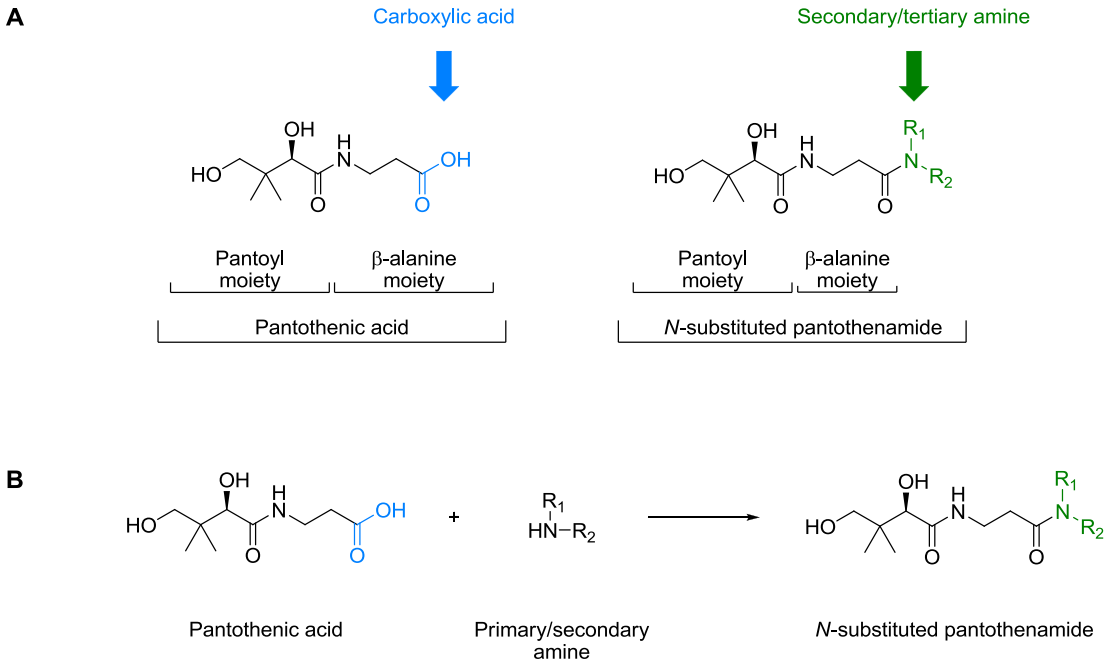


**Scheme 1.4. (A) Structural differences between pantothenic acid and *N*-substituted pantothenamides. (B) General illustration of the preparation of pantothenamides by condensing a primary or secondary amine to the carboxylic acid of pantothenic acid to form a new secondary or tertiary amide bond.**

Previous studies investigated numerous types of pantothenamides (Scheme 1.5) on *S. aureus*, which included linear and branched alkyl substitutions as well as various aromatic and polar substituents. Virga *et al*. [12], tested a series of pantothenamides against *Sa*PanK-II and found that molecules with linear alkyl tails, as well as linear alkyl tails with polar substituents displayed the highest percentage inhibition of the enzyme's pantothenic acid phosphorylation activity. However, when these pantothenamides where tested against *S. aureus* in whole cell inhibition studies, only the pantothenamides with linear alkyl substitutions showed inhibition. This was unexpected, since both groups displayed inhibition of the enzyme. Further experiments suggested that the introduction of a polar atom into the linear alkyl chain must prevent the uptake of such pantothenamides into the cell. The compounds that showed the most potent inhibition of *S. aureus* and *Sa*PanK-II were N5-Pan and N7-Pan; indicated in the blue box in Scheme 1.5. These results indicated that linear alkyl substitutions have a higher inhibitory effect than aromatic or polar substituents [12, 29]. Additionally, N7-Pan and *N*-nonyl pantothenamide (N9-Pan) were tested for their cytotoxicity potential against human HepG2 liver cells and it was found that neither compound strongly inhibited the growth of human hepatocytes (the lowest concentrations causing ≥50% reduction in cell viability were 64 and 128 µg/mL, respectively), suggesting that pantothenamides are viable leads for developing selective antimicrobial agents [30].

The inhibition of *Sa*PanK-II by these pantothenamides can be explained using the four available enzyme crystal structures (PDB codes: 2EWS, 4M7Y, 4M7X and 4NB4). All of these structures either have ADP or a non-hydrolyzable ATP analogue bound to the active site of the enzyme. The pantothenic acid binding pocket is completely exposed to the solvent when no other substrate apart from ADP or the non-hydrolyzable ATP analogue is bound to the active site. This would thus create space for the extended pantothenic acid analogues to bind in the active site pocket [32]. The crystal structures show that when the pantothenamides (i.e. N5-Pan, N7-Pan and N-[2-(1,3-benzodioxol-5-yl)-ethyl] pantothenamide (N354-Pan) [37]) bind to the active site, a conformational change occurs and the active site gets closed off from the surrounding solvent. This closed conformation is predicted to be the active form of the enzyme; however, since there is no crystal structure available with pantothenic acid bound in the active site, this still needs to be confirmed.

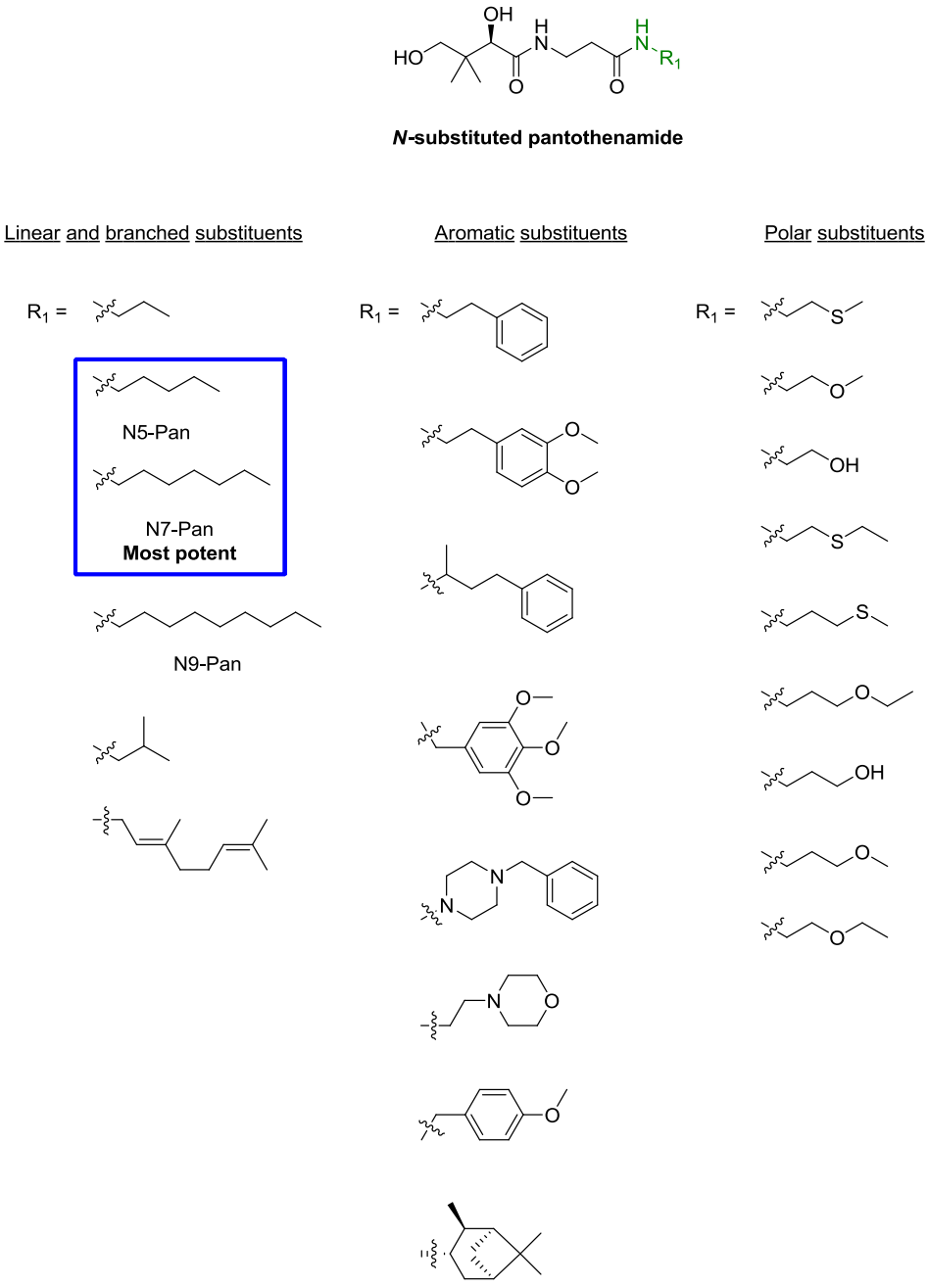


**Scheme 1.5. Various amide functional groups that have been used as pantothenic acid analogues in previous studies against *Sa*PanK-II and *S. aureus* [12]. N5-Pan and N7-Pan (indicated in the blue box) are the most potent inhibitors of *S. aureus* and *Sa*PanK-II.**

Given that pantothenamides could potentially have a similar binding mode to pantothenic acid, they could either act as competitive inhibitors of the enzyme (i.e. acting on Target 2 in Figure 1.6), or as alternative substrates. In the latter case, they will be phosphorylated by *Sa*PanK-II and subsequently be converted into CoA antimetabolites and inactive ACPs (i.e. act on Targets 3 and 4 in Figure 1.6) [44-46]. This has resulted in uncertainty about the exact mode of action of these

compounds in *S. aureus* – an uncertainty which is reflected in the current literature. For example, Leonardi *et al*. [29], discovered that pantothenamides (specifically N7-Pan) are converted into CoA antimetabolites in *S. aureus* (i.e. N7-Pan acts as a substrate for *Sa*PanK-II), followed by the biosynthesis of inactive downstream products (such as inactive ACPs) in intact cells through radioactive labelled compounds. On the other hand, findings by Choudhry *et al*. [30] suggested that these compounds are inhibitors of the *Sa*PanK-II enzyme itself and that it does not act as a substrate for *Sa*PanK-II. However, it is also possible that the direct spectrophotometric assay used by Choudhry *et al*. was not sensitive enough to detect phosphorylation of the pantothenamides; these authors also did not examine the metabolism of pantothenamides in intact cells [29].

Taken together, these studies illustrate that pantothenamides are excellent potential small molecule inhibitors of *S. aureus*, with low cytotoxicity towards human HepG2 liver cells; however, our poor understanding of their exact mechanism of action has hampered their development as clinically relevant agents.

## 1.7.2 Pantothenic acid analogues tested on *Plasmodium*

### 1.7.2.1 Overview of pantothenic acid analogues tested on *Plasmodium*

Since Trager illustrated in 1943 that pantothenic acid is a prerequisite for the survival of *Plasmodium lophurae* parasites in infected erythrocytes, the pursuit of pantothenic acid analogues as feasible leads for the development of antimalarials became possible [70]. Given that pantoyltaurine and pantoyltauramide (Scheme1.6) previously showed antibacterial activity towards bacteria that also require pantothenic acid for survival, these two pantothenic acid analogues were tested first for antimalarial activity. Pantoyltaurine and pantoyltauramide, together with several other *N*-substituted pantoyltauramides, were screened first against avian malaria infected ducks, canaries and chickens, because the procedures for *in vitro* cultivation of *P. falciparum* parasites were not yet established. These compounds were found to be inactive against *P. lophurae*-infected ducks, *Plasmodium gallinaceum*-infected chickens and *Plasmodium relictum*-infected canaries when included into their diets; however, pantoyltauramide showed some activity against *P. gallinaceum*-infected chickens when it was administered intravenously. This antimalarial activity was antagonized when pantothenic acid was co-administered with pantoyltauramide, which suggested that the antimalarial activity of pantoyltauramide is as a result of inhibition of pantothenic acid utilization [27].

Another series of *N*-substituted pantoyltauramides (Scheme1.6) were synthesized by Winterbottom *et al*. [71], in 1947 in an attempt to increase their absorption and excretion characteristics relative to pantoyltaurine. These compounds were found to be more active when included into the diets of

*P. gallinaceum*-infected chickens. Indeed, some of the compounds tested showed similar or increased activity towards *P. gallinaceum*-infected chickens compared to the standard antimalarial, quinine. The most active compound was four times and sixteen times more potent than quinine when tested against a standardized, blood induced infection of *P. gallinaceum*, in which peak parasitaemia was reached four days postinfection and seven days postinfection, respectively. Furthermore, a variety of pantothenone analogues (Scheme 1.6) were also tested against various *Plasmodium* parasites; some of the compounds showed good antiplasmodial activity and the activity was antagonized upon the addition of pantothenic acid [27].

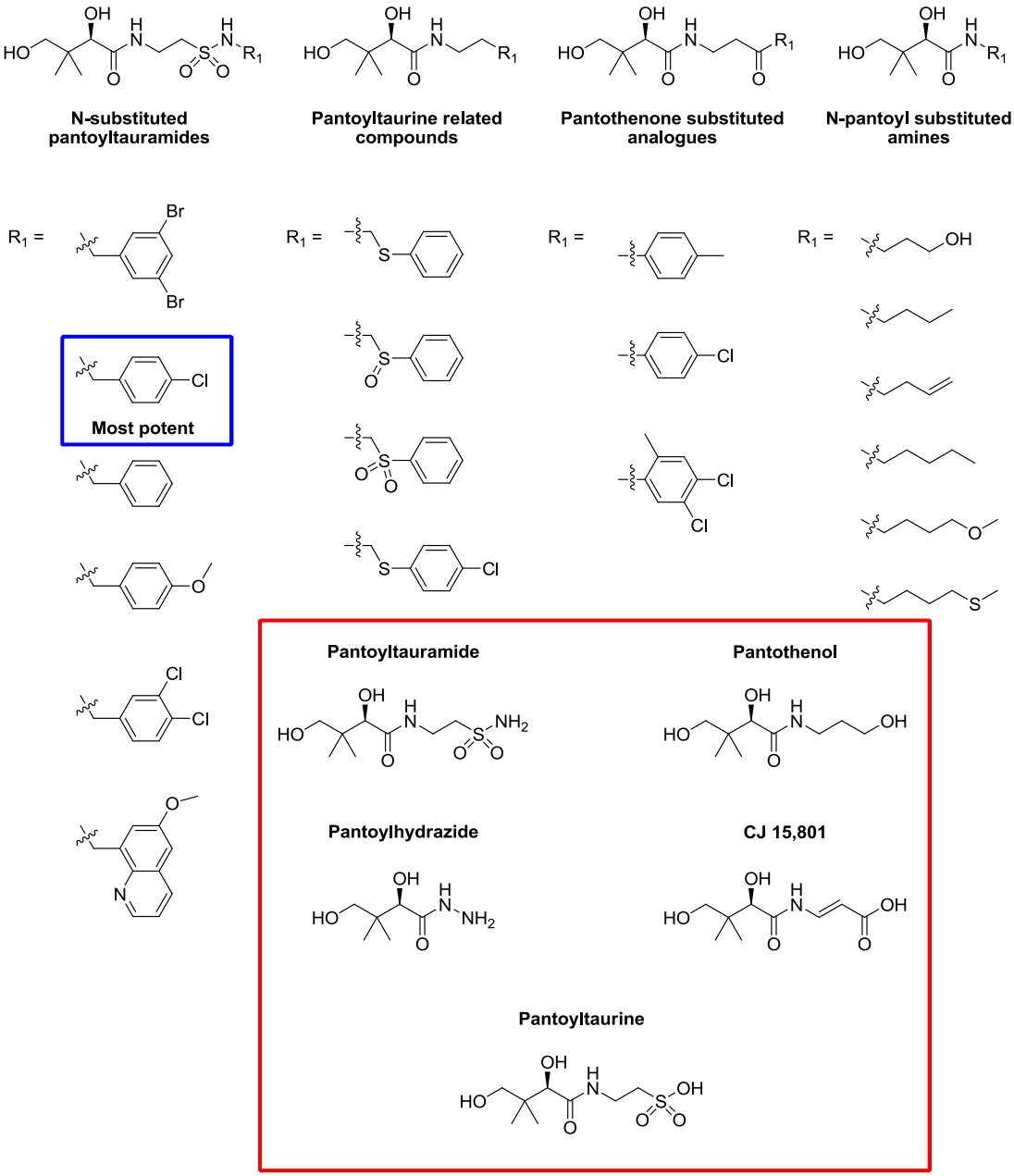


**Scheme 1.6. Various pantothenic acid analogues tested against a variety of *Plasmodium* species *in vivo*.**

After the procedure to cultivate blood-stage *Plasmodium* parasites *in vitro* was established, numerous studies were carried out with the same compounds to test their *in vitro* antiplasmodial activity and the results obtained were similar to that of the previous *in vivo* results. The most potent inhibitor, *p*-chloro-benzyl pantoyltauramide, indicated in the *N*-substituted pantoyltauramide series (Scheme 1.6, blue box), was also tested against *P. falciparum.* This inhibitor showed increased antiplasmodial activity compared to what was seen in ducks. Various other analogues such as *N*-aryl substituted and halogenated phenyl-substituted pantoyltauramides were also tested against a variety of *Plasmodium* parasites, with some promise of antimicrobial activity [27].

More recently, Saliba *et al*. [58, 72] showed that *P. falciparum* is also inhibited by pantothenol (Scheme 1.6, indicated in the red box), which is the provitamin form of pantothenic acid, through a mechanism that involved competition with pantothenic acid. The $H^+$-coupled transport of pantothenic acid across the parasite plasma membrane was not inhibited by pantothenol; instead pantothenol inhibited the phosphorylation of pantothenic acid by *Pf*PanK. However, it is still unclear whether pantothenol actually undergoes phosphorylation and whether this is the only site of action within the parasite [58]. Another example of a pantothenic acid analogue that acts as an inhibitor of *P. falciparum* is CJ-15,801 (Scheme 1.6, indicated in the red box), which is a fungal natural product isolated from *Seimatosporium sp*. CL28611 [72]. CJ-15,801 exerts its antiplasmodial activity on the parasite via competitive inhibition of pantothenic acid metabolism (inhibiting the utilization of pantothenic acid), given that the antiplasmodial activity is completely antagonized by the addition of extracellular pantothenic acid [72]. Various other compounds based on the pantothenol structure (referred to as *N*-pantoyl substituted amines; Scheme 1.6) have shown antiplasmodial activity towards *P. falciparum* in a similar manner to pantothenol. The *in vitro* antiplasmodial activity of these compounds ranged between 10–200 µM, which suggests that these compounds could translate into potent inhibitors of *P. falciparum* [27, 58, 60, 72].

#### 1.7.2.2 *N*-substituted pantothenamides tested on *P. falciparum*

The discovery of the *in vitro* antiplasmodial activity of pantothenol and CJ 15,801 in 2005 by Saliba *et al.* [58, 72], lead to an increased interest in targeting CoA metabolism in *P. falciparum* with pantothenic acid analogues [58, 72]. Although pantothenamides have been investigated as possible inhibitors of bacteria since 1970, the first pantothenamides tested for antiplasmodial activity against *P. falciparum in vitro* was only completed in 2013 [73-74]. The two pantothenamide libraries that were tested included a range of amines that represented four chemical motifs, i.e. primary alkyl amines, primary aliphatic amines containing heteroatom substituents, secondary cyclic amines, and primary amines containing aromatic substituents (some of the pantothenamides tested are shown in Scheme 1.7). Both of the pantothenamide libraries were tested for inhibition of

the proliferation of *P. falciparum* (3D7 strain). Surprisingly, none of the pantothenamides tested showed antiplasmodial activity at a clinically relevant concentration, with most of the compounds having an $IC_{50}$ >200 µM; the best hit compound was *N*-phenethyl pantothenamide (*N*-PE-PanAm) (indicated in the blue box) with an $IC_{50}$ of 53 ± 11 µM [46, 73-74].

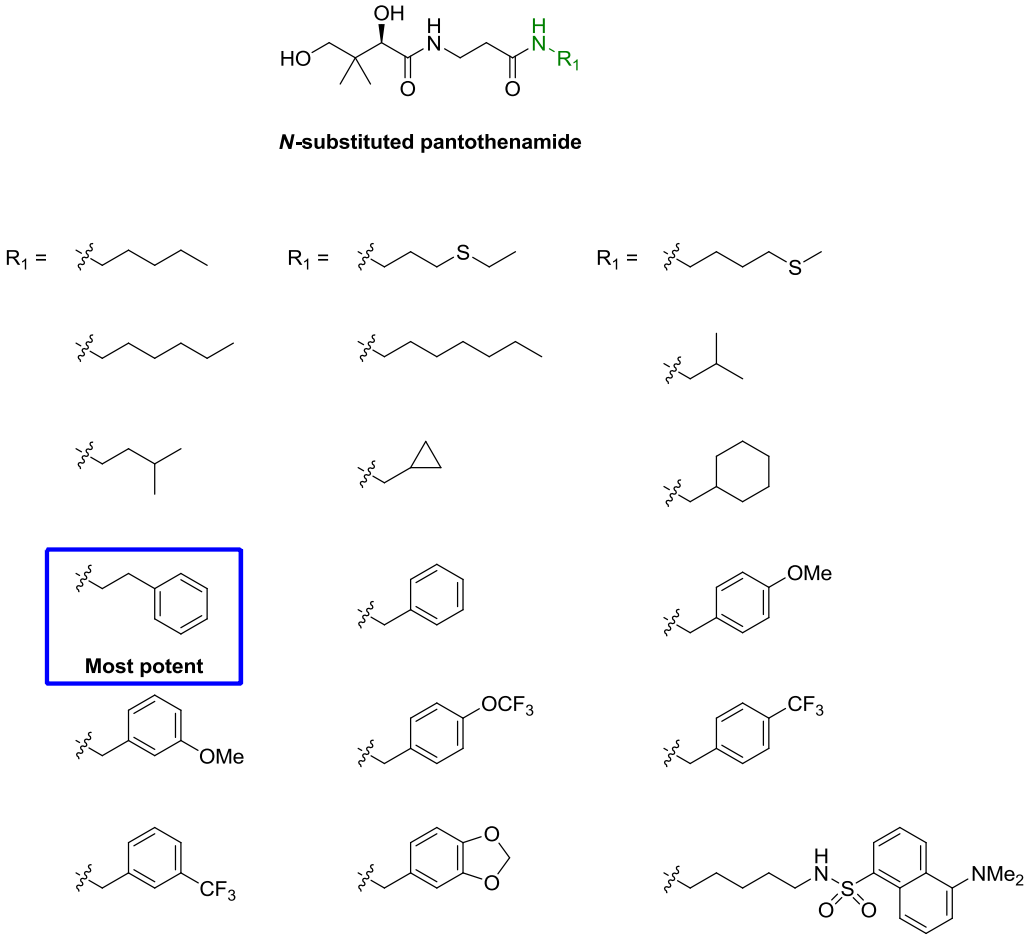


**Scheme 1.7. Various pantothenamides tested against *P. falciparum*. *N*-phenethyl pantothenamide (indicated in the blue box) was the most potent inhibitor.**

## 1.8 *N*-substituted pantothenamides are susceptible to enzyme-mediated hydrolysis

Inhibitor tests done with both N5-Pan and N7-Pan to determine the inhibitor activity against *Sa*PanK-II gave $K_i$-values in the nanomolar range in the *in vitro* studies, but the promising antimicrobial activity is lost when such tests are performed *in vivo.* A possible explanation for this loss of antimicrobial activity was uncovered in December 2011 when a patent application was published by Jansen *et al*. [75], regarding the antimicrobial activity of pantothenamides. They discovered that in 1% tryptone medium N5-Pan acted as an antimicrobial agent, but with the

addition of 10% serum or plasma, its antimicrobial activity was completely eradicated. Subsequently, they proposed that this effect might be due to enzymatic degradation of one specific amide bond (indicated in red in Scheme 1.8) in the pantothenamides by pantetheinase enzymes; this would lead to the formation of pantothenic acid and the corresponding amine (Scheme 1.8). Such a degradation pathway would account for the observed loss of antimicrobial activity [75].

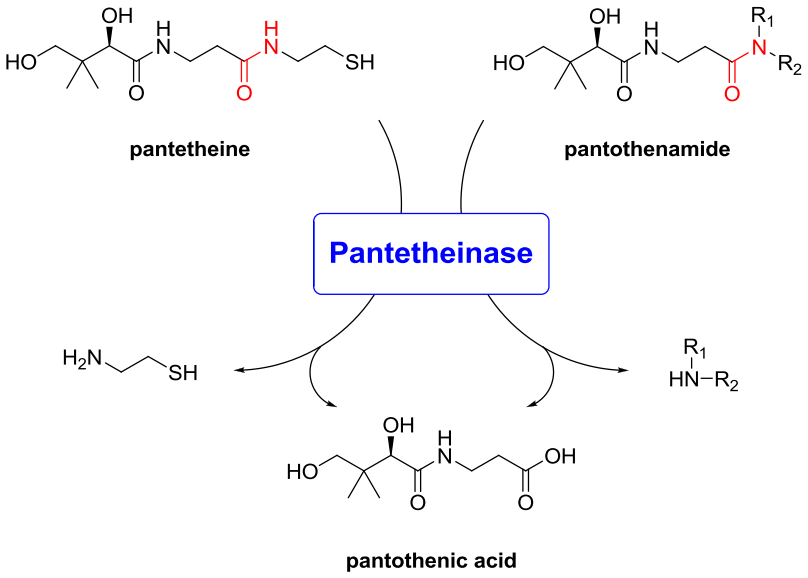


**Scheme 1.8. Pantothenamide degradation by the enzyme pantetheinase. (Left) The native function of pantetheinase is to catalyze the hydrolysis of the CoA metabolite pantetheine (PantSH) to pantothenic acid and cysteamine. (Right) The scissile amide bond (indicated in red) of pantothenamides is susceptible to degradation by pantetheinase.**

Jansen *et al*. [76] also tested this hypothesis against *P. falciparum*. Although N5-Pan and N7-Pan act as potent inhibitors of bacteria *in vitro*, these pantothenamides are not known to have activity against *P. falciparum* parasites [27]. N5-Pan is a poor inhibitor of *P. falciparum* growth *in vitro* and only achieves >90% inhibition at a concentration of 1 mM, which is clinically irrelevant [76]. Since *P. falciparum* parasites are cultured with human serum, it was hypothesized that the pantothenamides are also degraded by pantetheinases present in the serum, thereby reducing its potency. Indeed, when N5-Pan was tested against *P. falciparum* parasites in the presence of an inhibitor of pantetheinase activity, the antimalarial activity of N5-Pan was maintained, with an increase in anti-parasite potency ($IC_{90}$) by a factor of 200 compared to N5-Pan alone [76].

Furthermore, Spry *et al*. [73] found that if pantothenamides are tested as inhibitors of the *P. falciparum* parasite in aged media, i.e. media in which the pantetheinases present in the commonly used serum substitute Albumax were deactivated through pre-incubation at 37°C, the potency of

the pantothenamides tested were enhanced. Even pantothenamides that previously showed no inhibition in freshly prepared medium (i.e. with the pantetheinase activity intact), displayed inhibition of parasite growth at sub-micromolar concentrations in aged (pre-incubated) media [73].

Pantetheinases are encoded by the Vanin gene family (that forms part of the nitrilase superfamily), of which three human genes (VNN1, VNN2 and VNN3), two murine genes (Vanin-1 and Vanin-2) and one homologue in *Drosophila* are known [77-78]. Pantetheinase, also known as pantetheine hydrolyse, plays a major role in recycling CoA by catalyzing the hydrolysis of one specific amide linkage in PantSH (Scheme 1.9) via an invariant Glu-Lys-Cys catalytic triad to yield pantothenic acid (for reuse in CoA biosynthesis) and the small aminothiol cysteamine (β-mercaptoethylamine), a powerful antioxidant [79-81]. Numerous studies have provided evidence that suggests that the oxidative state of a cell is regulated by cysteamine [78-79, 82]. Cysteamine controls cellular levels of glutathione, interacts with cysteines, reduces peroxides and inhibits various enzymes, including transglutaminases. It has also been shown that both, cysteamine and cystamine (the disulphide of cysteamine) are cytoprotective and may also remove toxic, reactive aldehyde species [81]. Moreover, recent findings were put forward that Vanin does not only play a role in oxidative stress, but also in cell migration, inflammation and diseases such as cardiovascular disease, although their exact roles have not yet been identified [78-79, 83]. From a substrate recognition perspective, pantetheinase is extremely selective for compounds containing the pantothenate moiety, while the nature of the amide substituent is not as relevant and can be modified to a range of different functional groups [77, 79-80].

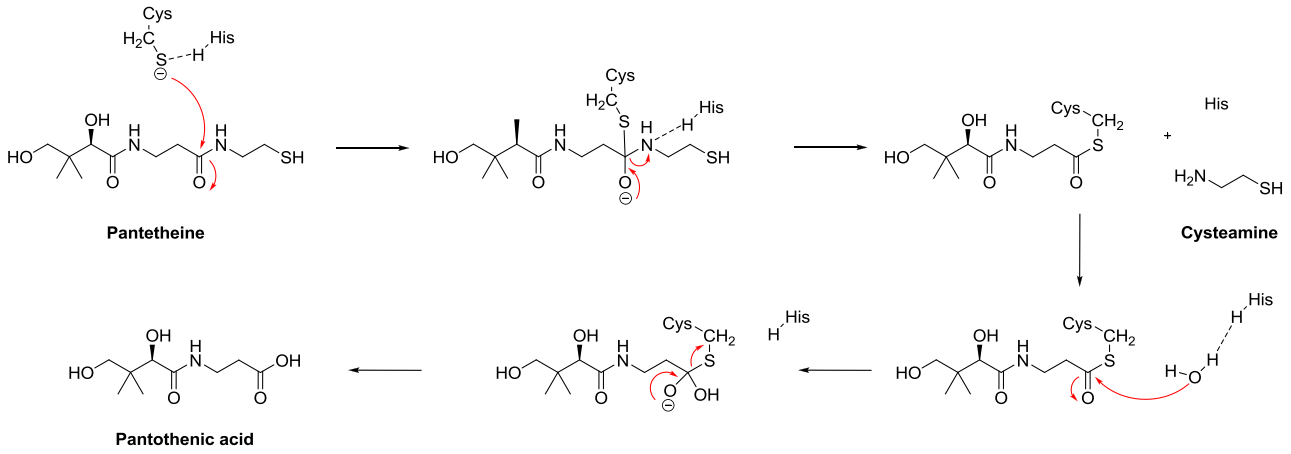


**Scheme 1.9. Mechanism for the hydrolysis of pantetheine (PantSH) as catalyzed by pantetheinase to produce pantothenic acid (for recycling to CoA biosynthesis) and the small aminothiol cysteamine (a powerful antioxidant).**

In the patent application mentioned above, the authors also investigated whether inhibition of pantetheinase activity might possibly keep the antimicrobial activity of pantothenamides intact, since inhibition of pantetheinase eliminates the potential hydrolysis of these compounds. They found that by inhibiting pantetheinase activity (through combination with an inhibitory PantSH analogue), breakdown of pantothenamides were prevented and their antimicrobial activity were preserved. Therefore, Jansen *et al*. suggested the use of a combination of an antimicrobial pantothenamide with an inhibitor of host panthetheinase as a strategy for the development of new antimalarials [75].

Since such a strategy would involve the separate optimization of the properties of two compound sets that may lead to other complications, de Villiers *et al*. [74] instead decided to modify the pantothenamides in such a way that they are resistant to pantetheinase-mediated degradation, while maintaining their antiplasmodial potency. This modification was achieved by displacing the amide bond that is normally cleaved by pantetheinase by exchanging the β-alanine moiety of the pantothenamides with either a glycine (to give α-pantothenamides) or a γ-aminobutyric acid (to give homopantothenamides) moiety (Figure 1.8). First, they tested to see if these modifications made the pantothenamides more resistant to hydrolysis by performing *in vitro* pantetheinase assays. They found that the modified analogues experienced only 5–15% hydrolysis in 24h, in comparison to pantothenamides that contained the normal β-alanine moiety which were hydrolyzed completely within this time-frame. Furthermore, they also determined that these modified pantothenamides have increased antiplasmodial potency when growth assays were conducted with ring-stage *P. falciparum* parasites. These results confirm that the degradation of pantothenamides by pantetheinase can be prevented by the modification of their structures [74].

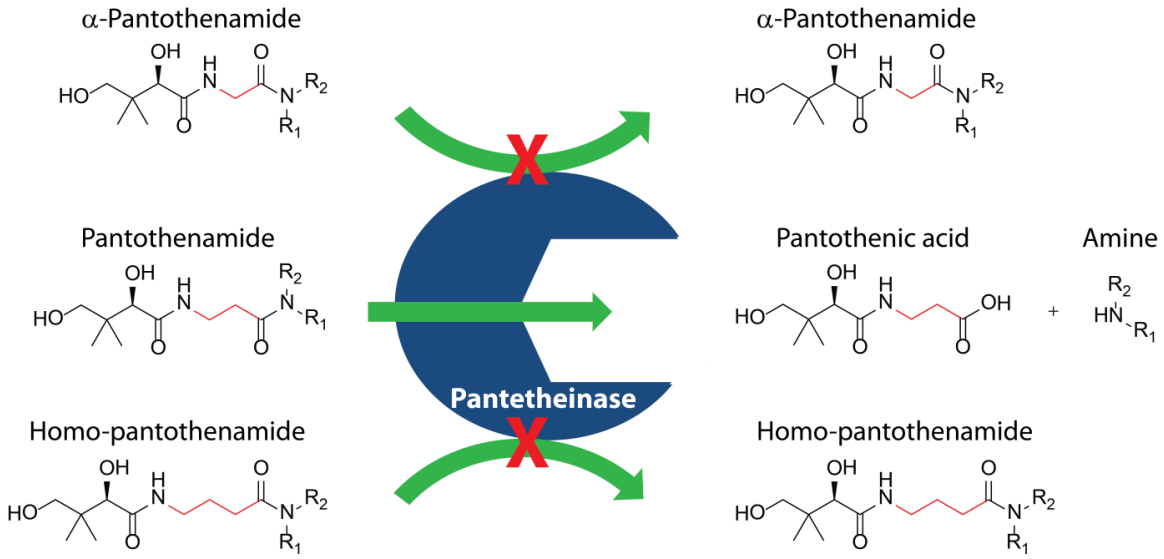


**Figure 1.8. Displacement of the scissile amide bond of pantothenamides leads to increased pantetheinase resistance. α-Pantothenamides have the β-alanine moiety of pantothenamides replaced with glycine and homo-pantothenamides have it replaced with γ-aminobutyric acid. These moieties are indicated in red.**

## 1.9 Problem statement

Our current knowledge was reviewed in the previous sections to serve as background to highlight the two main objectives of this study:

*i)* To elucidate the role of PanK in the mode of action of inhibitory pantothenamides in *S. aureus.*

ii) To develop inhibitors that are resistant to pantetheinase-mediated degradation while retaining good antimicrobial activity.

### i) Mode of action of the pantothenamides in *S. aureus*

The first part of this project builds upon previous studies of the pantothenamides performed in our research group. In these studies, a method was developed to synthesize a library of pantothenamides, which were then screened against various organisms for growth inhibitory potential, including *S. aureus* [46, 84]. While selected compounds were also characterized through various *in vitro* assays [46], their exact mode of action still had not been determined. Since the previous studies showed that *S. aureus* is only inhibited by pantothenamides that retained the β-alanine moiety (i.e. was highly selective), this suggested a role for PanK (the first point where selectivity can be exerted) in the mode of action of these compounds. Therefore, the first goal of this study was to elucidate the role of PanK in the mode of action of inhibitory pantothenamides in *S. aureus*.

Two mechanisms of action have been proposed for pantothenamide-mediated inhibition, with PanK playing a central role in both: 1) Inhibition based on the pantothenamides inhibiting PanK activity directly (Target 2 in Figure 1.6), and 2) metabolic activation of the molecules by PanK (i.e. by them acting as alternative substrates of PanK), followed by their conversion to CoA antimetabolites for subsequent inhibition of the ACPs and/or other CoA-dependent processes (Targets 3 and 4 in Figure 1.6).

Consequently, these two mechanisms can be distinguished based on the nature of the interaction of the pantothenamides with PanK, i.e. as inhibitors, or as alternative substrates. Such a distinction would shed light on the mode of action of the pantothenamides in a particular organism. This distinction can be achieved by means of detailed kinetic analyses of *Sa*PanK-II's activity towards the various compounds in comparison to its native substrate, and by testing the growth inhibition of a pantothenamide analogue in which the terminal hydroxyl has been removed (Figure 1.9). Such an analogue cannot act as a PanK substrate and be phosphorylated; consequently, it can only act as an inhibitor of PanK.

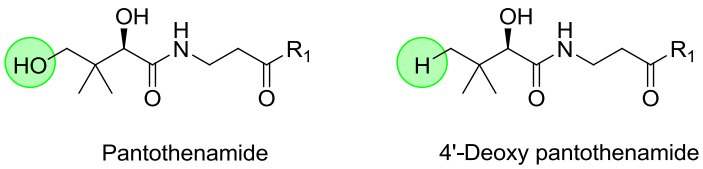


**Figure 1.9. Pantothenamides. (Left) Pantothenamide with the 4'-hydroxyl-group. (Right) Pantothenamide in which the 4'-hydroxyl is removed (4'-deoxy-pantothenamide).**

In Chapter 2 our findings towards answering this research question is presented in the form of a published article [47] of which I am co-first author, followed by additional supporting experiments which were not included in the publication.

### ii) Developing antimicrobial pantothenamides that are resistant to pantetheinase-mediated degradation

The discovery by Jansen *et al*. [75] that pantothenamides lost their *in vivo* antimicrobial activity due to degradation by pantetheinase, an enzyme found in plasma and serum, indicated that the inhibitors could retain their potency if the pantetheinase activity was inhibited. This was confirmed by experiments in which pantetheinase inhibitors were used in combination with pantothenamides. Under these conditions the breakdown of the pantothenamides was prevented and their antimicrobial activity was preserved [75, 85]. However, the pantetheinase inhibitors used in these

proof of concept studies are not suited for medicinal use due to poor selectivity for microbial versus host targets.

The second goal of this study was therefore to develop PanK inhibitors that are also resistant to pantetheinase-mediated degradation. In view of the fact that de Villiers *et al*. [74], already established that a modification to the β-alanine moiety of pantothenamides prevented it from being hydrolyzed by pantetheinase, we decided to further expand on this strategy. The proposal in this regard was to protect the pantothenamide scissile amide bond from hydrolysis by either increasing the steric bulk around this group though the addition of adjacent methyl groups, or by replacing it with bioisostere moieties that should withstand degradation. Additionally, since pantetheinase is highly substrate specific for the pantoyl moiety of the pantothenamides, removal or replacement of the 4'-hydroxyl should result in it not being recognized as a substrate. In the second part of the study these various strategies were evaluated using the N7-Pan and *N*-PE-PanAm scaffolds, since these pantothenamides were previously shown to have excellent potential as inhibitors of *S. aureus* and *P. falciparum* proliferation, respectively. This allowed us to determine which modifications can be made to counter breakdown by pantetheinase, while retaining inhibitory potency.

The findings addressing this research question are discussed in detail in Chapters 3 and 4, with one aspect of the work resulting in another publication [86] (see manuscript as attached addendum in this thesis), while a second aspect of the work is currently being incorporated into an additional manuscript. Finally, a general conclusion, future strategies and perspectives on this work are presented in Chapter 5.

## 1.10 References

1. Outterson, K., Powers, J. H., Daniel, G. W. and McClellan, M. B., Repairing the broken market for antibiotic innovation. *Health Affairs*, 2015**. 34** (2), 277-285.
2. Lin, J., Nishino, K., Roberts, M. C., Tolmasky, M., Aminov, R. I. and Zhang, L., Mechanisms of antibiotic resistance. *Frontiers in Microbiology*, 2015**. 6** (article 34), 1-3.
3. Spellberg, B., Blaser, M., Guidos, R. J., Boucher, H. W., Bradley, J. S., Eisenstein, B. I., Gerding, D., Lynfield, R., Reller, L. B., Rex, J., Schwartz, D., Septimus, E., Tenover, F. C. and Gilbert, D. N., Combating antimicrobial resistance: Policy recommendations to save lives. *Clinical Infectious Diseases* 2011**. 52 Suppl 5**, S397-428.
4. Spellberg, B., Guidos, R., Gilbert, D., Bradley, J., Boucher, H. W., Scheld, W. M., Bartlett, J. G. and Edwards, J., Jr., The epidemic of antibiotic-resistant infections: A call to action for the medical community from the Infectious Diseases Society of America. *Clinical Infectious Diseases* 2008**. 46** (2), 155-164.
5. Blair, J. M., Webber, M. A., Baylay, A. J., Ogbolu, D. O. and Piddock, L. J., Molecular mechanisms of antibiotic resistance. *Nature Reviews Microbiology*, 2015**. 13** (1), 42-51.
6. Frieden, T. Antibiotic resistance threats in the United States; *Centers for Disease Control & Prevention*: United States, 2013; pp 1-114.
7. Akinnusi, T. O., Vong, K. and Auclair, K., Geminal dialkyl derivatives of *N*-substituted pantothenamides: Synthesis and antibacterial activity. *Bioorganic & Medicinal Chemistry*, 2011**. 19** (8), 2696-2706.
8. Chadha, P., Mariano, N., LaBombardi, V., Segal-Maurer, S. and Urban, C., *In vitro* activities of mupirocin, tigecycline, ceftaroline, vancomycin, linezolid and daptomycin in clinical isolates of methicillin-resistant *Staphylococcus aureus* by E-test methodology. *Open Journal of Medical Microbiology*, 2015**. 5** (1), 12-16.
9. Theuretzbacher, U., Global antibacterial resistance: The never-ending story. *Journal of Global Antimicrobial Resistance*, 2013**. 1** (2), 63-69.
10. Rodriguez-Rojas, A., Rodriguez-Beltran, J., Couce, A. and Blazquez, J., Antibiotics and antibiotic resistance: A bitter fight against evolution. *International Journal of Medical Microbiology*, 2013**. 303** (6-7), 293-297.
11. Meissner, H. C., How to combat growing threat of antimicrobial resistance. *AAP News* 2015.
12. Virga, K. G., Zhang, Y. M., Leonardi, R., Ivey, R. A., Hevener, K., Park, H. W., Jackowski, S., Rock, C. O. and Lee, R. E., Structure-activity relationships and enzyme inhibition of pantothenamide-type pantothenate kinase inhibitors. *Bioorganic & Medicinal Chemistry*, 2006**. 14** (4), 1007-1020.
13. Otto, M., Basis of virulence in community-associated methicillin-resistant *Staphylococcus aureus*. *Annual Review of Microbiology*, 2010**. 64**, 143-162.

14. Guillemot, D., Antibiotic use in humans and bacterial resistance. *Microbiology*, 1999**. 2** (5), 494-498.
15. Walsh, C. T. and Wencewicz, T. A., Prospects for new antibiotics: A molecule-centered perspective. *Journal of Antibiotics*, 2014**. 67** (1), 7-22.
16. Fischbach, M. A. and Walsh, C. T., Antibiotics for emerging pathogens. *Science*, 2009**. 325** (5944), 1089-1093.
17. Spellberg, B., Bartlett, J., Wunderink, R. and Gilbert, D. N., Novel approaches are needed to develop tomorrow's antibacterial therapies. *American Journal of Respiratory & Critical Care Medicine*, 2015**. 191** (2), 135-140.
18. Theuretzbacher, U., Accelerating resistance, inadequate antibacterial drug pipelines and international responses. *International Journal of Antimicrobial Agents*, 2012**. 39** (4), 295-299.
19. Nikaido, H., Multidrug resistance in bacteria. *Annual Review of Biochemistry*, 2009**. 78**, 119-146.
20. Wright, G. D., Molecular mechanisms of antibiotic resistance. *Chemical Communications*, 2011**. 47** (14), 4055-4061.
21. Sanakal, R. D. and Kaliwal, B. B., Vancomycin resistance genes in various organisms - An *insilico* study. *International Journal of Biometrics & Bioinformatics*, 2001**. 5** (2), 111-129.
22. Chopra, I. and Roberts, M., Tetracycline antibiotics: Mode of action, applications, molecular biology, and epidemiology of bacterial resistance. *Microbiology & Molecular Biology Reviews*, 2001**. 65** (2), 232-260.
23. Hooper, D. C., Mechanisms of action of antimicrobials: Focus on fluoroquinolones. *Clinical Infectious Diseases*, 2001**. 32** (Suppl 1), S9-15.
24. Kotra, L. P., Haddad, J. and Mobashery, S., Aminoglycosides: Perspectives on mechanisms of action and resistance and strategies to counter resistance. *Antimicrobial Agents & Chemotherapy*, 2000**. 44** (12), 3249-3256.
25. McCallum, N., Berger-Bachi, B. and Senn, M. M., Regulation of antibiotic resistance in *Staphylococcus aureus*. *International Journal of Medical Microbiology*, 2010**. 300** (2-3), 118-129.
26. Jeljaszewicz, J., Mlynarczyk, G. and Mlynarczyk, A., Antibiotic resistance in Gram-positive cocci. *International Journal of Antimicrobial Agents*, 2000**. 16** (4), 473-478.
27. Spry, C., Kirk, K. and Saliba, K. J., Coenzyme A biosynthesis: An antimicrobial drug target. *FEMS Microbiology Reviews*, 2008**. 32** (1), 56-106.
28. Begley, T. P., Kinsland, C. and Strauss, E., The biosynthesis of coenzyme A in bacteria. *Vitamins & Hormones*, 2001**. 61** (2), 157-171.
29. Leonardi, R., Chohnan, S., Zhang, Y. M., Virga, K. G., Lee, R. E., Rock, C. O. and Jackowski, S., A pantothenate kinase from *Staphylococcus aureus* refractory to feedback regulation by coenzyme A. *Journal of Biological Chemistry*, 2005**. 280** (5), 3314-3322.

30. Choudhry, A. E., Mandichak, T. L., Broskey, J. P., Egolf, R. W., Kinsland, C., Begley, T. P., Seefeld, M. A., Ku, T. W., Brown, J. R., Zalacain, M. and Ratnam, K., Inhibitors of pantothenate kinase: Novel antibiotics for staphylococcal Infections. *Antimicrobial Agents & Chemotherapy*, 2003**. 47** (6), 2051-2055.
31. Leonardi, R., Zhang, Y. M., Rock, C. O. and Jackowski, S., Coenzyme A: Back in action. *Progress in Lipid Research*, 2005**. 44** (2-3), 125-153.
32. Hong, B. S., Yun, M. K., Zhang, Y. M., Chohnan, S., Rock, C. O., White, S. W., Jackowski, S., Park, H. W. and Leonardi, R., Prokaryotic type II and type III pantothenate kinases: The same monomer fold creates dimers with distinct catalytic properties. *Structure*, 2006**. 14** (8), 1251-1261.
33. Yang, K., Strauss, E., Huerta, C. and Zhang, H., Structural basis for substrate binding and the catalytic mechanism of type III pantothenate kinase. *Biochemistry*, 2008**. 47** (5), 1369-1380.
34. Van der Westhuyzen, R., Hammons, J. C., Meier, J. L., Dahesh, S., Moolman, W. J., Pelly, S. C., Nizet, V., Burkart, M. D. and Strauss, E., The antibiotic CJ-15,801 is an antimetabolite that hijacks and then inhibits CoA biosynthesis. *Chemistry & Biology*, 2012**. 19** (5), 559-571.
35. Rock, C. O., Karim, M. A., Zhang, Y. M. and Jackowski, S., The murine pantothenate kinase (*Pank1*) gene encodes two differentially regulated pantothenate kinase isozymes. *Gene*, 2002**. 291** (1-2), 35-43.
36. Hong, B. S., Senisterra, G., Rabeh, W. M., Vedadi, M., Leonardi, R., Zhang, Y. M., Rock, C. O., Jackowski, S. and Park, H. W., Crystal structures of human pantothenate kinases. Insights into allosteric regulation and mutations linked to a neurodegeneration disorder. *Journal of Biological Chemistry*, 2007**. 282** (38), 27984-27993.
37. Hughes, S. J., Antoshchenko, T., Kim, K. P., Smil, D. and Park, H. W., Structural characterization of a new *N*-substituted pantothenamide bound to pantothenate kinases from *Klebsiella pneumoniae* and *Staphylococcus aureus*. *Proteins*, 2014**. 82** (7), 1542-1548.
38. Ivey, R. A., Zhang, Y. M., Virga, K. G., Hevener, K., Lee, R. E., Rock, C. O., Jackowski, S. and Park, H. W., The structure of the pantothenate kinase·ADP·pantothenate ternary complex reveals the relationship between the binding sites for substrate, allosteric regulator, and antimetabolites. *Journal of Biological Chemistry*, 2004**. 279** (34), 35622-35629.
39. Song, W. J. and Jackowski, S., Kinetics and regulation of pantothenate kinase from *Escherichia coli*. *Journal of Biological Chemistry*, 1994**. 269** (43), 27051-27058.
40. Chohnan, S., Murase, N., Kurikawa, K., Higashi, K. and Ogata, Y., Antimicrobial activity of pantothenol against Staphylococci possessing a prokaryotic type II pantothenate kinase. *Microbes & Environments*, 2014**. 29** (2), 224-226.

41. Strauss, E., Coenzyme A biosynthesis and enzymology. In *Comprehensive Natural Products II*, Lew, M.; Hung-Wen, L., Eds. Elsevier: Oxford: 2010; pp 351-410.
42. Mercer, A. C., Meier, J. L., Hur, G. H., Smith, A. R. and Burkart, M. D., Antibiotic evaluation and *in vivo* analysis of alkynyl coenzyme A antimetabolites in *Escherichia coli*. *Bioorganic & Medicinal Chemistry Letters*, 2008**. 18** (22), 5991-5994.
43. Lambalot, R. H. and Walsh, C. T., Cloning, overproduction, and characterization of the *Escherichia coli* holo-acyl carrier protein synthase. *Journal of Biological Chemistry*, 1995**. 270** (42), 24658-24661.
44. Thomas, J. and Cronan, J. E., Antibacterial activity of *N*-pentylpantothenamide is due to inhibition of coenzyme A synthesis. *Antimicrobial Agents & Chemotherapy*, 2010**. 54** (3), 1374-1377.
45. Jackowski, S. and Rock, C. O., Turnover of the 4'-phosphopantetheine prosthetic group of acyl carrier protein. *Journal of Biological Chemistry* 1984**. 259** (3), 1891-1895.
46. Van Wyk, M. A study of *N*-substituted pantothenamides, antimicrobials acting on coenzyme A biosynthesis and utilization. PhD, University of Stellenbosch, 2009.
47. de Villiers, M., Barnard, L., Koekemoer, L., Snoep, J. L. and Strauss, E., Variation in pantothenate kinase type determines the pantothenamide mode of action and impacts on coenzyme A salvage biosynthesis. *FEBS Journal*, 2014**. 281** (20), 4731-4753.
48. Yao, J. and Rock, C. O., How bacterial pathogens eat host lipids: Implications for the development of fatty acid synthesis therapeutics. *Journal of Biological Chemistry*, 2015**. 290** (10), 5940-5946.
49. Saliba, K. J., Horner, H. A. and Kirk, K., Transport and metabolism of the essential vitamin pantothenic acid in human erythrocytes infected with the malaria parasite *Plasmodium falciparum*. *Journal of Biological Chemistry*, 1998**. 273** (17), 10190-10195.
50. Spry, C. and Saliba, K. J., The human malaria parasite *Plasmodium falciparum* is not dependent on host coenzyme A biosynthesis. *Journal of Biological Chemistry*, 2009**. 284** (37), 24904-24913.
51. Augagneur, Y., Jaubert, L., Schiavoni, M., Pachikara, N., Garg, A., Usmani-Brown, S., Wesolowski, D., Zeller, S., Ghosal, A., Cornillot, E., Said, H. M., Kumar, P., Altman, S. and Mamoun, C. B., Identification and functional analysis of the primary pantothenate transporter, *Pf*PAT, of the human malaria parasite *Plasmodium falciparum*. *Journal of Biological Chemistry*, 2013**. 288** (28), 20558-20567.
52. Saliba, K. J. and Kirk, K., $H^+$-coupled pantothenate transport in the intracellular malaria parasite. *Journal of Biological Chemistry*, 2001**. 276** (21), 18115-18121.
53. Mehlin, C., Structure based drug discovery for *Plasmodium falciparum*. *Combinatorial Chemistry & High Throughput Screening*, 2005**. 8** (1), 5-14.

54. Jayaraman, V., Bulusu, V. and Balaram, H., Crosstalk between purine nucleotide metabolism and mitochondrial pathways in *Plasmodium falciparum*. *Current science*, 2012**. 102** (5), 757-766.

55. Nagaraj, V. A., Sundaram, B., Varadarajan, N. M., Subramani, P. A., Kalappa, D. M., Ghosh, S. K. and Padmanaban, G., Malaria parasite-synthesized heme is essential in the mosquito and liver stages and complements host heme in the blood stages of infection. *PLoS Pathogens*, 2013**. 9** (8), e1003522.

56. Yu, M., Kumar, T. R., Nkrumah, L. J., Coppi, A., Retzlaff, S., Li, C. D., Kelly, B. J., Moura, P. A., Lakshmanan, V., Freundlich, J. S., Valderramos, J. C., Vilcheze, C., Siedner, M., Tsai, J. H., Falkard, B., Sidhu, A. B., Purcell, L. A., Gratraud, P., Kremer, L., Waters, A. P., Schiehser, G., Jacobus, D. P., Janse, C. J., Ager, A., Jacobs, W. R., Jr., Sacchettini, J. C., Heussler, V., Sinnis, P. and Fidock, D. A., The fatty acid biosynthesis enzyme FabI plays a key role in the development of liver-stage malarial parasites. *Cell Host Microbe*, 2008**. 4** (6), 567-578.

57. Vaughan, A. M., O'Neill, M. T., Tarun, A. S., Camargo, N., Phuong, T. M., Aly, A. S., Cowman, A. F. and Kappe, S. H., Type II fatty acid synthesis is essential only for malaria parasite late liver stage development. *Cellular Microbiology*, 2009**. 11** (3), 506-520.

58. Saliba, K. J., Ferru, I. and Kirk, K., Provitamin B5 (pantothenol) inhibits growth of the intraerythrocytic malaria parasite. *Antimicrobial Agents & Chemotherapy*, 2005**. 49** (2), 632-637.

59. Zhang, Y. M., Rock, C. O. and Jackowski, S., Biochemical properties of human pantothenate kinase 2 isoforms and mutations linked to pantothenate kinase-associated neurodegeneration. *Journal of Biological Chemistry*, 2006**. 281** (1), 107-114.

60. Spry, C., Chai, C. L., Kirk, K. and Saliba, K. J., A class of pantothenic acid analogs inhibits *Plasmodium falciparum* pantothenate kinase and represses the proliferation of malaria parasites. *Antimicrobial Agents & Chemotherapy* 2005**. 49** (11), 4649-4657.

61. Fletcher, S. and Avery, V. M., A novel approach for the discovery of chemically diverse anti-malarial compounds targeting the *Plasmodium falciparum* coenzyme A synthesis pathway. *Malaria Journal*, 2014**. 13**, 343.

62. Prigge, S. T., He, X., Gerena, L., Waters, N. C. and Reynolds, K. A., The initiating steps of a type II fatty acid synthase in *Plasmodium falciparum* are catalyzed by *pf*ACP, *pf*MCAT, and *pf*KASIII. *Biochemistry*, 2003**. 42** (4), 1160-1169.

63. Derbyshire, E., Mota, M. and Clardy, J., The next opportunity in anti-malaria drug discovery: The liver stage. *PLoS Pathogens*, 2011**. 7** (9), e1002178.

64. March, S., Ng, S., Velmurugan, S., Galstian, A., Shan, J., Logan, D. J., Carpenter, A. E., Thomas, D., Sim, B. K., Mota, M. M., Hoffman, S. L. and Bhatia, S. N., A microscale human

liver platform that supports the hepatic stages of *Plasmodium falciparum* and *vivax*. *Cell Host & Microbe*, 2013**. 14** (1), 104-115.

65. Strauss, E. and Begley, T. P., The antibiotic activity of *N*-pentylpantothenamide results from its conversion to ethyldethia-coenzyme A, a coenzyme A antimetabolite. *Journal of Biological Chemistry*, 2002**. 277** (50), 48205-48209.
66. Barnett, J. W. and Robinson, F. A., Analogues of pantothenic acid: Attempted preparation of growth promoters. *Biochemical Journal*, 1942**. 36** (3-4), 257-363.
67. Williams, R. J., Weinstock, H. H., Jr., Rohrmann, E., Truesdail, J. H., Mitchell, H. K. and Meyer, C. E., Pantothenic Acid. III. Analysis and determination of constituent groups. *Journal of the American Chemical Society*, 1939**. 61** (2), 454-457.
68. Pollack, M. A., Growth effects of α-methyl homologs of pantothenic acid and β-alanine. *Journal of the American Chemical Society*, 1943**. 65** (7), 1335-1339.
69. Clifton, G., Bryant, S. R. and Skinner, C. G., $N^1$-(substituted) pantothenamides, antimetabolites of pantothenic acid. *Archives of Biochemistry & Biophysics*, 1970**. 137** (2), 523-528.
70. Trager, W., Further studies on the survival and development *in vitro* of a malarial parasite. *Journal of Experimental Medicine*, 1943**. 77** (5), 411-420.
71. Winterbottom, R., Clapp, J. W., Miller, W. H., English, J. P. and Roblin, R. O., Studies in chemotherapy. XV. Amides of pantoyltaurine. *Journal of the American Chemical Society*, 1947**. 69** (6), 1393-1401.
72. Saliba, K. J. and Kirk, K., CJ-15,801, a fungal natural product, inhibits the intraerythrocytic stage of *Plasmodium falciparum in vitro* via an effect on pantothenic acid utilisation. *Molecular & Biochemical Parasitology*, 2005**. 141** (1), 129-131.
73. Spry, C., Macuamule, C., Lin, Z., Virga, K. G., Lee, R. E., Strauss, E. and Saliba, K. J., Pantothenamides are potent, on-target Inhibitors of *Plasmodium falciparum* growth when serum pantetheinase is inactivated. *PLoS One*, 2013**. 8** (2), e54974.
74. de Villiers, M., Macuamule, C., Spry, C., Hyun, Y. M., Strauss, E. and Saliba, K. J., Structural modification of pantothenamides counteracts degradation by pantetheinase and improves antiplasmodial activity. *ACS Medicinal Chemistry Letters*, 2013**. 4** (8), 784-789.
75. Zeeuwen, P. L. J. M., Jansen, P. A. M., Schalkwijk, J., Rutjes, F. P. J. T., Ritzen, B. and Hermkens, P. H. H. Pantothenic acid derivatives and their use in the treatment of microbial infections (OCR). WO 2011/152720 A1, 8 December 2011.
76. Jansen, P. A. M., Schalkwijk, J., Rutjes, F. P. J. T., Sauer-wein, R. and Hermkens, P. H. H. Derivatives of pantothenic acid and their use for the treatment of malaria. WO2011152721A1, 8 December 2011.
77. Pitari, G., Malergue, F., Martin, F., Philippe, J. M., Massucci, M. T., Chabret, C., Maras, B.,

Dupre, S., Naquet, P. and Galland, F., Pantetheinase activity of membrane-bound Vanin-1: Lack of free cysteamine in tissues of Vanin-1 deficient mice. *FEBS Letters*, 2000**. 483** (2-3), 149-154.

78. Van Diepen, J. A., Jansen, P. A., Ballak, D. B., Hijmans, A., Hooiveld, G. J., Rommelaere, S., Galland, F., Naquet, P., Rutjes, F. P., Mensink, R. P., Schrauwen, P., Tack, C. J., Netea, M. G., Kersten, S., Schalkwijk, J. and Stienstra, R., PPAR-alpha dependent regulation of Vanin-1 mediates hepatic lipid metabolism. *Journal of Hepatology*, 2014**. 61** (2), 366-372.
79. Kaskow, B. J., Proffitt, J. M., Blangero, J., Moses, E. K. and Abraham, L. J., Diverse biological activities of the vascular non-inflammatory molecules - The Vanin pantetheinases. *Biochemical & Biophysical Research Communications*, 2012**. 417** (2), 653-658.
80. Maras, B., Barra, D., Dupre, S. and Pitari, G., Is pantetheinase the actual identity of mouse and human Vanin-1 proteins? *FEBS Letters*, 1999**. 461** (3), 149-152.
81. Min-Oo, G., Ayi, K., Bongfen, S. E., Tam, M., Radovanovic, I., Gauthier, S., Santiago, H., Rothfuchs, A. G., Roffe, E., Sher, A., Mullick, A., Fortin, A., Stevenson, M. M., Kain, K. C. and Gros, P., Cysteamine, the natural metabolite of pantetheinase, shows specific activity against *Plasmodium*. *Experimental Parasitology*, 2010**. 125** (4), 315-324.
82. Berruyer, C., Martin, F. M., Castellano, R., Macone, A., Malergue, F., Garrido-Urbani, S., Millet, V., Imbert, J., Dupre, S., Pitari, G., Naquet, P. and Galland, F., Vanin-1$^{-/-}$ mice exhibit a glutathione-mediated tissue resistance to oxidative stress. *Molecular & Cellular Biology*, 2004**. 24** (16), 7214-7224.
83. Martin, F., Malergue, F., Pitari, G., Philippe, J. M., Philips, S., Chabret, C., Grandjeaud, S., Mattei, M. G., Mungall, A. J., Naquet, P. and Galland, F., Vanin genes are clustered (human 6q22–24 and mouse 10A2B1) and encode isoforms of pantetheinase ectoenzymes. *Immunogenetics*, 2001**. 53** (4), 296-306.
84. Van Wyk, M. and Strauss, E., Development of a method for the parallel synthesis and purification of *N*-substituted pantothenamides, known inhibitors of coenzyme A biosynthesis and utilization. *Organic & Biomolecular Chemistry*, 2008**. 6** (23), 4348-4355.
85. Jansen, P. A., Hermkens, P. H., Zeeuwen, P. L., Botman, P. N., Blaauw, R. H., Burghout, P., van Galen, P. M., Mouton, J. W., Rutjes, F. P. and Schalkwijk, J., Combination of pantothenamides with Vanin inhibitors as a novel antibiotic strategy against Gram-positive bacteria. *Antimicrobial Agents & Chemotherapy*, 2013**. 57** (10), 4794-4800.
86. Macuamule, C. J., Tjhin, E. T., Jana, C. E., Barnard, L., Koekemoer, L., de Villiers, M., Saliba, K. J. and Strauss, E., A pantetheinase-resistant pantothenamide with potent, on-target, and selective antiplasmodial activity. *Antimicrobial Agents & Chemotherapy*, 2015**. 59** (6), 3666-3668.

*Chapter 2*

# Variation In Pantothenate Kinase Type Determines The Mode of Action In Bacteria

Marianne de Villiers, **Leanne Barnard**, Lizbé Koekemoer, Jacky L. Snoep and Erick Strauss

*FEBS Journal*

Vol. 281 (2014) pp. 4731–4753[1]

**Author's Contribution:**

MdV and LB shared first authorship of this manuscript. They contributed equally to the syntheses, growth inhibition assays and enzyme kinetic analyses, as well as to the data analysis. Specifically, MdV prepared the pantothenamide library and determined the MIC values given in Table 1 as well as the enzyme specific activities shown in Figure 2A-B. She also performed initial experiments of the data reported in Figures 2C-F and 3A/C, as well as Table 2. LB repeated all these experiments a minimum of two times to improve the statistical significance of the data. LB also synthesized the (2*R*/*S*)-4'-deoxy-*N*-pentylpantothenamide and performed all relevant experiments with this compound. LK performed preliminary enzyme kinetic assays and data analysis. JLS constructed the kinetic model and performed the associated data analysis. ES directed the project, contributed to the data analysis and wrote the paper with significant contributions from all of the authors.

the FEBS Journal

# Variation in pantothenate kinase type determines the pantothenamide mode of action and impacts on coenzyme A salvage biosynthesis

Marianne de Villiers*, Leanne Barnard*, Lizbé Koekemoer, Jacky L. Snoep and Erick Strauss

Department of Biochemistry, Stellenbosch University, South Africa

**Keywords**
coenzyme A; growth inhibition; pantetheine; pantothenamide; pantothenate kinase

**Correspondence**
E. Strauss, Department of Biochemistry, Stellenbosch University, Stellenbosch 7600, South Africa
Fax: +27 21 808 5863
Tel: +27 21 808 5866
E-mail: estrauss@sun.ac.za

*These authors contributed equally to this work.

(Received 30 May 2014, revised 18 July 2014, accepted 18 August 2014)

doi:10.1111/febs.13013

*N*-substituted pantothenamides are analogues of pantothenic acid, the vitamin precursor of CoA, and constitute a class of well-studied bacterial growth inhibitors that show potential as new antibacterial agents. Previous studies have highlighted the importance of pantothenate kinase (PanK; EC 2.7.1.33) (the first enzyme of CoA biosynthesis) in mediating pantothenamide-induced growth inhibition by one of two proposed mechanisms: first, by acting on the pantothenamides as alternate substrates (allowing their conversion into CoA antimetabolites, with subsequent effects on CoA- and acyl carrier protein-dependent processes) or, second, by being directly inhibited by them (causing a reduction in CoA biosynthesis). In the present study we used structurally modified pantothenamides to probe whether PanKs interact with these compounds in the same manner. We show that the three distinct types of eubacterial PanKs that are known to exist ($PanK_I$, $PanK_{II}$ and $PanK_{III}$) respond very differently and, consequently, are responsible for determining the pantothenamide mode of action in each case: although the promiscuous $PanK_I$ enzymes accept them as substrates, the highly selective $PanK_{III}$s are resistant to their inhibitory effects. Most unexpectedly, *Staphylococcus aureus* PanK (the only known example of a bacterial $PanK_{II}$) experiences uncompetitive inhibition in a manner that is described for the first time. In addition, we show that pantetheine, a CoA degradation product that closely resembles the pantothenamides, causes the same effect. This suggests that, in *S. aureus*, pantothenamides may act by usurping a previously unknown role of pantetheine in the regulation of CoA biosynthesis, and validates its PanK as a target for the development of new antistaphylococcal agents.

## Introduction

The *N*-substituted pantothenamides are a class of pantothenic acid (Pan, vitamin $B_5$) analogues that were first described in 1970 as growth inhibitors of selected lactic acid bacteria and *Escherichia coli* [1]. Because Pan is the biosynthetic precursor of the universal acyl group carrier CoA (Fig. 1A), which serves to activate

**Abbreviations**
ACP, acyl carrier protein; AcpH, [ACP]hydrolase; dN5, DL-4′-deoxy-*N*-pentylpantothenamide; DPCK, dephospho-CoA kinase; *Ec*$PanK_I$, *Escherichia coli* type I pantothenate kinase; HoPanAm, homopantothenamide; HoPan, homopantothenic acid; HRMS, high resolution mass spectrometry; LDH, lactate dehydrogenase; MIC, minimal inhibitory concentration; N354-Pan, *N*-[2-(1,3-benzodioxol-5-yl)ethyl] pantothenamide; N5-Pan, *N*-pentyl pantothenamide; N7-Pan, *N*-heptyl pantothenamide; *n*-PanAm, *n*-pantothenamide; PanK, pantothenate kinase; Pan, pantothenic acid; PantSH, pantetheine; PK, pyruvate kinase; P-Pan, 4′-phosphopantothenic acid; P-PantSH, 4′-phosphopantetheine; PPAT, phosphopantetheine adenylyltransferase; *Sa*$PanK_{II}$, *Staphylococcus aureus* type II pantothenate kinase; α-PanAm, α-pantothenamide.

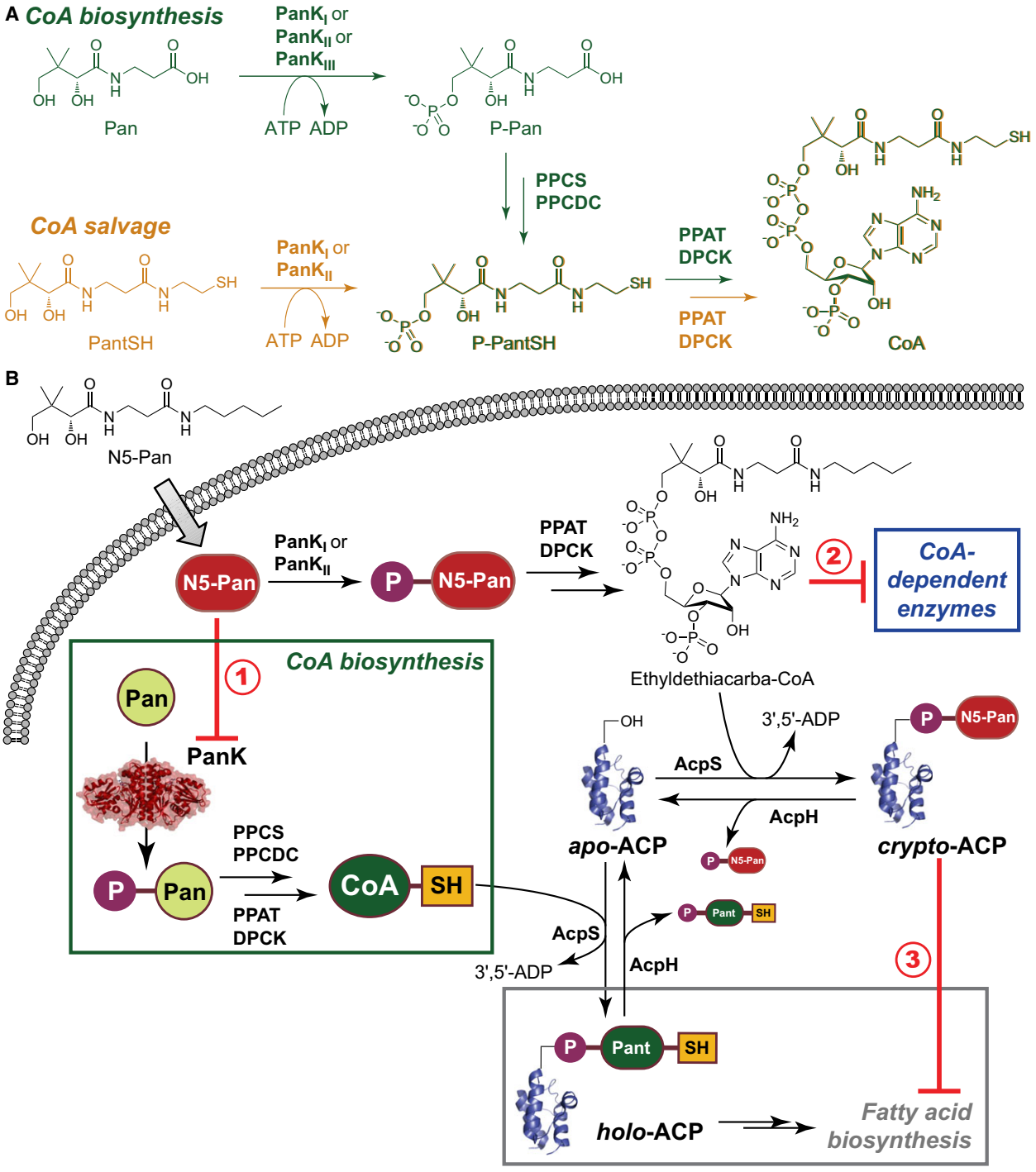


**Fig. 1.** Biosynthesis of CoA and the potential targets of the pantothenamide mode of action. (A) Biosynthesis of CoA from Pan in the five-step pathway catalyzed by panothenate kinase (PanK), phosphopantothenoylcysteine synthetase (PPCS), phosphopantothenoylcysteine decarboxylase (PPCDC), phosphopantetheine adenylyltransferase (PPAT) and dephospho-CoA kinase (DPCK), or from PantSH in the three-step salvage pathway consisting of PanK, PPAT and DPCK. (B) The three major biological targets of N5-Pan: (i) PanK, the first CoA biosynthetic enzyme; (ii) CoA-dependent enzymes, after its transformation into the antimetabolite ethyldethiacarba-CoA; and (iii) fatty acid biosynthesis, when ethyldethiacarba-CoA serves as substrate for AcpS to form a *crypto*-ACP instead of the catalytically active *holo*-ACP. *Holo*- and *crypto*-ACP are recycled back to *apo*-ACP by AcpH.

these groups for both acyl transfer reactions and biological Claisen condensation reactions [2], pantothenamides have raised much interest as antimetabolite-based lead compounds for the development of new selective antimicrobial agents [3]. Although recent studies have again highlighted the potential of these compounds [4–6], attempts at improving their potency are hampered by the fact that their mode of action still has not been unambiguously defined and appears to show variation between different organisms.

The first mode of action study, which was conducted in *E. coli* using *N*-pentyl pantothenamide (N5-Pan), the prototypical example of the class, showed that it is transformed into the CoA antimetabolite ethyldethiacarba-CoA by three of the five CoA biosynthetic enzymes (Fig. 1B) [7]. These enzymes are pantothenate kinase (PanK; EC 2.7.1.33), the first enzyme of the pathway that usually catalyzes the ATP-dependent phosphorylation of Pan to give 4′-phosphopantothenic acid (P-Pan), and the fourth and fifth enzymes phosphopantetheine adenylyltransferase (PPAT) and dephospho-CoA kinase (DPCK), which transform 4′-phosphopantetheine (P-PantSH) into CoA through the addition of adenylyl and phosphate groups, respectively (Fig. 1A). Moreover, the formation of ethyldethiacarba-CoA took place faster than the five-step conversion of Pan into CoA when conducted under competitive conditions *in vitro*. This suggested that N5-Pan exerted its inhibitory effect by reducing the rate of CoA synthesis, and/or through its biosynthetic product inhibiting enzymes and processes dependent on CoA.

A second study focused on fatty acid biosynthesis as the target for pantothenamide-induced bacterial growth inhibition, based on the essential requirement of the *holo*-acyl carrier protein (*holo*-ACP) in type II fatty acid synthase systems (as found in *E. coli*) [8]. Although *holo*-ACP is formed when [ACP]synthase transfers the P-PantSH group from CoA to *apo*-ACP [9], it is also possible for CoA analogues such as ethyldethiacarba-CoA to serve as the substrate instead; this leads to the formation of *crypto*-ACPs that do not have the requisite thiol group and are therefore unable to act as acyl carriers (Fig. 1B). N5-Pan treatment led to the formation of the N5-Pan-containing *crypto*-ACP (ethyldethiacarba-ACP) as predicted, and to a reduction in normal *holo*-ACP levels. CoA levels apparently remained unaffected. Ethyldethiacarba-ACP was also shown to accumulate and persist in N5-Pan-treated cells even after N5-Pan was removed from the culture, suggesting that ethyldethiacarba-ACP is a poor substrate for the [ACP]hydrolase (AcpH) that is responsible for ACP prosthetic group turnover [10,11]. In combination, these factors were considered to result in the complete inhibition of fatty acid biosynthesis; this has subsequently been hailed as the major target for pantothenamide-induced growth inhibition in bacteria.

Several subsequent studies have drawn this assertion into question. First, studies of the purified AcpH and *E. coli* strains in which the *acpH* gene was either knocked out or overexpressed indicated that the accumulation of ethyldethiacarba-ACP following N5-Pan treatment is not a result of reduced ACP turnover because this *crypto*-ACP was found to be readily hydrolyzed by AcpH [12]. Instead, N5-Pan treatment caused a significant reduction in the CoA pool (in contrast to the previous findings), indicating N5-Pan-mediated inhibition of CoA biosynthesis. Attempts at identifying the specific target by individual overexpression of the CoA biosynthetic genes failed because these strains instead showed an increase in N5-Pan sensitivity. This again pointed to the increased flux of the antimetabolite through the pathway as an important additional determinant of pantothenamide-meditated growth inhibition. Second, an investigation of pantothenamide-mediated inhibition of *Staphylococcus aureus* identified PanK as its point of action [13] because only pantothenamides that caused inhibition of the *S. aureus* PanK enzyme *in vitro* (using a standard kinase assay that couples ADP formation to NADH reduction) showed cell growth inhibition. However, a subsequent study revisited these results and used [$\gamma$-$^{32}$P]ATP to demonstrate that *S. aureus* PanK phosphorylates both N5-Pan and its heptyl analogue N7-Pan, and that this (as in the case of *E. coli*) also leads to the formation of modified *crypto*-ACPs and the inhibition of fatty acid synthesis [14]. However, because no studies have investigated the relative importance of the two inhibition modes, the role of PanK in the pantothenamide-mediated growth inhibition of *S. aureus* remains unresolved.

Although the exact mode of action of the pantothenamides still remains a matter of debate, these studies have all clearly highlighted the importance of PanK in mediating their growth inhibitory effects by one of two mechanisms: (a) by acting as the cellular target of inhibition, leading to the suppression of CoA biosynthesis or (b) by accepting pantothenamides as substrates, thereby allowing them to be converted into CoA analogues that exert their effects on CoA- and ACP-dependent processes. Unfortunately, structure–activity relationship studies that set out to establish a correlation between the growth inhibitory potency of a a pantothenamide and its potential to act as either an

inhibitor or substrate of the target organism's PanK have not been able to provide more insight into the enzyme's apparent dual role in pantothenamide-based inhibition [15,16].

Importantly, the distinction between a pantothenamide acting as either a PanK substrate or inhibitor may be linked to other aspects of CoA metabolism. For example, only organisms with PanKs that show poor substrate selectivity are able to form CoA from pantetheine (PantSH) (a CoA-derived degradation product structurally related to the pantothenamides) by means of a salvage pathway made up of PanK, PPAT and DPCK (Fig. 1A) [2]. PanKs occur as one of three distinct forms, known as type I, type II and type III PanK enzymes, respectively [17–20], with only $PanK_I$ and $PanK_{II}$ (the subscript denotes the type) showing activity towards both Pan and PantSH [21]. Organisms such as *Pseudomonas aeruginosa* that have $PanK_{III}$ enzymes cannot salvage CoA from pantetheine [22] and are also resistant to pantothenamide-induced growth inhibition [17,20]. This suggests that the inhibition mode of the pantothenamides (as structural mimics of PantSH) may be linked to the targeted organism's PanK type and its ability to salvage CoA.

In the present study, we explored the existence of such links through a combination of bacterial cell growth inhibition and kinetic characterization studies. We find that PanK type is the major determinant of the pantothenamide mode of action, and particularly so in *S. aureus*, which has a unique CoA metabolism supported by a $PanK_{II}$ with several exceptional features [14,20]. These results not only provide significant new insights for antimetabolite-based antimicrobial drug design, but also add to our understanding of the implications of PanK diversity for CoA metabolism and regulation.

## Results

### Pantothenamide library and study design

The link between PanK type and pantothenamide-induced bacterial cell growth inhibition was investigated using a library of *N*-substituted pantothenamides that was previously prepared in our laboratory and recently used to identify antiplasmodial pantothenamides that are resistant to pantetheinase-mediated degradation [5,23]. The library was constructed from Pan and two Pan analogues: α-pantothenic acid, which has the β-alanine of Pan replaced with glycine, and homopantothenic acid (HoPan) in which it is exchanged for γ-aminobutyric acid. The acids were subsequently coupled to 47 different amines representing a variety of chemical motifs, yielding three sets of pantothenamides, referred to as α-pantothenamides (α-PanAm), *n*-pantothenamides (*n*-PanAm, where *n* signifies 'normal') and homopantothenamides (HoPanAm), respectively (Table 1).

Although α-pantothenic acid has not previously been studied in the context of PanK and/or CoA inhibitors, HoPan was shown to act as a competitive inhibitor of a murine $PanK_{II}$ (*Mm*PanK1α) and to negatively affect CoA levels in mice *in vivo* [24]. The same result was found in insect cells [25]. By contrast, *E. coli* type I PanK (*Ec*$PanK_I$), which is known to accept a range of pantothenic acid analogues [21], does not accept HoPan as a substrate, nor is it significantly inhibited by it [15,24,26]. This diverse response indicated that such modifications in the Pan structure could successfully be used to probe PanK activity and inhibition.

### Organisms with different PanK types exhibit different pantothenamide-induced growth inhibition profiles

Three bacterial species, representing all three PanK types, were selected to evaluate the potency of the pantothenamide library members: *E. coli*, a Gram-negative bacterium with a typical $PanK_I$, the Gram-positive *S. aureus*, the only bacterium known to have an active (albeit atypical) $PanK_{II}$ (normally only eukaryotes have $PanK_{II}$ enzymes) and *P. aeruginosa*, a Gram-negative $PanK_{III}$-containing bacterium [2]. Although *P. aeruginosa* has been shown to be resistant to N5-Pan inhibition as a result of the selectivity of its $PanK_{III}$ enzyme [20], it was included in the present study because we considered that the smaller α-PanAm series could potentially be accommodated in its active site. As in several previous studies [16,27], growth inhibition assays were conducted in 1% tryptone (pancreatic digest of casein), a medium that contains low amounts (< 1 μM) of Pan [28]. Such Pan concentrations are not strictly physiologically relevant to humans with bacterial infections because the concentration of total Pan (i.e. free Pan and Pan bound up in CoA and other Pan-derived metabolites) in human whole blood ranges between 1 and 3 μM [29,30]. However, it allows susceptibility data to be obtained under conditions where Pan is not sufficiently abundant to counteract any potential inhibition, and therefore serves the point of investigating the mode of action of these compounds.

Susceptibility tests were performed by obtaining minimal inhibitory concentration (MIC) values for those compounds that showed inhibition in initial screens performed at 200 and 50 μM, respectively. The structures and MIC values for the pantothenamides

**Table 1.** MIC values for the inhibition of *E. coli* or *S. aureus* grown for 20 h in 1% tryptone medium in the presence of the indicated pantothenamides at different concentrations. The reported values represent the mean of two or more independent experiments; the errors indicate the range/2. References to compounds tested in previous studies are provided in the main text.

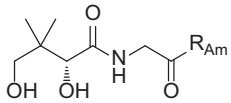

α-PanAm

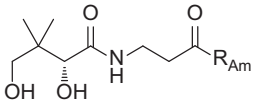

*n*-PanAm

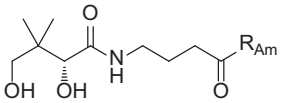

HoPanAm

| PanAm entry | $R_{Am}$ group | *E. coli* MIC (μM) | | | *S. aureus* MIC (μM) | | |
|---|---|---|---|---|---|---|---|
| | | α-PanAm | *n*-PanAm | HoPanAm | α-PanAm | *n*-PanAm | HoPanAm |
| 1 |  | **50–200** | > 200 | > 200 | > 200 | **30.8 ± 4.3** | > 200 |
| 2 | 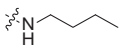 | **50–200** | > 200 | > 200 | > 200 | **50–200** | > 200 |
| 3 | 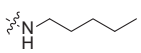 | **50–200** | **64.4 ± 8.2** | > 200 | > 200 | **18.0 ± 0.6** | > 200 |
| 4 | 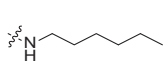 | **50–200** | **50–200** | > 200 | > 200 | **3.14 ± 1.20** | > 200 |
| 5 | 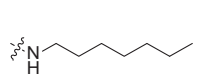 | > 200 | > 200 | > 200 | > 200 | **0.77 ± 0.04** | > 200 |
| 6 | 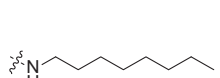 | > 200 | > 200 | > 200 | > 200 | **0.74 ± 0.17** | > 200 |
| 7 |  | > 200 | > 200 | > 200 | > 200 | **50–200** | > 200 |
| 8 | 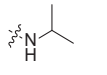 | > 200 | > 200 | > 200 | > 200 | **50–200** | > 200 |
| 9 | 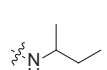 | **101 ± 3** | > 200 | > 200 | **50–200** | **34.7 ± 4.2** | > 200 |
| 10 | 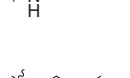 | > 200 | > 200 | > 200 | > 200 | > 200 | > 200 |
| 11 | 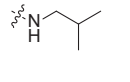 | **50–200** | > 200 | > 200 | > 200 | **50–200** | > 200 |
| 12 | 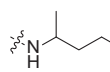 | **55.3 ± 0.8** | > 200 | > 200 | > 200 | **22.3 ± 1.8** | > 200 |
| 13 |  | > 200 | > 200 | > 200 | > 200 | **50–200** | > 200 |
| 14 | 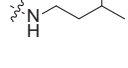 | **136 ± 26** | > 200 | > 200 | > 200 | **24.7 ± 0.3** | > 200 |

**Table 1.** (Continued).

| PanAm entry | $R_{Am}$ group | *E. coli* MIC (μM) | | | *S. aureus* MIC (μM) | | |
|---|---|---|---|---|---|---|---|
| | | α-PanAm | *n*-PanAm | HoPanAm | α-PanAm | *n*-PanAm | HoPanAm |
| 15 | 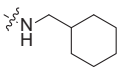 | > 200 | > 200 | > 200 | > 200 | **50–200** | > 200 |
| 16 | 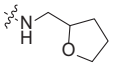 | > 200 | > 200 | > 200 | > 200 | **50–200** | > 200 |
| 17 | 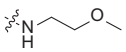 | > 200 | > 200 | > 200 | > 200 | > 200 | > 200 |
| 18 | 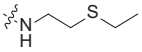 | **50–200** | > 200 | > 200 | > 200 | **50–200** | > 200 |
| 19 | 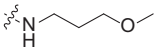 | > 200 | > 200 | > 200 | > 200 | > 200 | > 200 |
| 20 | 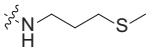 | **50–200** | **50–200** | > 200 | > 200 | **50–200** | > 200 |
| 21 | 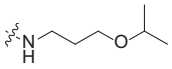 | > 200 | > 200 | > 200 | > 200 | **50–200** | > 200 |
| 22 | 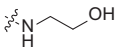 | > 200 | > 200 | > 200 | > 200 | > 200 | > 200 |
| 23 | 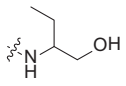 | > 200 | > 200 | > 200 | > 200 | **50–200** | > 200 |
| 24 | 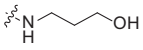 | > 200 | > 200 | > 200 | **50–200** | > 200 | > 200 |
| 25 | 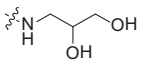 | > 200 | > 200 | > 200 | > 200 | > 200 | > 200 |
| 26 | 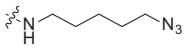 | > 200 | > 200 | > 200 | > 200 | **50–200** | > 200 |
| 27 | 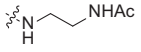 | > 200 | > 200 | > 200 | > 200 | > 200 | > 200 |

**Table 1.** (Continued).

| PanAm entry | $R_{Am}$ group | *E. coli* MIC (μM) | | | *S. aureus* MIC (μM) | | |
|---|---|---|---|---|---|---|---|
| | | α-PanAm | *n*-PanAm | HoPanAm | α-PanAm | *n*-PanAm | HoPanAm |
| 28 | 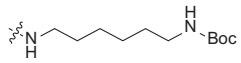 | > 200 | > 200 | > 200 | > 200 | > 200 | > 200 |
| 29 | 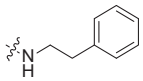 | > 200 | > 200 | > 200 | > 200 | **47.7 ± 7.9** | > 200 |
| 30 | 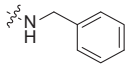 | > 200 | > 200 | > 200 | > 200 | > 200 | > 200 |
| 31 | 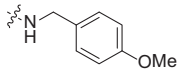 | > 200 | > 200 | > 200 | > 200 | > 200 | > 200 |
| 32 | 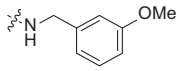 | > 200 | > 200 | > 200 | > 200 | **55.0 ± 10.2** | > 200 |
| 33 | 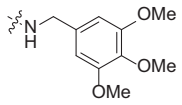 | > 200 | > 200 | > 200 | > 200 | > 200 | > 200 |
| 34 | 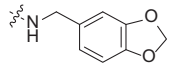 | > 200 | > 200 | > 200 | > 200 | **50–200** | > 200 |
| 35 | 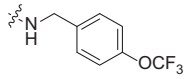 | > 200 | > 200 | > 200 | > 200 | > 200 | > 200 |
| 36 | 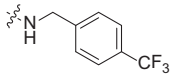 | > 200 | > 200 | > 200 | > 200 | > 200 | > 200 |
| 37 | 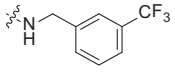 | > 200 | > 200 | > 200 | > 200 | > 200 | > 200 |
| 38 | 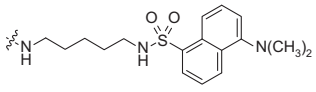 | > 200 | > 200 | > 200 | > 200 | > 200 | > 200 |
| 39 |  | > 200 | > 200 | > 200 | > 200 | > 200 | > 200 |

**Table 1.** (Continued).

| PanAm entry | $R_{Am}$ group | *E. coli* MIC (μM) | | | *S. aureus* MIC (μM) | | |
|---|---|---|---|---|---|---|---|
| | | α-PanAm | *n*-PanAm | HoPanAm | α-PanAm | *n*-PanAm | HoPanAm |
| 40 |  | > 200 | > 200 | > 200 | > 200 | > 200 | > 200 |
| 41 | 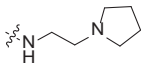 | > 200 | > 200 | > 200 | > 200 | > 200 | > 200 |
| 42 | 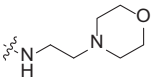 | > 200 | > 200 | > 200 | > 200 | > 200 | > 200 |
| 43 | 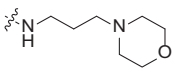 | > 200 | > 200 | > 200 | > 200 | > 200 | > 200 |
| 44 | 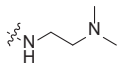 | > 200 | > 200 | > 200 | > 200 | > 200 | > 200 |
| 45 | 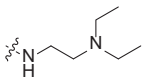 | > 200 | > 200 | > 200 | > 200 | > 200 | > 200 |
| 46 | 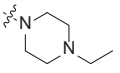 | > 200 | > 200 | > 200 | > 200 | > 200 | > 200 |
| 47 | 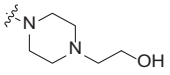 | > 200 | > 200 | > 200 | > 200 | > 200 | > 200 |

tested are given in Table 1. Importantly, the data obtained for the *n*-PanAm set correlate well with the results of previous pantothenamide structure–activity relationship studies, with the MIC values differing by no more than 10-fold (some differences are expected due to variation in the amount of Pan present in tryptone) [8,14,15].

Comparative analysis of the results indicated that *E. coli* was only inhibited by a small number of α-PanAm and *n*-PanAm series members, most of which had MIC values in the 50–100 μM range. Previous studies have demonstrated that, at least in some cases (such as with *n*-PanAm-5, otherwise known as *N*-heptyl pantothenamide or N7-Pan), this relatively poor inhibition profile can be ascribed to TolC-dependent efflux because TolC-defective strains do show sensitivity [8,15]. By contrast, *S. aureus* was only inhibited by *n*-PanAm compounds. These showed MIC values that varied by almost two orders of magnitude, with the best inhibitors (*n*-PanAm-5/N7-Pan and *n*-PanAm-6) having MIC values of ~ 0.7 μM. As expected, *P. aeruginosa* showed no inhibition by any of the pantothenamides tested, including the smaller sized α-PanAm series.

## Pantothenamide-mediated growth inhibition correlates with PanK activity in *E. coli* but not *S. aureus*

Next, we investigated whether the differences in the *E. coli* and *S. aureus* growth inhibition profiles could

be correlated with the activity and/or selectivity of their respective PanKs. The pantothenamides that showed the most potent growth inhibition were tested as substrates of the purified overexpressed enzymes at a fixed concentration (100 μM) using an established pyruvate kinase/lactate dehydrogenase (PK/LDH)-based coupled enzyme assay that links ADP production to the consumption of NADH [7]. Although this assay measures the enzymes' activity indirectly, it has been shown previously that the expected monophosphorylated ester is produced and that the PK/LDH-assay is a viable alternative for measuring PanK activity [7,13,21,31]. The corresponding compounds that have the same amide substituent but different substitutions of the β-alanine moiety were included for comparison. The data indicate that, for *Ec*PanK$_{I}$, compounds that show growth inhibition belong to the α- and *n*-PanAm series and have specific activities very similar to that measured for Pan, whereas the HoPanAms, which do not inhibit *E. coli* growth, show poor PanK activity (Fig. 2A). However, PanK activity is not necessarily a predictor of growth inhibition because even α- and *n*-PanAm compounds that do not show growth inhibition still show similar specific activity levels. Unexpectedly, the situation is reversed in *S. aureus*, with only the non-inhibitory HoPanAm members showing *S. aureus* type II PanK (*Sa*PanK$_{II}$) activity approaching that seen for Pan (Fig. 2B).

To further investigate these differences and their relevance to the pantothenamide mode of action, kinetic profiles were obtained for both enzymes with Pan and the three pantothenamides with *N*-pentyl substituents [i.e. α-PanAm-3, *n*-PanAm-3 (referred to as N5-Pan from here on) and HoPanAm-3] (Fig. 2C). These confirm that the pantothenamides that acted as *E. coli* inhibitors (N5-Pan and α-PanAm-3) have *Ec*PanK$_{I}$ activity profiles that closely resemble that of Pan. HoPanAm-3, which did not act as an *E. coli* growth inhibitor, is clearly a poor *Ec*PanK$_{I}$ substrate. By contrast, the *S. aureus* growth inhibitor N5-Pan has a very different activity profile that shows both a lower apparent $K_m$ ($K_m^{app}$) and significantly reduced turnover compared to Pan (Fig. 2D). The two pantothenamides that did not show inhibition of *S. aureus*, α-PanAm-3 and HoPanAm-3, are apparently poor and excellent substrates, respectively.

To confirm these trends, we extended the studies to other selected growth inhibitory pantothenamides. We found that *Ec*PanK$_{I}$ also accepts α-PanAm-12 and α-PanAm-14 as substrates (Fig. 2E), whereas *Sa*PanK$_{II}$ shows the same unusual kinetic profile for *n*-PanAm-5, *n*-PanAm-9, *n*-PanAm-12 and *n*-PanAm-29 that combines a low $K_m^{app}$ with low turnover (Fig. 2F). Among these compounds, *n*-PanAm-5 (N7-Pan) showed the lowest turnover; importantly, it is also the pantothenamide that exhibits the most potent growth inhibition of *S. aureus* identified to date [13,14]. These results strongly suggest that in *E. coli* PanK activity is a necessary (but not sufficient) requirement for pantothenamides to show growth inhibition. By contrast, pantothenamides that show growth inhibition of *S. aureus* bind its PanK enzyme with high apparent affinity, yet show poor turnover.

## Quantifying the variations in PanK kinetics: constructing a kinetic model

Several previous studies have used the Michaelis–Menten equation to obtain kinetic parameters for both *Ec*PanK$_{I}$ and *Sa*PanK$_{II}$ acting on a range of substrates [7,13,14,16,32–34]. In the present study we took special care to obtain all measurements during the initial phase of the reaction (< 10% substrate consumed), and found that *Ec*PanK$_{I}$ has a hyperbolic activity profile only for Pan, whereas it shows sigmoidal saturation curves for the pantothenamides (Fig. 3A). *Sa*PanK$_{II}$ has sigmoidal saturation curves for both Pan and HoPanAm-3 (the low $K_m^{app}$ for N5-Pan limited our ability to determine if this is also true in its case). These findings indicate that some substrates have a positive cooperative effect on PanK catalysis, a phenomenon that has previously only been described for certain PanK$_{III}$s [35].

The sigmoidal saturation data were best described by a simple Hill-type equation (Eqn 1) derived according to a mechanism based on a dimeric enzyme with one active site per subunit; the available structural data shows that both *Ec*PanK$_{I}$ and *Sa*PanK$_{II}$ conform to this description [20,26,36]. This mechanism, shown schematically for *Sa*PanK$_{II}$ acting on Pan in Fig. 3B, is based on the assumption that only enzyme states with both of the active sites occupied (e.g. $E_{Pan.Pan}$) have to be considered and lead to product formation (as is usually the case for cooperative enzymes). The differential binding of the substrate to the two active sites is described by the parameter α that modifies the dissociation constant for the enzyme form with substrate bound in both active sites. In Eqn (1), $k_f$ denotes the rate of transformation (phosphorylation) of Pan, $E_T$ is the total enzyme concentration and $K_{Pan}$ is the dissociation

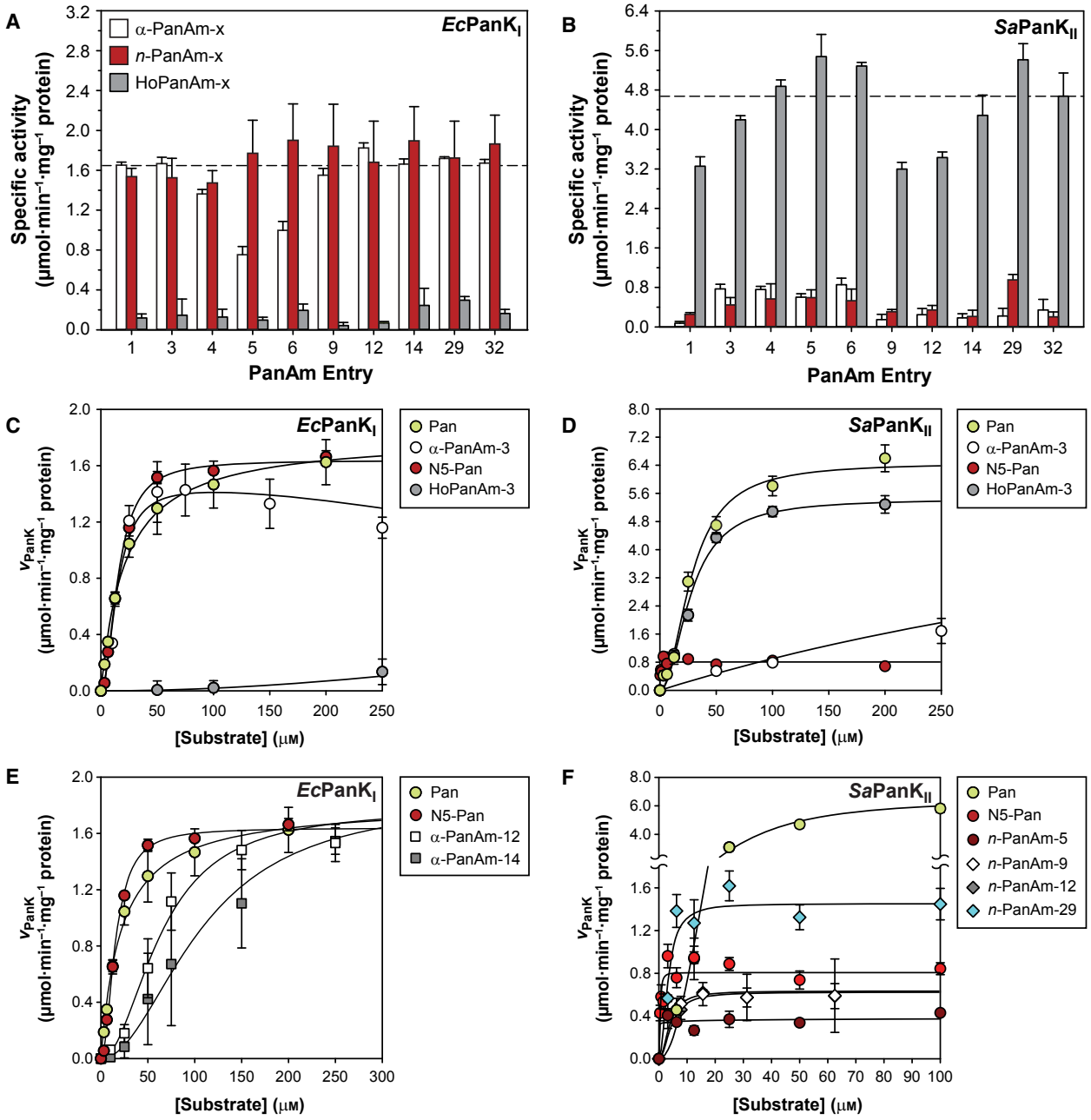


**Fig. 2.** Activity of *Ec*PanK$_I$ and *Sa*PanK$_{II}$ towards selected pantothenamides. (A) The specific activities for *Ec*PanK$_I$ towards Pan (dashed line) and the pantothenamides (bars) at 100 μM. The data were obtained from a single experiment performed in triplicate; the error bars denote the SD. (B) The data for *Sa*PanK$_{II}$ against Pan (dashed line) and the same panel of pantothenamides (bars). (C) Activity profiles for *Ec*PanK$_I$ with Pan, α-PanAm-3, N5-Pan and HoPanAm-3 as substrates. For information on statistical analysis and equations used to fit the data, see Table 2. (D) As for (C) but with *Sa*PanK$_{II}$. (E) *Ec*PanK$_I$ activity profiles with the *E. coli* growth inhibitory pantothenamides N5-Pan, α-PanAm-12 and α-PanAm-14 as substrates, with the Pan profile shown for comparison. Description and data analysis is as indicated for (C). (F) *Sa*PanK$_{II}$ activity profiles of the *S. aureus* growth inhibitory pantothenamides N5-Pan, *n*-PanAm-5 (N7-Pan), *n*-PanAm-9, *n*-PanAm-12 and *n*-PanAm-29, with the Pan profile shown for comparison. Note the *y*-axis break. Description and data analysis is as indicated for (C).

constant of Pan; $V_{max}$ is then equal to $2{\cdot}k_f{\cdot}E_T$, and $K_{0.5}^{Pan}$ (the $K_{0.5}$ value for Pan) is numerically equal to the concentration of Pan where $v_{PanK} = 0.5{\cdot}V_{max}$. Note that, from these conditions, it follows that $K_{Pan} = \sqrt{\alpha \cdot (K_{0.5}^{Pan})^2}$.

$$v_{\mathrm{PanK}} = 2 \cdot k_f \cdot [E_{\mathrm{Pan\cdot Pan}}] = \frac{2 \cdot k_f \cdot E_T \cdot \alpha \left(\frac{[\mathrm{Pan}]}{K_{\mathrm{Pan}}}\right)^2}{1 + \alpha \cdot \left(\frac{[\mathrm{Pan}]}{K_{\mathrm{Pan}}}\right)^2} = \frac{V_{\max} \cdot \left(\frac{[\mathrm{Pan}]}{K_{0.5}^{\mathrm{Pan}}}\right)^2}{1 + \left(\frac{[\mathrm{Pan}]}{K_{0.5}^{\mathrm{Pan}}}\right)^2} \quad (1)$$

Fitting Eqn (1) to the saturation data showed a good fit in all cases, as exemplified by the curve of *Sa*PanK$_{II}$ with Pan (Fig. 3C), and allowed determination of the relevant kinetic parameters. These values, summarized in Table 2, indicate that although for *E. coli* there is general agreement between a pantothenamide's growth inhibitory potency and the specific activity that *Ec*PanK$_I$ shows towards it, there is no direct correlation, as would be expected if the enzyme merely served as a gateway for the metabolic activation of these compounds, which subsequently have their inhibitory effect elsewhere. For *S. aureus*, potency correlates with compounds that have the unusual combination of very low (< 5 μM) values of $K_{0.5}$ and low turnover rates, and, consequently, very high apparent specificity constants ($k_{cat}/K_{0.5}$).

## N5-Pan has an inhibitory binding interaction with *Sa*PanK$_{II}$ but not with *Ec*PanK$_I$

To further investigate the importance of the activity profile differences, we obtained kinetic profiles for both enzymes acting on mixtures of Pan and N5-Pan; this pantothenamide was chosen for this particular experiment because it inhibits both *E. coli* and *S. aureus* growth and therefore allows for a comparative analysis. For each experiment, the total substrate concentration was increased at the same time as maintaining a constant ratio of Pan:N5-Pan; in subsequent experiments, the amount of Pan in the ratio was increased in a stepwise manner, from 0% (pure N5-Pan) to 100% (pure Pan). The combined turnover of Pan and N5-Pan was measured using the PK/LDH-based assay that responds to the formation of ADP.

The results demonstrate that, for *Ec*PanK$_I$, the resulting activity profiles show very small differences, and that there is a gradual progression from the profile for Pan to that for N5-Pan (Fig. 4A). However, for *Sa*PanK$_{II}$, even small amounts (i.e. 5%) of N5-Pan exert both an inhibitory effect (at mixture concentrations of 50 μM and higher) and an apparent stimulatory effect (at mixture concentrations of ~ 12.5 μM and below) on activity (Fig. 4B). Overall, the impact of N5-Pan on *Sa*PanK$_{II}$ activity is unexpectedly complex. In comparison, mixtures of Pan and HoPanAm-3, which acts as a substrate of *Sa*PanK$_{II}$ but does not show *S. aureus* growth inhibition, yielded essentially the same kinetic profile regardless of the composition of the substrate mixture (Fig. 4C). These results confirm that pantothenamides that show growth inhibition in

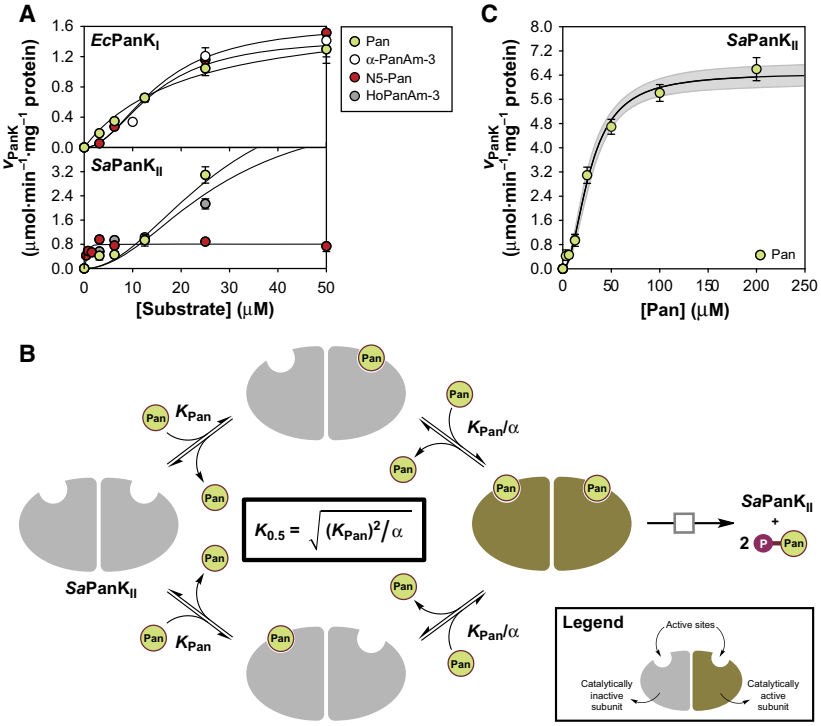


**Fig. 3.** Constructing a kinetic model for *Sa*PanK$_{II}$ activity. (A) Activity profiles for *Ec*PanK$_I$ and *Sa*PanK$_{II}$ shown in Fig. 2C,D at low substrate concentration to highlight the sigmoidal nature of the curves. (B) Schematic representation of the *Sa*PanK$_{II}$ kinetic model, based on an enzyme with two subunits, from which Eqn (1) is derived. $K_{Pan}$ is the dissociation constant of Pan, and α denotes the change in dissociation constant in the enzyme form with Pan bound to both subunits. This is the active form of the enzyme (shown in green), which catalyzes the phosphorylation reaction as denoted by the arrow with the open square. (C) Fitting Eqn (1) to the data points for the activity of *Sa*PanK$_{II}$ towards Pan, with the line indicating the best fit and the shaded area showing the 90% confidence interval. Parameter values and SEs are given in Table 2.

*S. aureus* have multifaceted interactions with its PanK enzyme, and that they do not simply act as alternative substrates.

### DL-4′-Deoxy-N5-Pan acts as an inhibitor of *Sa*PanK$_{II}$ turnover and *S. aureus* growth

To simplify the analysis of the interaction of N5-Pan with *Sa*PanK$_{II}$, we prepared its structural analogue DL-4′-deoxy-*N*-pentylpantothenamide (dN5) by $NaBH_4$-mediated reduction of a ketoamide precursor, to give the product as the racemate (Fig. 5A). This compound is expected to exclusively act as an inhibitor because it has the 4′-OH group of N5-Pan removed, thereby preventing it from being a PanK substrate (although all other binding interactions are retained).

Experiments were performed on both *Ec*PanK$_I$ and *Sa*PanK$_{II}$ using reaction mixtures that contained 25 μM Pan and increasing concentrations of either N5-Pan or dN5. The addition of N5-Pan increased the total observed activity for *Ec*PanK$_I$ as expected for an alternate substrate, whereas dN5 acted as a very poor inhibitor of the enzyme ($IC_{50}$ ~ 500 μM) (Fig. 5B). Full kinetic analysis subsequently indicated that this is the result of a minor reduction of the $V_{max}^{app}$ (data not shown), confirming that the 4′-OH group is an important determinant for ligand binding in *Ec*PanK$_I$ [26].

By contrast, both N5-Pan and dN5 showed the same apparent inhibitory effect on *Sa*PanK$_{II}$ with $IC_{50}$ values of 4.8 ± 1.2 and 7.3 ± 0.9 μM, respectively (Fig. 5C). For this enzyme, full kinetic analysis again showed a dual effect (Fig. 5D), with dN5 causing a small but significant reduction in the $K_{0.5}^{app}$ for Pan and a large reduction in the $V_{max}^{app}$. Additionally, growth inhibition tests performed in minimal medium showed that dN5 has a MIC of ~ 50 μM for *S. aureus* but does not inhibit *E. coli* (Fig. 6). By comparison, N5-Pan still has a much lower MIC (approximately 1.5 μM) for *S. aureus* under these conditions. Nonetheless, this result unambiguously shows that even pantothenamide analogues unable to act as PanK substrates have a negative impact on *S. aureus* growth.

### Expanding the kinetic model to account for complex interaction of N5-Pan with *Sa*PanK$_{II}$

We next used the dN5 data to expand the kinetic model for *Sa*PanK$_{II}$ to include a mechanism that could account for the dual stimulatory/inhibitory effect exerted by both dN5 and N5-Pan. Because the N5-Pan saturation kinetics did not show substrate inhibition at high concentrations, we started with an uncompetitive inhibition mechanism for dN5 [i.e. one in which it only binds to the *Sa*PanK$_{II}$–Pan ([$E_{Pan}$]) complex]. In addition, we also included a competitive inhibition mechanism in which dN5 can bind to any unoccupied active site. This led to the mechanistic scheme shown in Fig. 7A, which can be translated into a rate equation that assumes that only the [$E_{Pan.Pan}$], [$E_{Pan.dN5}$] and [$E_{dN5.Pan}$] complexes have catalytic activity, and in which no enzyme form that has only one active site occupied is considered (Eqn 2). The parameters in this equation are defined as those used in Eqn (1), with the addition of $K_{dN5}$ (dissociation constant for the competitive inhibition by dN5) and $K_{dN5'}$ (dissociation constant for the uncompetitive inhibition by dN5): Equation (2) was able to describe the data very well (Fig. 5D, solid lines) and accounted for both the stimulatory effect of the inhibitor at low substrate concentrations and the reduction in $V_{max}^{app}$ at high substrate concentrations. These effects are based on the dissociation constants for the binding of dN5 in a competitive ($K_{dN5}$ = 3.81 ± 0.45 μM) and uncompetitive ($K_{dN5'}$ = 41.0 ± 7.1 μM) binding mode, respectively, which clearly show that, for dN5, the former is the stronger interaction (Table 3). Additionally, the dissociation constant for Pan ($K_{Pan}$ = 9.31 ± 0.70 μM) and the value for α (0.111 ± 0.017 μM) were also calculated in this manner. The $K_{0.5}$ value of 27.9 μM calculated from these values is almost identical to the value of 27.8 μM obtained by fitting Eqn 1 to the Pan activity profile (Fig. 3C and Table 2).

The newly expanded mechanism can easily account for the data obtained from *Sa*PanK$_{II}$ acting on mixtures of Pan and N5-Pan (Fig. 4B) by modifying the competitive inhibition component exerted by dN5 to that of a competitive substrate with catalytic turnover. This confers activity on the two boxed complexes in

$$v_{PanK} = 2 \cdot k_f \cdot [E_{Pan\cdot Pan}] + 2 \cdot k_f \cdot [E_{Pan\cdot dN5}] = \frac{V_{max} \cdot \left(\frac{[Pan]}{K_{Pan}}\right) \cdot \left(\alpha \cdot \frac{[Pan]}{K_{Pan}} + \frac{[dN5]}{K_{dN5}}\right)}{1 + \alpha \cdot \left(\frac{[Pan]}{K_{Pan}}\right)^2 \cdot \left(1 + \left(\frac{[dN5]}{K_{dN5'}}\right)^2\right) + 2 \cdot \left(\frac{[Pan]\cdot[dN5]}{K_{Pan}\cdot K_{dN5}}\right) \cdot \left(1 + \frac{[dN5]}{K_{dN5'}}\right) + \left(\frac{[dN5]}{K_{dN5}}\right)^2} \quad (2)$$

**Table 2.** PanK kinetic parameters with Pan and various pantothenamides. Kinetic parameters were determined by keeping the ATP concentration constant at 1.5 mM in all cases. All reported parameters are the mean of those obtained by fitting the given equation to the data obtained for each individual experiments; the error values represent the range/2 (for parameters obtained from two independent experiments) or SEM (for parameters obtained from three or more independent experiments). References to compounds tested in previous studies are provided in the main text. ND, not determined.

| | *Ec*PanK$_I$ | | | | | | *Sa*PanK$_{II}$ | | | | | |
|---|---|---|---|---|---|---|---|---|---|---|---|---|
| Compound | $K_{0.5}$[a] (μM) | $k_{cat}$ ($s^{-1}$) | $k_{cat}/K_{0.5}$[a] ($mM^{-1}.s^{-1}$) | $N$[b] | Equation fitted | $R^2$ value[c] | $K_{0.5}$ (μM) | $k_{cat}$ ($s^{-1}$) | $k_{cat}/K_{0.5}$ ($mM^{-1}.s^{-1}$) | $N$[b] | Equation fitted | $R^2$ value[c] |
| Pan | 21.3 ± 1.4 | 1.16 ± 0.14 | 54.5 ± 3.1 | 2 | Michaelis–Menten | 0.9955 | 27.8 ± 3.3 | 3.37 ± 0.24 | 124 ± 7 | 4 | Eqn (1) | 0.9928 |
| α-PanAm-3 | 14.6 ± 1.1 | 0.95 ± 0.13 | 64.3 ± 4.3 | 2 | Modified Eqn (1)[d] | 0.9679 | 783 ± 64 | 4.14 ± 0.14 | 5.29 ± 0.62 | 1[e] | Michaelis–Menten | 0.8719 |
| *n*-PanAm-3 [N5-Pan] | 15.6 ± 1.2 | 1.06 ± 0.03 | 68.6 ± 3.4 | 2 | Eqn (1) | 0.9988 | < 1.5[f] | 0.44 ± 0.03 | > 290 | 4 | Eqn (1) | 0.8606 |
| HoPanAm-3 | 720 ± 95 | 0.62 ± 0.04 | 0.87 ± 0.17 | 1[e] | Eqn (1) | 0.8866 | 27.8 ± 2.3 | 2.85 ± 0.11 | 103 ± 6 | 3 | Eqn (1) | 0.9740 |
| α-PanAm-12 | 63 ± 11 | 1.05 ± 0.12 | 18.2 ± 4.3 | 3 | Eqn (1) | 0.9881 | ND | | | | | |
| α-PanAm-14 | 151 ± 56 | 1.37 ± 0.15 | 13.8 ± 6.6 | 3 | Eqn (1) | 0.9911 | ND | | | | | |
| *n*-PanAm-5 [N7-Pan] | ND | | | | | | 2.04 ± 0.54 | 0.22 ± 0.02 | 118 ± 41 | 2 | Eqn (1) | 0.8677 |
| *n*-PanAm-9 | ND | | | | | | 4.94 ± 0.94 | 0.33 ± 0.12 | 65.4 ± 11.8 | 2 | Eqn (1) | 0.9711 |
| *n*-PanAm-12 | ND | | | | | | 4.47 ± 0.11 | 0.32 ± 0.04 | 72.7 ± 10.0 | 2 | Eqn (1) | 0.9326 |
| *n*-PanAm-29 | ND | | | | | | 3.49 ± 0.50 | 0.75 ± 0.06 | 232 ± 59 | 3 | Eqn (1) | 0.9326 |
| PantSH | 23.6 ± 2.1 | 1.00 ± 0.09 | 42.4 ± 0.3 | 3 | Michaelis–Menten | 0.9949 | < 1.5[f] | 0.39 ± 0.09 | > 260 | 4 | Eqn (1) | 0.8714 |

[a] In those cases where the Michaelis–Menten equation was used to fit the data, $K_{0.5}$ is $K_m$.

[b] Number of independent experiments.

[c] $R^2$ value for the indicated equation fitted to the data averaged from all the experiments.

[d] α-PanAm-3 showed inhibition of *Ec*PanK$_I$ at high substrate concentrations; using a modified version of Eqn (1) that accounts for the uncompetitive substrate inhibition, a $K_i$ of 720 ± 120 μM was determined.

[e] As a result of the high $K_{0.5}$ value, kinetic parameters were determined by fitting the equation to the data from a single experiment performed in triplicate; errors indicate the SE of the fit.

[f] The low $K_{0.5}^{app}$ values of these compounds cannot be reported with accuracy because they fall below the sensitivity limit of the assay.

Fig. 7A as shown in Fig. 7B, and gives the corresponding rate equation Eqn (3) that was fitted to the Pan/N5-Pan experimental data, constraining the values for $V_{max}^{Pan}$ (the $V_{max}$ for Pan), $K_{Pan}$ and α to those obtained before. In this equation, $k_f^{Pan}$ and $k_f^{N5\text{-}Pan}$ denote the rates of phosphorylation of Pan and N5-Pan respectively, giving $V_{max}^{Pan} = 2 \cdot k_f^{Pan} \cdot E_T$ for Pan and $V_{max}^{N5\text{-}Pan} = 2 \cdot k_f^{N5\text{-}Pan} \cdot E_T$ for N5-Pan. Additionally, $K_{N5\text{-}Pan}$ is the dissociation constant of N5-Pan acting as a substrate, whereas $K_{N5\text{-}Pan'}$ is the dissociation constant for the uncompetitive inhibition component that it exerts:

The equation provided a very good description of the experimental data set (Fig. 8A) and gave the parameter values listed in Table 3. These indicate that, although the dissociation constant of N5-Pan for binding at the active site (i.e. as a substrate) is similar to that of dN5 ($K_{N5\text{-}Pan}$ = 2.22 ± 0.48 μM), its dissociation constant for binding as an uncompetitive inhibitor ($K_{N5\text{-}Pan'}$ = 4.89 ± 0.66 μM) is much smaller. Because N5-Pan also has a much reduced MIC compared to dN5, this provides additional evidence for the uncompetitive inhibition of *Sa*PanK$_{II}$ as an important contributor to the inhibition of *S. aureus* growth by N5-Pan.

$$\begin{aligned} v_{PanK} &= 2 \cdot k_f^{Pan} \cdot [E_{Pan\cdot Pan}] + 2 \cdot k_f^{Pan} \cdot [E_{Pan\cdot N5\text{-}Pan}] + 2 \cdot k_f^{N5\text{-}Pan} \cdot [E_{N5\text{-}Pan\cdot N5\text{-}Pan}] + 2 \cdot k_f^{N5\text{-}Pan} \cdot [E_{N5\text{-}Pan\cdot Pan}] \\ &\quad + 2 \cdot k_f^{N5\text{-}Pan} \cdot [E_{N5\text{-}Pan\cdot Pan}^{N5\text{-}Pan}] \\ &= \frac{V_{max}^{Pan} \cdot \left(\frac{[Pan]}{K_{Pan}}\right) \cdot \left(\alpha \cdot \frac{[Pan]}{K_{Pan}} + \frac{[N5\text{-}Pan]}{K_{N5\text{-}Pan}}\right) + V_{max}^{N5\text{-}Pan} \cdot \left(\frac{[N5\text{-}Pan]}{K_{N5\text{-}Pan}}\right) \cdot \left(\frac{[N5\text{-}Pan]}{K_{N5\text{-}Pan}} + \frac{[Pan]}{K_{Pan}} + \left(1 + \frac{[N5\text{-}Pan]}{K_{N5\text{-}Pan'}}\right)\right)}{1 + \alpha \cdot \left(\frac{[Pan]}{K_{Pan}}\right)^2 \cdot \left(1 + \left(\frac{[N5\text{-}Pan]}{K_{N5\text{-}Pan'}}\right)^2\right) + 2 \cdot \left(\frac{[Pan]\cdot[N5\text{-}Pan]}{K_{Pan}\cdot K_{N5\text{-}Pan}}\right) \cdot \left(1 + \frac{[N5\text{-}Pan]}{K_{N5\text{-}Pan'}}\right) + \left(\frac{[N5\text{-}Pan]}{K_{N5\text{-}Pan}}\right)^2} \end{aligned} \quad (3)$$

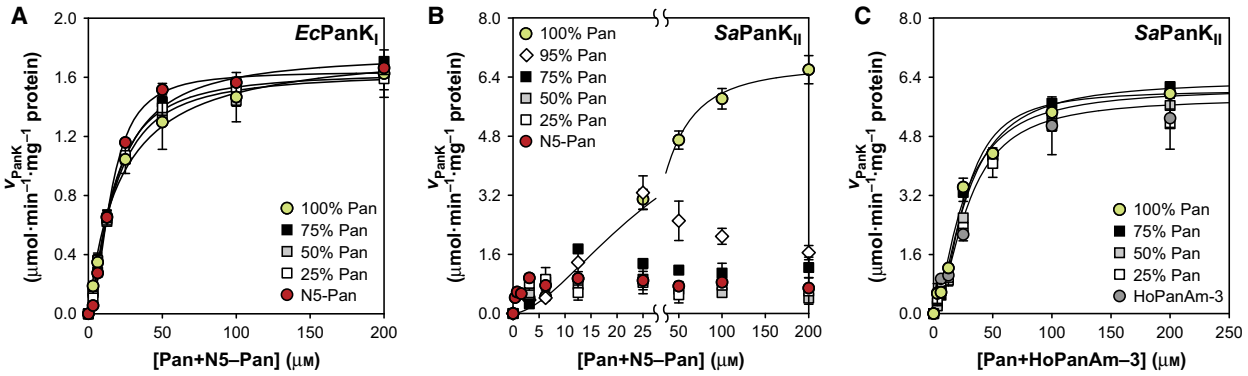


**Fig. 4.** Analyzing the interaction of Pan and N5-Pan with *Ec*PanK$_I$ and *Sa*PanK$_{II}$ under competitive conditions. (A) Kinetic profiles of mixtures of Pan and N5-Pan determined with *Ec*PanK$_I$. The *x*-axis indicates the total substrate concentration (Pan and N5-Pan combined); for each data set, the ratio of Pan:N5-Pan was kept at a constant value. The data points represent the mean of two independent experiments, each performed in triplicate; the error bars denote the range/2. Because the curves progress from a hyperbolic to a sigmoidal shape, the solid lines represent the best fit of the data to the Hill equation with the value for *h* (Hill coefficient) constrained to between 1 and 2. (B) Kinetic profiles of mixtures of Pan and N5-Pan determined with *Sa*PanK$_{II}$ as described for (A). The solid line represents the best fit of Eqn (1) to the 100% Pan data. (C) Kinetic profiles of mixtures of Pan and HoPanAm-3 determined for *Sa*PanK$_{II}$ as described for (A).

In the absence of Pan, Eqn (3) reduces to a much simpler form (Eqn 4), which describes the saturation kinetics of inhibitory pantothenamides such as N5-Pan.

$$v_{\mathrm{PanK}} = 2 \cdot k_f^{\mathrm{N5\text{-}Pan}} \cdot [E_{\mathrm{N5-Pan\cdot N5\text{-}Pan}}] = \frac{V_{\mathrm{max}}^{\mathrm{N5-Pan}} \cdot \left(\frac{[\mathrm{N5\text{-}Pan}]}{K_{\mathrm{N5\text{-}Pan}}}\right)^2}{1 + \left(\frac{[\mathrm{N5\text{-}Pan}]}{K_{\mathrm{N5\text{-}Pan}}}\right)^2} \quad (4)$$

This equation is equivalent to Eqn (1), which was used to obtain the parameters shown in Table 2, if $K_{0.5} = K_{\mathrm{Pan}}$ (i.e. if $\alpha = 1$). This would indicate that there is no differentiation in the binding of N5-Pan to the enzyme's two active sites.

## *Sa*PanK$_{II}$ atypical kinetic mechanism follows from its role in CoA salvage biosynthesis

The question arises as to why there is such a selective binding site in *Sa*PanK$_{II}$ that it accepts N5-Pan at the same time as excluding HoPanAm-3 (note that the latter did not show any uncompetitive inhibition mode; Fig. 4C). Clearly, the selectivity is for compounds that contain the natural β-alanine moiety, suggesting that the site is predisposed to bind compounds containing the native pantothenoyl group. Based on its close structural similarity to *n*-PanAm series compounds (such as N5-Pan), we considered PantSH (the substrate of the CoA salvage pathway; Fig. 1A) as the most likely natural ligand for this binding site.

To test such a hypothesis, we measured the activity of *Ec*PanK$_I$ and *Sa*PanK$_{II}$ against mixtures that contained 25 μM Pan and increasing concentrations of PantSH. The results are strikingly similar to those obtained for N5-Pan, with PantSH increasing the total observed activity for *Ec*PanK$_I$ but inhibiting *Sa*PanK$_{II}$ activity (Fig. 8B). Similarly, when constant ratio mixtures of Pan and PantSH were analyzed as conducted for N5-Pan, the profiles clearly demonstrate that PantSH has the same complex interaction with *Sa*PanK$_{II}$ (Fig. 8C), showing both a stimulatory (at low concentrations) and an inhibitory (at high concentrations) effect on turnover that is even more pronounced than that caused by N5-Pan. Based on the similarity between N5-Pan and PantSH, Eqn (3) was used to describe the Pan/PantSH experimental data by substituting PantSH for N5-Pan, and again constraining the $V_{\mathrm{max}}^{\mathrm{app}}$, $K_{\mathrm{Pan}}$ and α values to those obtained previously. The equation was able to describe the experimental data set well (Fig. 8C), and gave values for $K_{\mathrm{PantSH}}$ (binding at the active site, i.e. as substrate) and $K_{\mathrm{PantSH'}}$ (binding in an uncompetitive mode) of $0.46 \pm 0.08$ μM and $6.03 \pm 1.27$ μM, respectively (Table 3). In comparison with the values obtained for N5-Pan, PantSH appears to be the better substrate at the same time as showing similar uncompetitive inhibition to N5-Pan. Consequently, PantSH is more effective at activating *Sa*PanK$_{II}$ at low substrate concentrations (Fig. 8A,C, insets). Interestingly, when the activity of *Sa*PanK$_{II}$ activity against constant ratio mixtures of Pan and *n*-PanAm-5 (N7-Pan, the most potent *S. aureus* growth inhibitor) was measured and analyzed in a similar manner, the obtained kinetic parameters were almost identical to those found for PantSH (data not shown). Taken together, these results strongly suggest that pantothenamides showing

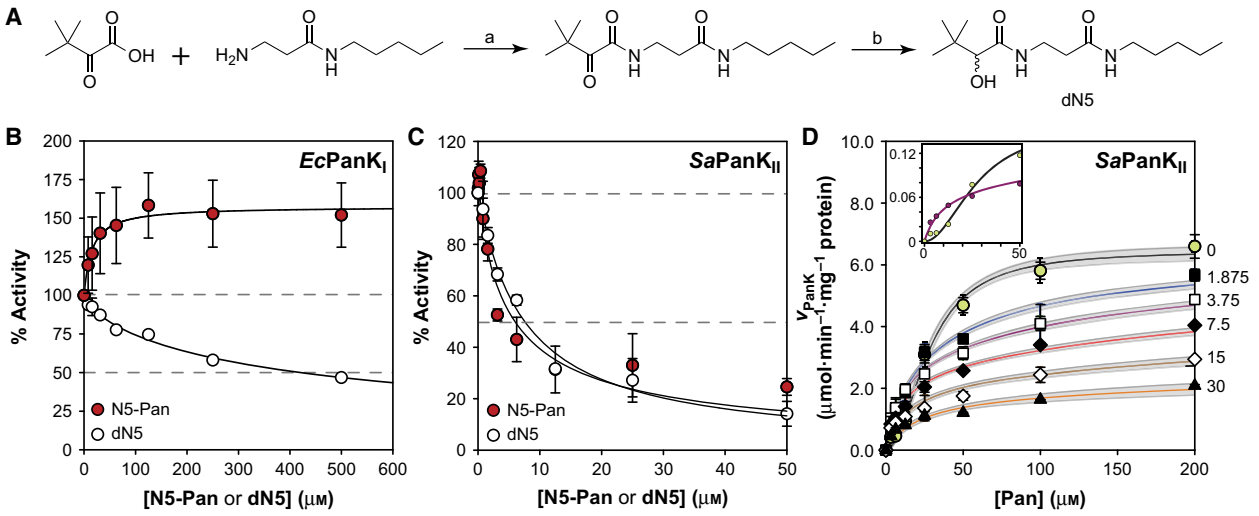


**Fig. 5.** dN5 as a PanK inhibitor. (A) Synthetic scheme for the preparation of dN5. (a) 1-Ethyl-3-(3-dimethylaminopropyl) carbodiimide hydrochloride (EDC), hydroxybenzotriazole (HOBt), *N,N*-diisopropylethylamine (DIPEA), $CH_2Cl_2$; (b) $NaBH_4$, methanol. (B) Activity/inhibition profiles for *Ec*PanK$_I$ when treated with N5-Pan and dN5 at a fixed concentration of 25 μM Pan. The data points represent the mean of two independent experiments, each performed in triplicate; the error bars denote the range/2. The solid lines represent the best fits to the Michaelis–Menten equation (for N5-Pan) or to Eqn (5) (for dN5). (C) Inhibition profiles for *Sa*PanK$_{II}$ as described for *Ec*PanK$_I$ in (A). (D) Kinetic profiles for *Sa*PanK$_{II}$ with Pan in the presence of increasing concentrations of dN5 (indicated on the right of each curve). The data points represent the mean of two independent experiments, each performed in triplicate; the error bars denote the range/2. The solid lines represent the best fit curves obtained by fitting Eqn (2) to all the data; the shaded areas indicate the 90% confidence intervals. The insert shows the stimulatory effect of the inhibitor at low substrate concentrations which results from the change Pan's saturation kinetics profile from sigmoidal for Pan only (black) to hyperbolic for Pan in the presence of 3.75 μM dN5 (purple).

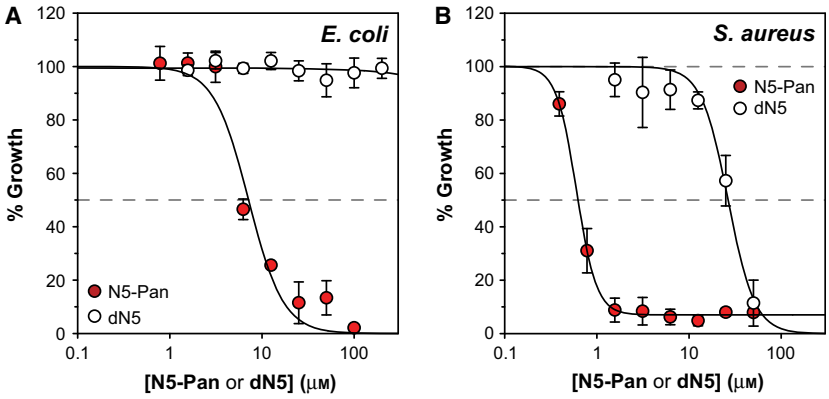


**Fig. 6.** dN5 as a bacterial cell growth inhibitor. (A) Growth inhibition profiles for *E. coli* grown in minimal medium in the presence of increasing concentrations of N5-Pan and DL-4′-deoxy-N5-Pan (dN5). The data points represent the mean of two independent experiments, each performed in triplicate; the error bars denote the range/2. The solid lines represent the best fits to Eqn (5). (B) Growth inhibition profiles for *S. aureus* grown in minimal medium as described for *E. coli* in (A).

inhibition of *S. aureus* growth mimic the interactions of PantSH with *Sa*PanK$_{II}$.

## Discussion

Although several previous studies have investigated the growth inhibitory potency of pantothenamides against various bacteria, and/or have shown that these compounds act as substrates of the target organisms' PanK enzymes, none have been able to establish a clear link between these two features [1,6–8,12,14–16,26,32,37]. In the present study, we performed the first detailed comparative kinetic analysis of pantothenamides that cause bacterial growth inhibition, showing that PanK type determines their mode of action. For organisms with PanK$_I$ enzymes, our data indicate that pantothenamides only show growth inhibition if they are accepted as alternate PanK substrates. This corresponds to these compounds having a mode of action

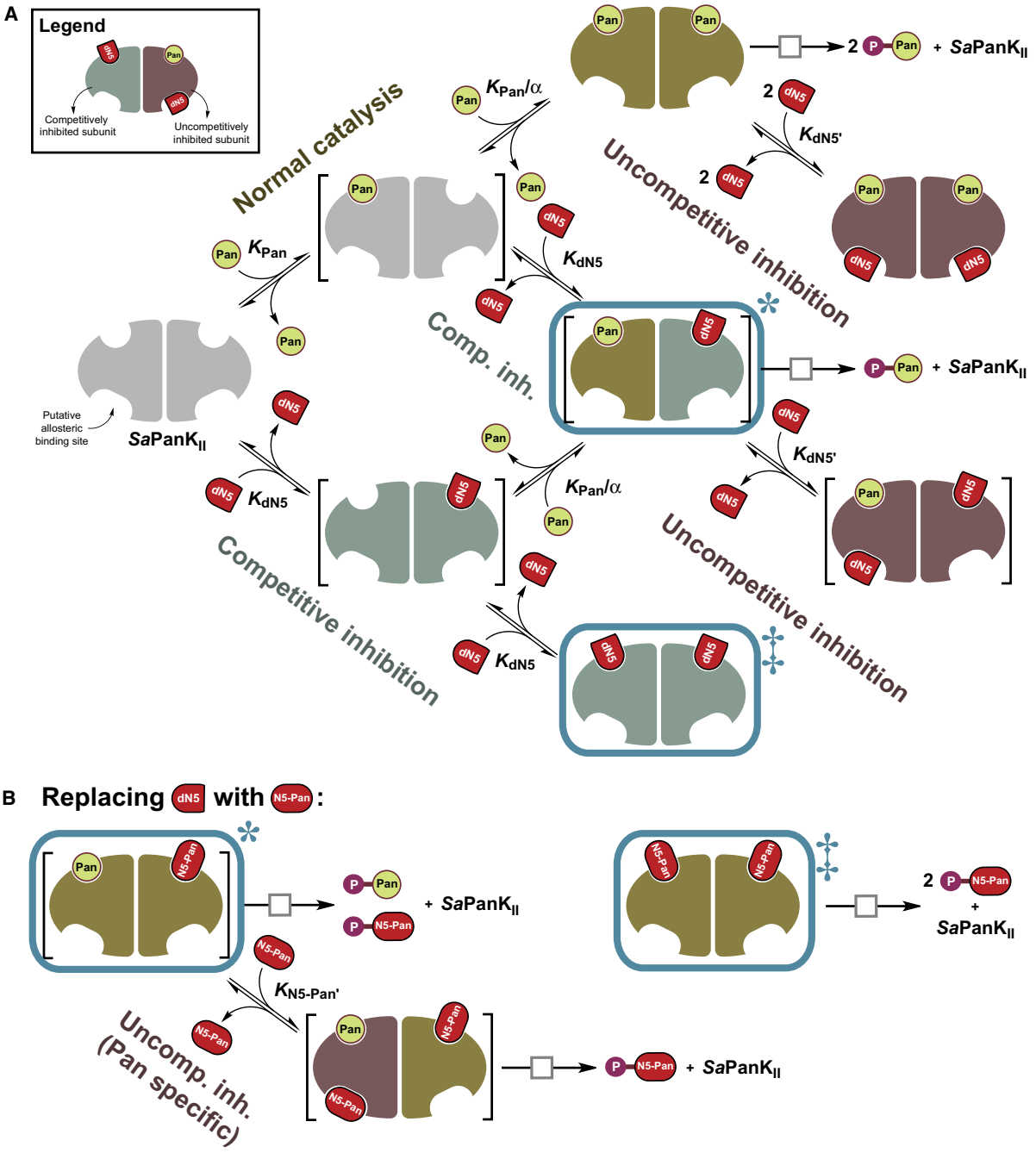


**Fig. 7.** Kinetic model for the interaction of dN5 and N5-Pan with *Sa*PanK$_{II}$. (A) Schematic representation of the *Sa*PanK$_{II}$ kinetic model adapted to account for the dual stimulatory/inhibitory effect shown by d5N. $K_{Pan}$ is the dissociation constant of Pan and α denotes the change in dissociation constant in the enzyme form with Pan bound to both subunits. $K_{dN5}$ denotes the dissociation constant for competitive inhibition, whereas $K_{dN5'}$ is the dissociation constant for uncompetitive inhibition. Note that, for the latter, it is assumed that inhibition takes place through binding at an allosteric site as shown, although no evidence for such a site has yet been found. For enzyme complexes shown in square brackets, the symmetrical alternative complex is not shown but implied. All active enzyme subunits are shown in green, whereas the competitively and uncompetitively inhibited complexes are shown in shades of grey as indicated. (B) The model shown in (A) can be modified to account for the interaction of the N5-Pan with *Sa*PanK$_{II}$ by converting the two competitively inhibited complexes [boxed and identified with an asterisk (*) and double dagger (‡), respectively] to catalytically active complexes that phosphorylates N5-Pan (and Pan) as indicated. $K_{N5\text{-}Pan'}$ is the dissociation constant for the uncompetitive inhibition shown by N5-Pan.

**Table 3.** Kinetic parameters for *Sa*PanK$_{II}$ determined from fitting various data sets to the indicated equations.

| Data set | Equation | Parameter | Value[a] | Unit |
|---|---|---|---|---|
| dN5 inhibition data (Fig. 5D) | Eqn (2) | $V_{max}$ | 6.47 ± 0.15 | μmol·min$^{-1}$·mg |
| | | $K_{Pan}$ | 9.31 ± 0.70 | μM |
| | | α | 0.111 ± 0.017 | |
| | | $K_{dN5}$ (competitive inhibition) | 3.81 ± 0.45 | μM |
| | | $K_{dN5'}$ (uncompetitive inhibition) | 41.0 ± 7.1 | μM |
| Pan:N5-Pan mix data (Fig. 4B; Fig. 8A) | Eqn (3) | $V_{max}^{N5\text{-}Pan}$ | 0.755 ± 0.100 | μmol·min$^{-1}$·mg |
| | | $K_{N5\text{-}Pan}$ (substrate) | 2.22 ± 0.48 | μM |
| | | $K_{N5\text{-}Pan'}$ (uncompetitive inhibition) | 4.89 ± 0.66 | μM |
| Pan:PantSH mix data (Fig. 8C) | Eqn (3)[b] | $V_{max}^{PantSH}$ | 0.656 ± 0.061 | μmol·min$^{-1}$·mg |
| | | $K_{PantSH}$ (substrate) | 0.46 ± 0.08 | μM |
| | | $K_{PantSH'}$ (uncompetitive inhibition) | 6.03 ± 1.27 | μM |

[a]Errors indicate the SE.
[b]PantSH replaces N5-Pan in Eqn (3) as written.

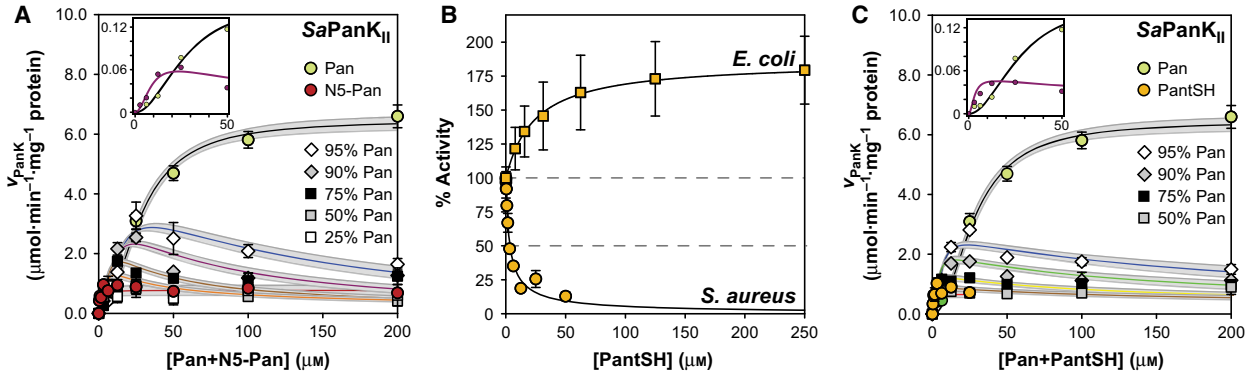


**Fig. 8.** The interaction of *Sa*PanK$_{II}$ with PantSH mimics that of N5-Pan. (A) Fitting Eqn (3) to the data obtained from *Sa*PanK$_{II}$ acting on mixtures of Pan and N5-Pan (Fig. 3B); the solid lines represent the best fit curves, whereas the shaded areas indicate the 90% confidence intervals. The insert shows the stimulatory effect caused by the presence of 5% N5-Pan (purple) compared to the 100% Pan curve (black). (B) Inhibition profiles for *Ec*PanK$_I$ and *Sa*PanK$_{II}$ treated with PantSH at a fixed concentration of 25 μM Pan. The data points represent the mean of two independent experiments, each performed in triplicate; the error bars denote the range/2. The solid lines represent the best fits to the Michaelis–Menten equation (for *Ec*PanK$_I$) or Eqn (S5) (for *Sa*PanK$_{II}$). (C) Kinetic profiles of mixtures of Pan and PantSH determined with *Sa*PanK$_{II}$ performed and analyzed as for (A).

that is dependent on their metabolic activation to form inhibitory CoA antimetabolites and/or inactive *crypto*-ACPs, and that these act as inhibitors of target(s) downstream of CoA biosynthesis. Such an analysis is in agreement with the conclusions of previous studies [8,12] and is supported by recent crystallographic data showing that growth inhibitory pantothenamides bind to PanK$_I$ enzymes in a manner similar to Pan [38,39].

For *S. aureus*, which is the only bacterium known to have an active type II PanK, the situation is very different. Specifically, we demonstrate that growth inhibitory pantothenamides have a complex interaction with this organism's PanK enzyme, acting as substrates that stimulate its activity when present at low concentrations but turning into uncompetitive inhibitors as their concentrations gradually increase. Additionally, we show that a pantothenamide analogue that cannot act as PanK substrates can still inhibit *S. aureus* growth. Taken together, these results clearly show that, in this organism, growth inhibition is likely the result of several factors working in combination: first, by being converted into CoA antimetabolites and *crypto*-ACPs (and having concomitant negative effects on fatty acid biosynthesis as was found in a previous study) [14] and, second, by reducing CoA levels by inhibiting the first step of its biosynthesis. This multifaceted mode of action is most likely one of the reasons why the pantothenamides (such as N7-Pan) show much higher potency against

*S. aureus* than any other bacterium that has been tested to date.

The kinetic model that was constructed for *Sa*PanK$_{II}$ provides an accurate description of the various data sets obtained for the enzyme acting on its native substrate (Pan), on various pantothenamides and on combinations of the two. Specifically, our model indicates that *Sa*PanK$_{II}$ is inhibited by the pantothenamides (and by PantSH) via an uncompetitive mechanism, which would imply the existence of an allosteric site in which *n*-PanAm series compounds bind. However, only two *Sa*PanK$_{II}$ structures have been deposited in the Protein Data Bank to date, neither of which has the natural substrate Pan bound. These structures provide no indication of the likely location of such an allosteric site. Moreover, the more recently published structure [i.e. that of a ternary complex of the enzyme bound to a phosphorylated pantothenamide (N354-Pan) and ADP (Protein Data Bank code: 4NB4)] [39] indicates that the enzyme has distinct open and closed conformations, with the latter preventing the product from being released; this discovery complicates the structural investigation of a potential uncompetitive inhibition mode through allosteric inhibition even further. Consequently, we cannot exclude the possibility that alternative kinetic models (including those that do not need to invoke the existence of an allosteric site) could also provide accurate descriptions of our data. Nonetheless, our proposed mechanism is the simplest one giving an accurate description of the total data set at the same time as taking all the information that is currently available on the enzyme into account.

Regardless of the mechanism or structural basis of the interaction between the growth inhibitory pantothenamides and *Sa*PanK$_{II}$, our finding that PantSH (the only pantothenamide known to occur naturally) [40,41] mirrors this complex and specific interaction suggests that it is a native ligand of the enzyme. Such a characteristic could be a compensatory regulatory mechanism for *Sa*PanK$_{II}$ because, unlike other type I and type II PanKs, this enzyme does not experience any feedback inhibition by CoA or its thioesters [14]. This is most likely as result of *S. aureus* maintaining higher levels of intracellular CoA as part of its unique redox biology because it does not contain any glutathione but instead uses CoA (and most likely the recently discovered low molecular weight thiol bacillithiol), as well as a highly specific CoA disulfide reductase, to maintain its intracellular redox potential [42,43]. Our findings suggest that CoA biosynthesis in *S. aureus* may be regulated by a unique mechanism in which PantSH stimulates *Sa*PanK$_{II}$ activity when it is present at low concentrations but inhibits it at high concentrations. Such an analysis is supported by previous findings showing that P-PantSH does not accumulate in either intra- or extracellular compartments, confirming that the regulation of CoA biosynthesis in *S. aureus* apparently occurs at the level of *Sa*PanK$_{II}$ [14].

Clearly, such a conclusion has important implications for *S. aureus* physiology that will have to be explored further, especially in light of the fact that the CoA and ACP degradation pathways responsible for PantSH formation remain very poorly characterized in all organisms [2]. Nonetheless, the evidence reported in the present study suggests that the specific interaction of *Sa*PanK$_{II}$ with PantSH presents a unique opportunity for the development of new antistaphylococcal agents, one which the pantothenamides have already started to exploit.

## Materials and methods

### General materials and methods

All the pantothenamides and precursors were prepared and their purity confirmed by $^{1}$H NMR analysis, as described previously [23]. The pantothenamides were dissolved in 50% acetonitrile–water solution to yield stock solutions at a concentration of 50 mM and assays were performed with the final acetonitrile concentration never exceeding 3% (v/v). Pantetheine was obtained by the reduction of the disulfide pantethine (Sigma-Aldrich, St Louis, MO, USA) in the presence of 1.5 equivalents of dithiothreitol or tris(2-carboxyethyl)phosphine. General chemicals, reagents and media were purchased from Sigma-Aldrich, Merck Chemicals (Darmstadt, Germany) or Acros Organics (Thermofisher, Fair Lawn, NJ, USA) and were of the highest purity. Solvents used for reactions were Chromasolv HPLC grade solvents (Sigma-Aldrich) and the hexanes, dichloromethane and ethyl acetate used for purification were purchased from Merck Chemicals. Dry *N*,*N*-dimethylformamide was prepared by shaking up over potassium hydroxide, distilled under reduced pressure and a nitrogen atmosphere, and finally stored over 4-Å molecular sieves in the dark. Dry dichloromethane was distilled from $CaH_2$ under a nitrogen atmosphere.

The *E. coli* K12 strain was available in our laboratory, whereas *S. aureus* RN4220 and *P. aeruginosa* ATCC 27853 where kind gifts from L. M. T. Dicks at the Department of Microbiology (Stellenbosch University). *Ec*PanK$_{I}$ and *Sa*PanK$_{II}$ were overexpressed and purified as described previously [7,14,34]. PK and LDH used in the kinetic assays were obtained from Roche (Basel, Switzerland).

All $^{1}$H and $^{13}$C NMR spectra were obtained using a 300-MHz Varian VNMRS (75 MHz for $^{13}$C) or 400-MHz Varian Unity Inova (100 MHz for $^{13}$C) instruments (Varian

Inc., Palo Alto, CA, USA) at the Central Analytical Facility (CAF) of the University of Stellenbosch. All chemical shifts (δ) were recorded using the residual solvent peak and reported in p.p.m. All high resolution mass spectrometry (HRMS) was performed on a Waters API Q-TOF Ultima spectrometer (Waters, Milford, MA, USA) at the MS unit of CAF. All $OD_{600}$ measurements and kinetic studies were performed using a Thermo Varioskan spectrophotometer (Thermo Scientific, Bremen, Germany). Inhibition studies were performed in Greiner Bio-One Cellstar flat-bottomed 96-well suspension plates (Greiner Bio-One GmbH, Frickenhausen, Germany). Kinetic studies were performed in Greiner Bio-One polystyrene flat-bottomed 96-well plates. The MICs were determined by plotting the percentage (relative to a control containing no inhibitor) bacterial cell growth against the logarithm of increasing compound concentration, followed by fitting Eqn (5) to the data (with the values of $y_0$ and $a$ generally fixed at 0 and 100, respectively).

$$y = y_0 + \frac{a}{1 + \left(\frac{x}{IC_{50}}\right)^b} \quad (5)$$

Kinetic data were fitted according to the derived equations. Analysis of all concentration–response curves and kinetic data was carried out using SIGMAPLOT, version 12 (Systat Software Inc., Chicago, IL, USA) or MATHEMATICA (Wolfram Research, Champaign, IL, USA).

## Synthesis of dN5

### Benzyl-3-oxo-3(pentylamino)propylcarbamate

Pentylamine (803 μL, 6.96 mmol) and diethyl phosphoryl cyanide (1.05 mL, 7.25 mmol) were added to a solution of CBz-β-alanine (1.41 g, 6.32 mmol) in dry *N*,*N*dimethylformamide (8 mL) at room temperature. The reaction mixture was cooled to 0 °C before triethylamine (1.85 mL, 13.3 mmol) was added. The reaction mixture was stirred for 2 h at 0 °C and left to stir overnight at room temperature. Ethyl acetate (50 mL) was added and the organic layer was washed sequentially with 5% citric acid (3 × 10 mL), 1 M aqueous $NaHCO_3$ (2 × 10 mL) and saturated sodium chloride (1 × 10 mL). The organic layer was dried ($Na_2SO_4$), filtered and concentrated *in vacuo* before purification by flash column chromatography (3:2 to 4:1 ethyl acetate:hexanes) afforded the carbamate (1.50 g, 81%) as a white solid. $R_f$ = 0.18. $\delta_H$ (300 MHz; $CDCl_3$) 0.87 (3H, t, $J$ = 6.9 Hz, $-CH_3$), 1.26–1.33 (4H, m, $-CH_2-$), 1.54 (2H, m, $-CH_2-$), 2.38 (2H, t, $J$ = 6.0 Hz, $-CH_2-$), 3.19 (2H, q, $J$ = 7.2, 12.9 Hz, $-CH_2-$), 3.45 (2H, q, $J$ = 6.2, 11.8 Hz, $-CH_2-$), 5.09 (2H, s, $-CH_2-$), 5.34 (2H, br s, –NH–) and 7.32–7.36 (5H, m, –CH–). $\delta_C$ (400 MHz; $CDCl_3$; 25 °C) 14.0, 22.3, 29.0, 29.2, 36.1, 37.1, 39.5, 66.6, 128.0, 128.1, 128.5, 136.5, 156.8 and 171.3. HRMS: $m/z$ $[M+H]^+$ 293.1866 (calculated $[C_{16}H_{25}N_2O_3]^+$ = 293.1860).

### 3-Amino-*N*-pentylpropanamide

Benzyl-3-oxo-3(pentylamino)propylcarbamate (1.50 g, 5.13 mmol) was dissolved in methanol (80 mL) at room temperature followed by the addition of palladium on activated carbon (Pd/C) (80.0 mg, 0.752 mmol). The reaction mixture was stirred overnight at room temperature under a $H_2$ gas balloon. Additional Pd/C (100 mg, 0.940 mmol) was added and the reaction mixture was stirred for a further 5 h under $H_2$. The reaction mixture was filtered and concentrated *in vacuo* to give the desired amide (800 mg, 99%) as a white solid. $R_f$ = 0.05 (10% methanol/dichloromethane). $\delta_H$ (300 MHz; $CDCl_3$) 0.87 (3H, t, $J$ = 7.1 Hz, $-CH_3$), 1.29–1.33 (4H, m, $-CH_2-$), 1.50 (2H, m, $-CH_2-$), 2.28 (2H, t, $J$ = 5.6 Hz, $-CH_2-$), 2.98 (2H, t, $J$ = 6.1 Hz, $-CH_2-$), 3.20 (2H, q, $J$ = 7.3, 12.9 Hz, $-CH_2-$) and 6.85 (1H, br s, –NH–). $\delta_C$ (300 MHz; $CDCl_3$; 25 °C) 14.4, 22.7, 29.5, 29.6, 38.0 38.3, 39.7 and 172.4. HRMS: $m/z$ $[M+H]^+$ 159.1499 (calculated $[C_8H_{19}N_2O]^+$ = 159.1492).

### 3,3-Dimethyl-2-oxo-butyric acid

A solution of pinacolone (10 mL, 83.4 mmol) in water (160 mL) was added to a solution of NaOH (8.00 g, 200 mmol) and potassium permanganate (12.2 g, 77.2 mmol) in water (196 mL) at 0 °C. The reaction mixture was stirred for 1 h at 0 °C, allowed to warm up to room temperature and stirred for an additional 2 h. The reaction mixture was filtered through celite, acidified to pH 2 with concentrated sulphuric acid, and the aqueous layer was extracted with diethyl ether (3 × 40 mL). The combined organic extracts were dried ($Na_2SO_4$), filtered and concentrated *in vacuo*. Bulb-to-bulb distillation (110 °C, 27.5 mmHg) gave the acid (3.99 g, 77%) as a clear oil. $\delta_H$ (300 MHz; $CDCl_3$) 1.23–1.33 (9H, m, $-CH_3$). $^1H$ NMR data are consistent with those reported previously [44].

### 3,3-Dimethyl-2-oxo-*N*-[3-oxo-3-(pentylamino)propyl] butanamide

*N*,*N*-Diisopropylethylamine (1.23 mL, 7.06 mmol) was added dropwise over 5 min to a solution of 3-amino-*N*-pentylpropanamide (800 mg, 5.06 mmol) in dichloromethane (40 mL) at 0 °C. Hydroxybenzotriazole (172.2 mg, 1.27 mmol), 3,3-dimethyl-2-oxo-butyric acid (820 mg, 6.30 mmol) and 1-ethyl-3-(3-dimethylaminopropyl) carbodiimide hydrochloride (1.34 g, 6.99 mmol) were then added consecutively and the reaction mixture was stirred overnight at room temperature. The reaction was quenched by the addition of 3 M HCl (50 mL) and the organic layer was washed with 3 M HCl (1 × 50 mL) and saturated $NaHCO_3$

(1 × 50 mL). The organic layer was dried ($Na_2SO_4$), filtered and concentrated *in vacuo* before purification by flash column chromatography (0.75 : 1 ethyl acetate : hexanes) afforded the desired amide (700 mg, 57%) as a white solid. $R_f$ = 0.27. $\delta_H$ (300 MHz; $CDCl_3$) 0.75 (3H, t, $J$ = 7.0 Hz, –$CH_3$), 1.14–1.19 (13H, m, –$CH_3$–, –$CH_2$–), 1.33–1.40 (2H, m, –$CH_2$–), 2.34 (2H, t, $J$ = 6.1 Hz, –$CH_2$–), 3.07 (2H, q, $J$ = 7.0, 13.1 Hz, –$CH_2$–), 3.42 (2H, q, $J$ = 6.1, 12.6 Hz, –$CH_2$–), 5.57 (1H, br s, –NH–) and 7.47 (1H, br s, –NH–). $\delta_C$ (400 MHz; $CDCl_3$; 25 °C) 13.9, 22.3, 26.2, 29.0, 29.2, 35.2, 35.4, 39.6, 42.9, 160.4 and 170.6, 203.0. HRMS: $m/z$ $[M+H]^+$ 271.2014 (calculated $[C_{14}H_{27}N_2O_3]^+$ = 271.2016).

### DL-4′-Deoxy-*N*-pentylpantothenamide

3,3-Dimethyl-2-oxo-*N*-[3-oxo-3-(pentylamino)propyl]butanamide (700 mg, 2.89 mmol) was dissolved in methanol (28 mL) at 0 °C under an inert atmosphere followed by the addition of sodium borohydride ($NaBH_4$, 163.44 mg, 4.32 mmol) in portions. The reaction mixture was stirred for 1 h at 0 °C and left to stir overnight at room temperature. Additional $NaBH_4$ (163.44 mg, 4.32 mmol) was added and the reaction mixture was stirred for another 3 h at room temperature. The reaction was quenched by the addition of saturated ammonium chloride (28 mL) and methanol was removed *in vacuo*. The aqueous solution was extracted with ethyl acetate (3 × 30 mL) and the combined organic extracts were dried ($Na_2SO_4$), filtered and concentrated *in vacuo* to yield dN5 (760 mg, 96%) as a colourless oil. $R_f$ = 0.39 (10% methanol/dichloromethane). $\delta_H$ (300 MHz; $CDCl_3$): 0.83 (3H, t, $J$ = 7.1 Hz, –$CH_3$), 0.93–0.95 (9H, m, –$CH_3$–), 1.24–1.27 (4H, m, –$CH_2$–), 1.43–1.48 (2H, m, –$CH_2$–), 2.37 (2H, t, $J$ = 6.2 Hz, –$CH_2$–), 3.13 (2H, q, $J$ = 7.0, 13.6 Hz, –$CH_2$–), 3.47 (2H, q, $J$ = 6.6, 12.7 Hz, –$CH_2$–), 3.66 (1H, s, –CH–), 6.38 (1H, br s, –NH–) and 7.17 (1H, br s, –NH–); $\delta_C$ (400 MHz; $CDCl_3$; 25 °C): 13.9, 22.3, 25.9, 29.0, 29.2, 35.0, 35.2, 35.6, 39.6, 79.4, 171.1 and 172.7. HRMS: $m/z$ $[M+H]^+$ 273.2172 (calculated $[C_{14}H_{29}N_2O_3]^+$ = 273.2173).

## Bacterial growth inhibition tests of pantothenamide library

The MICs of the library of *N*-substituted pantothenamides (Table 1, entries 1–47) against *E. coli* K12, *S. aureus* RN4220 or *P. aeruginosa* ATCC 27853 were determined by microbroth dilution in 96-well microtiter flat-bottomed plates and turbidometric analysis at $OD_{600}$. Starter cultures of either *E. coli* K12, *S. aureus* RN4220 or *P. aeruginosa* ATCC 27853 in 1% tryptone were prepared by inoculation with four separate colonies grown on LB agar plates. The starter culture was grown to exponential phase and then diluted 10 000-fold in the same medium. A 10-μL aliquot of the diluted cell suspension was used to inoculate each well of a 96-well plate containing 100 μL of 1% tryptone broth supplemented with the specific compound of interest (diluted from 50 mM stock solutions prepared in 50% aqueous acetonitrile to aid solubility). The compounds that exhibited positive results in initial screens at 200 μM were subsequently tested at 50 μM; those that still showed inhibition at this concentration were submitted to concentration–response analysis. Final concentrations of compounds were in the range 0.039–200 μM depending on the potency of the pantothenamide. The plates were incubated at 37 °C for 20 h before the cell densities were measured ($OD_{600}$). The extent of growth in each well was determined by normalizing the $OD_{600}$ values relative to those of the negative control (containing 3% acetonitrile instead of pantothenamide), which was taken as 100% bacterial cell growth. Each compound was tested in triplicate and all experiments were repeated at least once after the initial experiment.

## Bacterial growth inhibition studies of N5-Pan and dN5 in minimal media

The inhibition of *E. coli* K12 and *S. aureus* RN4220 by N5-Pan and dN5 was tested in minimal media appropriate for each bacterium. For *E. coli*, this medium consisted of 0.8 mM $MgSO_4$, 10 mM citric acid, 60 mM $K_2HPO_4$, 20 mM $NaNH_4HPO_4$ and 0.5% glucose; for *S. aureus*, it contained 40 mM KCl, 160 mM NaCl, 5.3 mM $MgSO_4$, 30 mM $(NH_4)_2SO_4$, 0.11 mM $CaCl_2$, 1.0 mM $KH_2PO_4$, 0.02 mM $FeSO_4$, 0.04 mM $MnSO_4$, 0.03 mM citric acid, 100 mM Tris, 28 mM glucose, 0.8 mM L-arginine, 1.0 mM L-proline, 1.9 mM L-glutamic acid, 1.5 mM L-valine, 1.5 mM L-threonine, 1.0 mM L-phenylalanine, 1.3 mM L-leucine, 0.78 mM L-cysteine, 0.4 μM biotin, 6.6 μM thiamine and 16 μM nicotinic acid [45]. The inhibition was determined by concentration–response analysis as described above with minor modifications. Briefly, starter cultures of *E. coli* K12 and *S. aureus* RN4220 in 1% tryptone were inoculated with four separate colonies grown on LB agar plates. The starter culture was grown to exponential phase and then diluted 10-fold into the applicable minimal media. A 10-μL aliquot of the diluted cell suspension was used to inoculate each well of a 96-well flat-bottomed plate containing 100 μL of minimal medium. Subsequently, the media was supplemented with either N5-Pan or dN5. For *E. coli* and *S. aureus*, the final concentrations of N5-Pan varied in the range 0.781–100 μM and 0.391–50 μM, respectively; for both organisms, dN5 was varied in the range 1.56–200 μM. The plates were incubated at 37 °C for 24 h before the cell densities were measured ($OD_{600}$) and analyzed further as described above. Each compound was tested in either two (*E. coli*) or three (*S. aureus*) independent experiments, each performed triplicate.

## PanK assays

PanK activity was determined using a continuous spectrophotometric assay that coupled the production of ADP to the consumption of NADH and was monitored by the

decrease in $A_{340}$, as described previously [7]. An extinction coefficient of 6220 $M^{-1} \cdot cm^{-1}$ was used for NADH. Each 300-μL reaction mixture contained 50 mM Tris-HCl (pH 7.6), 10 mM $MgCl_2$, 20 mM KCl, 1.5 mM ATP, 0.5 mM NADH, 0.5 mM phosphoenolpyruvate, 3 units of PK, 3 units of LDH and either 3.0 μg of *Ec*PanK$_I$ or 1.5 μg of *Sa*PanK$_{II}$. When PantSH was tested as substrate, 0.5 mM of tris(2-carboxyethyl)phosphine was also added to the reaction mixture. The concentration ranges (and ratios of substrate used in the mixture experiments) are indicated as appropriate. The reaction was initiated by the addition of substrate (or mixtures of substrates, or mixtures of substrates and inhibitors) and was monitored for 5 min at 25 °C.

### Statistical analysis

Using the raw kinetic data, initial velocities were calculated for each substrate concentration (or substrate mixture, or substrate/inhibitor mixture) by linear regression of the readings made in the 50s period after the initial 10 s (i.e. the period from 10 to 60 s after the reaction was started). For each experiment, the three readings made for each data point were averaged and plotted with the SD to give the respective kinetic profile. Kinetic parameters reported in Table 2 were determined for each experiment by fitting the appropriate equation to the data; the reported values are the mean values of the parameters determined from all the individual independent experiments, and are given with errors that indicate the range/2 or SEM as appropriate. The parameters (Table 3) were determined in a global fit by minimizing the squared difference between experimental data points and model simulation of the appropriate equation, and are given with errors that indicate the SE.

## Acknowledgements

We thank Professor Willem van Otterlo for providing advice and guidance regarding the synthesis of dN5. This project was funded by grants from the National Research Foundation (NRF) of South Africa (CPR20110726000022216) and Medical Research Council of South Africa to ES. JLS is supported by the South African Research Chairs Initiative of the Department of Science and Technology and the NRF of South Africa. MdV, LB and LK were supported by bursaries from the NRF.

## Author contributions

MdV and LB contributed equally to the syntheses, growth inhibition assays and enzyme kinetic analyses, as well as to the data analysis. LK performed enzyme kinetic assays and data analysis. JLS constructed the kinetic model and performed the associated data analysis. ES conceived the project, contributed to the data analysis and wrote the paper with contributions from all of the authors.

## References

1 Clifton G, Bryant SR & Skinner CG (1970) $N^1$-(substituted) pantothenamides, antimetabolites of pantothenic acid. *Arch Biochem Biophys* **137**, 523–528.
2 Strauss E (2010) Coenzyme A biosynthesis and enzymology. In Comprehensive Natural Products II Chemistry and Biology (Mander L & Liu H-W, eds), pp. 351–410. Elsevier, Oxford.
3 Spry C, Kirk K & Saliba KJ (2008) Coenzyme A biosynthesis: an antimicrobial drug target. *FEMS Microbiol Rev* **32**, 56–106.
4 Spry C, Macuamule C, Lin Z, Virga KG, Lee RE, Strauss E & Saliba KJ (2013) Pantothenamides are potent, on-target inhibitors of *Plasmodium falciparum* growth when serum pantetheinase is inactivated. *PLoS One* **8**, e54974.
5 de Villiers M, Macuamule C, Spry C, Hyun Y-M, Strauss E & Saliba KJ (2013) Structural modification of pantothenamides counteracts degradation by pantetheinase and improves antiplasmodial activity. *ACS Med Chem Lett* **4**, 784–789.
6 Jansen PAM, Hermkens PHH, Zeeuwen PLJM, Botman PNM, Blaauw RH, Burghout P, van Galen PM, Mouton JW, Rutjes FPJT & Schalkwijk J (2013) Combination of pantothenamides with vanin inhibitors as a novel antibiotic strategy against Gram-positive bacteria. *Antimicrob Agents Chemother* **57**, 4794–4800.
7 Strauss E & Begley TP (2002) The antibiotic activity of *N*-pentylpantothenamide results from its conversion to ethyldethia-coenzyme A, a coenzyme A antimetabolite. *J Biol Chem* **277**, 48205–48209.
8 Zhang Y-M, Frank MW, Virga KG, Lee RE, Rock CO & Jackowski S (2004) Acyl carrier protein is a cellular target for the antibacterial action of the pantothenamide class of pantothenate antimetabolites. *J Biol Chem* **279**, 50969–50975.
9 Mercer AC & Burkart MD (2007) The ubiquitous carrier protein – a window to metabolite biosynthesis. *Nat Prod Rep* **24**, 750–773.
10 Jackowski S & Rock CO (1984) Turnover of the 4′-phosphopantetheine prosthetic group of acyl carrier protein. *J Biol Chem* **259**, 1891–1895.
11 Thomas J & Cronan JE (2005) The enigmatic acyl carrier protein phosphodiesterase of *Escherichia coli*. *J Biol Chem* **280**, 34675–34683.
12 Thomas J & Cronan JE (2010) Antibacterial activity of *N*-pentylpantothenamide is due to inhibition of coenzyme A synthesis. *Antimicrob Agents Chemother* **54**, 1374–1377.

13 Choudhry AE, Mandichak TL, Broskey JP, Egolf RW, Kinsland C, Begley TP, Seefeld MA, Ku TW, Brown JR, Zalacain M *et al.* (2003) Inhibitors of pantothenate kinase: novel antibiotics for staphylococcal infections. *Antimicrob Agents Chemother* **47**, 2051–2055.
14 Leonardi R, Chohnan S, Zhang Y-M, Virga KG, Lee RE, Rock CO & Jackowski S (2005) A pantothenate kinase from *Staphylococcus aureus* refractory to feedback regulation by coenzyme A. *J Biol Chem* **280**, 3314–3322.
15 Virga KG, Zhang Y-M, Leonardi R, Ivey RA, Hevener K, Park H-W, Jackowski S, Rock CO & Lee RE (2006) Structure–activity relationships and enzyme inhibition of pantothenamide-type pantothenate kinase inhibitors. *Bioorg Med Chem* **14**, 1007–1020.
16 Mercer AC, Meier JL, Hur GH, Smith AR & Burkart MD (2008) Antibiotic evaluation and *in vivo* analysis of alkynyl coenzyme A antimetabolites in *Escherichia coli*. *Bioorg Med Chem Lett* **18**, 5991–5994.
17 Brand LA & Strauss E (2005) Characterization of a new pantothenate kinase isoform from *Helicobacter pylori*. *J Biol Chem* **280**, 20185–20188.
18 Nicely NI, Parsonage D, Paige C, Newton GL, Fahey RC, Leonardi R, Jackowski S, Mallett TC & Claiborne A (2007) Structure of the type III pantothenate kinase from *Bacillus anthracis* at 2.0 Å resolution: implications for coenzyme A-dependent redox biology. *Biochemistry* **46**, 3234–3245.
19 Yang K, Eyobo Y, Brand LA, Martynowski D, Tomchick D, Strauss E & Zhang H (2006) Crystal structure of a type III pantothenate kinase: insight into the mechanism of an essential coenzyme A biosynthetic enzyme universally distributed in bacteria. *J Bacteriol* **188**, 5532–5540.
20 Hong BS, Yun MK, Zhang Y-M, Chohnan S, Rock CO, White SW, Jackowski S, Park H-W & Leonardi R (2006) Prokaryotic type II and type III pantothenate kinases: the same monomer fold creates dimers with distinct catalytic properties. *Structure* **14**, 1251–1261.
21 Strauss E, de Villiers M & Rootman I (2010) Biocatalytic production of coenzyme A analogues. *ChemCatChem* **2**, 929–937.
22 Balibar CJ, Hollis-Symynkywicz MF & Tao J (2011) Pantethine rescues phosphopantothenoylcysteine synthetase and phosphopantothenoylcysteine decarboxylase deficiency in *Escherichia coli* but not in *Pseudomonas aeruginosa*. *J Bacteriol* **193**, 3304–3312.
23 van Wyk M & Strauss E (2008) Development of a method for the parallel synthesis and purification of *N*-substituted pantothenamides, known inhibitors of coenzyme A biosynthesis and utilization. *Org Biomol Chem* **6**, 4348–4355.
24 Zhang Y-M, Chohnan S, Virga KG, Stevens RD, Ilkayeva OR, Wenner BR, Bain JR, Newgard CB, Lee RE, Rock CO *et al.* (2007) Chemical knockout of pantothenate kinase reveals the metabolic and genetic program responsible for hepatic coenzyme A homeostasis. *Chem Biol* **14**, 291–302.
25 Siudeja K, Srinivasan B, Xu L, Rana A, de Jong J, Nollen EAA, Jackowski S, Sanford L, Hayflick S & Sibon OCM (2011) Impaired coenzyme A metabolism affects histone and tubulin acetylation in *Drosophila* and human cell models of pantothenate kinase associated neurodegeneration. *EMBO Mol Med* **3**, 755–766.
26 Ivey RA, Zhang Y-M, Virga KG, Hevener K, Lee RE, Rock CO, Jackowski S & Park H-W (2004) The structure of the pantothenate kinase.ADP.pantothenate ternary complex reveals the relationship between the binding sites for substrate, allosteric regulator, and antimetabolites. *J Biol Chem* **279**, 35622–35629.
27 van der Westhuyzen R, Hammons JC, Meier JL, Dahesh S, Moolman WJA, Pelly SC, Nizet V, Burkart MD & Strauss E (2012) The antibiotic CJ-15,801 is an antimetabolite that hijacks and then inhibits CoA biosynthesis. *Chem Biol* **19**, 559–571.
28 Wittwer CT, Beck S, Peterson M, Davidson R, Wilson DE & Hansen RG (1990) Mild pantothenate deficiency in rats elevates serum triglyceride and free fatty acid levels. *J Nutr* **120**, 719–725.
29 Wittwer CT, Schweitzer C, Pearson J, Song WO, Windham CT, Wyse BW & Hansen RG (1989) Enzymes for liberation of pantothenic acid in blood: use of plasma pantetheinase. *Am J Clin Nutr* **50**, 1072–1078.
30 Shibata K, Fukuwatari T, Ohta M, Okamoto H, Watanabe T, Fukui T, Nishimuta M, Totani M, Kimura M, Ohishi N *et al.* (2005) Values of water-soluble vitamins in blood and urine of Japanese young men and women consuming a semi-purified diet based on the Japanese dietary reference intakes. *J Nutr Sci Vitaminol* **51**, 319–328.
31 Spry C, Saliba KJ & Strauss E (2014) A miniaturized assay for measuring small molecule phosphorylation in the presence of complex matrices. *Anal Biochem* **451**, 76–78.
32 Meier JL, Mercer AC, Rivera H Jr & Burkart MD (2006) Synthesis and evaluation of bioorthogonal pantetheine analogues for in vivo protein modification. *J Am Chem Soc* **128**, 12174–12184.
33 Worthington AS & Burkart MD (2006) One-pot chemo-enzymatic synthesis of reporter-modified proteins. *Org Biomol Chem* **4**, 44–46.
34 van Wyk M & Strauss E (2007) One-pot preparation of coenzyme A analogues via an improved chemo-enzymatic synthesis of pre-CoA thioester synthons. *Chem Commun*, 398–400.
35 Yang K, Strauss E, Huerta C & Zhang H (2008) Structural basis for substrate biding and the catalytic

mechanism of type III pantothenate kinase. *Biochemistry* **47**, 1369–1380.
36 Yun M, Park C-G, Kim J-Y, Rock CO, Jackowski S & Park H-W (2000) Structural basis for the feedback regulation of *Escherichia coli* pantothenate kinase by coenzyme A. *J Biol Chem* **275**, 28093–28099.
37 Akinnusi TO, Vong K & Auclair K (2011) Geminal dialkyl derivatives of *N*-substituted pantothenamides: synthesis and antibacterial activity. *Bioorg Med Chem* **19**, 2696–2706.
38 Li B, Tempel W, Smil D, Bolshan Y, Schapira M & Park H-W (2013) Crystal structures of *Klebsiella pneumoniae* pantothenate kinase in complex with *N*-substituted pantothenamides. *Proteins* **81**, 1466–1472.
39 Hughes SJ, Antoshchenko T, Kim KP, Smil D & Park H-W (2014) Structural characterization of a new *N*-substituted pantothenamide bound to pantothenate kinases from *Klebsiella pneumoniae* and *Staphylococcus aureus*. *Proteins* **82**, 1542–1548.
40 Peters VJ, Brown GM, Williams WL & Snell EE (1953) Isolation of the *Lactobacillus bulgaricus* factor from natural sources. *J Am Chem Soc* **75**, 1688–1691.
41 Jackowski S & Rock CO (1984) Metabolism of 4′-phosphopantetheine in *Escherichia coli*. *J Bacteriol* **158**, 115–120.
42 Van Laer K, Hamilton CJ & Messens J (2013) Low-molecular-weight thiols in thiol-disulfide exchange. *Antioxid Redox Signal* **18**, 1642–1653.
43 Gaupp R, Ledala N & Somerville GA (2012) Staphylococcal response to oxidative stress. *Front Cell Info Microbiol* **2**, 33.
44 Tuck KL, Saldanha SA, Birch LM, Smith AG & Abell C (2006) The design and synthesis of inhibitors of pantothenate synthetase. *Org Biomol Chem* **4**, 3598–3610.
45 Rudin L, Sjöström J-E, Lindberg M & Philipson L (1974) Factors affecting competence for transformation in *Staphylococcus aureus*. *J Bacteriol* **118**, 155–164.

*Chapter 2 (continued)*

# Variation In Pantothenate Kinase Type Determines The Mode of Action In Bacteria

## *Additional Information*

Apart from the work presented in the accompanying manuscript, a number of additional experiments were performed to corroborate some of the findings. The results of these studies were not published, but are reported below. In addition, the synthetic strategies that were used to obtain valuable substrates/inhibitors needed for this study are also discussed.

## 2.1 Additional kinetic parameters

### 2.1.1 N7-Pan: pantothenic acid mixed kinetics with *Sa*PanK-II

During the initial review of the manuscript reprinted in the preceding section, one of the reviewers questioned our decision to use N5-Pan instead of N7-Pan for all kinetic analyses, given that N7-Pan is the most potent pantothenamide inhibitor against *S. aureus* (see Table 1 in the manuscript). Our reasoning was that N5-Pan inhibits bacterial growth for both *E. coli* and *S. aureus* allowing for a comparative kinetic analysis, while N7-Pan inhibits only *S. aureus.*

Nonetheless, and in view of the reviewer's comment, we set out to perform an additional experiment where constant ratio mixtures of pantothenic acid and N7-Pan (instead of N5-Pan) were used. This was done to confirm that the trend observed for N5-Pan also holds for N7-Pan. The experiment was performed as described in the manuscript. Figure 2.1A shows the interaction of pantothenic acid and N7-Pan with *Sa*PanK-II under competitive conditions. This indicates that N7-Pan has a significant inhibitory effect on the activity of the enzyme at higher concentrations, even in mixtures containing only 5% N7-Pan. In addition, it also shows increased activity at lower substrate concentrations. These results are consistent with the results shown in Figures 8A and 8C in the manuscript obtained for mixtures of N5-Pan/pantothenic acid and PantSH/pantothenic acid, respectively. Figure 2.1B shows the fit of the kinetic model described in the article to the pantothenic acid/N7-Pan mix data. The kinetic parameters obtained in this manner were nearly identical to those obtained for constant ratio mixtures of pantothenic acid and PantSH (Table 3 in the manuscript). This indicates that the pantothenamides that do show inhibition of *S. aureus* growth mimic the interactions of PantSH with *Sa*PanK-II.

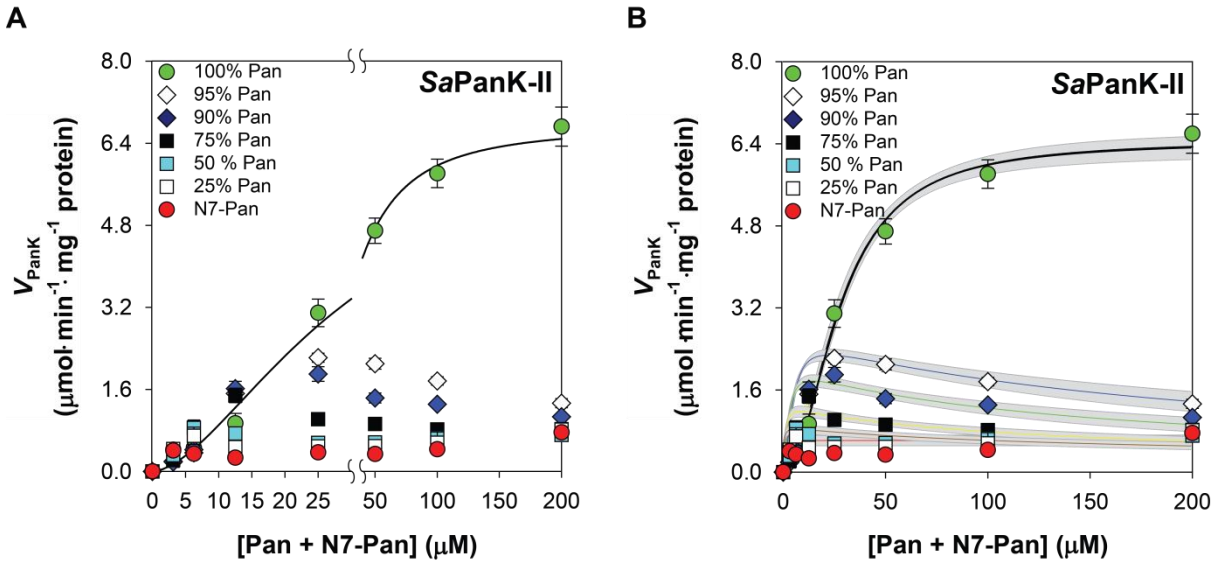


**Figure 2.1. (A) The kinetic profiles of mixtures of pantothenic acid (Pan) and N7-Pan with *Sa*PanK-II under competitive conditions. The concentration indicated on the X-axis (note the axis-break) is the total substrate concentration (Pan and N7-Pan combined); for each data set, the ratio of Pan: N7-Pan was kept constant as indicated. The data points represent the mean of two independent experiments, each performed in triplicate; the error bars denote the range/2. The solid line represents the best fit of Equation 1 (see manuscript) to the 100% Pan data. (B) Fitting Equation 3 (see manuscript) to the experimental data obtained in (A). The solid lines represent the best fit curves, while the shaded area indicates the 90% confidence intervals for these fits.**

## 2.2 Synthetic strategies for the production of 4'-deoxy-*N*-pentyl pantothenamide (2.9)

In the published manuscript we described the synthesis of 4'-deoxy-*N*-pentylpantothenamide (**2.9**, 4'-deoxy-N5-Pan), a N5-Pan analogue in which the 4'-hydroxyl (OH) group has been removed. This modification gives an analogue that can only act as an inhibitor of *Sa*PanK-II, providing a very useful tool to help determine the exact mode of action of the pantothenamides in *S. aureus*. In the manuscript, the synthesis of racemic 4'-deoxy-N5-Pan **2.9** [(*R*/*S*)-4'-deoxy-N5-Pan **2.9**] is described (Figure 5A). The synthetic preparation of (*R*/*S*)-4'-deoxy-N5-Pan **2.9** is straightforward given that a ketone at the 2'-position can be selectively reduced in the final step to afford both enantiomers of the alcohol at this position. However, the resulting racemic mixture cannot be separated into the respective enantiomers, making it impossible to confirm that the data of the kinetic characterization studies in fact only reflect that of the *R*-isomer as expected. To do this would require a stereoselective synthetic preparation of (*R*)-4'-deoxy-N5-Pan **2.9**; this is significantly more challenging given that we either have to make use of a chiral reducing agent , or a starting material that contains the correct stereocenter. Below the various attempts at the synthesis of racemic (*R*/*S*)-4'-deoxy-N5-Pan **2.9** as well as the enantiomerically pure (*R*)-4'-deoxy-N5-Pan **2.9** are outlined and discussed.

### 2.2.1 Synthesis of (*R*/*S*)-4'-deoxy-*N*-pentyl pantothenamide [(*R*/*S*)-2.9]

Synthetically it is challenging to selectively remove the 4'-OH-group of N5-Pan, due to the presence of a second hydroxy and two amide functionalities in the molecule. The envisioned strategies for the synthesis of (*R*/*S*)-4'-deoxy-N5-Pan **2.9** [(*R*/*S*)-**2.9**] were therefore based on using a starting material that already has the hydroxyl functional group at the 4'-carbon removed to construct the target molecule. Two methods were envisaged whereby this could be accomplished based on the retrosynthesis shown in Scheme 2.1.

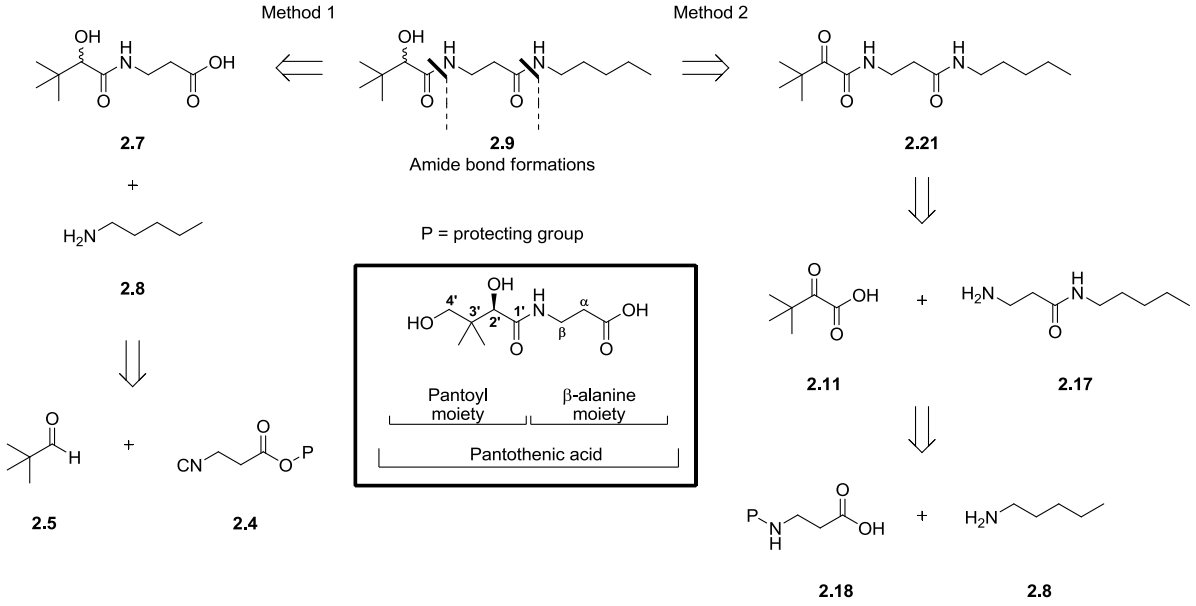


**Scheme 2.1. Proposed retrosynthesis of (*R*/*S*)-4'-deoxy-*N*-pentyl pantothenamide 2.9. (Method 1) Reaction of pivaldehyde 2.5 with an isocyanide 2.4, followed by removal of the carboxylate protecting group and coupling of pentylamine 2.8 in the final step of the synthesis. (Method 2) Coupling a moiety with no hydroxyl functional group at the 4'-carbon (2.11) to a primary amine which already contains the pentyl functional group (2.17).**

The retrosynthesis of both methods were based on the coupling of three fragments via two amide bond formations. In method 1 there is a disconnection between the 1'- and 2'-carbons in the pantoyl moiety, and a second disconnection between the carbonyl carbon of the β-alanine moiety and the *N*-substituent. The first amide bond is formed during the 1' and 2' carbon bond formation by coupling aldehyde **2.5** to isocyanide **2.4** through Lewis acid activation. The second amide bond is formed during the coupling of acid **2.7** and heptylamine **2.8** to afford racemic **2.9**. In method 2 there is a disconnection between the carbonyl carbon of the β-alanine moiety and the *N*-substituent, and a second disconnection between the 1'-carbon of the pantoyl moiety and the amine at the β-carbon position of the β-alanine moiety. In this method the amide bond between acid **2.18** and heptylamine **2.8** is formed first, while the second amide bond is formed during the

coupling of ketoacid **2.11** and amine **2.17**. While method 1 was attempted without success (discussed in detail below), racemic **2.9** was successfully synthesized using method 2 (this is the method reported in the accompanying manuscript).

Method 1, shown in Scheme 2.2, was based on the synthesis of (*R*/*S*)-4'-deoxy pantothenic acid prepared in a previous study in our group [1], and involved five linear steps that included two coupling reactions. During the first step, β-alanine benzyl ester (**2.1**; prepared from β-alanine benzyl ester tosylate salt) was formylated to amide **2.3** by the addition of acetic formic anhydride (**2.2**; prepared by stirring acetic anhydride with formic acid). The acetic acid ($CH_3COOH$) that formed during the course of the reaction was removed through an aqueous work-up step that proved to be adequate to obtain pure amide **2.3** in 72% yield, which correlates well with the previously reported yield of 64% [1].

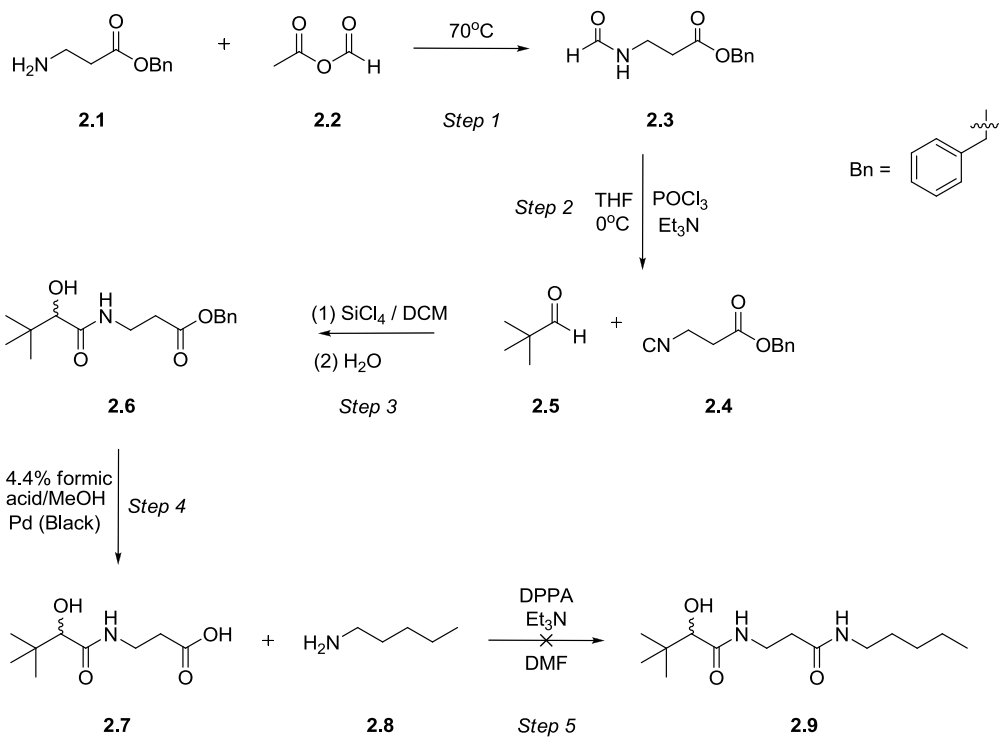


**2.1** **2.2** **2.3** **2.4** **2.5** **2.6** **2.7** **2.8** **2.9**

**Scheme 2.2. Synthesis route of (*R*/*S*)-4'-deoxy-*N*-pentyl pantothenamide 2.9 using Method 1. Formation of a C–C bond through the reaction of isocyanide 2.4 with pivaldehyde 2.5. Deprotection of ester 2.6 successfully gave acid 2.7; however, the final step did not give adequate amounts of material to allow for successful purification of the final product (2.9).**

In addition to Koekemoer's method, an alternative method, described by Suchý *et al.* [2], was attempted to formylate the β-alanine benzyl ester tosylate salt directly. This method involves

treatment of amino acid esters with imidazole in warm (60°C) dimethylformamide (DMF), and does not require dry, inert conditions. Mechanistically, DMF acts as the formyl donor, whereas imidazole acts as an acyl transfer agent. β-alanine benzyl ester tosylate salt was accordingly treated with imidazole and heated in DMF for 48h. However, we obtained a very low yield (29%) compared to published results (79% yield) [2]. Additionally, this method also proved to be time-consuming, since the reaction has to stir for 48h compared to Koekemoer's method that only has to stir for 4.5h. As a result, we continued to use the three-step formylating procedure developed by Koekemoer [1], since no purification, other than an aqueous work-up, was required and a satisfactory 72% yield was obtained.

The second step entailed the dehydration of amide **2.3** to isocyanide **2.4** by phosphoryl chloride ($POCl_3$) and triethylamine ($Et_3N$). Initial dehydration of amide **2.3** with $POCl_3$ did not proceed to completion as $^1H$ NMR spectroscopic analysis indicated that only 50% of amide **2.3** was dehydrated. This might be attributed to experimental conditions not being thoroughly anhydrous or to the use of poor quality $POCl_3$ reagent. $POCl_3$ reacts with water ($H_2O$) to give hydrochloric acid (HCl) and phosphoric acid ($H_3PO_4$), which can lead to an inadequate amount of $POCl_3$ to fully dehydrate amide **2.3**. The dehydration step was therefore repeated on the same reaction using the same number of $POCl_3$ equivalents (equiv.) to ensure full conversion of amide **2.3** to isocyanide **2.4**. Isocyanide **2.4** was next used in the first C–C bond formation reaction by adding it to aldehyde **2.5**. This reaction was facilitated through Lewis acid activation with silicon tetrachloride ($SiCl_4$). The reaction was quenched, with subsequent hydration leading to the formation of amide **2.6**. Unfortunately, only a 20% yield was obtained after purification by flash column chromatography (FCC), but this gave sufficient material to allow the next step to be attempted.

Step 4 entailed the deprotection of ester **2.6** with palladium black (Pd black) in a 4.4% formic acid/methanol (MeOH) solution. The benzyl protecting group was removed within 4h to afford carboxylic acid **2.7** in an excellent 94% yield after filtration and the purity was confirmed with $^1H$ NMR spectroscopic analysis. To form the final amide bond a diphenylphosphoryl azide (DPPA)-mediated coupling (adapted from Shioiri *et al*. [3]) was attempted by treating a solution of carboxylic acid **2.7** and pentylamine **2.8** in DMF with DPPA and $Et_3N$. Regrettably, the reaction gave a mixture of products that did not lend itself to further purification. As a result of the very poor overall yield (only 11% up to carboxylic acid **2.7**), along with the formation of a mixture of products in the final step, this synthetic route was not pursued any further. Consequently, method 2 was investigated as an alternative, and it finally allowed for the successful synthesis of (*R*/*S*)-**2.9.** A detailed description of this method is reported in the accompanying manuscript.

## 2.2.2 Synthesis of (*R*)-4'-deoxy-*N*-pentyl pantothenamide [(*R*)-2.9]

Due to the lack of stereo control in the synthetic procedures used for the preparation of (*R*/*S*)-**2.9** as outlined above, a racemic mixture is obtained. Virga *et al*. [4] reported that the *R*-configuration at the 2'–OH position of substrates/inhibitors is necessary for optimal binding of the 4'–OH group to the PanK binding pocket. Therefore, only one of the enantiomers in the racemic mixture is postulated to act as an inhibitor. Consequently, we wanted to develop a stereoselective synthetic procedure allowing for the preparation of (*R*)-**2.9**; this could then be used for physiologically more relevant inhibition studies on *S. aureus*. A stereoselective synthesis of (*R*)-**2.9** could be achieved by using a chiral reducing agent or by using a starting material with the correct stereochemistry. Scheme 2.3 proposes an asymmetric synthesis for (*R*)-**2.9** in five linear steps. Overall, the synthetic strategy is a modification of method 2 outlined for the preparation of the (*R*/*S*)-**2.9**, with the addition of a chiral auxiliary in the second step to control the stereoselectivity of the subsequent reduction.

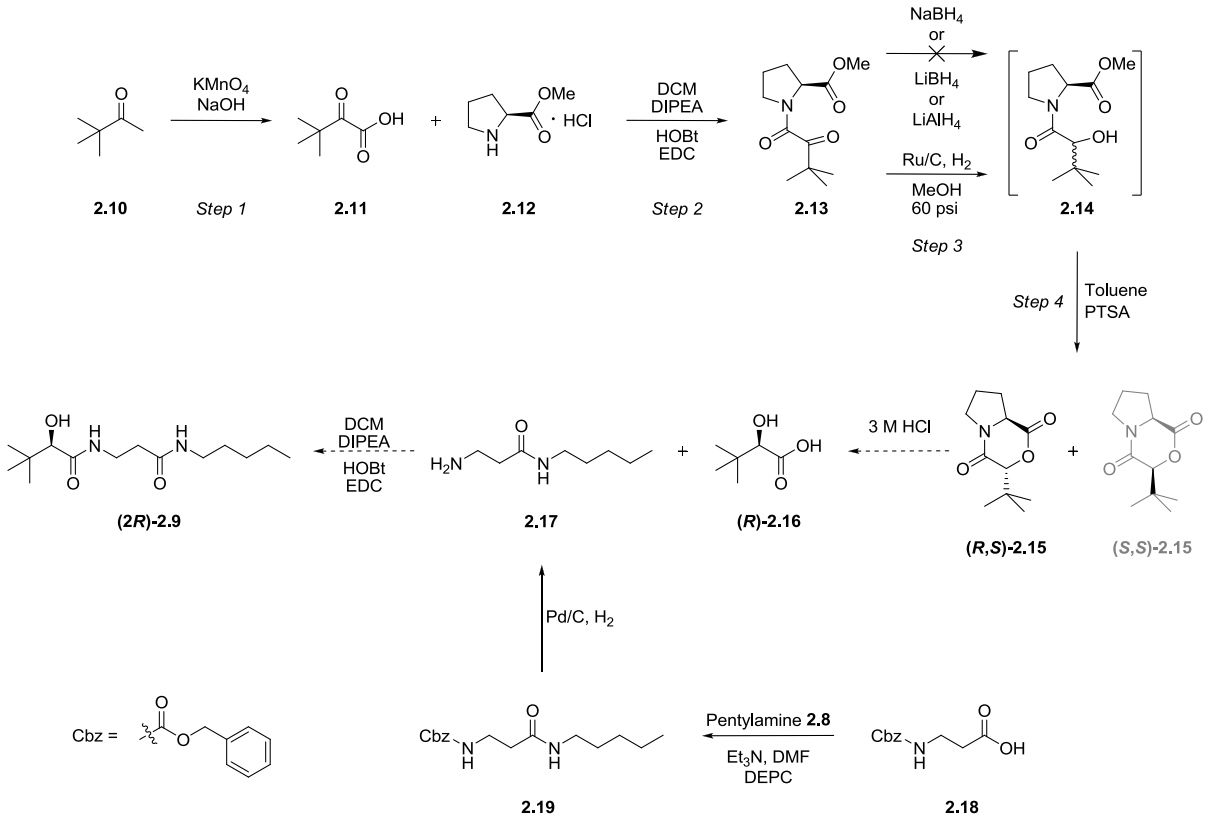


**Scheme 2.3. Proposed synthetic route for the preparation of (*R*)-4'-deoxy-*N*-pentyl pantothenamide 2.9 in six steps starting from pinacolone (2.10). Solid arrows indicate synthetic steps that were successfully performed, whereas arrows in dotted lines indicate theoretical synthetic procedures that were not performed.**

In step one, ketoacid **2.11** is synthesised according to Tuck *et al*. [5], through the oxidation of pinacolone **2.10** by potassium permanganate ($KMnO_4$) in a single step which produced ketoacid **2.11** in a 77% yield. This is followed by an amide coupling, which entails the coupling of ketoacid **2.11** with (*R*)-proline methyl ester HCl salt **2.12** in the presence of *N*-(3-dimethylaminopropyl)-*N*′-ethylcarbodiimide (EDC) hydrochloride, *N*,*N*-diisopropylethylamine (DIPEA) and hydroxy-benzotriazole (HOBt) to give ketoamide **2.13**. EDC acts as an activating agent for the carboxyl group, allowing for nucleophilic acyl substitution with an amine. The experimental procedure for this coupling reaction was done as described by Nelson *et al*. [6]. Although these authors reported an 84% yield for this coupling, only a 60% yield of ketoamide **2.13** was obtained after purification by FCC. Theoretically, the subsequent reduction of ketoamide **2.13** in step 3 and lactonization of hydroxy amide **2.14** in step 4 should generate lactone **2.15** in an *R*:*S* ratio of 93:7. The more rapid lactonization of the *R,S*-isomer is due to the lower energy transition state or intermediate along the lactonization pathway [6]. Separation of the diastereomers via FCC should be possible after the lactonization of hydroxy amide **2.14** to (*R*,*S*)- and (*S*,*S*)-**2.15** [6].

Nelson *et al*. [6] used 5% ruthenium on activated carbon (Ru/C) under 60 psi hydrogen ($H_2$) gas in a Parr reactor to reduce ketoamide **2.13**. However, since a similar ketoamide was successfully reduced using a metal hydride in the synthesis of (*R*/*S*)-**2.9**, we decided to use this method in our first attempt to reduce ketoamide **2.13**. Consequently, sodium borohydride ($NaBH_4$) was first used as a reducing agent in step 3, since it is a mild reducing agent and is selective toward ketones as opposed to amides. Various reaction conditions were tested (shown in Table 2.1) which included changes in temperature, time and the number of equiv. of reducing agent; however, the reduction of the ketone was unsuccessful and the starting material was recovered, even at 6 equiv. of $NaBH_4$. Following this, we attempted to reduce ketoamide **2.13** with either lithium borohydride ($LiBH_4$) or lithium aluminium hydride ($LiAlH_4$) using varying reaction conditions as summarized in Table 2.1. Unfortunately, none of these reagents were able to reduce ketoamide **2.13** successfully, since the starting material was recovered after each reaction.

Given that we were unsuccessful in reducing ketoamide **2.13** using a metal hydride, we finally attempted the reduction by using a Parr reactor and 5% Ru/C as described in literature [6]. To this end, 5% Ru/C and ketoamide **2.13** was heated to 50°C and stirred for 72h under 60 psi $H_2$ gas pressure, followed by lactonization of hydroxy amide **2.14** [in the presence of *p*-toluenesulfonic acid (PTSA)] to (*R*,*S*)- and (*S*,*S*)-lactone **2.15** under vacuum to remove the MeOH side product. From the $^1$H NMR spectrum of the crude product it was unclear whether the reduction was successful; however, High Resolution Mass Spectroscopy (HRMS) did not show any product formation and the starting material was recovered. The procedure was repeated, but this time the

reaction mixture was degassed by three alternating nitrogen/vacuum cycles to remove dissolved oxygen from within the solvent, before it was inserted into the Parr reactor. Additionally, the lactonization step was performed without vacuum and the time was increased from 5h to 48h. The reduction of ketoamide **2.13** was successful and (*R*,*S*)- and (*S*,*S*)-**2.15** were separated by FCC and obtained in a combined yield of 48% over the two steps. Although literature [6] reported a 10:1 ratio for (*R*,*S*):(*S*,*S*) we obtained only a 5:1 ratio. $^{1}$H NMR data were consistent with those reported previously for (*R,S*)-**2.15** [6] and confirmed that *R,S* is indeed the major diastereomer.

**Table 2.1. Various reaction conditions attempted for the reduction of ketoamide 2.13**.

| Reducing agent | Attempt 1 | Attempt 2 |
|---|---|---|
| **$NaBH_4$** | 1) 0°C, 1h, 3 equiv. then<br>2) overnight at rt | 1) 0°C, 1h, 6 equiv. then<br>2) 36h at rt |
| **$LiBH_4$** | 1) 0°C, 1h, 2 equiv. then<br>2) overnight at rt | 1) 0°C, 1h, 4 equiv. then<br>2) 24h at rt then<br>3) additional 2 equiv., 24h at rt |
| **$LiAlH_4$** | 1) -78°C, 2h, 1 equiv. then<br>2) 0°C, 2h then<br>3) overnight at rt | 1) -78°C, 2h, 2 equiv. then<br>2) 0°C, 2h then<br>3) overnight at rt. |

[b] rt, room temperature

Since the reduction of ketoamide **2.13** was challenging and Parr reactors are not readily available in many research facilities, we decided to pursue an alternative strategy in which the racemic hydroxy acid **2.16** is prepared first, followed by its coupling to (*R*)-proline methyl ester HCl salt **2.12** to form the hydroxy amide **2.14**. This would be followed by lactonization (mediated by PTSA catalysis) to give (*R*,*S*)- and (*S*,*S*)-lactone **2.15** as shown in Scheme 2.4. Given that this method does not involve any stereochemical control, the product is expected to be obtained a 1:1 ratio of *R*:*S* enantiomers; however, it should be possible to separate these stereoisomers after the formation of the diastereomers (*R*,*S*)- and (*S*,*S*)-lactone **2.15**.

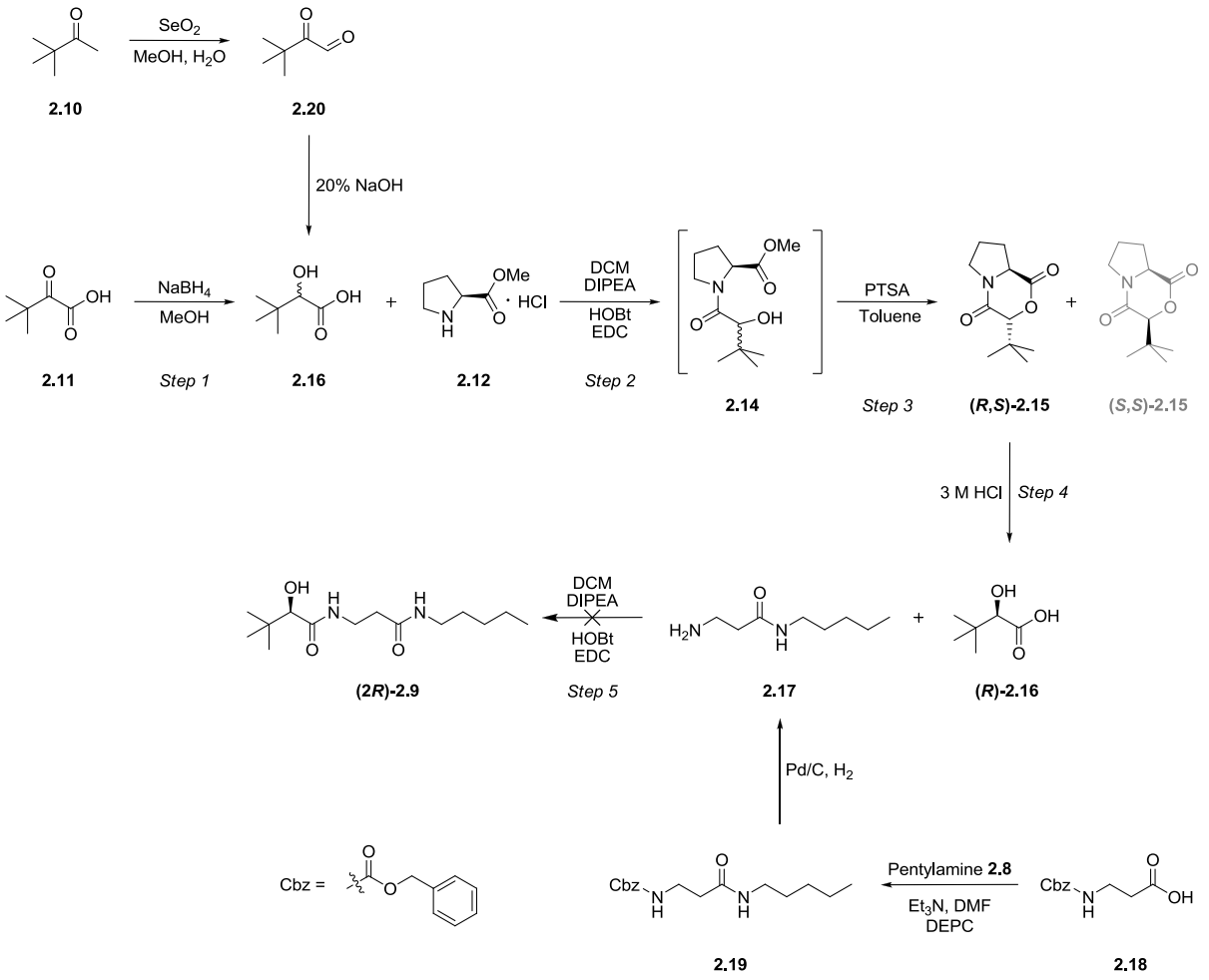


**Scheme 2.4. Proposed alternative synthetic route for the synthesis of (*R*)-4'-deoxy-*N*-pentyl pantothenamide 2.9 starting either from 3,3-dimethyl-2-oxo-butyric acid (2.11) or from pinacolone (2.10). This synthesis was successfully executed except for the final amide coupling in step 5.**

Our first attempt at the synthesis of racemic hydroxy acid **2.16** was through the reduction of ketoacid **2.11** based on a method reported in the literature [7]. In this method 1 equiv. of $NaBH_4$ was used and the reaction was stirred for 2h at 0°C. However, in our hands this was not sufficient to give complete reduction of the ketone. Therefore, 2 equiv. of $NaBH_4$ was used and the reaction was stirred for 4h at 0°C, followed by stirring overnight at room temperature (rt). Thin layer chromatography (TLC) showed that all of the starting material was consumed. The protocol stipulates that the reaction mixture must be acidified to pH 2 before extraction with diethyl ether. Subsequently, the organic layer is washed with $H_2O$ until a pH of 4 is reached. Using this method we only obtained a 5% yield of racemic hydroxy acid **2.16**, instead of the 67% yield that was reported [7]. We expect that this low yield is due to the loss of the product during the extensive aqueous work-up. Consequently an alternative method for the preparation of racemic hydroxy acid **2.16** was explored.

Hydroxy acid **2.16** can also be prepared from pinacolone **2.10** in a two-step synthesis (Scheme 2.4). A method by Fuson *et al*. [8], was used to oxidize pinacolone **2.10** with selenium dioxide ($SeO_2$) to form keto aldehyde **2.20** which was purified using a Claisen Vigreux distillation at atmospheric pressure and used without any further purification in the next step. In the following step, as described by Köntös *et al*. [9], aldehyde **2.20** was heated in an aqueous sodium hydroxide (NaOH) solution and underwent an internal Cannizzaro reaction in the strong basic medium resulting in the formation of the sodium salt of racemic hydroxy acid **2.16**, which, after acidification and recrystallization with 1,2-dichloroethane (DCE), was obtained in an overall yield (over the two steps) of 34% [9]. This method was preferentially used for the synthesis of racemic hydroxy acid **2.16** due to the higher overall yield. Additionally, in an effort to separate the two hydroxy acid **2.16** isomers a resolution was attempted by conversion to the (1*S*, 2*R*)-(+)-ephedrine salt followed by fractional crystallization; however, this method did not give satisfactory results.

Consequently, racemic hydroxy acid **2.16** was coupled to (*R*)-proline methyl ester HCl salt **2.12** using an amide coupling reaction in the presence of EDC, DIPEA and HOBt to give the diastereomers of hydroxy amide **2.14**. After an aqueous work-up this was immediately lactonized to (*R*,*S*)- and (*S*,*S*)-lactone **2.15** in the presence of PTSA, followed by purification by FCC. The isomers were obtained in a 1:1 ratio in a combined yield of 64% (over the two steps). Even though the Ru/C reduction method gave a 5:1 ratio of (*R*,*S*):(*S*,*S*)-**2.15** compared to the 1:1 ratio obtained for the coupling of racemic hydroxy acid **2.16**, the Ru/C method has an overall lower yield and will only give a marginally higher yield for (*R*,*S*)-**2.15**. Therefore, either method can be used for the synthesis of (*R*,*S*)-**2.15**.

Following the successful separation of (*R*,*S*)- and (*S*,*S*)-**2.15** in step 3, the (*R*,*S*)-isomer (stereochemistry was confirmed with $^1$H NMR spectroscopic analysis [6]) was subjected to acid hydrolysis in step 4 to afford the *R*-hydroxy acid HCl salt (**2.16**) in a 73% yield. The final step of the synthesis entailed an amide bond formation between **2.16** and amine **2.17**. The amine was prepared by coupling commercially available carboxylic acid **2.18** to pentylamine **2.8** using diethyl phosphoryl cyanide (DEPC) in the presence of $Et_3N$ by adapting a method from Yamada *et al*. [10] to form **2.19**, followed by successful removal of the benzyl carbamate protecting group through hydrogenation with $H_2$ gas in the presence of palladium on activated carbon (10% Pd/C) to yield amine **2.17** as a pure white solid upon filtration in an excellent yield (89%) over two steps. The purity of amine **2.17** was confirmed with $^1$H NMR spectroscopic analysis. Subsequently, amine **2.17** and *R*-hydroxy acid HCl salt **2.16** were coupled using an EDC coupling reaction with DIPEA and HOBt. The reaction gave a mixture of products which were subsequently separated by FCC. Unfortunately, according to NMR spectroscopic analysis, none of these were target compound (*R*)-

**2.9**. The coupling was also attempted by using DPPA as activation reagent, but regrettably NMR spectroscopic analysis indicated that this coupling was also unsuccessful. Consequently, after several months of attempting to synthesize (*R*)-**2.9** with no success, we decided to use (*R*/*S*)-**2.9** in the biological experiments set out in the accompanying manuscript.

## 2.3 Conclusion

The biological results obtained for N7-Pan in combination with pantothenic acid were consistent with the results obtained for N5-Pan in combination with pantothenic acid in the manuscript (Figures 8A and 8C). Additionally, the model described in the manuscript also fitted our experimental data well, with the kinetic parameters being nearly identical to those obtained for constant ratio mixtures of pantothenic acid and PantSH.

Virga *et al*. [4] reported that PanK enzymes require the *R*-configuration at the 2'-OH position of their substrates or inhibitors for optimal binding of the 4'-OH group in the active site. Therefore, we attempted the asymmetric synthesis of (*R*)-**2.9**; however, after numerous attempts this synthesis was not pursued any further due to low yielding reactions and a failure to perform the final amide bond formation. Consequently, we decided to use (*R*/*S*)-**2.9** in our biological experiments, and demonstrated that it showed excellent inhibition of the enzyme. It would be beneficial to attempt to synthesize (*R*)-**2.9** once more in future experiments. However, (*S*)-**2.9** should also be synthesized and tested to prove that it is indeed less effective than (*R*)-**2.9**. This will also confirm the reports by Virga *et al*. [4] that only the *R*-isomer is biologically active.

## 2.4 Experimental section

### 2.4.1 Materials and methods

General chemicals and reagents were purchased from Sigma-Aldrich, Merck Chemicals (Darmstadt, Germany) or Acros Organics (ThermoFisher, Fair Lawn, NJ, USA) and were of the highest purity. Solvents used for reactions were CHROMASOLV HPLC grade solvents from Sigma-Aldrich, while the hexanes, dichloromethane (DCM) and ethyl acetate (EtOAc) used for purification were purchased from Merck Chemicals. Dry DMF was prepared by shaking up over potassium hydroxide (KOH), distilled under reduced pressure and a nitrogen atmosphere, and finally stored over 4 Å molecular sieves in the dark. Dry DCM was distilled from calcium hydride ($CaH_2$) under a nitrogen atmosphere while dry tetrahydrofuran (THF) was distilled from sodium (Na) under a nitrogen atmosphere.

All $^{1}H$ and $^{13}C$ NMR spectra were obtained using a 300 MHz Varian VNMRS (75 MHz for $^{13}C$), 400 MHz Varian Unity Inova (100 MHz for $^{13}C$) or 600 MHz Varian Unity Inova (150 MHz for $^{13}C$) instruments at the Central Analytical Facility (CAF) of the University of Stellenbosch. All chemical shifts (δ) were recorded using the residual solvent peak and reported in p.p.m. All HRMS were performed on a Waters API Q-TOF Ultima spectrometer (Waters, Milford, MA, USA) at the Mass Spectrometry unit of CAF.

### 2.4.2 Synthetic preparation of 4'-deoxy N5-Pan (2.9)

*N-Formyl* β-*alanine benzyl ester* (**2.*3***)

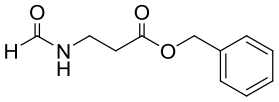

To a solution of β-alanine benzyl ester tosylate salt (3.00 g, 8.46 mmol) in $H_2O$ (20 mL) was added 1 M NaOH until the pH was adjusted to 10.5. The aqueous solution was extracted with DCM (4 × 25 mL) and dried ($Na_2SO_4$). The solvent was removed *in vacuo* to yield β-alanine benzyl ester (**2.1**) (1.29 g, 7.19 mmol) as a colourless oil. Acetic formic anhydride (**2.2**), prepared by stirring acetic anhydride (7.50 mL) with formic acid (3.30 mL) for 2.5h at 55°C, was added. The reaction mixture was refluxed at 70°C for 2h and cooled to rt. DCM (25 mL) was added and the organic layer was washed with saturated sodium bicarbonate ($NaHCO_3$) (2 × 25 mL) and $H_2O$ (2 × 25 mL). The organic layer was dried ($Na_2SO_4$), filtered and concentrated *in vacuo* to yield ester **2.3** (1.26 g, 72%) as a yellow oil. $R_f$ = 0.38 (3:1 EtOAc: Hexanes). $\delta_H$ (300 MHz; $CDCl_3$; 25°C) 2.60 (2H, t, *J* = 6.0 Hz, -$CH_2$-), 3.56 (2H, q, *J* = 7.0 Hz, -$CH_2$-), 5.15 (2H, s, -$CH_2$-), 6.11 (1H, br s, -NH-), 7.32-7.39 (5H, m, arom) and 8.14 (1H, s, -CH). $^{1}H$ NMR data are consistent with those previously reported [1].

*Isocyanide β-alanine benzyl ester* (**2.*4***)

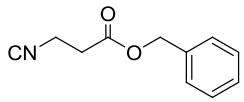

To a solution of ester **2.3** (1.26 g, 6.11 mmol) in THF (15 mL) at -78°C, under an inert atmosphere was added $Et_3N$ (4.26 mL, 30.6 mmol). A solution of $POCl_3$ (570 µL, 6.11 mmol) in THF (15 mL) was added slowly at -78°C while stirring continuously. After the addition was complete, the reaction mixture was stirred for an additional 3h at 0°C. The reaction was quenched by the addition of cold $H_2O$ (50 mL) and the aqueous layer was extracted with diethyl ether (3 × 30 mL). The combined organic extracts were washed with $H_2O$ (3 × 30 mL), dried ($MgSO_4$), filtered and concentrated *in vacuo* to yield isocyanide **2.4** (947 mg, 82%) as a black smelly oil. $R_f$ = 0.35 (3:1 EtOAc: Hexanes). $\delta_H$ (300 MHz; $CDCl_3$; 25°C) 2.75-2.81 (2H, m, -$CH_2$-), 3.68-3.73 (2H, m, -$CH_2$-), 5.18 (2H, s, -$CH_2$-) and 7.34-7.39 (5H, m, arom). $^{1}H$ NMR data are consistent with those previously reported [1].

*(R/S)-Benzyl 4'-deoxy-pantothenate* (**2.6**)

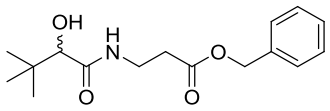

$SiCl_4$ (689 µL, 6.01 mmol) was added to a solution of isocyanide **2.4** (947 mg, 5.01 mmol) in dry DCM (25 mL) at 0°C under an inert atmosphere. The reaction mixture was stirred vigorously for 5 min before aldehyde **2.5** (653 µL, 6.01 mmol) was added at 0°C. The reaction mixture was warmed to 25°C and stirred for an additional 2h. The reaction was quenched by the addition of saturated potassium carbonate ($K_2CO_3$) (5 mL), filtered through Celite and the aqueous layer was extracted with DCM (3 × 30 mL). The combined organic extracts were washed with $H_2O$ (3 × 30 mL), dried ($MgSO_4$), filtered and concentrated *in vacuo*. Purification by FCC (1:1 EtOAc: Hexanes) yielded deoxy ester **2.6** (294 mg, 20%) as a light yellow oil. $R_f$ = 0.23 (FCC conditions). $\delta_H$ (400 MHz; $CDCl_3$; 25°C) 0.95 (9H, s, $-CH_3$), 2.60 (2H, t, *J* = 5.8 Hz, $-CH_2-$), 3.56 (2H, q, *J* = 6.2 Hz, $-CH_2-$), 3.64 (1H, d, *J* = 5.0 Hz, -CH-), 5.13 (2H, s, $-CH_2-$), 6.61 (1H, br s, -NH-) and 7.33-7.36 (5H, m, arom). OH proton not observed. $^1$H NMR data are consistent with those previously reported [1].

*(R/S)-4'-Deoxy-pantothenic acid* (**2.7**)

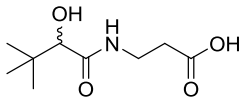

To a solution of deoxy ester **2.6** (294 mg, 1.00 mmol) in 4.4% formic acid/MeOH (20 mL) was added Pd (black) (147 mg, 1.38 mmol) at rt. The reaction mixture was stirred for 4h at rt before Pd (black) was removed by filtration and the filtrate was concentrated *in vacuo* to afford acid **2.7** (191 mg, 94%) as a colourless oil. $R_f$ = 0.21 (5% MeOH in DCM). $\delta_H$ (300 MHz; $CDCl_3$; 25°C) 0.98 (9H, s, $-CH_3$), 2.59 (2H, t, *J* = 5.9 Hz, $-CH_2-$), 3.55 (2H, q, *J* = 5.9 Hz, $-CH_2-$), 3.72 (1H, s, -CH-) and 6.82 (1H, br s, -NH-). OH protons not observed. $^1$H NMR data are consistent with those previously reported [1].

*3,3-Dimethyl-2-oxo-butyric acid* (**2.11**)

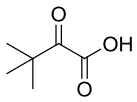

To a solution of NaOH (8.00 g, 200 mmol) and $KMnO_4$ (12.2 g, 77.2 mmol) in $H_2O$ (196 mL) at 0°C, was added a solution of pinacolone (**2.10**) (10 mL, 83.4 mmol) in $H_2O$ (160 mL). The reaction mixture was stirred for 1h at 0°C and an additional 2h at rt. The reaction mixture was filtered through Celite, acidified to pH 2 with concentrated sulphuric acid ($H_2SO_4$), and the aqueous layer was extracted with diethyl ether (3 × 40 mL). The combined organic extracts were dried ($Na_2SO_4$), filtered and concentrated *in vacuo*. Bulb-to-bulb distillation (110°C, 27.5 mmHg) gave carboxylic acid **2.11** (3.99 g, 77%) as a clear oil. $\delta_H$ (300 MHz; $CDCl_3$; 25°C) 1.32 (9H, s, $-CH_3$). OH proton not observed. $^1$H NMR data are consistent with those previously reported [7].

*(3R,8S)-3-Tert-butyltetrahydro-1H-pyrrolo[2,1-c][1,4]oxazine-1,4(3H)-dione* (**2.15**)

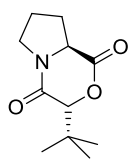

DIPEA (3.00 mL, 17.2 mmol) was added drop-wise over 5 min to a solution of (*R*)-proline methyl ester HCl salt (**2.12**) (2.76 g, 16.6 mmol) in DCM (54 mL) at 0°C. HOBt (396 mg, 2.93 mmol), racemic hydroxy acid **2.16** (2.00 g, 15.1 mmol) and EDC hydrochloride (3.19 g, 16.6 mmol) were then added consecutively at 0°C and the reaction mixture was stirred overnight at rt. The reaction was quenched by the addition of 3 M HCl (54 mL) and the organic layer was washed with 3 M HCl (1 × 54 mL) and saturated $NaHCO_3$ (1 × 54 mL). The organic layer was dried ($Na_2SO_4$), filtered and concentrated *in vacuo* to afford crude racemic hydroxy amide **2.14**. To a solution of racemic hydroxy amide **2.14** in toluene (50 mL) was added PTSA (432 mg, 2.27 mmol) and the reaction mixture was stirred for 48h at rt. The toluene was removed *in vacuo* before purification with FCC (9:1 DCM: EtOAc) afforded (*R*,*S*)- and (*S*,*S*)-lactone **2.15** as white solids in a combined yield of 64%. The ratio of (*R*,*S*)-lactone **2.15** to (*S*,*S*)-lactone **2.15** was 1:1.

(*R*,*S*)-lactone **2.15** $R_f$ = 0.19 (FCC conditions). $\delta_H$ (400 MHz; $CDCl_3$; 25°C) 1.11 (9H, s, $-CH_3$), 1.86-2.08 (3H, m, $-CH_2-$), 2.45-2.52 (1H, m, $-CH_2-$), 3.52-3.57 (1H, m, $-CH_2-$), 3.71-3.78 (1H, m, $-CH_2-$), 4.19 (1H, dd, *J* = 6.6, 10.2 Hz, -CH-) and 4.50 (1H, s, -CH-). $^1$H NMR data are consistent with those previously reported [6].

(*S*,*S*)-lactone **2.15** $R_f$ = 0.37 (FCC conditions). $\delta_H$ (400 MHz; $CDCl_3$; 25°C) 1.19 (9H, s, $-CH_3$), 1.88-2.05 (2H, m, $-CH_2-$), 2.26-2.41 (2H, m, $-CH_2-$), 3.48-3.64 (2H, m, $-CH_2-$), 4.22 (1H, t, *J* = 7.8 Hz, -CH-) and 4.33 (1H, s, -CH-). $^1$H NMR data are consistent with those previously reported [6].

*(3R,8S)-3-Tert-butyltetrahydro-1H-pyrrolo[2,1-c][1,4]oxazine-1,4(3H)-dione* (**2.15**)

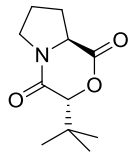

To a solution of ketoamide **2.13** (1.00 g, 4.14 mmol) in MeOH (50 mL) was added 5% Ru/C (500 mg, 4.95 mmol) and the reaction mixture was degassed by three alternating nitrogen/vacuum cycles. The reaction mixture was heated to 50°C and pressurized to 60 psi of $H_2$ pressure and stirred for 72h. The reaction mixture was cooled to rt, depressurized, filtered through a pad of Celite and concentrated *in vacuo* to afford crude racemic hydroxy amide **2.14**. To a solution of racemic hydroxy amide **2.14** in toluene (30 mL) was added PTSA (120 mg, 0.63 mmol) and the reaction mixture was stirred for 48h at rt. The toluene was removed *in vacuo* before purification with FCC (9:1 DCM: EtOAc) afforded (*R*,*S*)- and (*S*,*S*)-lactone **2.15** as white solids in a combined yield of 48%. The ratio of (*R*,*S*)-lactone **2.15** to (*S*,*S*)-lactone **2.15** was 5:1. Analytical data are identical to those reported above.

*2-Hydroxy-3,3-dimethylbutanoic acid* (**2.16**)

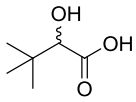

To a solution of ketoacid **2.11** (3.00 g, 23.1 mmol) in MeOH (100 mL) at 0°C under an inert atmosphere was added $NaBH_4$ (1.75 g, 46.1 mmol) in small portions. The reaction mixture was stirred for 4h at 0°C, and left to stir overnight at rt. The solvent was removed *in vacuo* and the resulting crude residue was dissolved in $H_2O$ (20 mL) and acidified to pH 2 (with cooling) with 3 M HCl. The aqueous layer was extracted with diethyl ether (4 × 25 mL) and the combined organic extracts were washed with $H_2O$ until the pH of a washing became pH 4. The combined organic extracts were dried ($Na_2SO_4$), filtered, concentrated *in vacuo* and lyophilized to yield racemic hydroxy acid **2.16** (152 mg, 5%) as a white solid. $R_f$ = product on baseline (10% MeOH in DCM). $\delta_H$ (400 MHz; $CDCl_3$; 25°C) 1.02 (9H, s, -$CH_3$) and 3.87 (1H, s, -$CH_3$). O<u>H</u> protons not observed. $^1$H NMR data are consistent with those previously reported [7].

*2-Hydroxy-3,3-dimethylbutanoic acid* (**2.16**)

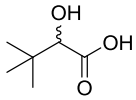

NaOH (20% aqueous, 220 mL, 550 mmol) was added slowly to a solution of keto aldehyde **2.20** (56.1 g, 491 mmol) heated to 80°C. The reaction mixture was stirred overnight at 80°C. The reaction mixture was cooled to 0°C and acidified to pH 2 with concentrated HCl. The aqueous layer was extracted with diethyl ether (4 × 200 mL). The combined organic extracts were dried ($MgSO_4$), filtered, concentrated *in vacuo* and lyophilized. The crude product was recrystallized from DCE to afford racemic hydroxy acid **2.16** (43.5 g, 67%) as white crystals. Analytical data are identical to those reported above.

*(R)-2-Hydroxy-3,3-dimethylbutanoic acid* (**(*R*)-2.16**)

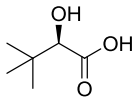

(*R*,*S*)-lactone **2.15** (500 mg, 2.37 mmol) was dissolved in 3 M HCl (30 mL) and refluxed overnight. The reaction mixture was lyophilized before purification with FCC (5:1:1:1 EtOAc: $H_2O$: MeOH: Acetonitrile ($CH_3CN$)). Purified *R*-hydroxy acid **2.16** was lyophilized to afford a white solid (230 mg, 73%). $R_f$ = 0.44 (FCC conditions). $\delta_H$ (400 MHz; $CDCl_3$; 25°C) 1.03 (9H, s, -$CH_3$) and 3.91 (1H, s, -CH-). O<u>H</u> protons not observed.

*3-Amino-N-pentylpropanamide* (**2.17**)

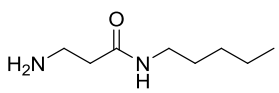

To a solution of carbamate **2.19** (1.50 g, 5.13 mmol) in MeOH (80 mL) at rt was added Pd/C (80.0 mg, 0.752 mmol). The reaction atmosphere was filled with $H_2$ gas and the reaction mixture was stirred overnight at rt under $H_2$. Additional Pd/C (100 mg, 0.940 mmol) was added and the reaction mixture was stirred for a further 5h under $H_2$. The reaction mixture was filtered and concentrated *in vacuo* to give amide **2.17** (800 mg, 99%) as a white solid. $R_f$ = product on baseline (10% MeOH in DCM). $\delta_H$ (300 MHz;

$CDCl_3$; 25°C) 0.87 (3H, t, *J* = 7.1 Hz, $-CH_3$), 1.29-1.33 (4H, m, $-(CH_2)_2-$), 1.50-1.59 (4H, m, $-CH_2-$ and $-NH_2$), 2.28 (2H, t, *J* = 5.6 Hz, $-CH_2-$), 2.98 (2H, t, *J* = 6.1 Hz, $-CH_2-$), 3.20 (2H, q, *J* = 7.3 Hz, $-CH_2-$) and 6.85 (1H, br s, -NH-). $\delta_C$ (300 MHz; $CDCl_3$; 25°C) 14.4, 22.7, 29.5, 29.6, 38.0 38.3, 39.7 and 172.4. (MS) $[M+H]^+$ 159.1499 (Calculated $[C_8H_{19}N_2O]^+$ = 159.15).

*Benzyl 3-oxo-3-(pentylamino) propylcarbamate* (**2.19**)

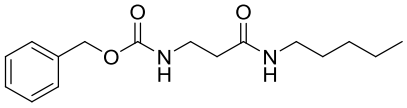

Pentylamine (**2.8**) (803 µL, 6.96 mmol) and DEPC (1.05 mL, 6.96 mmol) were added to a solution of Cbz-β-alanine (**2.18**) (1.41 g, 6.32 mmol) in dry DMF (8 mL) at rt. The reaction mixture was cooled to 0°C before $Et_3N$ (1.85 mL, 13.3 mmol) was added. The reaction mixture was stirred for 2h at 0°C and left to stir overnight at rt. EtOAc (50 mL) was added and the organic layer was washed with 5% citric acid (3 × 10 mL), 1 M aqueous $NaHCO_3$ (2 × 10 mL) and saturated sodium chloride (NaCl) (1 × 10 mL). The organic layer was dried ($Na_2SO_4$), filtered and concentrated *in vacuo* before purification by FCC (3:2 to 4:1 EtOAc: Hexanes) afforded carbamate **2.19** (1.50 g, 81%) as a white solid. $R_f$ = 0.18 (FCC conditions). $\delta_H$ (300 MHz; $CDCl_3$; 25°C) 0.87 (3H, t, *J* = 6.9 Hz, $-CH_3$), 1.26-1.33 (4H, m, $-(CH_2)_2-$), 1.54-1.61 (2H, m, $-CH_2-$), 2.38 (2H, t, *J* = 6.0 Hz, $-CH_2-$), 3.19 (2H, q, *J* = 7.3 Hz, $-CH_2-$), 3.45 (2H, q, *J* = 6.3 Hz, $-CH_2-$), 5.09 (2H, s, $-CH_2-$), 5.44 (1H, br s, -NH-), 5.56 (1H, br s, -NH-) and 7.32-7.36 (5H, m, arom). $\delta_C$ (400 MHz; $CDCl_3$; 25°C) 14.0, 22.3, 29.0, 29.2, 36.1, 37.1, 39.5, 66.6, 128.0, 128.1, 128.5, 136.5, 156.8 and 171.3. (MS) $[M+H]^+$ 293.1866 (Calculated $[C_{16}H_{25}N_2O_3]^+$ = 293.19).

*3,3-Dimethyl-2-oxobutanal* (**2.20**)

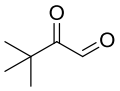

$SeO_2$ (111.2 g, 1.00 mol) was added to a solution of MeOH (100 mL) and $H_2O$ (5 mL) and the reaction mixture was refluxed until all the $SeO_2$ dissolved. Pinacolone (**2.10**) (122 mL, 976 mmol) was added rapidly and the clear solution became red and then black after a few minutes. The reaction mixture was refluxed overnight. The reaction mixture was cooled to rt and filtered to remove the precipitated selenium. The yellow to orange filtrate was distilled at atmospheric pressure using a Claisen vigreux distillation setup and the distillate was collected from 110 – 120°C to afford keto aldehyde **2.20** (56.1 g, 50%) as a yellow oil. The product was used without purification.

## 2.5 References

1. Koekemoer, L. Characterization of prokaryotic pantothenate kinase enzymes and the development of type-specific inhibitors. PhD, University of Stellenbosch, 2011.
2. Suchy, M., Elmehriki, A. A. H. and Hudson, R. H. E., A remarkably simple protocol for the *N*-formylation of amino acid esters and primary amines. *Organic Letters*, 2011**. 13** (15), 3952-3955.
3. Shioiri, T., Ninomiya, K. and Yamada, S., Diphenylphosphoryl azide. A new convenient reagent for a modified Curtius reaction and for peptide synthesis. *Journal of the American Chemical Society*, 1972**. 94** (17), 6203-6205.
4. Virga, K. G., Zhang, Y. M., Leonardi, R., Ivey, R. A., Hevener, K., Park, H. W., Jackowski, S., Rock, C. O. and Lee, R. E., Structure-activity relationships and enzyme inhibition of pantothenamide-type pantothenate kinase inhibitors. *Bioorganic & Medicinal Chemistry*, 2006**. 14** (4), 1007-1020.
5. Tuck, K. L., Saldanha, S. A., Birch, L. M., Smith, A. G. and Abell, C., The design and synthesis of inhibitors of pantothenate synthetase. *Organic & Biomolecular Chemistry* 2006**. 4**, 3598-3610.
6. Nelson, T. D., LeBlond, C. R., Frantz, D. E., Matty, L., Mitten, J. V., Weaver, D. G., Moore, J. C., Kim, J. M., Boyd, R., Kim, P.-Y., Gbewonyo, K., Brower, M., Sturr, M., McLaughlin, K., McMasters, D. R., Kress, M. H., McNamara, J. M. and Dolling, U. H., Stereoselective synthesis of a potent thrombin inhibitor by a novel P2-P3 lactone ring opening. *Journal of Organic Chemistry*, 2004**. 69**, 3620-3627.
7. Enholm, E. J., Lavieri, S., Cordóva, T. and Ghiviriga, I., 1,3-Diastereocontrol in acyclic radical allylations. *Tetrahedron Letters*, 2003**. 44** (3), 531-534.
8. Fuson, R. C., Gray, H. and Gouza, J. J., Acyloins from *t*-Butylglyoxal. *Journal of the American Chemical Society*, 1939**. 61** (8), 1937-1940.
9. Köntös, Z., Huszthy, P., Bradshaw, J. S. and Izatt, R. M., Enantioseparation of racemic organic ammonium perchlorates by a silica gel bound optically active di-*tert*-butylpyridino-18-crown-6 ligand. *Tetrahedron Asymmetry*, 1999**. 10** (11), 2087-2099.
10. Yamada, S., Kasai, Y. and Shioiri, T., Diethylphosphoryl cyanide. A new reagent for the synthesis of amides. *Tetrahedron Letters*, 1973**. 14** (18), 1595-1598.

*Chapter 3*

# Developing PanK Inhibitors That Are Resistant To Pantetheinase-Mediated Degradation

## 3.1 Introduction

Drug-resistant pathogens are a major cause for the increase in morbidity and mortality worldwide. These pathogens include, but are not limited to, MRSA, ESBL-producing *Escherichia coli*, vancomycin-resistant enterococci, MDR and XDR *M. tuberculosis* and penicillin- and macrolide-resistant pneumococci [1-2]. The current arsenal of available antibiotics which has been successfully used for decades as treatments against bacteria—including *S. aureus*—is being rendered ineffective due to bacteria becoming increasingly insensitive to these compounds [3-4]. Since *S. aureus* makes use of all known mechanisms to develop antibiotic resistance (as discussed in detail in Chapter 1), new antimicrobials with novel modes of action are needed to decrease the prospect of cross-resistance [5].

The CoA biosynthetic pathway, as well as the enzymes that subsequently utilize CoA, is seen as a potential novel target for antimicrobial chemotherapy development. The value of this pathway lies in CoA being an essential cofactor that needs to be synthesized *de novo* in all living organisms [6]. In *S. aureus*, CoA biosynthesis is an even more attractive target due to the accumulation of milimolar quantities of CoA in the organism. Moreover, CoA is involved in maintaining the redox balance in *S. aureus* through a unique CoA disulphide reductase system [1, 6].

Previous studies have established that pantothenamides—amide analogues of pantothenic acid—are potential small molecule inhibitors of CoA biosynthesis and utilization in *S. aureus* [1, 7-12]. Although the antibacterial activity of pantothenamides has been investigated since 1970 [6], our poor understanding of their mechanism of action hampered their development as clinically relevant agents. Furthermore, N5-Pan and N7-Pan, classical examples of the pantothenamide class, show inhibitor activity against *Sa*PanK-II as well as *S. aureus* in the micro- and nanomolar range in the *in vitro* studies; however, pantothenamides do not translate into potent inhibitors *in vivo* [1, 6, 12-13]. In 2011 Jansen *et al*. [13] discovered that this loss of antimicrobial activity *in vivo* is due to enzymatic degradation of the pantothenamides by pantetheinase enzymes. These enzymes are encoded by the Vanin gene family (that forms part of the nitrilase superfamily), of which three human genes (VNN1, VNN2 and VNN3), two murine genes (Vanin-1 and Vanin-2) and one homologue in *Drosophila* are known [14-15]. Pantetheinase, also known as PantSH hydrolyse, catalyzes the hydrolysis of one specific amide linkage in PantSH (Scheme 1.8 and 1.9, Chapter 1) via an invariant Glu-Lys-Cys catalytic triad to yield pantothenic acid (for reuse in CoA biosynthesis)

and cysteamine (a powerful antioxidant) [16-18]. Pantetheinase is highly substrate specific for the pantothenate moiety, while the cysteamine structure moiety is less specific and alternative functional groups can replace the sulfhydryl functional group in the substrate [17, 19]. As a result, the pantothenamides are also hydrolyzed by pantetheinase leading to the formation of pantothenic acid and the corresponding amine (Scheme 1.8, Chapter 1), resulting in the loss of antimicrobial activity [13, 20].

The results of our study of the mode of action of the pantothenamides in *S. aureus* (as related in Chapter 2) that showed that these compounds exert their growth inhibitory effects at least partially by inhibiting PanK has contributed significantly to our knowledge in this regard. Additionally, recent findings on the breakdown of pantothenamides by pantetheinase through the hydrolysis of a specific amide linkage rendering them ineffective; we now have greater insight into how these compounds exert their antimicrobial activity. In combination, these findings show that new potent antistaphylococcal inhibitors based on the pantothenamide scaffold should show two main characteristics: 1) they should be resistant to the degradation caused by the pantetheinase enzymes and 2) they should still bear enough structural similarity to PantSH to exhibit the same complex interaction with *Sa*PanK-II that causes the inhibitory profiles described in the previous Chapter.

## 3.2 Study design and strategy

With these requirements in mind, we set out to design and characterize new *Sa*PanK-II inhibitors by making modifications to the pantothenamide core structure that would protect it against pantetheinase-mediated hydrolysis, while retaining the important interactions required for recognition by *Sa*PanK-II. This can be achieved through one of three strategies: 1) by either making the scissile amide bond less accessible to the pantetheinase catalytic residues by increasing the steric bulk surrounding it, e.g. by addition of a methyl group, 2) by replacing the scissile amide bond with a bioisostere that would withstand pantetheinase degradation, or 3) by preventing the compound from being recognized as a substrate by pantetheinase by replacing or removing the 4'-hydroxyl group, since pantetheinase is highly substrate specific for the pantothenate motif (Figure 3.1) [17, 19].

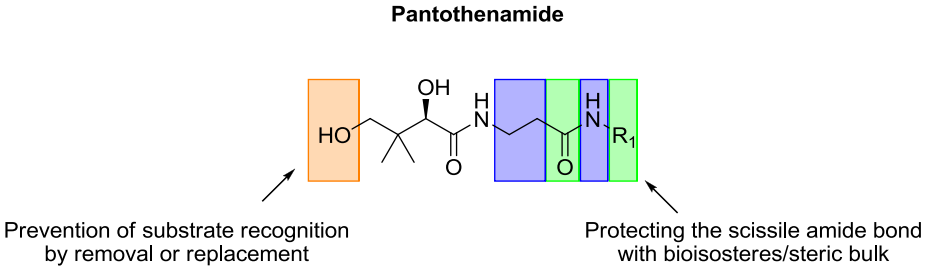


**Figure 3.1. Three strategies to protect the pantothenamide from pantetheinase mediated hydrolysis: 1) Addition of steric bulk in the regions of the molecule highlighted in blue, 2) Substitution of the scissile amide bond with a bioisostere in the regions highlighted in green, or 3) Removal or replacement of the 4'-hydroxyl highlighted in the orange block.**

*N*-Heptyl pantothenamide (**3.10**, N7-Pan), a member of the pantothenamide library designed and synthesized by de Villiers *et al*. [12], has previously been demonstrated to show the most potent inhibition against *S. aureus* with a MIC value in the nanomolar range. This also correlates with other studies of the pantothenamides in which N7-Pan **3.10** was also the best pantothenamide inhibitor of *S. aureus* [1]. We consequently decided to use N7-Pan **3.10** as scaffold to synthesize ten analogues that would show increased resistance to pantetheinase-mediated degradation, while retaining the structural feature required for *Sa*PanK-II binding (Figure 3.2).

The first strategy was based on increasing the steric bulk surrounding the scissile amide bond and the compounds based on this strategy are indicated with a blue box in Figure 3.2. In two N7-Pan analogues the scissile amide bond was retained, but a methyl group was added to either the α- or β-position relative to the amide bond. This was expected to introduce steric hindrance and prevent or slow the hydrolysis of the amide bond. Furthermore, backbone *N*-methylation is one of many ways nature has developed to stabilize highly rich peptidic scaffolds and to resist protease-mediated degradation. Chemists use *N*-methylation to enhance the pharmacological properties of peptides because it tends to increase the molecular cell permeability, as well as their stability towards enzymatic degradation [21]. Therefore, the third option for increasing steric bulk on N7-Pan **3.10** was by *N*-alkylation of the amide nitrogen. The final N7-Pan analogue that was based on strategy 1 involved the introduction of a double bond. Although the introduction of a double bond in the β-alanine moiety of the molecule is not technically seen as adding steric bulk in the vicinity of the scissile amide bond, the decreased rotational freedom that results from this modification may also reduce access to the amide carbonyl by preventing pantetheinase from binding the analogue in the orientation necessary for catalysis.

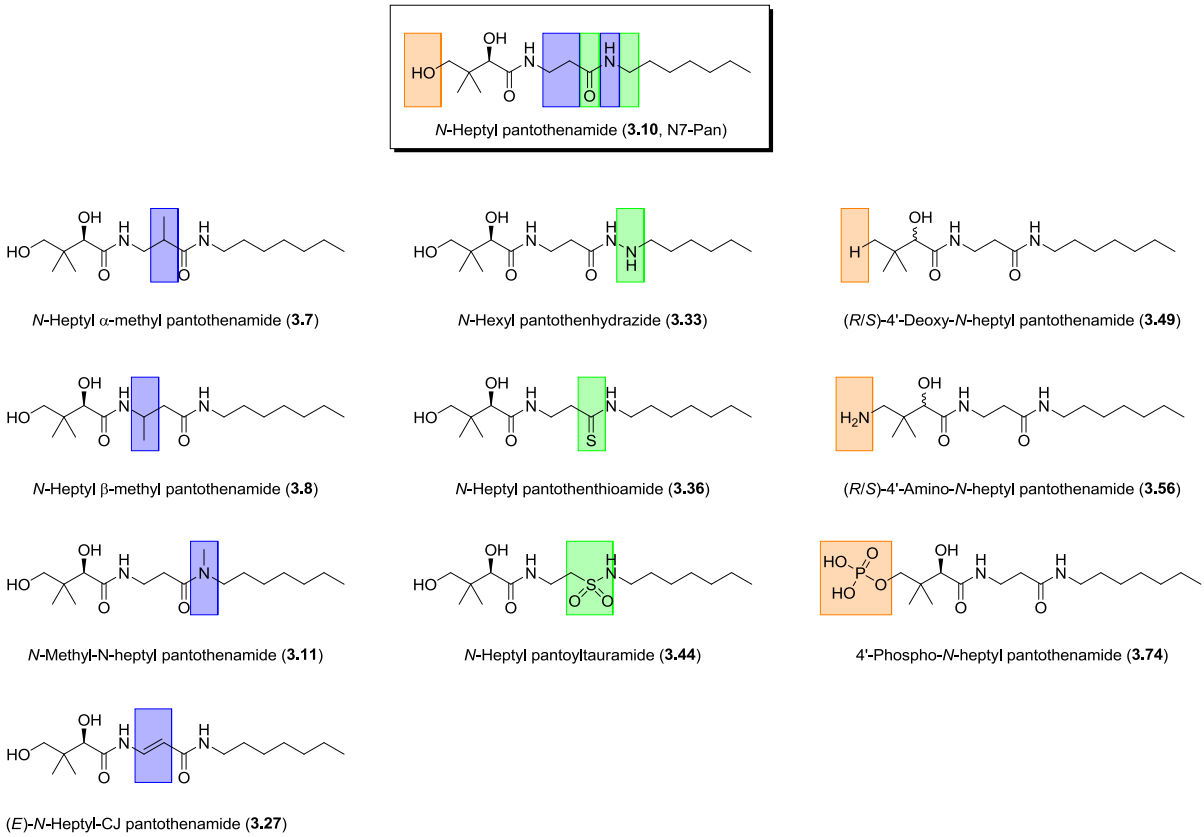


**Figure 3.2. Structures of N7-Pan analogues designed to withstand pantetheinase-mediated hydrolysis using the strategies outlined in Figure 3.1 and the text. In each case the boxed region highlights the structural modification, while the colour (legend as in Figure 3.1) indicates which specific strategy was used to introduce degradation resistance.**

The second strategy was based on replacing the scissile amide bond with a bioisostere (compounds indicated with a green box in Figure 3.2). Exchange of the scissile amide for a hydrazide is one of three bioisosteric replacements that were employed in an attempt to render the N7-Pan analogues less susceptible to pantetheinase degradation. Various hydrazide derivatives have been claimed to possess antimicrobial, antimalarial, anti-Human Immunodeficiency Virus (HIV), antitumor, antimycobacterial, trypanocidal and anti-inflammatory activities [22]. Therefore, we set out so synthesize a N7-Pan analogue that incorporated the hydrazide bioisostere.

The second bioisostere that we decided upon was a thioamide. Thioamides, formed by replacing the carbonyl oxygen in an amide bond with sulfur, has received considerable attention in synthetic medicinal chemistry, although less than a hand full of naturally occurring thioamides are known out of over 170 000 natural products [23-24]. Various thioamides have been developed as therapeutics against *M. tuberculosis*, as broad band anthelmintics and antifungals, and thioamides have also been discussed in support of inhibition of the anthrax lethal factor. Moreover, another thioamide,

closthioamide, represents an extremely active antibacterial agent against MRSA, with only moderate cytotoxicity [23]. The third and final bioisostere that we decided on was a bioisostere called sulfonamide ($R_1$-S(=O)$_2$-NH-$R_2$). These bioisosteres are widely used in the agricultural and pharmaceutical industry. Due to the fact that the main pharmaceutical applications of the sulfonamides as clinical medicines include antibacterial agents, diuretics and HIV protease inhibitors [25-27], we suspected that the sulfonamide moiety should be pantetheinase-resistant.

The third strategy was based on modifying the structure of N7-Pan **3.10** in such a way that pantetheinase would not recognize it as an alternative substrate (compounds indicated with an orange box in Figure 3.2). Previously, pantetheinase has been shown to require the pantothenate moiety for binding [17, 19]. We therefore wanted to test whether pantetheinase would still recognize pantothenamides as substrates if we either remove the 4'-hydroxyl group or replace the 4'-hydroxyl group with another functional group such as a primary amine or a phosphate.

## 3.3 Physicochemical properties of the proposed N7-Pan analogues

With the dramatic increase in MDR pathogens and the need for novel antibiotics, it is imperative to understand as much as possible from preceding efforts in drug discovery and drug development settings and to apply the lessons learned to the discovery of prospective antibiotics [28]. Lipinski's landmark study [29] epitomized the first systematic attempt to correlate the physicochemical properties of certain drugs within the World Drug Index (WDI) database which included the predicted successful initial hits as well as the subsequent late stage leads. By making use of experimental and computational approaches Lipinski *et al*. [29] connected the physicochemical properties of drugs with both, their oral bioavailability and the subsequent difficulties encountered during preclinical and clinical progression for the first time. The most important discovery in this study was the identification of an ideal property space for orally available drug candidates, now called "Lipinski's rules", "the rule of 5" or "Lipinski's rules of 5" since all four properties relate to the number 5. Today it is common to analyse these properties prior to synthesizing novel candidates [28-30]. Approximately 90% of all oral compounds pass three of the four following rules:

1. The molecular weight (M/W) **≤ 500** g.mol$^{-1}$
2. The lipophilicity, expressed as the partition coefficient (Log*P* or cLog*P*) **≤** 5 and **≥ 0**
3. The number of hydrogen bond (H-bond) donors **≤ 5**
4. The number of hydrogen bond (H-bond) acceptors **≤ 10**

Consequently, we analyzed the predicted physicochemical properties of the N7-Pan analogues described above. The Lipinski rule of 5 physicochemical properties for these compounds is shown in Table 3.1. The molecular weight of a compound is probably the most useful measure of molecular size as it is very easy to calculate. In literature, increasing molecular weight is related to poorer blood brain barrier permeability as well as poorer intestinal permeability [29]. According to Lipinski's rule of 5 most oral drugs have a molecular weight ≤ 500 g.mol$^{-1}$; all of the proposed N7-Pan analogues are compliant to this rule.

Lipophilicity is the most important physical property of a drug in relation to its absorption, distribution, potency, and elimination. If a drug is too lipophilic it may be insoluble in aqueous media such as blood or gastrointestinal fluid, or bind too strongly to plasma proteins and therefore the free blood concentration will be too low to produce the desired effect. Alternatively, the drug will distribute into lipid bi-layers and be unable to reach the inside of the cell. Conversely, if the drug is not lipophilic enough, it will not be absorbed through the gut wall due to a lack of membrane solubility. Lipophilicity is expressed as the partition coefficient (Log*P* or cLog*P*), where *P* (partition) is a measure of the relative affinity of a molecule for the lipid and aqueous phases in the absence of ionization. *P* is calculated by:

$$P = \frac{[X]_{Octanol}}{[X]_{Aqueous}}$$

Where $[X]_{Octanol}$ is equal to the concentration of the drug in the octanol phase and $[X]_{Aqueous}$ is equal to the concentration of the drug in the aqueous phase.

Octanol is the most frequently used lipid phase in pharmaceutical research since it is has a polar and non-polar region like a membrane phospholipid. $P_{\mathrm{Octanol/Aqueous}}$ is relatively easy to measure and frequently correlates well with various biological properties, in addition to being predicted fairly accurately with computational models. Using these computational models, cLog*P* for a molecule can be calculated from a sum of fragmental or atom-based terms plus various corrections [31-33]:

$$cLogP = \sum fragments + \sum corrections\ .$$

In this study, values of cLog*P* were calculated with calculator plugins in the program MarvinSketch 6.0.6. The calculation method that was used is a weighted method which uses equal weights of three individual methods. In the first method (VG) Log*P* data is applied from a publication by Viswanadhan *et al.* [34], in the second method (PHYS) Log*P* data is applied from the Physical Properties (PHYSPROP) database [35] distributed by the Syracuse Research Corporation and in the third method (KLOP) Log*P* data is applied from a publication by Klopman *et al*. [36]. We found

that all of the proposed N7-Pan analogues obey Lipinski's rule of 5 except *N*-hexyl-pantothenhydrazide (**3.33**, N6-pantothenhydrazide) which had a value of -0.02, indicating that it is not lipophilic enough to be considered a suitable drug candidate.

The last two rules of Lipinski are based on H-bond interactions. Intermolecular H-bonds are practically non-existent between small molecules in water, while intramolecular H-bonds are more easily formed in water since they are entropically more favoured. Consequently, de-solvation and formation of a neutral molecule is unfavourable if the compound forms many hydrogen or ionic bonds with water. Given that most oral drugs are absorbed through the gut wall by transcellular absorption, the number of H-bond donors or acceptors must be limited, otherwise the drug will not get absorbed from the gut into the blood [37]. When evaluating our proposed N7-Pan analogues against these criteria, we found that all are compliant to the desired amount of H-bond donors (≤ 5) and acceptors (≤ 10). The number of H-bond donors and H-bond acceptors were also calculated using the calculator plugins in the program MarvinSketch 6.0.6.

In recent years the Lipinski rule of 5 model has been expanded to include more *in silico* characterized properties such as the Polar Surface Area (PSA ≤ 140 Å$^2$), the number of rotatable bonds (NRotBs ≤ 10-20), the distribution coefficient (Log$D_{7.4}$ ≤ 5 and ≥ 0) and the fraction of $sp^3$-hybridized carbon atoms (F$sp^3$) [28, 30]. These additional physicochemical properties for the N7-Pan analogues are also shown in Table 3.1. The PSA is a measure of what proportion of the surface of the molecule is comprised of polar groups, compared to the proportion of hydrophobic groups. Our N7-Pan analogues are in good agreement with the optimal PSA of ≤ 140 Å$^2$, except for 4'-phospho-*N*-heptyl pantothenamide (**3.74**, 4'-phospho-N7-Pan). Furthermore, the NRotBs also play an important role in the absorption potential and permeability of a drug. A rotatable bond is defined as any single non-ring bond, attached to a non-terminal, non-hydrogen atom. However, amide C–N bonds are not counted because of their high barrier to rotation. All of the N7-Pan analogues have between 11 and 14 NRotBs which is in good agreement with the suggested 10-20 NRotBs [30].

The distribution coefficient is similar to the partition coefficient; however, if a drug can ionize then the observed partitioning (*P*) between water and octanol will be pH-dependent. Thus, the distribution coefficient is the effective lipophilicity of a drug at a given pH, and is a function of both the lipophilicity of the un-ionized drug and the degree of ionization. The distribution coefficient can be calculated using the equation:

$$LogD = \mathrm{Log}\frac{[X]_{Octanol}}{[X]_{Aqueous}^{Ionized} + [X]_{Aqueous}^{Un-ionized}}$$

Where $[X]_{Octanol}$ is equal to the concentration of the drug in the octanol phase, $[X]^{Ionized}_{Aqueous}$ is equal to the concentration of the ionized drug in the aqueous phase and $[X]^{Un-ionized}_{Aqueous}$ is equal to the concentration of the un-ionized drug in the aqueous phase.

For most of the N7-Pan analogues the partition coefficient is equal to the distribution coefficient since these analogues cannot ionize. It is only 4'-phospho-N7-Pan **3.74** and (*R*/*S*)-4'-amino-*N*-heptyl pantothenamide (**3.56**, (*R*/*S*)-4'-amino-N7-Pan) that are able to ionize due to the modifications made at the 4'-position of N7-Pan. Unfortunately, the Log$D_{7.4}$ values for these compounds fall outside the limits of the proposed Log$D_{7.4}$ values. The NRotBs and the distribution coefficients of each N7-Pan analogue were also calculated using the calculator plugins in the program MarvinSketch 6.0.6.

The final physicochemical property that we investigated was the molecular topology, F$sp^3$. F$sp^3$ is the number of $sp^3$-hybridized carbon atoms divided by the total number of carbon atoms. Aqueous solubility, plasma protein binding, potassium channel inhibition, as well as Caco-2 permeability are all influenced by F$sp^3$, some favourably and others unfavourably by increased F$sp^3$. Specifically, the aqueous solubility is increased by an increase in F$sp^3$ [38]. We found that the F$sp^3$ % calculated for the N7-Pan analogues are between 86.7% and 93.3%, except for (*E*)-*N*-heptyl CJ-pantothenamide (**3.27**, (*E*)-N7-CJ-Pan) with a F$sp^3$ % of 75%. Therefore, these N7-Pan analogues should have a high aqueous solubility.

All of the proposed N7-Pan analogues pass at least three of the four rules set by Lipinski's rules of 5, in addition to the expanded *in silico* characterized properties. We therefore expect that these compounds will be orally bioavailable if they translate into potent inhibitors.

**Table 3.1. Physicochemical properties of the N7-Pan analogues[a]. The values indicated in red fall outside the proposed limits.**

| Molecule | M/W (g.mol$^{-1}$) | cLog*P* | H-bond acceptors | H-bond donors | PSA (Å$^2$) | NRotBs | Log$D_{7.4}$ | F*sp*$^3$ |
|---|---|---|---|---|---|---|---|---|
| 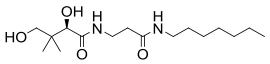 | 316.44 | 0.72 | 4 | 4 | 98.66 | 12 | 0.72 | 0.875 |
| 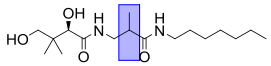 | 330.46 | 1.26 | 4 | 4 | 98.66 | 12 | 1.26 | 0.882 |
| 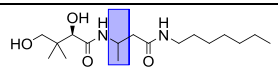 | 330.46 | 1.14 | 4 | 4 | 98.66 | 12 | 1.14 | 0.882 |
| 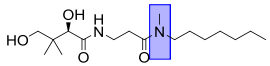 | 330.46 | 0.94 | 4 | 3 | 89.87 | 12 | 0.94 | 0.882 |
| 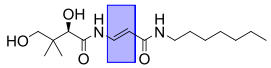 | 314.42 | 0.93 | 4 | 4 | 98.66 | 11 | 0.93 | 0.750 |
| 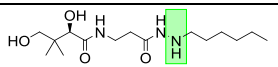 | 317.42 | -0.02 | 5 | 5 | 110.7 | 12 | -0.02 | 0.867 |
| 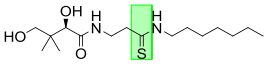 | 332.50 | 1.61 | 3 | 4 | 81.59 | 12 | 1.61 | 0.875 |
| 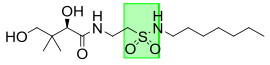 | 352.49 | 0.26 | 5 | 4 | 115.7 | 12 | 0.26 | 0.933 |
| 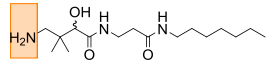 | 315.45 | 0.61 | 4 | 4 | 104.5 | 12 | -1.29 | 0.875 |
| 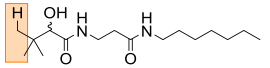 | 300.43 | 2.00 | 3 | 3 | 78.43 | 11 | 2.00 | 0.875 |
| 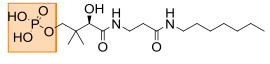 | 396.42 | 0.60 | 6 | 5 | 145.2 | 14 | -2.46 | 0.875 |

[a] Values of cLog*P* and Log$D_{7.4}$ were calculated with calculator plugins in the program MarvinSketch 6.0.6, 2013 from ChemAxon (Budapest, Hungary). cLog*P* and Log$D_{7.4}$ values were set at default: calculations used equal weights of VG, KLOP, and PHYS methods and electrolyte concentrations ($Na^+$,$K^+$ and $Cl^-$) set to 0.1 mol.dm$^{-3}$ [34-36]. We did not consider tautomerization in our calculations. PSA was calculated with the same program, but excluded sulfur and phosphorus atoms from the calculations. NRotB, H-bond donors and H-bond acceptors were calculated using the same program. The values that fall outside the limits of the physicochemical properties are indicated in red.

## 3.4 Synthesis of pantetheinase-resistant N7-Pan analogues

Since none of the proposed molecules are commercially available, a large portion of this study was dedicated to the synthesis of these potential pantetheinase-resistant *S. aureus* growth inhibitors based on the scaffold of N7-Pan. We first focused on the analogues that have steric bulk in close proximity to the scissile amide bond increased, followed by the preparation of the N7-Pan bioisosteres. Lastly, we prepared the required analogues where the 4'-hydroxyl group is removed or replaced to prevent substrate recognition.

### 3.4.1 Increasing steric bulk surrounding the N7-Pan scissile amide bond

#### 3.4.1.1 *N*-Heptyl α-methyl pantothenamide (3.7) and *N*-heptyl β-methyl pantothenamide (3.8)

In the first two N7-Pan analogues the scissile amide bond was retained, but a methyl group was added to either the α- or β-position relative to the amide bond. This should introduce steric hindrance and should prevent or slow the hydrolysis of the amide bond. The synthesis of *N*-heptyl α-methyl pantothenamide (**3.7**, N7-α-methyl-Pan) and *N*-heptyl β-methyl pantothenamide (**3.8**, N7-β-methyl-Pan) was based on a modified method of Jana [39] (Scheme 3.1), involving a condensation- and a coupling reaction. Since α- and β-methyl pantothenic acids (**3.4** and **3.5**) are not commercially available, these were synthesized first. (*R*/*S*)-3-Amino isobutyric acid **3.1** and (*R*/*S*)-3-aminobutyric acid **3.2** were condensed with (*R*)-(-)-pantolactone **3.3**. The compounds were partially purified by anion exchange chromatography (to remove the amines and protonate the carboxylate) before further purification by FCC gave amides **3.4** and **3.5** as white-yellow powders (which became oils upon standing) in 86% and 82% yield, respectively. Activation of the carboxylate by DPPA was used for the final amide bond formation. Specifically, a solution of carboxylic acid **3.4** or **3.5** and heptylamine (**3.6**) in DMF was treated with DPPA and $Et_3N$. Subsequent purification by FCC gave amide **3.7** (from **3.4**) as a yellow oil in 43% yield. Unfortunately, only a 17% yield was obtained for amide **3.8** (yellow oil) (from **3.5**) after purification. DPPA coupling reactions require strictly anhydrous conditions to achieve successful amide bond formations [40]. Given that carboxylic acid **3.5** was found to be very hygroscopic, the low yield obtained for amide **3.8** could be attributed to this fact. Additionally, the low yield could also be due to a possible competing coupling reaction at the unprotected 4'-hydroxyl position.

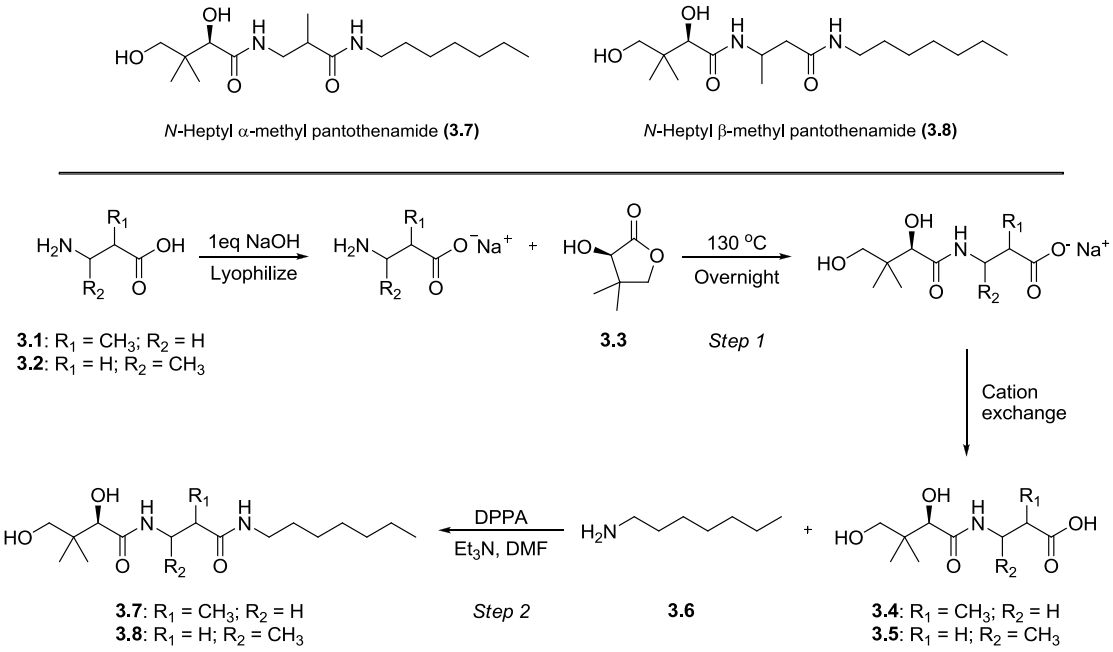


**Scheme 3.1. Synthetic route for the preparation of *N*-heptyl α-methyl pantothenamide (3.7) and *N*-heptyl β-methyl pantothenamide (3.8). *N*-heptyl α-methyl pantothenamide 3.7 was prepared from (*R*/*S*)-3-amino-isobutyric acid 3.1 in two steps, while *N*-heptyl β-methyl pantothenamide 3.8 was prepared from (*R*/*S*)-3-aminobutyric acid 3.2 in two steps.**

### 3.4.1.2 *N*-Methyl *N*-heptyl pantothenamide (3.11)

*N*-alkylation of amides is a useful way to prepare more substituted analogues. Generally, *N*-substituted amides are synthesized through nucleophilic substitution with alkyl halides under basic conditions; however, this method requires the use of strong bases and alkyl halides. Recently, Xia *et al*. [41] developed a method for *N*-alkylation of amides under neutral conditions that suppresses the overalkylation of primary amides. Therefore, we first attempted to synthesize *N*-methyl-*N*-heptyl pantothenamide (**3.11**, *N*-methyl-N7-Pan) using the method of Xia *et al*. This entails the Cu-catalyzed *N*-methylation of amides in which an organic peroxide, specifically dicumyl peroxide (DCP), serves as the methylating agent. It has been suggested that this mechanism proceeds via a radical process [41].

The first method that we attempted consisted of a two-step linear synthesis (Scheme 3.2, Method 1). In the first step, calcium pantothenate was exchanged to its free acid **3.9** using Amberlite IR120 $H^+$-cation exchange resin, followed by coupling to heptylamine (**3.6**) using DPPA in the presence of $Et_3N$. Subsequent purification by FCC gave amide **3.10** as a pure white solid in moderate yield (47%). In the final step, we attempted *N*-alkylation of amide **3.10** using DCP as the methylating agent in the presence of copper chloride (CuCl); however, this was unsuccessful and alkyl **3.11** was not obtained in this manner.

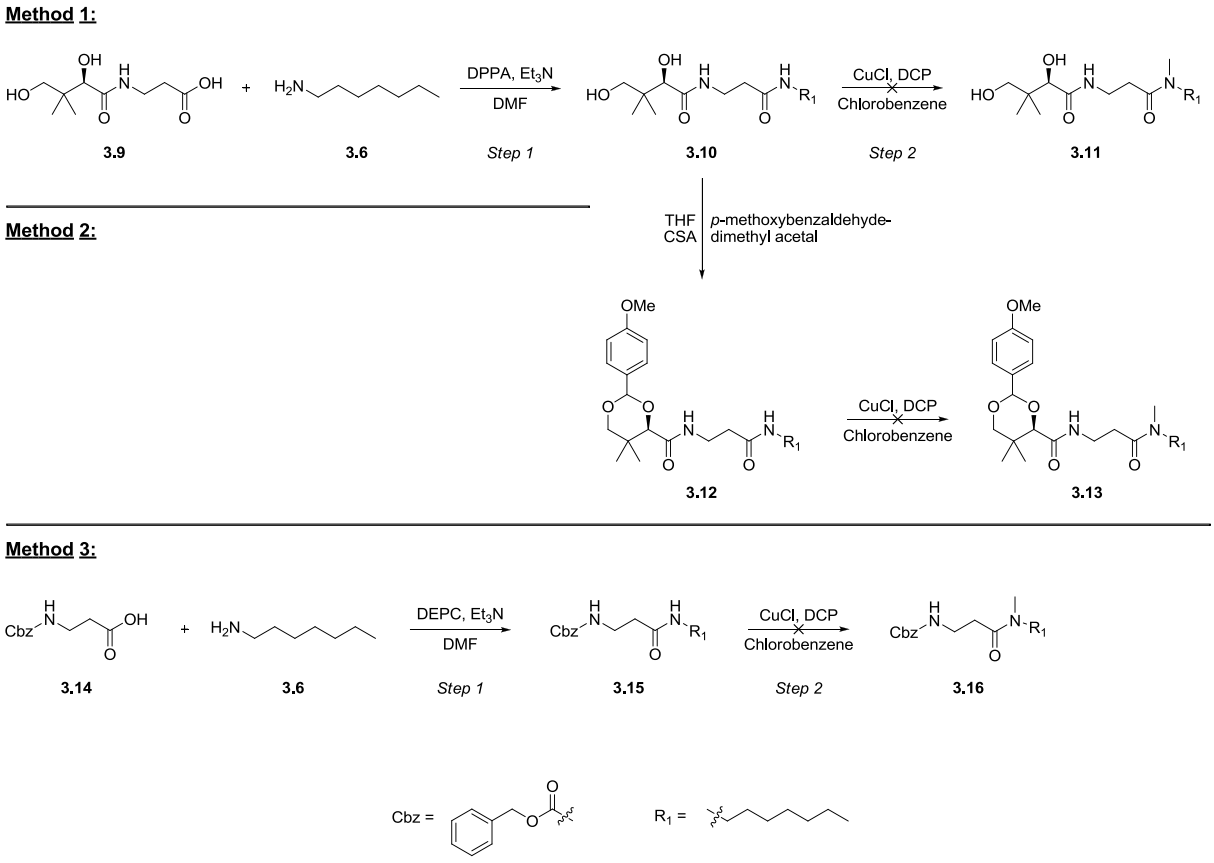


**Scheme 3.2. Proposed methods for the synthesis of *N*-methyl-*N*-heptyl pantothenamide (3.11) by Cu-catalyzed *N*-alkylation of the scissile amide's nitrogen atom using DCP as the methylating agent. In method 1 and 2 we attempted to prepare *N*-methyl-*N*-heptyl pantothenamide 3.11 from pantothenic acid 3.9, while in method 3 we attempted to prepare *N*-methyl-*N*-heptyl pantothenamide 3.11 from Cbz-β-alanine (3.14).**

Given that the *N*-alkylation failed on amide **3.10** (which has an unprotected 1,3-diol on the pantoyl moiety), we proposed that protection of the 1,3-diol might increase the likelihood of *N*-alkylation on the amide (Scheme 3.2, Method 2). Consequently, a standard method described by Van der Westhuyzen [42] was used to protect the 1,3-diol with a *p*-methoxybenzylidene (PMB) protecting group. 1,3-Diol **3.10** was protected using *p*-methoxy-benzaldehyde dimethyl acetal and a catalytic amount of (±)-10-camphorsulfonic acid (CSA) in THF. *p*-Methoxybenzylidene **3.12** was obtained in a good yield (76%) as a white solid upon purification by FCC. Subsequently, **3.12** was subjected to *N*-alkylation using DCP and CuCl. Unfortunately, even with protection of the 1,3-diol, the *N*-alkylation did not take place. Therefore, in a final attempt to alkylate the scissile amide we decided to use commercially available carboxybenzyl (Cbz) protected β-alanine (**3.14**) which does not contain the 1,3-diol (Scheme 3.2, Method 3). Seeing as DPPA and DEPC-activated coupling reactions are mechanistically and experimentally similar, a DEPC coupling reaction was explored as the first step of method 3. A solution of Cbz-β-alanine (**3.14**) and heptylamine (**3.6**) in DMF was

treated with DEPC and $Et_3N$. Purification by FCC gave carbamate **3.15** as a pure white powder in an excellent 93% yield. The next step of the synthesis entailed *N*-alkylation of the amide; amide **3.15** was subsequently treated with DCP and CuCl, but without success. After three attempts this method was not pursued any further.

In view of the fact that we were unsuccessful with the *N*-alkylation of the scissile amide's nitrogen, we decided to first mono-alkylate heptylamine (**3.6**) and to subsequently couple the resulting secondary amine (**3.17**) to pantothenic acid (**3.9**) to obtain the desired product **3.11** (Scheme 3.3). First, we set out to mono-alkylate heptylamine (**3.6**) through nucleophilic substitution with an alkyl halide under basic conditions (Scheme 3.3, Method 1). A method, described by Jablonski *et al*. [43], was used to attempt mono-alkylation with methyliodide ($CH_3I$) in the presence of a base (*N*-methylmorpholine), but this was unsuccessful. Alternatively, we decided to use methylamine·HCl as alkylating reagent and react it with heptylbromide (**3.18**) (Scheme 3.3, Method 2). While investigating this method as alternative it was found that Salvatore *et al*. [44-45] have developed an efficient method for the direct *N*-alkylation of amines that gives mono-alkylated amines predominantly or exclusively. This is achieved by performing this reaction in the presence of either cesium hydroxide (CsOH) or cesium carbonate ($Cs_2CO_3$) in DMF. Consequently, heptylbromide (**3.18**) was treated with either CsOH ($CsOH{\cdot}H_2O$ was scrupulously dried) or $Cs_2CO_3$ in the presence of methylamine·HCl in DMF, but once again, target compound **3.17** did not form during this reaction.

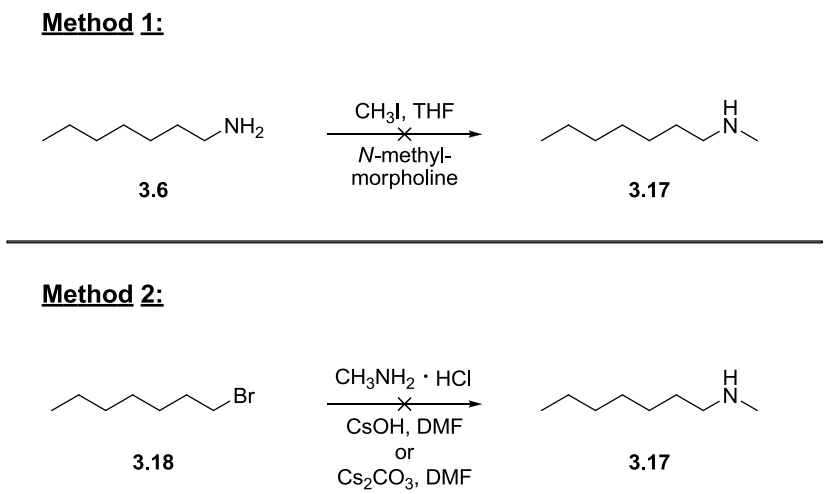


**Scheme 3.3. Direct *N*-alkylation of either heptylamine (3.6) with $CH_3I$ or methylamine·HCl with heptylbromide (3.18).**

While investigating possible alternative routes for the preparation of target compound **3.11**, the alkylated amine **3.17** became commercially available from Sigma-Aldrich, which greatly simplified the synthesis of the desired product. The synthesis of **3.11** was based on a method that exploits the known reactivity of activated thioesters towards amines in a two-step linear synthesis method (Scheme 3.4) previously published from our research group [46]. In the first step, calcium pantothenate was converted into its free acid **3.9** and was subsequently coupled to thiophenol (**3.19**) using a DEPC-assisted coupling in the presence of $Et_3N$. Following an aqueous work-up and purification by FCC, thioester **3.20** was obtained as a yellow oil (which solidified upon standing) in 53% yield. In the final step, **3.20** was coupled to *N*-methyl heptylamine (**3.17**) by aminolysis of the thioester; subsequent purification by FCC afforded target amide **3.11** as a yellow oil, in an excellent yield of 86%.

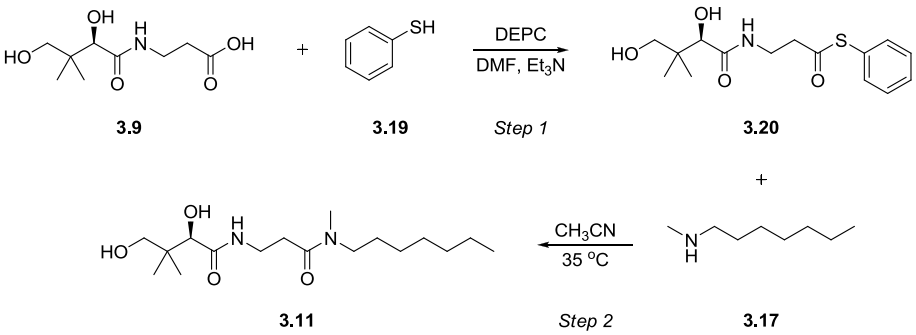


**Scheme 3.4. Synthetic route for the preparation of *N*-methyl-*N*-heptyl pantothenamide (3.11) from pantothenic acid 3.9 using a two-step linear method that was developed by Van Wyk and Strauss [46].**

### 3.4.1.3 (*E*)-*N*-Heptyl CJ pantothenamide ((*E*)-3.27)

In 2001, Sugie *et al*. [47] reported that the pantothenic acid analogue CJ-15,801 (a fermentation product of *Seimatosporium sp*., Scheme 1.6, Chapter 1), inhibits the growth of three MDR strains of *S. aureus* with MIC values ranging from 28.8-230 µM [47]. Unpublished results from related studies in our laboratory indicated that amide analogues of CJ-15,801 are resistant to pantetheinase degradation. Consequently, we decided to incorporate the double bond from CJ-15,801 into our N7-Pan analogues. Although the introduction of a double bond in the β-alanine moiety of the molecule is not technically seen as adding steric bulk in the vicinity of the scissile amide bond, the decreased rotational freedom that results from this modification may also reduce access to the amide carbonyl by preventing pantetheinase from binding the analogue in the orientation necessary for catalysis. The synthesis of (*E*)-N7-CJ-Pan **3.27** was based on a method developed by Van der Westhuyzen [42] that consists of six steps; two fragments are prepared separately which are then coupled using a Pd-catalyzed coupling to introduce the enamide moiety, which is subsequently deprotected to afford target compound (*E*)-**3.27** (Scheme 3.5).

The first step in the synthesis of fragment 1 (amide **3.22**) consisted of the ring opening and subsequent aminolysis of (*R*)-(-)-pantolactone **3.3**, which was achieved with 30% ammonia ($NH_3$) in MeOH. The product was partially purified by the removal of $NH_3$ and MeOH *in vacuo*. The crude amide **3.21** was lyophilized to afford a white powder in excellent yield (94%) which was subsequently used in the next step without further purification. In the second step, amide **3.21** was treated with isopropenyl methyl ether (IPM) and a catalytic amount of PTSA in a 1:1 ratio of DCM and acetone to protect the 2,4-diol. After purification by FCC, acetonide **3.22** (fragment 1), was obtained in 79% yield, a slightly higher yield than the 62% obtained by Van der Westhuyzen [42].

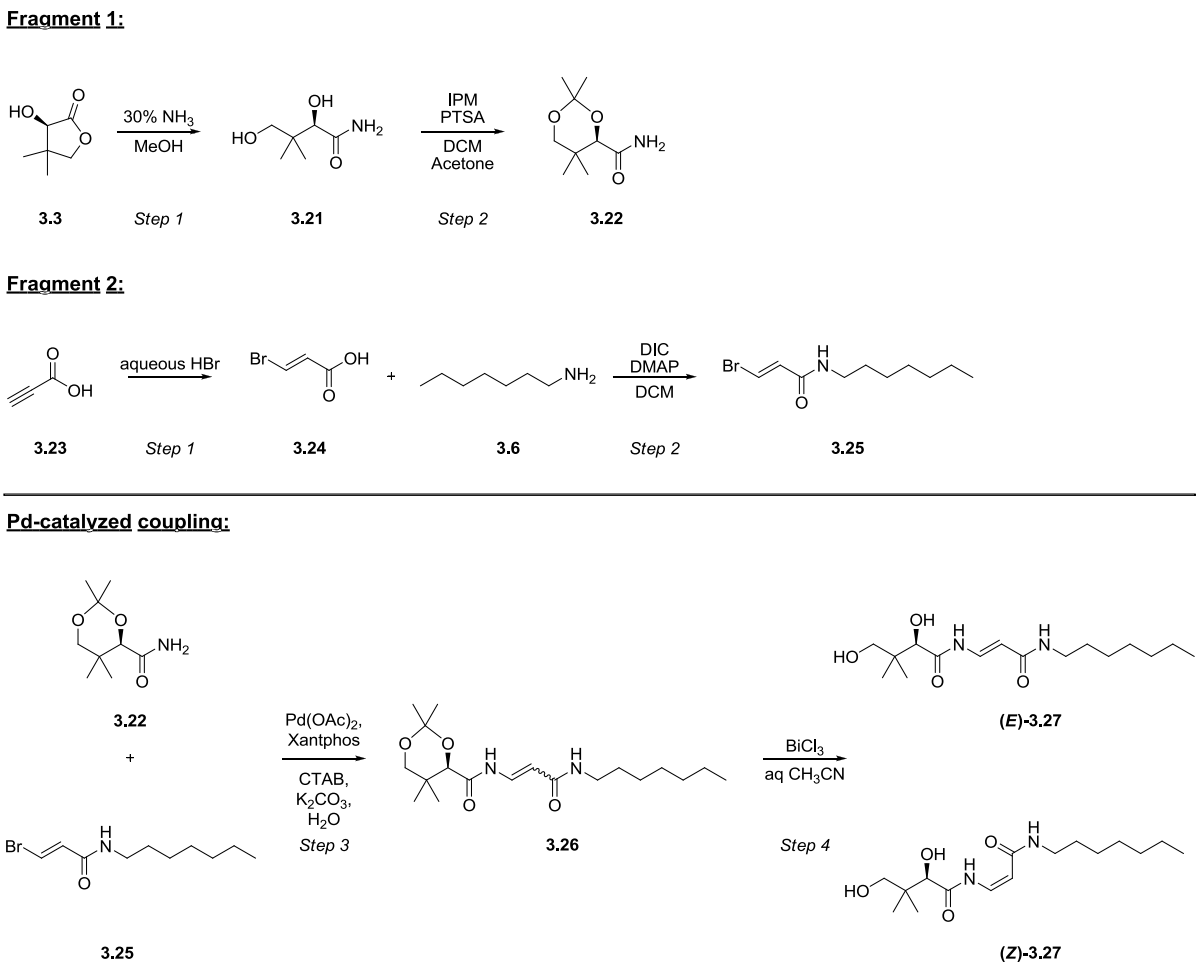


**Scheme 3.5. Synthetic route for the preparation of (*E*)-*N*-Heptyl CJ pantothenamide (3.27) from (*R*)-(-)-pantolactone 3.3 and propiolic acid 3.23 using a six-step method that was developed by Van der Westhuyzen [42].**

Next, we had to prepare fragment 2 (bromo acrylamide **3.25**). In the first step of the synthesis, propiolic acid (**3.23**) was mono-brominated by refluxing in 48% aqueous hydrobromic acid (HBr), followed by cooling on an ice bath. Pure bromo acid **3.24** was isolated as a grey solid upon

filtration of the resulting precipitate. Unfortunately, only a 20% yield was obtained, but this gave sufficient material to allow the next step to be attempted. In the second step the bromo acid **3.24** was successfully coupled to heptylamine (**3.6**) using a standard *N*,*N*-diisopropylcarbodiimide (DIC) and 4-*N*,*N*-dimethylaminopyridine (DMAP)-mediated coupling procedure in DCM, after which purification by FCC afforded the second fragment, acrylamide **3.25**, as yellow solid in a moderate yield (46%).

After the successfully completed syntheses of fragment 1 and 2, a Pd-catalyzed coupling procedure was used to introduce the enamide moiety (step 3). This coupling reaction is known to stereoselectively prepare *E*-enamides in excellent yield from amides and bromo acrylamides using commercially available reagents [48]. In addition to the Pd-catalyst, a base (in this case we used potassium carbonate, $K_2CO_3$) is needed to neutralize the HBr that forms during the course of the reaction, while a phase transfer-catalyst (cetyltrimethylammonium bromide, CTAB) assists in this neutralization process. An appropriate ligand for the Pd is also required. The ligand employed by Van der Westhuyzen [42] was the bisphosphine ligand, Xantphos (4,5-Bis(diphenylphosphino)-9,9-dimethyl-xanthene), a ligand often employed in Pd-catalyzed C–N bond formation systems [42]. Bromo acrylamide **3.25** (fragment 2) and amide **3.22** (fragment 1) were therefore coupled and subsequently purified by FCC (to separate the *E*- and *Z*-isomers) to afford enamide (*E*)-**3.26** and (*Z*)-**3.26** in 50% and 10% yield, respectively, with an *E:Z* ratio of 5:1. Given that the deprotected pantoyl moiety is extremely acid sensitive and will lactonize at a low pH, the deprotection of the acetonide was carried out using mild conditions at a neutral pH. In the final step the acetonide protecting group was successfully removed from both (*E*)-**3.26** and (*Z*)-**3.26** using bismuth (III) chloride ($BiCl_3$) in aqueous $CH_3CN$. Subsequent purification by FCC gave (*E*)-**3.27** as a white solid in 30% yield and (*Z*)-**3.26** as a yellow oil in 62% yield, respectively. The absolute stereochemistry of the *E*- and *Z*-isomers was confirmed with $^1$H NMR spectroscopic analysis – the vinylic proton shifts as well as the *J*-couplings were consistent with those previously reported by Van der Westhuyzen [42].

## 3.4.2 Preparation of bioisosteres of N7-Pan

### 3.4.2.1 *N*-Hexyl pantothenhydrazide (3.33)

The first bioisosteric replacement that we decided upon was a hydrazide. Methodologies reported for the direct preparation of carboxylic acid hydrazides from carboxylic acids are generally inefficient. Instead, the standard method for preparing carboxylic acid hydrazides is by hydrazinolysis of the corresponding esters in MeOH or EtOH [22, 49-50]. However, in the case of α,β-unsaturated esters, the main product is usually the pyrazolidinone due to an undesired Michael-type cyclization. Consequently, Zhang *et al*. [49] developed an alternative method for the

synthesis of hydrazides—including those of α,β-unsaturated acids—involving preforming activated esters or amides by means of HOBt and EDC hydrochloride treatment, followed by their reaction with hydrazine [49]. We based our method for the synthesis of N6-Pantothenhydrazide **3.33** (a N7-Pan analogue) on the known reactivity of activated thioesters towards amines and decided to activate the carboxylic acid for hydrazinolysis with a thioester, rather than an ester.

This synthetic route that was developed consisted of a four-step linear synthesis that included a thioesterification, as well as reductive amination (Scheme 3.6). In step 1, calcium pantothenate was converted into free acid **3.9** using Amberlite IR120 resin and was subsequently coupled to ethanethiol (**3.28**) using a DEPC-assisted coupling reaction in the presence of $Et_3N$ to facilitate the thioesterification. Following an aqueous work-up and purification by FCC, thioester **3.29** was obtained as a yellow oil in 60% yield. Next, **3.29** was treated with hydrazine hydrate in EtOH and refluxed overnight. Following this, hydrazide **3.30** was obtained as a yellow oil upon removal of the solvent *in vacuo* and was subsequently used in the next step without any further purification.

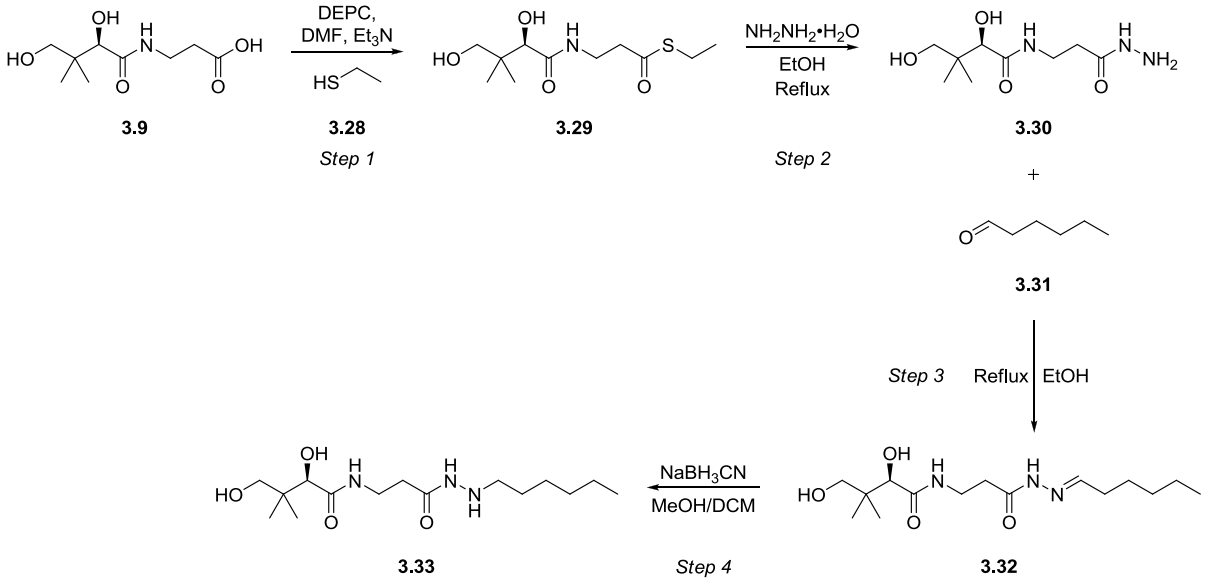


**Scheme 3.6. Synthetic route for the preparation of *N*-hexyl pantothenhydrazide (3.33) from pantothenic acid 3.9 in four steps.**

The final two steps entailed a reductive amination for which a general method described by Andreini *et al*. [50] was used. Hydrazide **3.30** was reacted with hexanal (**3.31**) in EtOH by stirring at reflux for 48h. After purification by FCC, imine **3.32** was obtained in a satisfactory yield of 77%. In the final step, **3.32** was reduced to afford the target compound N6-pantothenhydrazide **3.33**. Initially we attempted the reduction of imine **3.32** with $NaBH_4$ in MeOH; however, the reduction was

unsuccessful and the starting material was recovered. Next, imine **3.32** was treated with sodium cyanoborohydride ($NaBH_3CN$)—a reagent that is only reactive towards protonated imines [51]—in a 3:2 mixture of MeOH and DCM and the pH was adjusted first to pH 3, and then to pH 1 after the first half hour. Purification by FCC afforded **3.33** as a yellow oil, but unfortunately only in a 27% yield.

#### 3.4.2.2 *N*-Heptyl pantothenthioamide (3.36)

The second bioisosteric replacement that we decided upon was a thioamide. The synthetic preparation of thioamides has been accomplished using various reagents, such as phosphorus pentasulfide, bis(tricyclohexyltin) sulfide with boron trifluoride, hydrogen sulfide in the presence of an acid, bis(trimethylsilyl) sulfide with cobalt (II) chloride hexahydrate, 2,4-bis(*p*-methoxyphenyl)-1,3-dithiaphosphetane 2,4-disulfide (Lawesson's reagent), as well as thionation of *gem*-dichlorides with thioacetic acid, potassium xanthate or sodium hydrogen sulfide [24, 52]. We decided to base the synthesis of *N*-heptyl pantothenthioamide (**3.36**, N7-pantothenthioamide) on the conversion of the carbonyl oxygen of the scissile amide bond to sulfur using Lawesson's reagent.

The synthetic route that we developed consisted of a four-step linear synthesis that included a thionation and a condensation reaction (Scheme 3.7). In step 1, a solution of Cbz-β-alanine (**3.14**) and heptylamine (**3.6**) in DMF was treated with DEPC and $Et_3N$ to facilitate the amide bond formation. The side products and unreacted amine were removed through an aqueous work-up, which proved to be adequate to obtain amide **3.15** as a pure white powder in an excellent 93% yield. The second step of the synthesis entailed the thionation of the scissile amide bond based on a method from Kuehne *et al*. [53] and Otani *et al*. [54]. Amide **3.15** was treated with Lawesson's reagent in toluene and the reaction mixture was refluxed overnight. Subsequent purification by FCC afforded thioamide **3.34** as a light yellow powder in good yield (67%).

The third step of the synthesis entailed the deprotection of carbamate **3.34**. The benzyl carbamate protecting group was successfully removed by refluxing overnight in a 1:1 solution of MeOH and concentrated HCl. The crude product was lyophilized to afford the HCl salt of amine **3.35** (white powder) which was subsequently used in the next step without any further purification. In the final step amine **3.35** was condensed with (*R*)-(-)-pantolactone **3.3** in the presence of $Et_3N$ to facilitate the amide bond formation. Subsequent purification by FCC afforded target compound **3.36** as a yellow oil. Unfortunately, a very low yield (7%) was obtained in the final step. This low yield could be attributable to the fact that the HCl salt of amine **3.35** was used which decreased the total $Et_3N$ concentration in the reaction mixture. Furthermore, a large quantity of (*R*)-(-)-pantolactone **3.3** was recovered during FCC. The formation of amide bonds from esters are extremely difficult and

usually require high temperatures. In the final step we condensed amine **3.35** with (*R*)-(-)-pantolactone **3.3**, which is a very stable ester in the form of a five membered ring lactone.

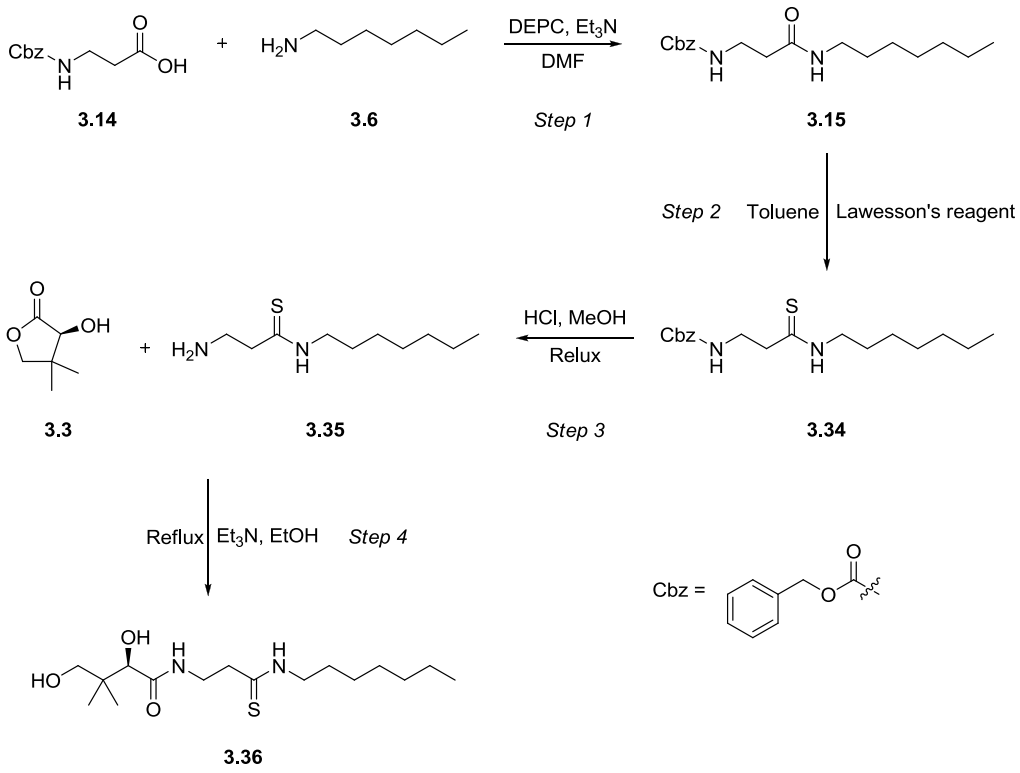


**Scheme 3.7. Synthetic route for the preparation of *N*-heptyl pantothenthioamide (3.36) from Cbz-β-alanine (3.14) in a four-step synthesis.**

### 3.4.2.3 *N*-Heptyl pantoyltauramide (3.44)

The third and final bioisosteric replacement performed in this study involved the synthesis of *N*-heptyl pantoyltauramide (**3.44**, N7-pantoyltauramide). In this molecule the scissile amide bond was replaced with a sulfonamide ($R_1$-S(=O)$_2$-NH-$R_2$) moiety. The synthesis of N7-pantoyltauramide **3.44** was based on a method developed by Jana [39] and comprised of five linear steps that included a protection and activation reaction (Scheme 3.8).

Taurine (2-aminoethanesulfonic acid, **3.37**) was protected with benzyl chloroformate (CbzCl, **3.38**) and the excess CbzCl was azeotroped off by co-evaporation with toluene, EtOH and DCM. The crude carbamate **3.39** was lyophilized and subsequently used in the next step without any further purification. In the second step, the sulfonic acid on carbamate **3.39** was activated by fluorination using (diethylamino)sulphur trifluoride (DAST, **3.40**) to make it more reactive towards primary amines. After purification by FCC, tauryl fluoride **3.41** was obtained in 80% yield, a much higher yield than Jana's reported 44%. Step 3 entailed the aminolysis of tauryl fluoride **3.41** with

heptylamine (**3.6**) in DCM at 50°C. In this reaction, heptylamine (**3.6**) was successfully coupled after 20h to afford tauramide **3.42** as a yellow-orange powder in an excellent yield of 83% upon purification with FCC.

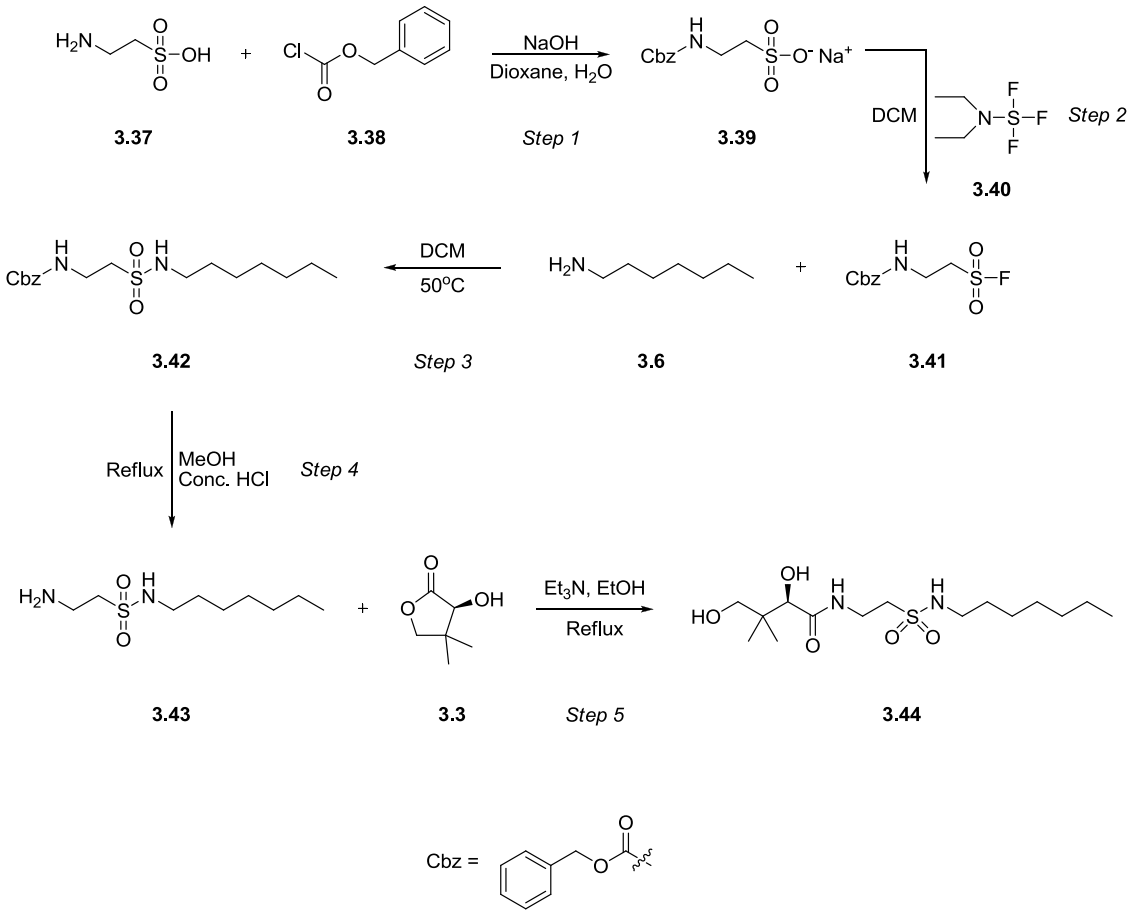


**Scheme 3.8. Synthetic route for the preparation of *N*-heptyl pantoyltauramide (3.44) from taurine 3.37 using the five-step linear method that was developed by Jana [39].**

The fourth step of the synthesis involved the deprotection of carbamate **3.42** using concentrated HCl in the presence of MeOH. The benzyl formate protecting group was successfully removed by refluxing overnight in a 1:1 solution of MeOH and concentrated HCl. The crude amine **3.43** was lyophilized to afford the product as the HCl salt (white powder) in an excellent yield (82%). It was subsequently used in the next step without any further purification. The final step of the synthesis entailed the formation of an amide bond by aminolysis of (*R*)-(-)-pantolactone **3.3** with amine **3.43** in the presence of $Et_3N$. The reaction was complete after refluxing for 7h and amide **3.44** was purified by FCC. Spectroscopic analysis confirmed the formation of the target compound; however, impurities were still present. As a result, amide **3.44** was subjected to further purification by solid

phase extraction (SPE). Amide **3.44**, dissolved in DCM, was loaded onto a DCS-$NH_2$ SPE column and eluted with $CH_3CN$. The second purification was successful and amide **3.44**, free of any impurities, was obtained, but unfortunately with only an 18% yield in the final step.

## 3.4.3 Removal of 4'-OH group from N7-Pan

### 3.4.3.1 (*R*/*S*)-4'-Deoxy-*N*-heptyl pantothenamide (3.49)

The first N7-Pan analogue in which the 4'-hydroxyl group was altered is structurally identical to (*R*/*S*)-4'-deoxy-N5-Pan **2.9**, the synthesis of which is described in the manuscript reproduced in Chapter 2. However, to maintain the same core structure of the series, (*R*/*S*)-4'-deoxy-*N*-heptyl pantothenamide (**3.49**, (*R*/*S*)-4'-deoxy-N7-Pan) was synthesized using the method developed previously for (*R*/*S*)-4'-deoxy-N5-Pan **2.9** (Scheme 3.9). The procedure consisted of a four-step linear synthesis that included two coupling reactions and a deprotection reaction.

A solution of Cbz-β-alanine (**3.14**) and heptylamine (**3.6**) in DMF was treated with DEPC and $Et_3N$ in the first step to facilitate the amide bond formation. The side products and unreacted amine were removed through an aqueous work-up, which proved to be adequate to obtain amide **3.15** as a pure white powder in an excellent 93% yield. The second step of the synthesis entailed the deprotection of carbamate **3.15**, with the benzyl carbamate protecting group being successfully removed with $H_2$ in the presence of 10% palladium on activated carbon (Pd/C), to yield amine **3.45** as a pure white powder in a yield of 96% upon filtration. The purity of amine **3.45** was confirmed with NMR spectroscopic analysis.

Step 3 entailed an amide coupling in the presence of EDC hydrochloride using amine **3.45** and acid **3.46** (synthesised according to Tuck *et al*. [55] through the oxidation of pinacolone (**3.47**) by $KMnO_4$). The coupling was assisted with HOBt and DIPEA, which resulted in the formation of the second amide bond. The experimental procedure (as described in Chapter 2) was followed; however, a yield of only 22% was obtained for **3.48** after purification by FCC compared to the 57% yield obtained in the equivalent coupling used to prepare (*R*/*S*)-4'-deoxy-N5-Pan **2.9**. This low yield could be attributed to the low purity of carboxylic acid **3.46** as it was found to degrade over time and it was not used immediately. The final step of the synthesis (step 4) entailed the reduction of ketone **3.48**. Since three carbonyl groups were present in the molecule (1 × ketone and 2 × amides), $NaBH_4$ was used for the reduction due to its selectivity toward ketones as opposed to amides. Ketone **3.48** was therefore treated with $NaBH_4$ to afford target compound **3.49** as a white powder in a good 78% yield after an aqueous work-up.

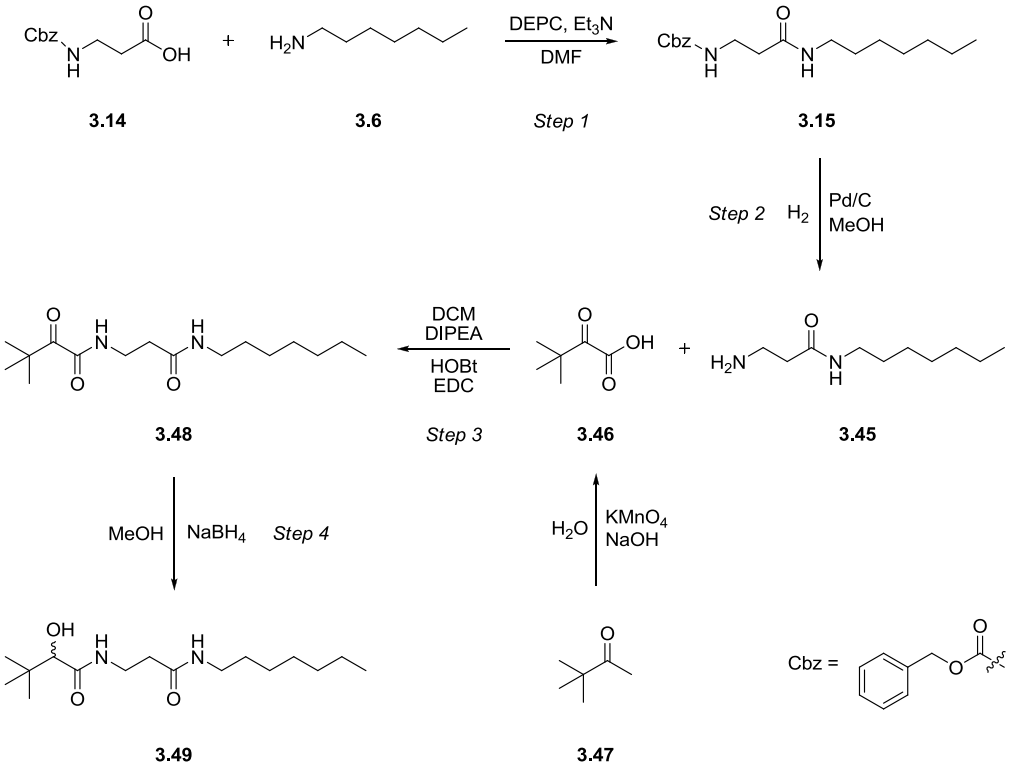


**Scheme 3.9. Synthetic route for the preparation of (*R*/*S*)-4'-deoxy-*N*-heptyl pantothenamide (3.49) from Cbz-β-alanine (3.14) through a four-step linear synthesis based on the equivalent protocol developed for preparation of the pentyl (N5-Pan) homologue as described the manuscript reproduced in Chapter 2 [12].**

### 3.4.3.2 (*R*/*S*)-4'-Amino-*N*-heptyl pantothenamide (3.56)

The second N7-Pan analogue in which the 4'-hydroxyl was modified had this group replaced with a 4'-amino group in order to prevent its recognition by pantetheinase as a substrate. The original synthetic procedure for the synthesis of (*R*)-4'-amino-N7-Pan **3.56** was based on a method developed by Yan *et al*. [56] for the preparation of (*R*)-4'-amino PantSH from pantethine (the disulfide of PantSH, Scheme 1.1B, Chapter 1). Yan *et al*. [56] first attempted to install the 4'-amine via activation of the 4'-hydroxyl, followed by nucleophilic substitution with sodium azide ($NaN_3$) and subsequent reduction of the azide to afford the 4'-amine. In this work, activation of the 4'-hydroxyl was first attempted with 4-toluenesulfonyl chloride (TsCl) and 2,4,6-triisopropyl-benzenesulfonyl chloride (TIPBSCl); however, these sulfonyl chlorides failed to activate the 4'-hydroxyl group. The more reactive methylsulfonyl chloride (MsCl) proved to be reactive enough to mesylate the 4'-hydroxyl group. However, when nucleophilic substitution of the mesylated 4'-OH was attempted with $NaN_3$, the reaction still failed to take place. This could be attributable to steric hindrance caused by the dimethyl groups on the adjacent quaternary carbon. Consequently, the authors used reductive amination to install the 4'-amine after preparation of the 4'-aldehyde; this method proved to be successful and allowed for the preparation of (*R*)-4'-amino PantSH [56]. We therefore also used this method in our first attempt of the synthesis of target compound **3.56** (Scheme 3.10).

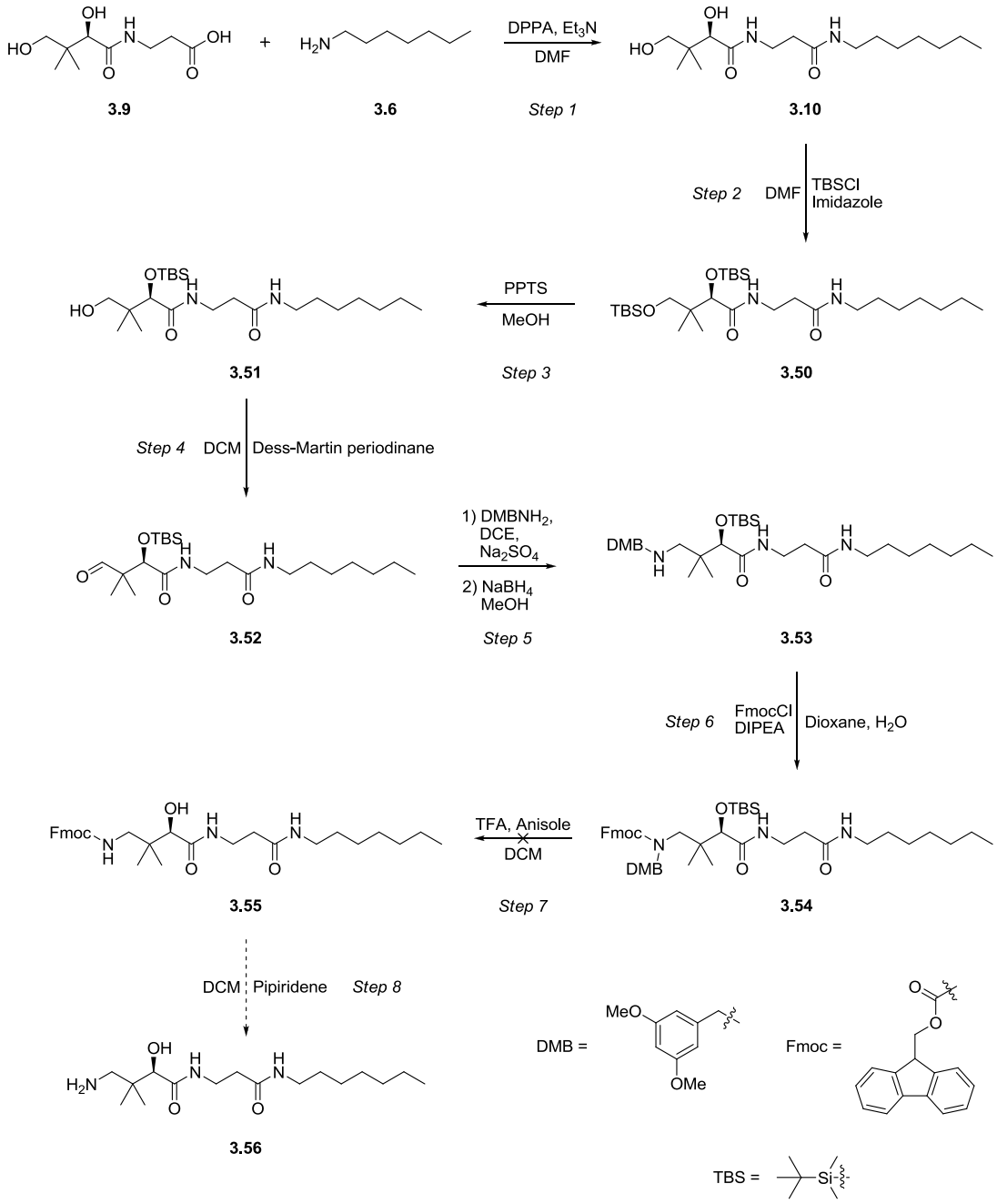


**Scheme 3.10. Proposed synthetic route for the preparation of (*R*)-4'-amino-*N*-heptyl pantothenamide (3.56) from pantothenic acid 3.9, adapted from the method developed by Yan *et al*. [56].**

The proposed synthetic route consisted of an eight-step linear synthesis which included protection, oxidation, reductive amination, and deprotection reactions. In the first step, calcium pantothenate was exchanged to the free acid **3.9** using Amberlite IR120 resin. This compound was subsequently coupled to heptylamine (**3.6**) using DPPA in the presence of $Et_3N$ to facilitate the amide bond formation. Subsequent purification by FCC gave amide **3.10** as a pure white solid in a moderate yield (47%). In the second step, *tert*-butyldimethylsilyl chloride (TBSCl) with imidazole was used to

protect both the primary and secondary hydroxyl groups of **3.10**, and the product was purified with FCC to afford the TBS ether **3.50** in 83% yield, slightly lower than the reported 98%. Step 3 entailed the selective removal of the TBS-protecting group from the primary alcohol of TBS ether **3.50.** This TBS protecting group was successfully cleaved with pyridinium *p*-toluenesulfonate (PPTS) in MeOH, before purification by FCC afforded hydroxyl **3.51** as a yellow oil in 86% yield that correlates well with the reported yield (92%) of Yan *et al.* [56]. Additionally, the $^{1}$H NMR data are consistent with those previously reported in literature [56]. Subsequently, in step 4, hydroxyl **3.51** was oxidized to the aldehyde using Dess-Martin periodinane, before purification by FCC gave aldehyde **3.52** as a yellow oil in an excellent yield of 96%.

Yan *et al*. [56] reported the execution of steps 4 to 7 with only partial purification in step 6 before carrying out step 7. Consequently, we also decided to carry out steps 5 to 7 (Scheme 3.10) in the same manner. Step 5 entailed the metal hydride-mediated reductive amination of aldehyde **3.52** using dimethoxybenzyl amine ($DMBNH_2$) in DCE, followed by $NaBH_4$-mediated reduction of the imine to afford amine **3.53**. The use of protecting groups on the amine is crucial during the metal hydride reductive amination to prevent over-alkylation. Without a protecting group, multiple alkylation reactions typically occur, resulting in the formation of undesired secondary or tertiary amine products. Removal of a DMB protecting group from a secondary amine is not widely reported and harsh reaction conditions are generally required; however, the removal of a DMB protecting group from an amide is much easier. Therefore, to facilitate the DMB deprotection, amine **3.53** was transformed into the corresponding 9-fluorenylmethyl carbamate (Fmoc) in step 6. Amine **3.53** was treated with Fmoc chloride and DIPEA in a 4:1 ratio of dioxane and $H_2O$ and carbamate **3.54** was partially purified by FCC to remove excess unreacted Fmoc chloride. The partially purified carbamate **3.54** was subsequently used in the next step without any further purification. In step 7, both the DMB and TBS protecting groups are removed using trifluoroacetic acid (TFA) under standard reaction conditions. Purification by FCC was performed to isolate the reaction product; however, NMR spectroscopic analysis indicated that none of the isolated compounds were the desired product (carbamate **3.55**).

Since we were unable to successfully synthesize carbamate **3.55** by carrying out steps 5 to 7 without purification, we decided to repeat these steps with purification after each reaction. Thus, aldehyde **3.52** was once more treated with $DMBNH_2$, followed by $NaBH_4$-mediated reduction of the imine. However, subsequent purification by FCC did not afford amine **3.53**. The reaction conditions were thus modified in an attempt to successfully synthesize amine **3.53**. Specifically, the reaction temperature was increased to reflux, the solvent was changed to toluene to increase the reflux temperature and the duration of the reaction was varied. Unfortunately, none of these conditions resulted in the successful formation of the desired product.

Given that we were unsuccessful in using the N7-Pan analogue for the synthesis of (*R*)-**3.56**, we decided to revert to the benzyl ester derivative of pantothenic acid **3.9** and to perform the reaction with this compound (Scheme 3.11). Briefly, in step 1 benzyl bromide (**3.57**) in DMF was used to alkylate the sodium salt of acid **3.9**, giving ester **3.58** as a yellow oil in good yield (74%) after purification by FCC and the $^{1}$H NMR data are consistent with those previously reported in literature [57]. The second step entailed the protection of the primary and secondary alcohols in the pantoyl moiety of **3.58** as TBS ethers. The side products were removed through an aqueous work-up, followed by FCC to remove unreacted TBS chloride. This method allowed for **3.59** to be obtained, which was then used in the next step without any further purification. In step 3, the primary hydroxyl of **3.59** was deprotected to afford **3.60** after purification by FCC; this was oxidized to the aldehyde **3.61** in step 4 with a 77% yield over the two steps. Next, we attempted the reductive amination of aldehyde **3.61** with $DMBNH_2$ and $NaBH_4$; however, once again we were unable to successfully synthesize protected amine **3.62**. Consequently, this method by Yan *et al*. [56] was not pursued any further.

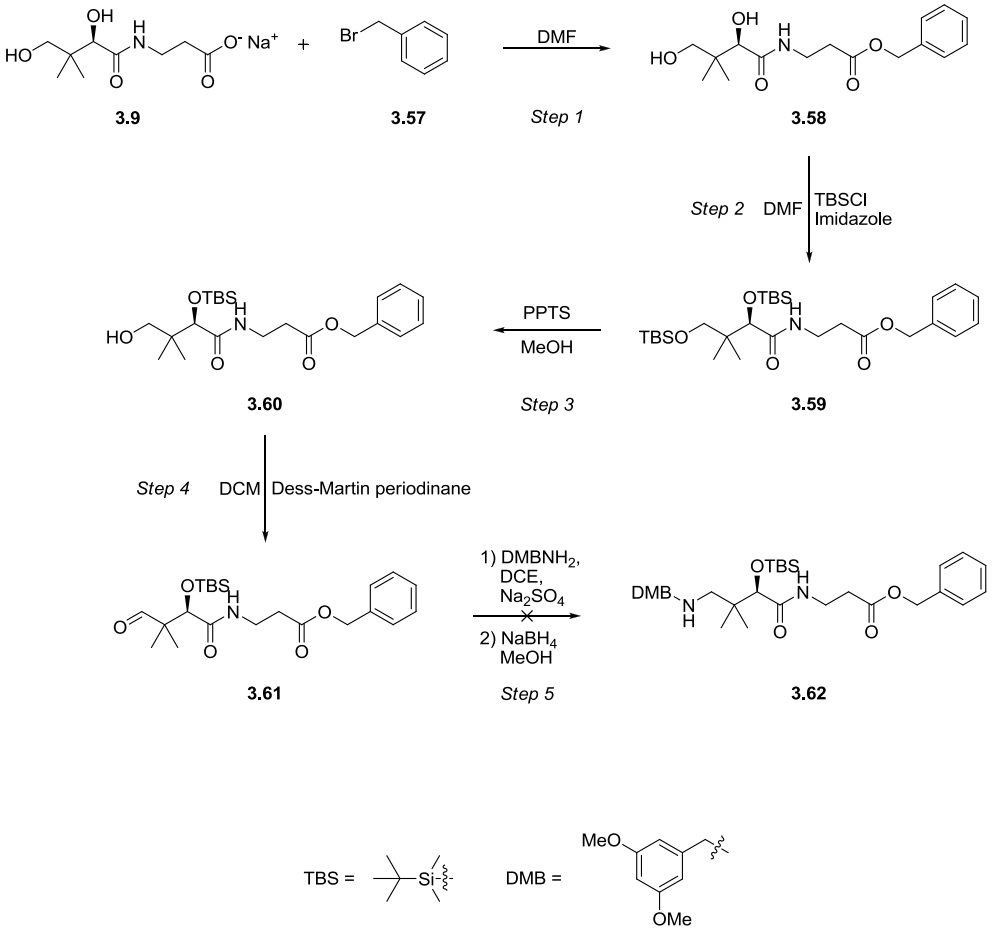


**Scheme 3.11. Alternative proposed synthetic route for the preparation of (*R*)-4'-amino-*N*-heptyl pantothenamide (3.56) from pantothenic acid 3.9, adapted from the method developed by Yan *et al*. [56].**

Seeing as we have already prepared aldehyde **3.61** and found it to be easier to visualize on TLC compared to aldehyde **3.52** due to the presence of a benzyl group, we decided to use this compound to attempt alternative metal hydride reductive amination methods. The formation of unwanted secondary and tertiary alkylated amines is a general problem during metal hydride reductive amination reactions; thus the ammonia source has to be protected. However, this in itself produces problems, since protecting groups add functional groups and structural complexity to a molecule, which can have unfavourable effects on reactivity, in addition to increasing the number steps in a synthetic route [58]. Mirriyala *et al*. [59] developed an alternative and more selective reductive amination method for the preparation of primary amines from ketones, using $NH_3$ and titanium (IV) isopropoxide-$NaBH_4$. Unfortunately, when this method was applied to aldehydes it predominately resulted in the formation of secondary amines [59].

Recently, Dangerfield *et al*. [58] developed a protecting group-free synthesis of primary amines by optimizing reaction conditions for the metal hydride/$NH_3$-mediated reductive amination of aldehydes. This new method primarily afforded primary amines and it was also found to be applicable to a wide range of functionalized substrates [58]. Consequently, we decided to use this method to synthesize amine **3.63** (Scheme 3.12, Method 1). Aldehyde **3.61** was dissolved in a saturated solution of ammonium acetate ($NH_4OAc$) in EtOH, followed by treatment with $NaBH_3CN$ and 30% aqueous ammonium hydroxide, and was then refluxed overnight. Subsequently, the mixture was concentrated *in vacuo* and the residue was loaded onto pre-washed Dowex W50-X8 $H^+$-ion exchange resin and washed several times with $H_2O$ to remove the excess salt. The product was then eluted with 15% to 30% aqueous ammonium hydroxide, the eluent was lyophilized and finally analyzed using NMR spectroscopy; however, no product was obtained.

In a final attempt to utilize aldehyde **3.61**, we tried a transamination procedure as described by de Kimpe *et al*. [60] (Scheme 3.12, Method 2). This method entails the formation of *N*-benzyl imine **3.65** by treating aldehyde **3.61** with benzylamine (**3.64**) in the presence of $MgSO_4$ (step 1), followed by isomerization with potassium *tert*-butoxide (*t*BuOK) to afford the conjugated *N*-(benzylidine) amine **3.66** (step 2). The final step (step 3) entails acid hydrolysis of **3.66** to remove the benzyl protecting group and subsequent addition of base to afford amine **3.63**. Therefore, in step 1 aldehyde **3.61** was treated with benzylamine **3.64**; however, the reaction did not proceed at room temperature, at reflux or when an additional equiv. of **3.64** was added. Consequently, after many failed attempts to introduce the 4'-amino group via reductive amination and transamination, this strategy was not pursued any further.

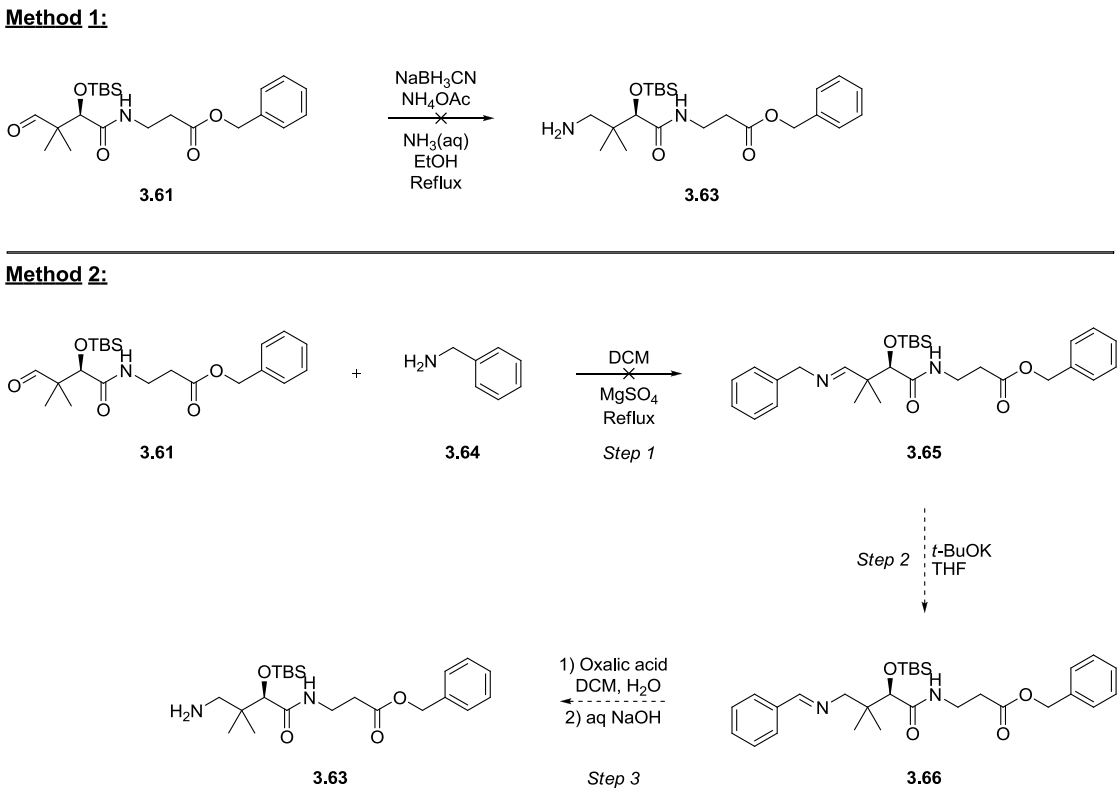


**Scheme 3.12. Alternative proposed synthetic routes for the preparation of (*R*)-4'-amino-*N*-heptyl pantothenamide (3.56). (Method 1) An alternative method for the metal hydride-mediated reductive amination of aldehyde 3.61 based on a method developed by Dangerfield *et al*. [58]. (Method 2) An alternative method for the transamination of aldehyde 3.61 based on a method that was developed by de Kimpe *et al*. [60].**

A thorough literature search revealed a method, developed by Kopelevich *et al*. [61] in 1979, that utilizes a Gabriel-type synthesis with potassium phthalimide (**3.67**) (Scheme 3.13) to introduce the 4'-amine functionality onto pantothenic acid **3.9**. This was achieved by preparing (*R*/*S*)-4'-amino-2-hydroxy-3,3-dimethylbutanoic acid (**3.69**), which was subsequently coupled to β-alanine (Scheme 1.3, Chapter 1) to afford (*R*/*S*)-4'-amino pantothenic acid. Given that a similar strategy in the synthesis of (*R*/*S*)-4'-deoxy-N7-Pan **3.49** to prepare acid **3.46** was used, before coupling it to amine **3.45** (Scheme 3.9), we decided to apply this method to the synthesis of (*R*/*S*)-**3.56**. While an important disadvantage of this method is the formation of a mixture of enantiomers at the 2'-hydroxyl group, as was the case with (*R*/*S*)-**3.49**, we decided to proceed with the synthesis with the intention of revisiting the enantioselective syntheses in the case that the racemate was found to have desirable biological activity.

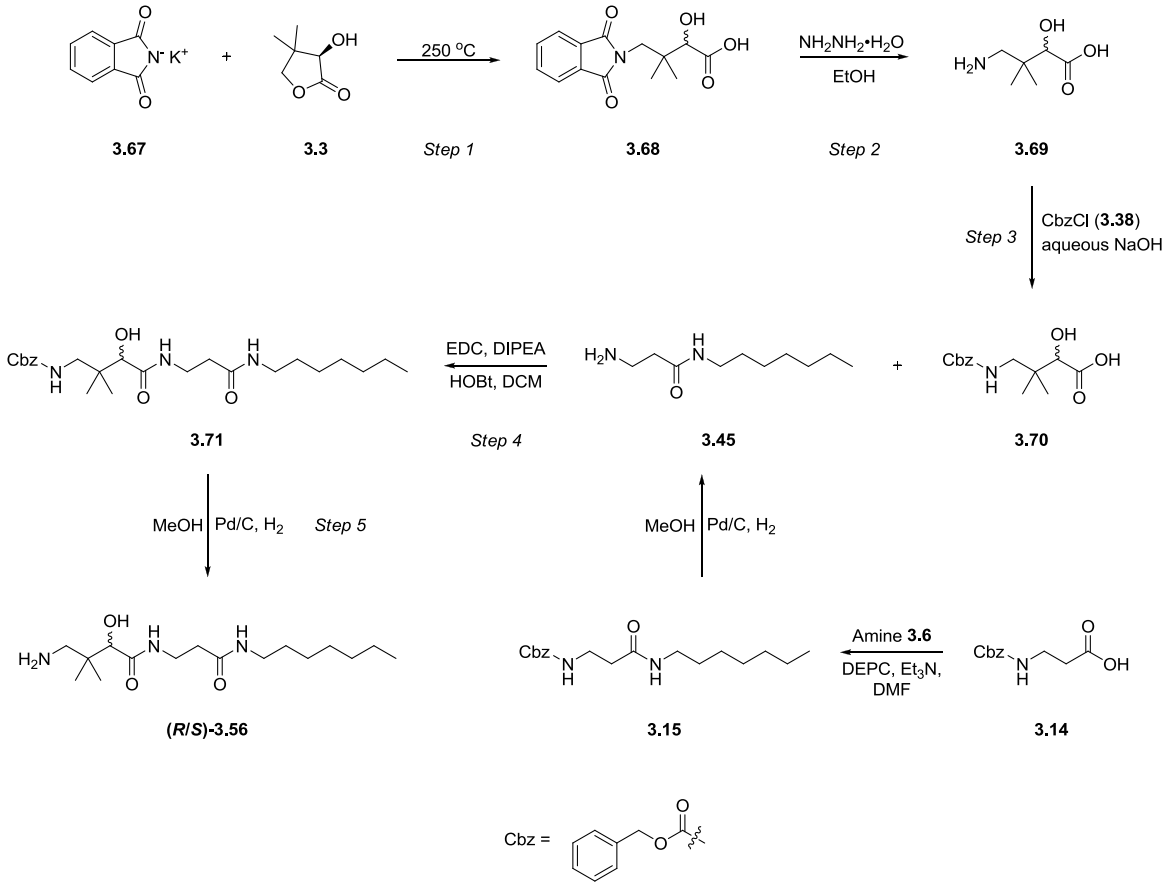


**Scheme 3.13. Synthetic route for the preparation of (*R*/*S*)-4'-amino-*N*-heptyl pantothenamide (3.56) using phthalimide to introduce the 4'-amine, based on methods adapted from Kopelevich *et al*. [62] and de Villiers *et al*. [12].**

We used an adapted experimental procedure from Kopelevich *et al*. [62], leading to a five-step linear synthesis that included a condensation and coupling reaction. In the first step, (*R*)-(-)-pantolactone **3.3** was condensed with potassium phthalimide (**3.67**) (synthesised according to Wang *et al*. [63] by stirring phthalimide with KOH in a mixture of MeOH and EtOH) at 250°C, before purification by FCC afforded phthalimide **3.68** as a pale yellow solid in excellent yield (86%) and the $^{1}$H NMR data are consistent with those previously reported in literature [62]. Although we start off with an *R*-configuration at the hydroxyl in (*R*)-(-)-pantolactone **3.3**, phthalimide **3.68** is a mixture of enantiomers. We hypothesize that this is due to potassium phthalimide (**3.67**) acting as a base that deprotonates at the α-carbon, i.e. at the (*R*)-hydroxyl position, leading enolization and racemization. In the second step, the phthaloyl protecting group was successfully removed using hydrazine hydrate in EtOH and amine **3.69** was obtained as a pure white powder upon recrystallization with chloroform in moderate yield (57%). Subsequently, in step 3, primary amine **3.69** was protected with CbzCl **3.38** in aqueous NaOH. The reaction mixture was washed with

diethyl ether to remove excess unreacted CbzCl **3.38** and the aqueous layer was lyophilized to afford carbamate **3.70** as a white powder in a much higher yield (93%) than the 67% yield reported by Kopelevich *et al*. [62].

Step 4 entailed an EDC-assisted coupling between acid **3.70** and amine **3.45** (as previously described in the synthesis of (*R*/*S*)-**3.49** in Chapter 2 [12]) in the presence of HOBt and DIPEA, which resulted in the formation of the second amide bond. After purification by FCC, amide **3.71** was obtained as a yellow oil in 50% yield; this result correlates well with the yield obtained in the similar coupling used to prepare (*R*/*S*)-4'-deoxy-N5-Pan **2.9** as described in Chapter 2. The final step of the synthesis involved the deprotection of carbamate **3.71** by treatment with $H_2$ in the presence of 10% Pd/C, to yield target compound (*R*/*S*)-**3.56** as a pure white solid upon filtration in an excellent 89% yield. The purity was confirmed by $^1$H NMR spectroscopic analysis.

#### 3.4.3.3 4'-Phospho-*N*-heptyl pantothenamide (3.74)

The synthetic route for preparation of 4'-phospho-N7-Pan **3.74** was based on a method developed by Strauss *et al*. [57] and comprised of three linear steps that included a phosphorylation and deprotection step (Scheme 3.14). In the first step, calcium pantothenate was converted into the free acid **3.9** using Amberlite IR120 resin and was subsequently coupled to heptylamine (**3.6**) using DEPC in the presence of $Et_3N$ to facilitate the amide bond formation. The side products and unreacted amine were removed through aqueous work-up; this proved to be adequate and amide **3.10** was subsequently used in the next step without any further purification. In the second step, hydroxyl **3.10** was phosphorylated with dibenzylchlorophosphate **3.72** (prepared *in situ* by reacting dibenzylphosphite and *N*-chlorosuccinimide in toluene for 2h, followed by filtration of the succinimide) in pyridine at -40°C, before purification by FCC afforded **3.73** as a yellow solid in a 34% yield. The final step of the synthesis entailed its deprotection; the benzyl protecting groups were successfully removed with $H_2$ in the presence of 10% Pd/C to yield target compound **3.74** as a clear oil in an excellent yield (98%) upon filtration and the purity was confirmed by $^1$H NMR spectroscopic analysis.

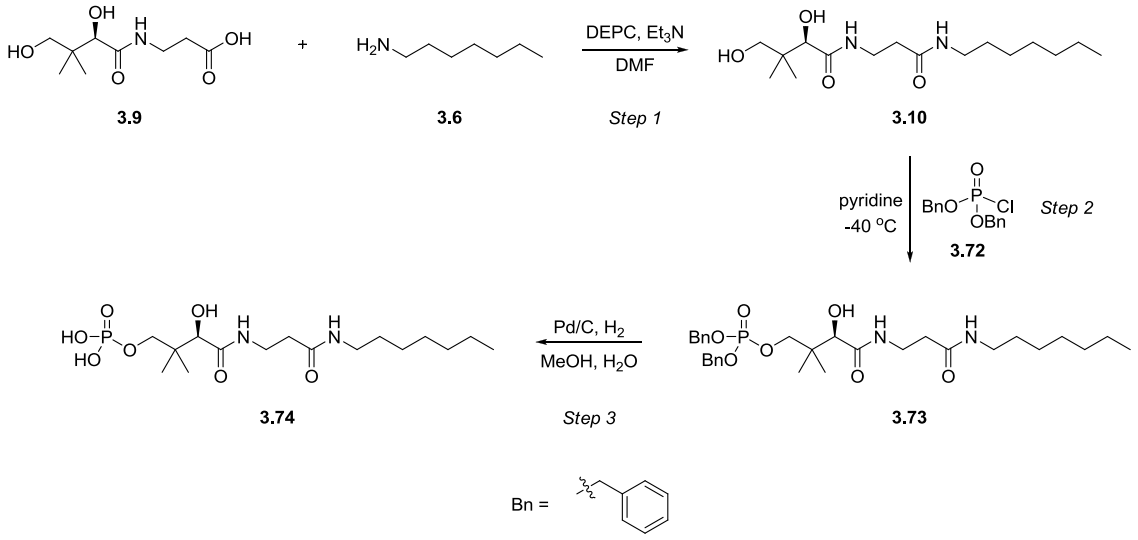


**Scheme 3.14. Synthetic route for the preparation of 4'-phospho-*N*-heptyl pantothenamide (3.74) from pantothenic acid using a method developed by Strauss *et al*. [57].**

## 3.5 Biological evaluation of N7-Pan analogues

The next objective was to evaluate whether the ten N7-Pan derivatives prepared above retained their potency towards *S. aureus*. We evaluated the compounds in two different ways: first, we subjected all of the N7-Pan derivatives to kinetic analysis using heterologously purified *Sa*PanK-II enzyme to determine whether they have the same kinetic parameters associated with the mode of action of the parent compound N7-Pan **3.10**. Second, we investigated the whole cell inhibition of *S. aureus* RN4220 by these compounds.

### 3.5.1 Kinetic characterization of *S. aureus* pantothenate kinase (*Sa*PanK-II) using the N7-Pan analogues as alternate substrates

*Sa*PanK-II was overexpressed in *E. coli* and purified using $Ni^{2+}$-based immobilized metal ion affinity chromatography (IMAC) in similar fashion as was described in the accompanying manuscript in Chapter 2. The purified *Sa*PanK-II was subsequently assayed for its ability to catalyze the ATP-dependent phosphorylation of the N7-Pan analogues using an established enzyme-coupled assay [64]. In this continuous assay (Figure 3.3), one molecule of substrate (pantothenic acid **3.9** in the figure; N7-Pan analogues in this study) reacts with one molecule of ATP to form the phosphorylated product (4'-phospho-pantothenic acid in Figure 3.3) and one molecule of ADP. Pyruvate kinase (PK) regenerates ATP from the ADP molecule by transferring the phosphate from phosphoenol pyruvate (PEP), leading to the formation of one molecule of pyruvate. This pyruvate molecule is consumed by lactose dehydrogenase (LDH) to generate one molecule of lactate with the concomitant oxidation of one molecule of NADH to $NAD^+$. The decrease of NADH is followed

spectrophotometrically at $A_{340}$ over time. From the slope of the curves obtained in this manner initial rates are calculated that are used to obtain the kinetic parameters.

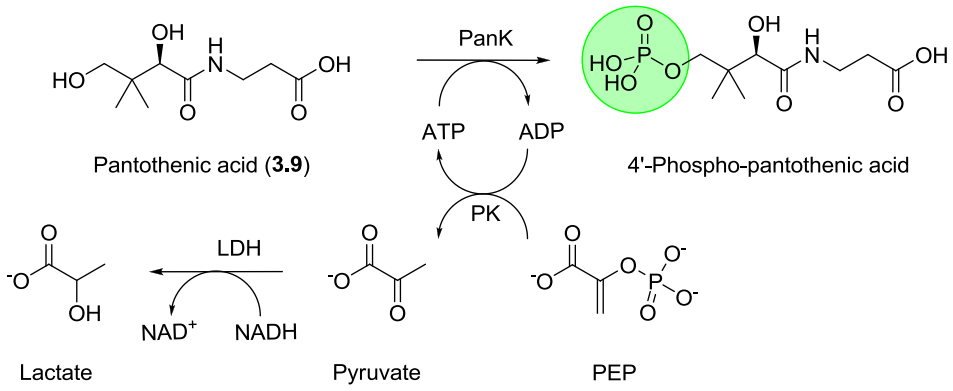


**Figure 3.3. Coupled enzymatic assay to quantify the [ADP] produced by the PanK reaction.**

Each N7-Pan analogue was tested as substrate of *Sa*PanK-II and the Michaelis-Menten kinetic parameters (summarized Table 3.2) were determined by utilizing measurements from the initial phase of each reaction (<10% substrate consumed). The kinetic profiles obtained are shown in Figure 3.4. We predicted that the N7-Pan analogues that would exhibit the same mode of action as N7-Pan **3.10**, would also show its unusual combination of kinetic parameters which includes a high apparent affinity ($K_M^{app}$) and low turnover ($k_{cat}$) resulting in a high apparent catalytic efficiency ($k_{cat}/K_M^{app}$). However, not one of the analogues exhibited such a profile.

**Table 3.2. Kinetic parameters determined for *Sa*PanK-II with the N7-Pan analogues.[a] ND, not determined.**

| | ***Sa*PanK-II** | | | | |
|---|---|---|---|---|---|
| **Compound** | $K_M^{app}$ **(μM)** | $k_{cat}$ **($s^{-1}$)** | $k_{cat}/K_M$ **($mM^{-1}.s^{-1}$)** | $N^b$ | **Equation fitted** |
| **3.9** | 27.8 ± 3.3 | 3.37 ± 0.24 | 124 ± 7 | 4 | Hill equation |
| **3.10** | 2.04 ± 0.54 | 0.22 ± 0.02 | 118 ± 41 | 2 | Michaelis-Menten |
| **3.7** | 35.3 ± 1.3 | 1.77 ± 0.02 | 50.3 ± 2.5 | 2 | Michaelis-Menten |
| **3.8** | 67.5 ± 16 | 1.64 ± 0.18 | 25.3 ± 5.3 | 4 | Michaelis-Menten |
| **3.11** | 487 ± 127 | 5.79 ± 1.4 | 12.0 ± 0.31 | 2 | Michaelis-Menten |
| **3.27** | 39.3 ± 2.9 | 2.46 ± 0.19 | 62.5 ± 0.41 | 2 | Michaelis-Menten[c] |
| **3.44** | 51.7 ± 27 | 5.29 ± 1.9 | 107 ± 15 | 3 | Michaelis-Menten[c] |
| **3.36** | 111 ± 96 | 3.46 ± 2.0 | 38.7 ± 13 | 4 | Michaelis-Menten[c] |

| | | | | | |
|---|---|---|---|---|---|
| **3.33** | 37.0 ± 17 | 1.74 ± 0.31 | 52.1 ± 16 | 4 | Michaelis-Menten |
| **3.56** | - | - | - | 2 | - |
| **3.49** | ND | ND | ND | ND | ND |
| **3.74** | ND | ND | ND | ND | ND |

[a] Kinetic parameters were determined by keeping the ATP concentration constant at 1.5 mM in all cases. All reported parameters are the mean of those obtained by fitting the given equation to each experiment's individual data set; errors indicate the range/2 (for parameters obtained from two independent experiments) and the SEM (for parameters obtained from three or more independent experiments).

[b] Number of independent experiments.

[c] Certain N7-Pan analogues showed inhibition of *Sa*PanK-II at high substrate concentrations; using a Michaelis-Menten equation that accounts for the uncompetitive substrate inhibition, a $K_i$ for each compound was determined – (*E*)-N7-CJ-Pan **3.27** = 205 ± 8.8 µM, N7-pantoyltauramide **3.44** = 279 ± 93 µM and N7-pantothenthioamide **3.36** = 225 ± 137 µM.

Compared to N7-Pan **3.10** which has a $K_M^{app}$ of 2.04 ± 0.54 µM, all of the N7-Pan analogues with steric bulk introduced (Figure 3.4A) had much lower affinities for *Sa*PanK-II, suggesting that they are poor substrates. N7-α-methyl-Pan **3.7** has the highest affinity with a $K_M^{app}$ of 35.3 ± 1.3 µM, which is comparable to that of the native substrate, pantothenic acid **3.9** ($K_M^{app}$ = 27.8 ± 3.3 µM), while *N*-Methyl-N7-Pan **3.11** is the poorest substrate with a $K_M^{app}$ of 487 ± 127 µM. This value is more than 15-fold higher than the $K_M^{app}$ of pantothenic acid **3.9**.

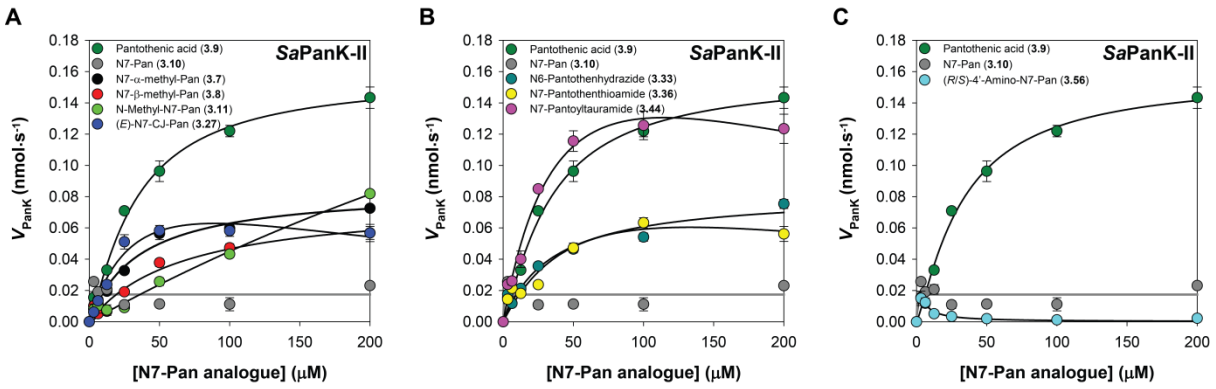


**Figure 3.4. (A) Kinetic profiles for *Sa*PanK-II with pantothenic acid 3.9 (dark green), N7-Pan 3.10 (grey) and the N7-Pan analogues with steric bulk introduced (N7-α-methyl-Pan 3.7 (black), N7-β-methyl-Pan 3.8 (red), *N*-methyl-N7-Pan 3.11 (light green) and (*E*)-N7-CJ-Pan 3.27 (dark blue)). (B) Kinetic profiles for *Sa*PanK-II with pantothenic acid 3.9 (dark green), N7-Pan 3.10 (grey) and the bioisostere N7-Pan analogues (N6-pantothenhydrazide 3.33 (cyan), N7-pantothenthioamide 3.36 (yellow) and N7-pantoyltauramide 3.44 (pink)). (C) Kinetic profiles for *Sa*PanK-II with pantothenic acid 3.9 (dark green), N7-Pan 3.10 (grey) and (*R*/*S*)-4'-amino-N7-Pan 3.56 (light blue).**

Furthermore, compared to the low turnover ($k_{cat}$ = 0.22 ± 0.02 $s^{-1}$) of N7-Pan **3.10**, all of the N7-Pan analogues with steric bulk introduced had a much higher turnover. N7-β-methyl-Pan **3.8** has the

lowest turnover with a $k_{cat}$ of 1.64 ± 0.18 $s^{-1}$, but this is still roughly 7-fold higher than for the N7-Pan **3.10** value. *N*-Methyl-N7-Pan **3.11** has the highest turnover with a $k_{cat}$ of 5.79 ± 1.4 $s^{-1}$, which is higher than what we observe for pantothenic acid **3.9** ($k_{cat}$ = 3.37 ± 0.24 $s^{-1}$), while (*E*)-N7-CJ-Pan **3.27** and N7-α-methyl-Pan **3.7** have $k_{cat}$-values of 2.46 ± 0.19 $s^{-1}$ and 1.77 ± 0.02 $s^{-1}$, respectively. Since none of the N7-Pan analogues with steric bulk added show the same unusual combination of kinetic parameters observed for N5-Pan and N7-Pan **3.10** (as described in Chapter 2) and consequently do not have the same complex interaction with *Sa*PanK-II, it is doubtful that they would act as uncompetitive inhibitors of the enzyme as is the case with N7-Pan.

Of the three N7-Pan bioisosteres (Figure 3.4B), the kinetic parameters of N6-pantothenhydrazide **3.33** was the closest to that of N7-Pan **3.10**. It had a relatively low affinity for *Sa*PanK-II ($K_M^{app}$ = 37.0 ± 17 vs. 2.04 ± 0.54 µM for N7-Pan **3.10**) and a higher turnover ($k_{cat}$ = 1.74 ± 0.31 vs. 0.22 ± 0.02 $s^{-1}$). N7-pantothenthioamide **3.36** was also a poor substrate for *Sa*PanK-II with a $K_M^{app}$ of 111 ± 96 µM. This large SEM is attributed to the variation in the parameters obtained from the standard kinetic equation fits due to **3.36** being a poor substrate. Furthermore, it has a turnover which is comparable to that of pantothenic acid **3.9**, with $k_{cat}$-values of 3.46 ± 2.0 $s^{-1}$ and 3.37 ± 0.24 $s^{-1}$, respectively. Consequently, it is unlikely that these two bioisosteres would act as uncompetitive inhibitors of the enzyme, given that they do not show the same complex interaction observed with N7-Pan **3.10**. In contrast, N7-pantoyltauramide **3.44** showed a lower affinity for *Sa*PanK-II compared to N7-Pan **3.10** ($K_M^{app}$ = 51.7 ± 27 vs. 2.04 ± 0.54 µM) with a much higher turnover ($k_{cat}$ = 5.29 ± 1.9 $s^{-1}$ vs. 0.22 ± 0.02 $s^{-1}$), suggesting that it is an excellent substrate for *Sa*PanK-II and not an inhibitor of the enzyme. This is supported by its turnover which is 1.5-fold higher than what we observe for pantothenic acid **3.9** ($k_{cat}$ = 3.37 ± 0.24 $s^{-1}$).

(*R*/*S*)-4'-Amino-N7-Pan **3.56**, the N7-Pan analogue in which the 4'-hydroxyl was replaced with a 4'-amine, was also tested as a substrate (Figure 3.4C). It showed a kinetic profile comparable to that of N7-Pan **3.10** with a very low turnover and high affinity for *Sa*PanK-II. We were unable to determine the kinetic parameters because the values obtained from fits of the standard kinetic equations fell below the sensitivity limit of the assay and were therefore not deemed trustworthy. Nonetheless, its kinetic profile suggests that like N7-Pan **3.10**, (*R*/*S*)-4'-amino-N7-Pan **3.56** also has an unusual combination of kinetic parameters and therefore might act as an uncompetitive inhibitor of the enzyme. We subsequently tested this compound as an inhibitor of *Sa*PanK-II (see below). Finally, neither (*R*/*S*)-4'-deoxy-N7-Pan **3.49** nor 4'-phospho-N7-Pan **3.74** were tested as substrates, since the terminal hydroxyl were removed in the case of the former, making it impossible to be phosphorylated; in the case of the second, the compound is a product analogue, since it is already phosphorylated.

Subsequently, these compounds were tested as inhibitors of *Sa*PanK-II using reaction mixtures that contained 25 µM pantothenic acid **3.9** and increasing concentrations of either (*R*/*S*)-4'-amino-N7-Pan **3.56**, (*R*/*S*)-4'-deoxy-N7-Pan **3.49** or 4'-phospho-N7-Pan **3.74**. Surprisingly, even though (*R*/*S*)-4'-amino-N7-Pan **3.56** showed a similar kinetic profile to that of N7-Pan **3.10** (i.e. high affinity with low turnover), it was a very poor inhibitor of *Sa*PanK-II with an $IC_{50}$ > 250 µM (Figure 3.5A). Therefore, (*R*/*S*)-4'-amino-N7-Pan **3.56** neither acts a substrate nor as an inhibitor of *Sa*PanK-II. (*R*/*S*)-4'-Deoxy-N7-Pan **3.49** showed the same apparent inhibitory effect on *Sa*PanK-II as N7-Pan **3.10**, with an $IC_{50}$ value of ~ 5.5 µM (Figure 3.5B). Full kinetic analysis with (*R*/*S*)-4'-deoxy-N7-Pan **3.49** showed a dual effect, with (*R*/*S*)-4'-deoxy-N7-Pan **3.49** causing a small but significant reduction in $K_M^{app}$ for pantothenic acid **3.9** and a large reduction in the $V_{max}^{app}$ (Figure 3.5C). These results are in agreement with the results obtained with (*R*/*S*)-4'-deoxy-N5-Pan **2.9** as described in Chapter 2.

Unexpectedly, the product analogue 4'-phospho-N7-Pan **3.74** also showed an inhibitory effect on *Sa*PanK-II with an $IC_{50}$ value of ~ 40.5 µM (Figure 3.5B). This was very surprising, given that we do not expect the product analogue to bind to the enzyme and consequently inhibit the enzyme activity. Full kinetic analysis showed the same overall effect observed for (*R*/*S*)-4'-deoxy-N7-Pan **3.49**, with 4'-phospho-N7-Pan **3.74** causing a small but significant reduction in $K_M^{app}$ for pantothenic acid **3.9** and a large reduction in the $V_{max}^{app}$ (Figure 3.5D). However, *Sa*PanK-II activity is positively influenced at very low concentrations of 4'-phospho-N7-Pan **3.74** and inhibited at higher concentrations. Even though the product analogue, 4'-phospho-N7-Pan **3.74** acts as an inhibitor of *Sa*PanK-II, it is ~7-fold less potent than (*R*/*S*)-4'-deoxy-N7-Pan **3.49** which does not contain the 4'-hydroxyl.

To summarise, the kinetic characterization results show that none of the N7-Pan analogues with steric bulk introduced or with bioisostere replacements showed a complex interaction (low turnover, high catalytic efficiency) with *Sa*PanK-II similar to what was observed for N5-Pan and N7-Pan **3.10**. (*R*/*S*)-4'-Amino-N7-Pan **3.56** is the only N7-Pan analogue that showed a similar interaction to what was observed for N7-Pan **3.10**, but enzyme inhibition assays showed that it acts as a very poor inhibitor of *Sa*PanK-II, in addition to being a very poor substrate. Both (*R*/*S*)-4'-deoxy-N7-Pan **3.49** and 4'-phospho-N7-Pan **3.74** were found to be good inhibitors of *Sa*PanK-II.

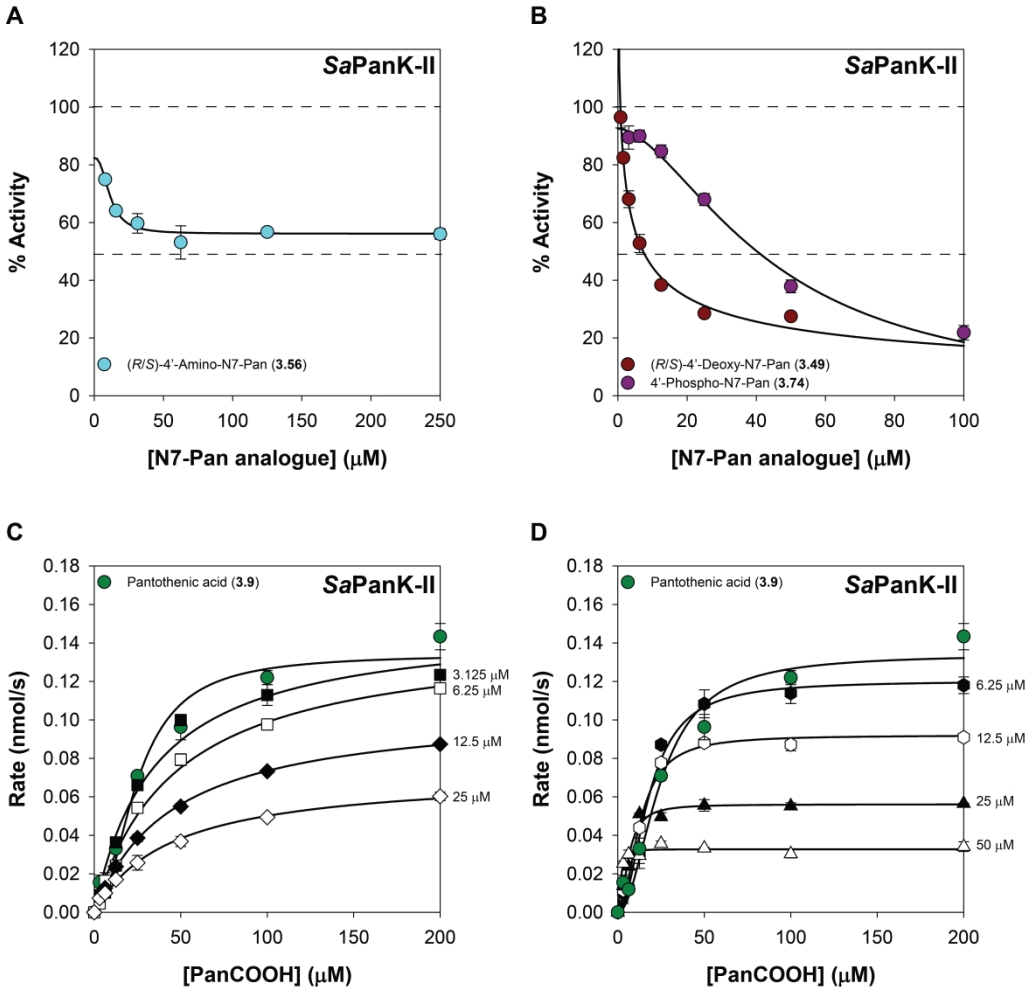


**Figure 3.5. N7-Pan analogues as inhibitors of *Sa*PanK-II. (A) Inhibition profile of *Sa*PanK-II when treated with (*R*/*S*)-4'-amino-N7-Pan 3.56 at a fixed concentration of 25 μM pantothenic acid 3.9. (B) Inhibition profile of *Sa*PanK-II when treated with (*R*/*S*)-4'-deoxy-N7-Pan 3.49 (dark red) and 4'-phospho-N7-Pan 3.74 (purple) at a fixed concentration of 25 μM pantothenic acid 3.9. (C) Kinetic profiles for *Sa*PanK-II with pantothenic acid 3.9 in the presence of increasing concentrations of (*R*/*S*)-4'-deoxy-N7-Pan 3.49 (indicated on the right of each curve). (D) Kinetic profiles for *Sa*PanK-II with pantothenic acid 3.9 in the presence of increasing concentrations of 4'-phospho-N7-Pan 3.74 (indicated on the right of each curve).**

## 3.5.2 Cell growth inhibition of *S. aureus* RN4220 by the N7-Pan analogues

To determine if the obtained kinetic parameters correlated with the growth inhibition potential of these analogues in any way, whole cell inhibition assays were performed using *S. aureus* RN4220. Inhibition assays were performed using minimal medium (i.e. with no pantothenic acid **3.9** present) that is appropriate for *S. aureus* (see experimental section for details) [65]. While using minimal medium does not give practically relevant results, it does allow for even low levels of inhibition to be observed, and for small differences to be characterized. The bacteria were incubated for 24h at 37°C with varying concentrations of each N7-Pan analogue and the $MIC_{80}$ (minimum concentration needed to kill 80% of the organism) values were calculated as shown in Table 3.3. Of all of the N7-

Pan analogues tested, only N7-β-methyl-Pan **3.8**, (*E*)-N7-CJ-Pan **3.27**, (*R*/*S*)-4'-deoxy-N7-Pan **3.49** and 4'-phospho-N7-Pan **3.74** had $MIC_{80}$ values lower than 200 µM, with (*R*/*S*)-4'-deoxy-N7-Pan **3.49** ($MIC_{80}$ ~25 µM) and 4'-phospho-N7-Pan **3.74** ($MIC_{80}$ ~1.8 µM) being the most potent. Surprisingly, 4'-phospho-N7-Pan **3.74** was the most potent inhibitor. This was also highly unexpected; given that it is generally believed that phosphorylated molecules are too polar to enter cells unassisted [66].

Consequently, the N7-Pan analogues that had $MIC_{80}$ values lower than 200 µM were tested on bacteria grown in 1% tryptone medium (which contains ~1–5 µM pantothenic acid **3.9**). The bacteria were incubated for 20h at 37°C with varying concentrations of each N7-Pan analogue. The results in Table 3.3 shows that of the four N7-Pan analogues tested, only 4'-phospho-N7-Pan **3.74** had a $MIC_{80}$ lower than 200 µM. The observed decrease in potency is due to the pantothenic acid **3.9** present in the growth medium antagonizing the inhibition exerted by the N7-Pan analogues. The $MIC_{80}$ for 4'-phospho-N7-Pan **3.74** in 1% tryptone broth is ~24 µM, a value that compares poorly to that of N7-Pan **3.10**, which has a $MIC_{80}$ <0.77 µM against *S. aureus* grown in the same medium.

**Table 3.3. MIC80 values determined for *S. aureus* RN4220 with the N7-Pan analogues.[a] ND, not determined.**

| | ***S. aureus* RN4220** | |
|---|---|---|
| **Compound** | **$MIC_{80}$ (minimal medium) (µM)** | **$MIC_{80}$ (1% tryptone) (µM)** |
| **3.10** | **<0.078** | **<0.77** |
| **3.7** | >200 | ND |
| **3.8** | **~50** | >200 |
| **3.11** | >200 | >200 |
| **3.27** | **~25** | >200 |
| **3.44** | >200 | ND |
| **3.36** | >200 | ND |
| **3.33** | >200 | ND |
| **3.56** | > 200 | ND |
| **3.49** | **~25** | >200 |
| **3.74** | **~1.8** | **~24** |

[a] *S. aureus* RN4220 was grown in either minimal medium for 24 h or in 1% tryptone medium for 20 h in the presence of the indicated N7-Pan analogue at 37°C. The reported values represent the mean of two or more independent experiments.

### 3.5.3 Pantetheinase resistance of the N7-Pan analogues

Given that the N7-Pan analogues did not show a complex interaction similar to that observed for N7-Pan **3.10**, and also did not show the same potency compared to N7-Pan **3.10**, the pantetheinase resistance of these analogues were not determined. However, unpublished results from related studies in our laboratory indicated that amide analogues of CJ-15,801 are resistant to pantetheinase degradation and we therefore expect that (*E*)-N7-CJ-Pan **3.27** will also be pantetheinase-resistant. Furthermore, Dr. Cristiano Macuamule determined during his PhD study that the α- and β-methyl pantothenamides, as well as the pantoyltauramides are pantetheinase-resistant [67]. Given that pantetheinase is highly substrate specific for the pantothenate moiety and consequently does not accept substrates with a modification at the 4'-position [17, 19], we expect that 4'-phospho-N7-Pan **3.74**, (*R*/*S*)-4'-deoxy-N7-Pan **3.49** and (*R*/*S*)-4'-amino-N7-Pan **3.56** will be pantetheinase-resistant seeing as the pantothenate moiety has been modified.

## 3.6 Rationalizing the poor inhibition observed for the N7-Pan analogues

After the completion of the aforementioned work, a crystal structure of *Sa*PanK-II with 4'-phospho-N7-Pan **3.73** bound in the active site was deposited into the Protein Data Bank (PDB) [68]. This crystal structure (PDB 4M7X) allowed us to rationalize why some of the N7-Pan analogues acted as poor substrates of *Sa*PanK-II and as poor inhibitors of *S. aureus* RN4220.

Figure 3.6 shows a representation of the active site of *Sa*PanK-II, which is a dimer with two identical subunits (indicated in red and green), bound to 4'-phospho-N7-Pan **3.74**. As seen in the picture, two amino acid residues have H-bonding interactions with 4'-phospho-N7-Pan **3.74**: Arg113 forms H-bonds with the carbonyl oxygens of its two amide groups, while Thr172 has an H-bonding interaction with the NH of one of the amide bonds. In the case of *N*-methyl-N7-Pan **3.11** the H-bonding interaction with Thr172 is lost when the scissile amide bond is methylated. Furthermore, when the carbonyl oxygen is replaced with a sulfur to form the thioamide in N7-pantothenthioamide **3.36**, the H-bonding interaction is weakened with Arg113, since a sulfur atom is an extremely poor H-bonding acceptor. Additionally, since the sulfur atom is larger than the oxygen atom, this could also have a steric effect. The loss or weakening of these binding interactions are reflected in the increase in the $K_M^{app}$-values for *N*-methyl-N7-Pan **3.11** ($K_M^{app}$ of 487 ± 127 μM) and N7-pantothenthioamide **3.36** ($K_M^{app}$ of 111 ± 96 μM) compared to that of pantothenic acid **3.9** ($K_M^{app}$ of 27.8 ± 3.3 μM). This could explain the poor inhibition of *S. aureus* observed for these compounds; they do not interact with or inhibit the enzyme as N7-Pan **3.10** does, nor are they good substrates of *Sa*PanK-II that would metabolically activate them to exert an inhibitory effect by being converted into antimetabolites of CoA.

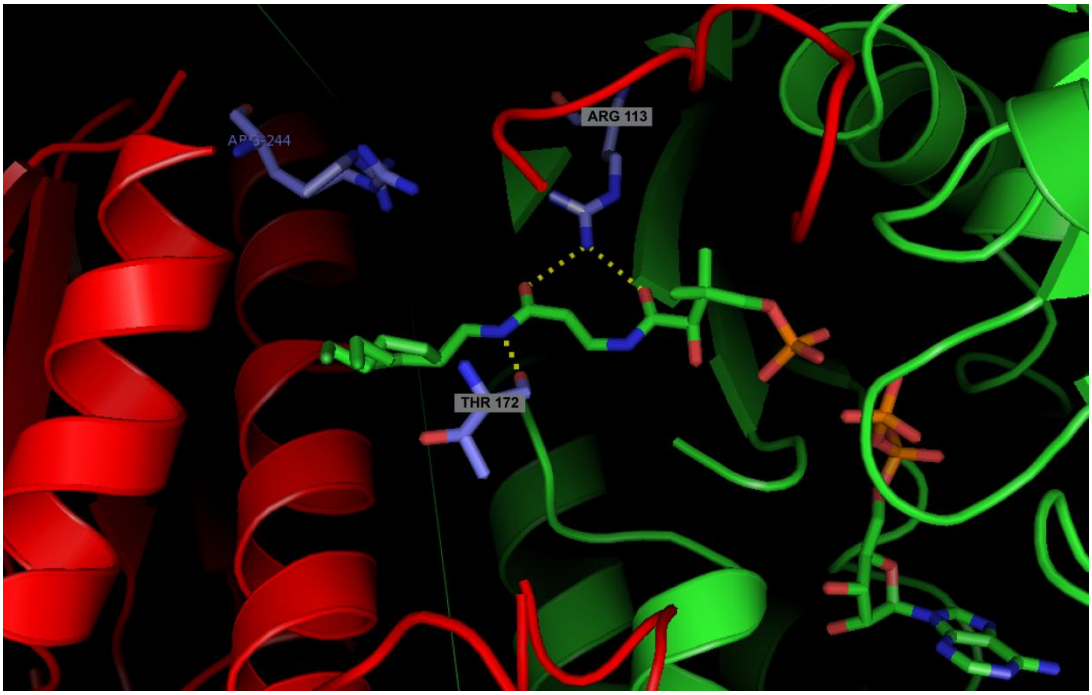


**Figure 3.6. Crystal structure of *Sa*PanK-II (PDB 4M7X), which is a dimer with two identical subunits (indicated in red and green), with 4'-phospho-N7-Pan 3.74 bound in the active site. 4'-Phospho-N7-Pan 3.74 forms H-bonding interactions with two amino acid residues; Arg113 forms H-bonding interactions with the two carbonyl oxygens of the amide bonds and Thr172 forms a H-bonding interaction with the NH of the scissile amide bond.**

Looking at the active site where 4'-phospho-N7-Pan **3.74** is bound (Figure 3.7) we can see that there is some space to accommodate structural modifications on the α- and β-carbons adjacent to the scissile amide bond (big yellow oval), as well as on the NH of the amide bond (small yellow oval). This suggests that the modifications resulting in the formation of N7-α-Methyl-Pan **3.7** and N7-β-methyl Pan **3.8**, both of which showed some inhibition of *S. aureus* whole cell growth, can be accommodated in the active site. Additionally, there is also space to accommodate the methyl group on the nitrogen of the scissile amide bond as in the case of *N*-methyl-N7-Pan **3.11**, although this leads to the loss of an H-bonding interaction as explained above. (*E*)-N7-CJ-Pan **3.27** contains a trans-enamide moiety which makes the molecule rigid and prevents the C–C bonds in the β-alanine moiety from rotating. Consequently, the two amide bonds of (*E*)-N7-CJ-Pan **3.27** are in the same plane as the double bond. However, this is not the case with 4'-phospho-N7-Pan **3.74** – the amide bonds are not in the same plane and the molecule is free to rotate. These differences in molecular geometry could result in *Sa*PanK-II not being able to bind (*E*)-N7-CJ-Pan **3.27** in the orientation necessary, and could explain why we observed poor inhibition against *S. aureus*, compared to the inhibition observed with 4'-phospho-N7-Pan **3.74**.

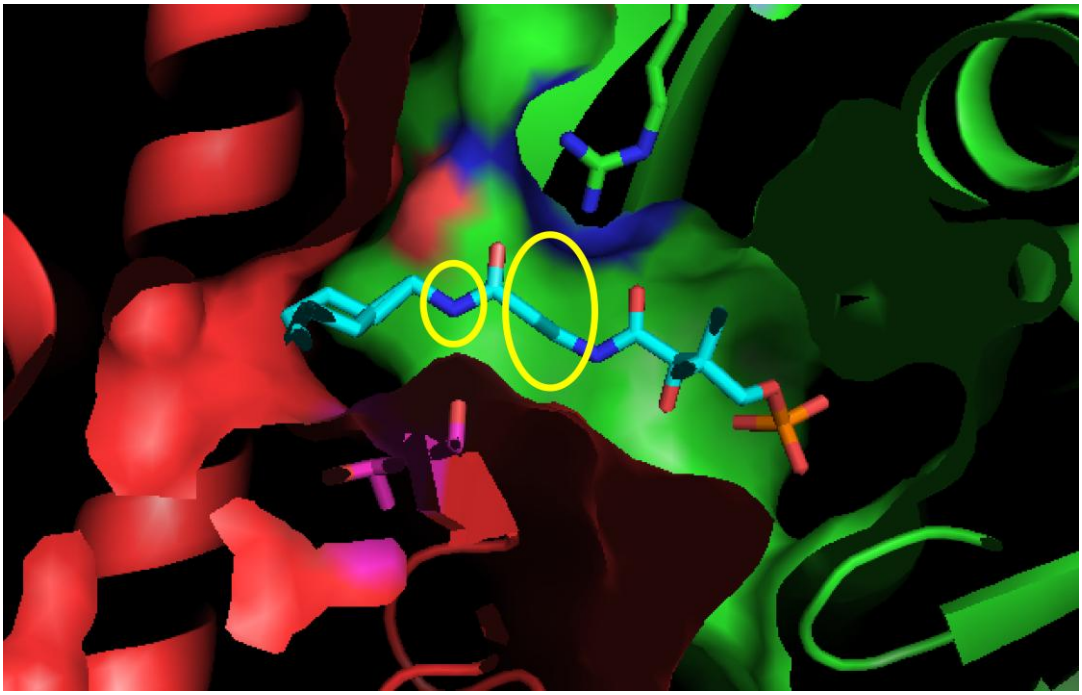

**Figure 3.7. Crystal structure of *Sa*PanK-II (PDB 4M7X) as shown in Figure 3.6, but with the surface of the active site shown. This highlights the space that is available in the active site to accommodate modifications of the parent compound. Specifically, the big yellow oval indicates the space around the α-and β-carbons adjacent to the scissile amide bond, while the small yellow oval indicates the space around the NH of the amide bond, both of which is large enough to accommodate the methyl groups found in the methylated analogues of N7-Pan.**

## 3.7 Conclusion

I have successfully synthesized ten N7-Pan analogues using various synthetic organic methods, and fully characterized all of the compounds analytically, kinetically and as bacterial growth inhibitors. The results presented here showed that none of the N7-Pan analogues showed the same complex interaction with *Sa*PanK-II that is observed for N7-Pan **3.10**, with the kinetic profiles of N7-α-methyl-Pan **3.7**, N7-β-methyl Pan **3.8**, (*E*)-N7-CJ-Pan **3.27** and N6-pantothenhydrazide **3.33** showing the closest resemblance to N7-Pan **3.10**. Both, (*R*/*S*)-4'-deoxy-N7-Pan **3.49** and 4'-phospho-N7-Pan **3.74** acted as inhibitors of *Sa*PanK-II. Inhibition from the latter was surprising, given that we did not expect the product analogue to bind to *Sa*PanK-II and consequently inhibit the enzyme activity. Furthermore, only four of the ten N7-Pan analogues showed growth inhibition of *S. aureus* RN4220 below 200 μM in minimal medium, while 4'-phospho-N7-Pan **3.74** is the only N7-Pan analogue that showed inhibition below 200 μM in 1% tryptone medium, with an $MIC_{80}$ of ~25 μM. This was highly unexpected, seeing as it is generally believed that phosphorylated molecules are too polar to enter cells unassisted [66]. It is therefore possible that *S. aureus* has a specific uptake mechanism for phosphorylated pantothenic acid analogues (most likely phospho-PantSH) but no reports on this have been made to date.

Additionally, we were able to use the *Sa*PanK-II crystal structure—that only became available after we had already completed most of the experiments—to rationalize why some of the N7-Pan analogues did not show inhibition of either *Sa*PanK-II or *S. aureus* RN4220. Two amino acid residues (Arg113 and Thr172) form critical H-bonding interactions with the pantothenamides in the active site; unfortunately, many of these were lost or weakened with the structural modifications that were implemented.

Overall, our findings indicate that it will be challenging to develop potent pantetheinase-resistant inhibitors for *S. aureus*. From the results above it is evident that the H-bonding interactions between Arg113 and the carbonyl oxygens of the two amide bonds, as well as the H-bond between Thr172 and the NH of the scissile amide are extremely important for binding in the active site. Additionally, the space within the active site for the addition of steric bulk is also limited, seeing as the addition of a methyl group to the α- or β-position is already too big a perturbation on the pantothenamide structure. Consequently, to design potent pantetheinase-resistant inhibitors, smaller steric bulk must be considered and the H-bonding interactions will have to be kept intact by using bioisosteres that can still form H-bonding interactions.

## 3.8 Experimental section

### 3.8.1 Material and methods

The N7-Pan analogues were dissolved in either a 50% $CH_3CN$-$H_2O$ solution or dimethyl sulfoxide (DMSO) to yield stock solutions at a concentration of 50-200 mM. Kinetic assays and growth inhibition assays were done with the final $CH_3CN$ or DMSO concentration never exceeding 3% (v/v). General chemicals, reagents and media were purchased from Sigma-Aldrich, Merck Chemicals (Darmstadt, Germany) or Acros Organics (ThermoFisher, Fair Lawn, NJ, USA) and were of the highest purity. Solvents used for reactions were CHROMASOLV HPLC grade solvents from Sigma-Aldrich, while the hexanes, DCM and EtOAc used for purification were purchased from Merck Chemicals. Dry DMF was prepared by shaking up over KOH, distilled under reduced pressure and a nitrogen atmosphere, and finally stored over 4 Å molecular sieves in the dark. Dry DCM was distilled from $CaH_2$ under a nitrogen atmosphere while dry THF was distilled from sodium under a nitrogen atmosphere.

All $^{1}H$ and $^{13}C$ NMR spectra were obtained using a 300 MHz Varian VNMRS (75 MHz for $^{13}C$), 400 MHz Varian Unity Inova (100 MHz for $^{13}C$) or 600 MHz Varian Unity Inova (150 MHz for $^{13}C$) instruments at the CAF of the University of Stellenbosch. All chemical shifts (δ) were recorded using the residual solvent peak and reported in p.p.m. All HRMS were performed on a Waters API

Q-TOF Ultima spectrometer (Waters, Milford, MA, USA) at the Mass Spectrometry unit of CAF. All $OD_{600}$ and kinetic studies were done using a Thermo Varioskan spectrophotometer (Thermo Scientific, Bremen, Germany). Inhibition studies were performed in Greiner Bio-one Cellstar flat-bottomed 96-well suspension plates (Greiner Bio-One GmbH, Frickenhausen, Germany). Kinetic studies were performed in Greiner Bio-one polystyrene flat-bottomed 96-well plates. The $MIC_{80}$s were determined by plotting the percentage (relative to a control containing no inhibitor) bacterial cell growth against the logarithm of increasing compound concentration. Kinetic data were fitted using Michaelis-Menten equations. Analysis of all concentration-response curves and kinetic data were done using Sigmaplot, version 12 (Systat Software Inc., Chicago, IL, USA).

### 3.8.2 Synthetic preparation of the N7-Pan analogues

*α-Methyl pantothenic acid* (**3.4**) *(mixture of diastereomers)*

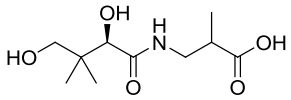

(*R*/*S*)-3-Amino isobutyric acid (**3.1**) (500 mg, 4.80 mmol) was dissolved in 1 M aqueous NaOH (4.80 mL, 4.80 mmol) and the solution was lyophilized. To the resulting white salt was added (*R*)-(-)-pantolactone **3.3** (700 mg, 5.28 mmol) and the mixture was stirred under an inert atmosphere overnight at 130°C. The resulting sticky oil was dissolved in $H_2O$ and loaded onto a column (1 cm diameter) containing prewashed Amberlite IR120 ($H^+$-form) ion exchange resin (500 mg). The free acid was eluted with $H_2O$ (1 × 10 mL) and lyophilized before purification by FCC (5:2:1:1 EtOAc: MeOH: $H_2O$: $CH_3CN$) afforded carboxylic acid **3.4** (0.97 mg, 86%) as a white-yellow powder. $R_f$ = 0.47 (FCC conditions). $\delta_H$ (300 MHz; $D_2O$; 25°C) 0.82 (3H, s, -$CH_3$), 0.85 (3H, s, -$CH_3$), 1.04 (3H, d, *J* = 7.1 Hz, -$CH_3$), 2.51-2.58 (1H, m, -CH-), 3.26-3.30 (2H, m, -$CH_2$-), 3.31 (1H, d, *J* = 11.1 Hz, -CH-), 3.42 (1H, d, *J* = 11.1 Hz, -CH-), 3.79 (1H, s, -CH-, diastereomer A) and 3.91 (1H, s, -CH-, diastereomer B). O<u>H</u> protons not observed. $^1$H NMR data are consistent with those previously reported [69].

*β-Methyl pantothenic acid* (**3.5**) *(mixture of diastereomers)*

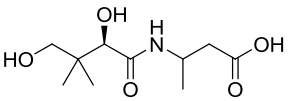

(*R*/*S*)-3-Aminobutyric acid (**3.2**) (500 mg, 4.80 mmol) was dissolved in 1 M aqueous NaOH (4.80 mL, 4.80 mmol) and the solution was lyophilized. To the resulting white-yellow salt was added (*R*)-(-)-pantolactone **3.3** (700 mg, 5.28 mmol) and the mixture was stirred under an inert atmosphere overnight at 130°C. The resulting sticky oil was dissolved in $H_2O$ and loaded onto a column (1 cm diameter) containing prewashed Amberlite IR120 ($H^+$-form) ion exchange resin (500 mg). The free acid was eluted with $H_2O$ (1 × 10 mL) and lyophilized before purification by FCC (5:2:1:1 EtOAc: MeOH: $H_2O$: $CH_3CN$) afforded carboxylic acid **3.5** (1.30 g, 82%) as a white-yellow powder. $R_f$ = 0.43 (FCC conditions).

$\delta_H$ (300 MHz; $D_2O$; 25°C) 0.91 (3H, s, -$CH_3$), 0.93 (3H, s, $CH_3$), 1.21 (3H, d, *J* = 5.9 Hz, -$CH_3$), 2.35-2.50 (2H, m, -$CH_2$-), 3.38 (1H, d, *J* = 11.2 Hz, -CH-), 3.51 (1H, d, *J* = 11.2 Hz, -CH-), 3.78 (1H, d, *J* = 3.5 Hz, -CH-, diastereomer A), 3.96 (1H, d, *J* = 3.5 Hz, -CH-, diastereomer B), and 4.26-4.34 (1H, m, -CH-). OH protons not observed. $^1$H NMR data are consistent with those previously reported (unpublished) [70].

*N-Heptyl α-methyl-pantothenamide* (**3.7**)

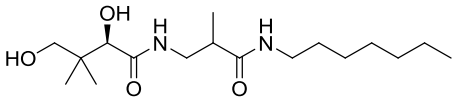

Heptylamine (**3.6**) (191 µL, 1.29 mmol) and DPPA (278 µL, 1.29 mmol) were added to a solution of carboxylic acid **3.4** (250 mg, 1.07 mmol) in anhydrous DMF (3 mL) at rt under an inert atmosphere. After cooling the mixture to 0°C, $Et_3N$ (180 µL, 1.29 mmol) was added. The reaction mixture was stirred for an additional 2h at 0°C and left to stir overnight at rt. DMF was removed *in vacuo* and Amberlite IR400 ($OH^-$-form) resin was added (2.50 g). The reaction mixture was filtered and lyophilized before purification by FCC (10% MeOH in DCM) afforded amide **3.7** (151 mg, 43%) as a yellow oil. $R_f$ = 0.41 (FCC conditions). $\delta_H$ (400 MHz; $CDCl_3$; 25°C) 0.85 (3H, t, *J* = 6.7 Hz, -$CH_3$), 0.92 (3H, s, -$CH_3$), 1.01 (3H, s, -$CH_3$), 1.15 (3H, d, *J* = 7.0 Hz, -$CH_3$), 1.25-1.34 (8H, m, -$(CH_2)_4$-), 1.46-1.50 (2H, m, -$CH_2$-), 2.50-2.61 (1H, m, -CH-), 3.14-3.27 (2H, m, -$CH_2$-), 3.31-3.45 (2H, m, -$CH_2$-), 3.49 (2H, s, -$CH_2$-), 3.94 (1H, s, -CH-, diastereomer A), 3.99 (1H, s, -CH-, diastereomer B), 5.89 (1H, br s, -NH-) and 7.29 (1H, br s, -NH-). OH protons not observed. $\delta_C$ (100 MHz; $CDCl_3$; 25°C) 14.3, 16.0, 21.9, 22.8, 22.8, 29.1, 29.7, 31.9, 39.5, 39.9, 40.9, 41.1, 42.4, 71.1, 77.8, 174.0, and 175.2. (HRMS) $[M+H]^+$ 331.2592 (Calculated $[C_{17}H_{35}N_2O_4]^+$ = 331.2597).

*N-Heptyl β-methyl-pantothenamide* (**3.8**)

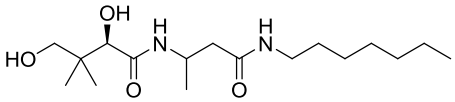

Heptylamine (**3.6**) (344 µL, 2.32 mmol) and DPPA (500 µL, 2.32 mmol) were added to a solution of carboxylic acid **3.5** (450 mg, 1.93 mmol) in anhydrous DMF (3 mL) at rt under an inert atmosphere. After cooling the mixture to 0°C, $Et_3N$ (323 µL, 2.32 mmol) was added. The reaction mixture was stirred for an additional 2h at 0°C and left to stir overnight at rt. DMF was removed *in vacuo* and Amberlite IR400 ($OH^-$-form) resin was added (2.50 g). The reaction mixture was filtered and lyophilized before purification by FCC (10% MeOH in DCM) afforded amide **3.8** (106 mg, 17%) as a white solid. $R_f$ = 0.19 (FCC conditions). $\delta_H$ (300 MHz; $CDCl_3$; 25°C) 0.86 (3H, apparent t, *J* = 6.7 Hz, -$CH_3$), 0.90 (3H, s, -$CH_3$), 1.00 (3H, s, -$CH_3$), 1.03 (3H, d, *J* = 3.2 Hz, -$CH_3$), 1.24-1.29 (8H, m, -$(CH_2)_4$-), 1.47-1.53 (2H, m, -$CH_2$-), 2.27-2.35 (1H, m, -$CH_2$-), 2.44-2.53 (1H, m, -$CH_2$-), 3.17-3.28 (2H, m, -$CH_2$-), 3.45-3.56 (2H, m, -$CH_2$-), 3.94 (1H, s, -CH-, diastereomer A), 3.99 (1H, s, -CH-, diastereomer B), 4.29-3.37 (1H, m, -CH-), 5.83 (1H, br s, -NH-) and 7.47 (1H, br

s, -NH-). OH protons not observed. $\delta_C$ (75 MHz; $CDCl_3$; 25°C) 14.1, 20.0, 20.2, 21.7, 22.6, 26.9, 28.9, 29.5, 31.7, 39.5, 39.7, 42.1, 42.6, 70.8, 77.2, 170.8 and 172.4. (HRMS) $[M+H]^+$ 331.2589 (Calculated $[C_{17}H_{35}N_2O_4]^+$ = 331.2597).

*N-Heptyl pantothenamide* (**3.10**)

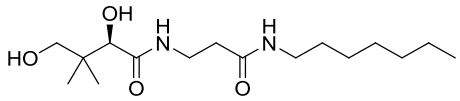

Calcium pantothenate (1.00 g, 4.15 mmol) was exchanged to the free acid by dissolving the salt in $H_2O$ (15 m) and passing the solution through a column (1.50 cm diameter) of pre-washed Amberlite IR-120 ($H^+$-form) ion exchange resin (1.10 g). The free carboxylic acid was eluted with $H_2O$ (1 × 15 mL), followed by lyophilization of the collected column eluate to afford the free carboxylic acid **3.9** as a clear oil (860 mg, 3.92 mmol). Heptylamine (**3.6**) (698 µL, 4.71 mmol) and DPPA (1.02 mL, 4.71 mmol) were added to a solution of carboxylic acid **3.9** (860 mg, 3.92 mmol) in anhydrous DMF (5 mL) at rt under an inert atmosphere. After cooling the mixture to 0°C, $Et_3N$ (656 µL, 4.71 mmol) was added. The reaction mixture was stirred for an additional 2h at 0°C and left to stir overnight at rt. DMF was removed *in vacuo* and Amberlite IR400 ($OH^-$ form) resin was added (5.00 g). The reaction mixture was filtered and lyophilized before purification by FCC (10% MeOH in DCM) afforded amide **3.10** (580 mg, 47%) as a white solid. $R_f$ = 0.27 (FCC conditions). $\delta_H$ (300 MHz; $CDCl_3$; 25°C) 0.85 (3H, t, *J* = 7.0 Hz, $-CH_3$), 0.92 (3H, s, $-CH_3$), 1.02 (3H, s, $-CH_3$), 1.25-1.34 (8H, m, $-(CH_2)_4-$), 1.46 (2H, t, *J* = 6.5 Hz, $-CH_2-$), 2.40 (2H, t, *J* = 6.0 Hz, $-CH_2-$), 3.19 (2H, q, *J* = 7.0 Hz, $-CH_2-$), 3.49 (2H, s, $-CH_2-$), 3.53-3.59 (2H, m, $-CH_2-$), 3.98 (1H, s, -CH-), 5.79 (1H, br s, -NH-) and 7.33 (1H, br t, *J* = 6.2 Hz, -NH-). OH protons not observed. $^1$H NMR data are consistent with those previously reported [1].

*N-Methyl-N-heptyl pantothenamide* (**3.11**)

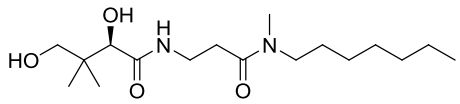

To a solution of thioester **3.20** (200 mg, 0.642 mmol) in $CH_3CN$ (7 mL) at rt was added *N*-methyl heptylamine (**3.17**) (130 µL, 0.771 mmol). The reaction mixture was stirred overnight at 35°C. The reaction mixture was concentrated *in vacuo* before purification by FCC (15% MeOH in DCM) afforded amide **3.11** (182 mg, 86%) as a yellow oil. $R_f$ = 0.28 (FCC conditions). $\delta_H$ (400 MHz; $CDCl_3$; 25°C) 0.85-0.89 (3H, m, $-CH_3$), 0.90 (3H, s, $-CH_3$), 1.00 (3H, s, $-CH_3$), 1.23-1.33 (8H, m, $-(CH_2)_4-$), 1.44-1.56 (2H, m, $-CH_2-$), 2.51 (2H, qin, *J* = 5.5, 9.4 Hz, $-CH_2-$), 2.90 (3H, d, *J* = 18.7 Hz, $-CH_3$), 3.20 (1H, t, *J* = 7.4, $-CH_2-$), 3.28-3.37 (1H, m, $-CH_2-$), 3.47 (2H, s, $-CH_2-$), 3.54 (2H, quin, *J* = 5.5 Hz, $-CH_2-$), 3.98 (1H, s, -CH-) and 7.47 (1H, br s, -NH-). OH protons not observed. $\delta_C$ (100 MHz; $CDCl_3$; 25°C) 14.2, 21.8, 21.8, 22.8, 27.0, 29.2, 29.3, 31.9, 32.7, 33.3, 39.6, 48.2, 50.2, 71.2, 77.2, 171.5 and 173.4. (HRMS) $[M+H]^+$ 331.2601 (Calculated $[C_{17}H_{35}N_2O_4]^+$ = 331.2597).

*(4R)-N-(3-(Heptylamino)-3-oxopropyl)-2-(4-methoxyphenyl)-5,5-dimethyl-1,3-dioxane-4-carboxamide* (**3.12**)

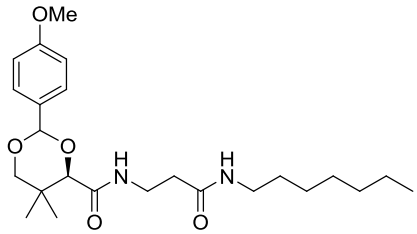

To an oven dried two-neck round bottomed flask containing 1,3-diol **3.10** (200 mg, 0.632 mmol) at rt under an inert atmosphere was added anhydrous THF (10 mL) and crushed molecular sieves (1.00 g). To the reaction mixture were added CSA (14.7 mg, 63.2 µmol) and *p*-methoxybenzaldehyde dimethyl acetal (215 µL, 1.26 mmol) and the reaction mixture was stirred overnight at rt. The reaction mixture was filtered and concentrated *in vacuo* before purification by FCC (5% MeOH in DCM) gave *p*-methoxybenzylidene **3.12** (230 mg, 76%) as a white solid. $R_f$ = 0.23 (FCC conditions). $\delta_H$ (400 MHz; $CDCl_3$; 25°C) 0.85 (3H, t, *J* = 6.6 Hz, $-CH_3$), 1.09 (6H, s, $-(CH_3)_2$), 1.24-1.33 (8H, m, $-(CH_2)_4-$), 1.41-1.52 (2H, m, $-CH_2-$), 2.38 (2H, t, *J* = 6.3 Hz, $-CH_2-$), 3.16-3.29 (2H, m, $-CH_2-$), 3.46-3.59 (2H, m, $-CH_2-$), 3.67 (2H, d, *J* = 7.3 Hz, $-CH_2-$), 3.82 (3H, s, $-CH_3$), 4.07 (1H, s, -CH-), 5.45 (1H, s, -CH-), 5.82 (1H, br s, -NH-), 6.89-6.94 (2H, m, arom), 7.01 (1H, br s, -NH-) and 7.28-7.44 (2H, m, arom). $\delta_C$ (100 MHz; $CDCl_3$; 25°C) 14.3, 19.3, 22.0, 22.8, 27.1, 29.1, 29.7, 32.0, 33.3, 35.3, 36.3, 39.8, 55.5, 78.6, 84.0, 101.5, 113.9, 128.1, 130.3, 159.9, 169.8 and 171.0. (HRMS) $[M+H]^+$ 435.2845 (Calculated $[C_{24}H_{39}N_2O_5]^+$ = 435.2859).

*Benzyl 3-(heptylamino)-3-oxopropylcarbamate* (**3.15**)

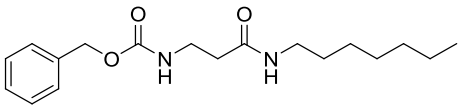

Heptylamine (**3.6**) (700 µL, 4.72 mmol) and DEPC (716 µL, 4.72 mmol) were added to a solution of Cbz-β-alanine (**3.14**) (1.00 g, 4.29 mmol) in anhydrous DMF (6 mL) at rt under an inert atmosphere. The reaction mixture was cooled to 0°C before $Et_3N$ (1.25 mL, 9.00 mmol) was added. The reaction mixture was stirred for 2h at 0°C and left to stir overnight at rt. EtOAc (50 mL) was added and the organic layer was washed with 5% aqueous citric acid (3 × 10 mL), 1 M aqueous $NaHCO_3$ (2 × 10 mL) and sat. aqueous NaCl (1 × 10 mL). The organic layer was dried ($Na_2SO_4$), filtered and concentrated *in vacuo* to afford carbamate **3.15** (1.28 g, 93%) as a white solid. $R_f$ = 0.21 (3:1 EtOAc: Hexanes). $\delta_H$ (400 MHz; $CDCl_3$; 25°C) 0.85 (3H, t, *J* = 6.7 Hz, $-CH_3$), 1.22-1.33 (8H, m, $-(CH_2)_4-$), 1.42-1.51 (2H, m, $-CH_2-$), 2.38 (2H, t, *J* = 5.9 Hz, $-CH_2-$), 3.19 (2H, q, *J* = 7.0, Hz, $-CH_2-$), 3.45 (2H, q, *J* = 6.2, Hz, $-CH_2-$), 5.09 (2H, s, $-CH_2-$), 5.43 (1H, br s, -NH-), 5.52 (1H, br s, -NH-) and 7.30-7.38 (5H, m, arom.). $\delta_C$ (100 MHz; $CDCl_3$; 25°C) 14.3, 22.8, 27.1, 29.2, 29.8, 31.9, 36.3, 37.4, 39.8, 66.8, 128.2, 128.3, 128.7, 136.8, 156.8 and 171.3. (HRMS) $[M+H]^+$ 321.2177 (Calculated $[C_{18}H_{29}N_2O_3]^+$ = 321.2178).

*S-Phenyl thiopantothenate* (**3.20**)

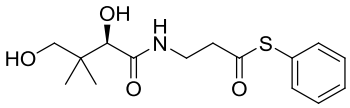

Calcium pantothenate (1.00 g, 4.15 mmol) was exchanged to the free acid by dissolving the salt in $H_2O$ (15 mL) and passing the solution through a column (1.50 cm diameter) of pre-washed Amberlite IR-120 ($H^+$-form) ion exchange resin (1.10 g). The free carboxylic acid was eluted with $H_2O$ (1 × 15 mL), followed by lyophilization of the collected column eluate to afford the free carboxylic acid **3.9** as a clear oil (860 mg, 3.92 mmol). Thiophenol (**3.19**) (443 µL, 4.31 mmol) and DEPC (654 µL, 4.31 mmol) were added to a solution of carboxylic acid **3.9** (860 mg, 3.92 mmol) in anhydrous DMF (5 mL) at rt under an inert atmosphere. The reaction mixture was cooled to 0°C before $Et_3N$ (1.15 mL, 8.23 mmol) was added. The reaction mixture was stirred for 2h at 0°C and left to stir overnight at rt. EtOAc (50 mL) was added and the organic layer was washed with 5% aqueous citric acid (3 × 10 mL), 1 M aqueous $NaHCO_3$ (2 × 10 mL) and sat. aqueous NaCl (1 × 10 mL). The organic layer was dried ($Na_2SO_4$), filtered and concentrated *in vacuo* before purification by FCC (2:1 to 4:1 EtOAc: Hexanes) afforded thioester **3.20** (0.650 g, 53%) as a yellow oil (which solidified upon standing). $R_f$ = 0.23 (3:1 EtOAc: Hexanes). $\delta_H$ (300 MHz; $CDCl_3$; 25°C) 3.92 (3H, s, $-CH_3$), 1.02 (3H, s, $-CH_3$), 2.91 (2H, t, *J* = 5.1 Hz, $-CH_2-$), 3.50 (2H, d, *J* = 5.0 Hz, $-CH_2-$), 3.59-3.66 (2H, m, $-CH_2-$), 4.01 (1H, s, -CH-), 7.12 (1H, br s, -NH-) and 7.39-9.45 (5H, m, arom). OH protons not observed. $^1$H NMR data are consistent with those previously reported [71-72].

*(R)-2,4-Dihydroxy-3,3-dimethylbutanamide* (**3.21**)

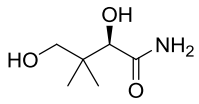

To an oven dried round bottomed flask containing (*R*)-(-)-pantolactone **3.3** (1.20 g, 9.22 mmol) was added anhydrous 30% $NH_3$ in MeOH (14 mL) at rt under an inert atmosphere. The reaction mixture was stirred overnight at rt. The reaction mixture was concentrated *in vacuo* to afford amide **3.21** (1.28 g, 94%) as a white solid which was subsequently used in the next step without any further purification. $\delta_H$ (300 MHz; DMSO-$d_6$; 25°C) 0.81 (3H, s, $-CH_3$), 0.83 (3H, s, $-CH_3$), 3.16 (1H, dd, *J* = 5.9, 10.6 Hz, $-CH_2-$), 3.28 (1H, dd, *J* = 5.6, 10.3 Hz, $-CH_2-$), 3.66 (1H ,d, *J* = 5.9 Hz, -CH-), 4.46 (1H, t, *J* = 5.6 Hz, -OH), 5.21 (1H, d, *J* = 5.3 Hz, -OH) and 7.12 (2H, s, $-NH_2$). $^1$H NMR data are consistent with those previously reported [73].

*(R)-2,2,5,5-Tetramethyl-1,3-dioxane-4-carboxamide* (**3.22**)

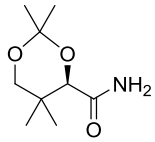

To an oven dried two-neck round bottomed flask containing 2,4-diol **3.21** (1.00 g, 6.79 mmol) was added anhydrous acetone (20 mL) and anhydrous DCM (20 mL) at rt under an inert atmosphere. The reaction mixture was cooled to 10°C before isopropenyl methyl ether (1.30 mL, 13.6 mmol) was added, followed by a solution of PTSA (129 mg, 0.679 mmol) in anhydrous acetone (5 mL) dropwise. The reaction mixture was stirred

overnight at rt and was subsequently neutralized by adding $Et_3N$ (500 µL). The resulting solution was dried ($Na_2SO_4$), filtered and concentrated *in vacuo* before purification by FCC (2:1 EtOAc: Hexanes) afforded acetonide **3.22** (1.00 g, 79%) as a white solid. $R_f$ = 0.36 (FCC conditions). $\delta_H$ (300 MHz; DMSO-$d_6$; 25°C) 0.91 (3H, s, -$CH_3$), 0.93 (3H, s, -$CH_3$), 1.36 (3H, s, -$CH_3$), 1.37 (3H, s, -$CH_3$), 3.16 (1H, d, *J* = 11.7 Hz, -$CH_2$-), 3.61 (1H, d, *J* = 11.7 Hz, -$CH_2$-), 3.97 (1H, s, -CH-), 6.82 (1H, br s, -$NH_2$) and 7.18 (1H, br s, -$NH_2$). $^1$H NMR data are consistent with those previously reported [73].

*(E)-β-Bromoacrylic acid* (**3.24**)

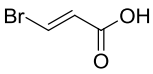


To a solution of 48% aqueous HBr (5.50 mL) was added propiolic acid (**3.23**) (880 µL, 14.3 mmol) dropwise at rt. The reaction mixture was stirred at reflux for 1.5h, where after it was cooled on an ice bath. The resulting precipitate was filtered and pure bromo acid **3.24** (425 mg, 20%) was obtained as a grey solid which was subsequently used in the next step without any further purification. $\delta_H$ (300 MHz; DMSO-$d_6$; 25°C) 6.54 (1H, d, *J* = 13.8 Hz, -CH-) and 7.71 (1H, d, *J* = 13.8 Hz, -CH-). O<u>H</u> proton not observed. $^1$H NMR data are consistent with those previously reported [42].

*(E)-3-Bromo-N-heptylacrylamide* (**3.25**)

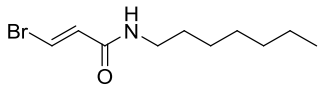


Heptylamine (**3.6**) (589 µL, 3.97 mmol) and DMAP (64.8 mg, 0.530 mmol) were added to a solution of bromo acid **3.24** (400 mg, 2.65 mmol) in anhydrous DCM (5 mL) at rt under an inert atmosphere. The reaction mixture was cooled to 0°C before DIC (451 µL, 2.91 mmol) was added dropwise. The reaction mixture was warmed to rt and left to stir overnight at rt. The reaction mixture was filtered through a pad of Celite and the solvent was removed *in vacuo*. The resulting crude residue was re-dissolved in EtOAc (30 mL) and the organic layer was washed with sat. aqueous $NaHCO_3$ (2 × 10 mL) and sat. aqueous NaCl (1 × 10 mL). The organic layer was dried ($Na_2SO_4$), filtered and concentrated *in vacuo* before purification by FCC (1:2 EtOAc: Hexanes) afforded amide **3.25** (300 mg, 46%) as a yellow solid. $R_f$ = 0.46 (FCC conditions). $\delta_H$ (400 MHz; $CDCl_3$; 25°C) 0.86 (3H, t, *J* = 6.7 Hz, -$CH_3$), 1.26-1.33 (8H, m, -$(CH_2)_4$-), 1.48-1.55 (2H, m, -$CH_2$-), 3.27 (2H, q, *J* = 5.9 Hz, -$CH_2$-), 5.44 (1H, br s, -NH-), 6.43 (1H, d, *J* = 13.5 Hz, -CH-) and 7.44 (1H, d, *J* = 13.5 Hz, -CH-). $\delta_C$ (100 MHz; $CDCl_3$; 25°C) 14.3, 22.8, 27.1, 29.1, 29.7, 31.9, 40.0, 122.5, 131.2 and 163.7. (HRMS) $[M+H]^+$ 248.0646 (Calculated $[C_{10}H_{19}Br^{79}NO]^+$ = 248.0650) and $[M+H]^+$ 250.0626 (Calculated $[C_{10}H_{19}Br^{81}NO]^+$ = 250.0650).

*(R)-N-(3-(Heptylamino)-3-oxoprop-1-enyl)-2,2,5,5-tetramethyl-1,3-dioxane-4-carboxamide* (**3.26**)

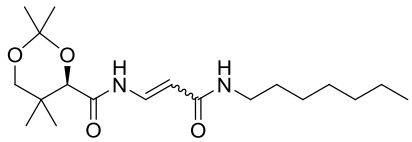

To an oven dried Schlenk tube were added palladium acetate ($Pd(OAc)_2$) (33.0 mg, 0.147 mmol), Xantphos (128 mg, 0.221 mmol), $K_2CO_3$ (406 mg, 2.94 mmol), CTAB (107 mg, 0.294 mmol), amide **3.22** (275 mg, 1.47 mmol), bromide **3.25** (400 mg, 1.61 mmol) and anhydrous toluene (3.70 mL) at rt under an inert atmosphere. The reaction mixture was degassed by three alternating nitrogen/vacuum cycles until no further gas evolution was observed. The reaction mixture was stirred for 1h at 50°C after which $H_2O$ (79.4 µL, 4.41 mmol) was added and the reaction mixture was stirred for an additional 4h at 55°C. The resulting reaction mixture was cooled to rt, diluted with EtOAc (50 mL) and the organic layer was washed with $H_2O$ (2 × 15 mL). The organic layer was dried ($Na_2SO_4$), filtered and concentrated *in vacuo* before purification by FCC (1:1 to 3:1 EtOAc: Hexanes) afforded (*E*)- and (*Z*)-amide **3.26** in a combined yield of 60% as a white-yellow solid and yellow oil respectively (*E*:*Z* ratio of 5:1).

(*E*)-amide **3.26**: $R_f$ = 0.28 (1:1 EtOAc: Hexanes). $\delta_H$ (300 MHz; $CDCl_3$; 25°C) 0.85 (3H, t, *J* = 6.7 Hz, $-CH_3$), 0.99 (3H, s, $-CH_3$), 1.05 (3H, s, $-CH_3$), 1.25-1.33 (8H, m, $-(CH_2)_4-$), 1.44 (2H, s, $-CH_2-$), 1.46 (3H, s, $-CH_3$), 1.50 (3H, s, $-CH_3$), 3.28 (2H, d, *J* = 12.9 Hz, $-CH_2-$), 3.30 (1H, d, *J* = 12.9 Hz, $-CH_2-$), 3.68 (1H, d, *J* = 11.7 Hz, $-CH_2-$), 4.17 (1H, s, -CH-), 5.37 (1H, br s, -NH-), 5.79 (1H, d, *J* = 13.8 Hz, -CH-), 7.71 (1H, dd, *J* = 10.7, 13.9 Hz, -CH-) and 8.23 (1H, br d, *J* = 10.0, -NH-). $\delta_C$ (75 MHz; $CDCl_3$; 25°C) 14.1, 18.7, 18.8, 22.6, 26.9, 26.9, 29.0, 29.7, 31.7, 32.9, 33.4, 39.6, 71.5, 99.1, 99.5, 106.4, 132.6, 166.1 and 168.1. (HRMS) $[M+H]^+$ 355.2599 (Calculated $[C_{19}H_{35}N_2O_4]^+$ = 355.2597).

(*Z*)-amide **3.26**: $R_f$ = 0.63 (1:1 EtOAc: Hexanes). $\delta_H$ (300 MHz; $CDCl_3$; 25°C) 0.86 (3H, t, *J* = 6.7 Hz, $-CH_3$), 1.05 (6H, s, $-(CH_3)_2$), 1.25-1.34 (8H, m, $-(CH_2)_4-$), 1.46 (3H, s, $-CH_3$), 1.49-1.54 (2H, m, $-CH_2-$), 1.61 (3H, s, $-CH_3$), 3.26-3.33 (2H, m, $-CH_2-$), 3.29 (1H, d, *J* = 11.7 Hz, $-CH_2-$), 3.69 (1H, d, *J* = 11.7 Hz, $-CH_2-$), 4.19 (1H, s, -CH-), 4.95 (1H, d, *J* = 8.8 Hz, -CH-), 5.32 (1H, br s, -NH-), 7.24 (1H, dd, *J* = 8.8, 11.2 Hz, -CH-) and 11.6 (1H, br d, *J* = 11.2, -NH-). $\delta_C$ (75 MHz; $CDCl_3$; 25°C) 14.3, 18.9, 19.3, 22.2, 22.8, 23.2, 27.1, 29.8, 29.9, 31.9, 33.5, 39.4, 71.6, 99.5, 100.8, 118.4, 133.4, 167.9 and 169.0. (HRMS) $[M+H]^+$ 355.2589 (Calculated $[C_{19}H_{35}N_2O_4]^+$ = 355.2597).

*(E)-N-Heptyl CJ-pantothenamide* (**(*E*)-3.27**)

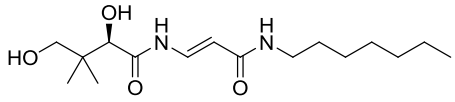

To a solution of acetonide (*E*)-**3.26** (200 mg, 0.564 mmol) in $CH_3CN$ (4.70 mL) at rt were added $H_2O$ (203 µL, 11.3 mmol) and $BiCl_3$ (35.6 mg, 0.113 mmol). The reaction mixture was

stirred overnight at rt. The reaction mixture was filtered through a pad of Celite and the solvent was removed *in vacuo*. The resulting crude residue was re-dissolved in EtOAc (20 mL) and the organic layer was washed with sat. aqueous $NaHCO_3$ (2 × 10 mL). The aqueous layer was extracted with EtOAc (1 × 10 mL) and the combined organic layers were dried ($Na_2SO_4$), filtered and concentrated *in vacuo* before purification by FCC (100% EtOAc) afforded hydroxyl (*E*)-**3.27** (53.1 mg, 30%) as a white solid. $R_f$ = 0.12 (FCC conditions). $\delta_H$ (400 MHz; DMSO-$d_6$; 25°C) 0.79 (3H, s, -$CH_3$), 0.82 (3H, s, -$CH_3$), 0.83 (3H, t, *J* = 7.0 Hz, -$CH_3$), 1.20-1.29 (8H, m, -$(CH_2)_4$-), 1.35-1.42 (2H, m, -$CH_2$-), 3.04 (2H, q, *J* = 6.2 Hz, -$CH_2$-), 3.13 (1H, dd, *J* = 5.1, 10.5 Hz, -$CH_2$-), 3.32 (1H, d, *J* = 5.5 Hz, -$CH_2$-), 3.84 (1H, d, *J* = 5.5 Hz, -CH-), 5.83 (1H, d, *J* = 14.1 Hz, -CH-), 7.55 (1H, dd, *J* = 10.9, 14.1 Hz, -CH-), 7.75 (1H, br t, *J* = 5.5 Hz, -NH-) and 10.1 (1H, br d, *J* = 10.9 Hz, -NH-). OH protons not observed. $\delta_C$ (100 MHz; DMSO-$d_6$; 25°C) 15.2, 21.1, 21.1, 23.3, 27.7, 29.6, 30.5, 32.5, 40.2, 46.8, 71.5, 76.1, 106.6, 134.0, 165.8 and 173.7. (HRMS) $[M+H]^+$ 315.2289 (Calculated $[C_{16}H_{31}N_2O_4]^+$ = 315.2284).

*(Z)-N-Heptyl CJ-pantothenamide* (**(*Z*)-3.27**)

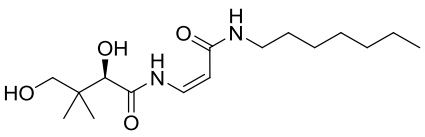

To a solution of acetonide (*Z*)-**3.26** (40.0 mg, 0.113 mmol) in $CH_3CN$ (1.00 mL) at rt were added $H_2O$ (40.7 µL, 2.26 mmol) and $BiCl_3$ (7.13 mg, 22.6 µmol). The reaction mixture was stirred overnight at rt. The reaction mixture was filtered through a pad of Celite and the solvent was removed *in vacuo*. The resulting crude residue was re-dissolved in EtOAc (10 mL) and the organic layer was washed with sat. aqueous $NaHCO_3$ (2 × 5 mL). The aqueous layer was extracted with EtOAc (1 × 10 mL) and the combined organic layers were dried ($Na_2SO_4$), filtered and concentrated *in vacuo* before purification by FCC (3:1 EtOAc: Hexanes) afforded hydroxyl (*Z*)-**3.27** (21.9 mg, 62%) as a yellow oil. $R_f$ = 0.35 (FCC conditions). $\delta_H$ (300 MHz; DMSO-$d_6$; 25°C) 0.79 (3H, s, -$CH_3$), 0.83 (3H, s, -$CH_3$), 0.84 (3H, apparent t, *J* = 7.3 Hz, -$CH_3$), 1.20-1.31 (8H, m, -$(CH_2)_4$-), 1.36-1.45 (2H, m, -$CH_2$-), 3.04-3.11 (2H, m, -$CH_2$-), 3.16 (1H, dd, *J* = 5.3, 10.6 Hz, -$CH_2$-), 3.34 (1H, d, *J* = 7.0 Hz, -$CH_2$-), 3.85 (1H, d, *J* = 4.7 Hz, -CH-), 5.13 (1H, d, *J* = 8.8 Hz, -CH-) 7.11 (1H, dd, *J* = 8.8, 11.2 Hz, -CH-), 7.97 (1H, t, *J* = 5.6 Hz, -NH-) and 11.8 (1H, br d, *J* = 11.2 Hz, -NH-). OH protons not observed. $\delta_C$ (75 MHz; DMSO-$d_6$; 25°C) 14.4, 20.4, 21.5, 22.5, 26.9, 29.5, 31.7, 38.6, 39.1, 40.7, 67.9, 75.0, 100.9, 132.6, 167.9 and 172.5. (HRMS) $[M+H]^+$ 315.2278 (Calculated $[C_{16}H_{31}N_2O_4]^+$ = 315.2284).

*S-Ethyl thiopantothenate* (**3.29**)

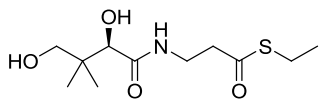

Calcium pantothenate (1.00 g, 4.15 mmol) was exchanged to the free acid by dissolving the salt in $H_2O$ (15 mL) and passing the solution through a column (1.50 cm diameter) of pre-washed Amberlite IR-120

($H^+$-form) ion exchange resin (1.10 g). The free carboxylic acid was eluted with $H_2O$ (1 × 15 mL), followed by lyophilization of the collected column eluate to afford the free carboxylic acid **3.9** as a clear oil (870 mg, 3.97 mmol). Ethanethiol (**3.28**) (324 µL, 4.37 mmol) and DEPC (633 µL, 4.37 mmol) were added to a solution of carboxylic acid **3.9** (870 mg, 3.97 mmol) in anhydrous DMF (8 mL) at rt under an inert atmosphere. The reaction mixture was cooled to 0°C before $Et_3N$ (1.16 mL, 8.33 mmol) was added. The reaction mixture was stirred for 2h at 0°C and left to stir overnight at rt. EtOAc (50 mL) was added and the organic layer was washed with 5% aqueous citric acid (3 × 10 mL), 1 M aqueous $NaHCO_3$ (2 × 10 mL) and sat. aqueous NaCl (1 × 10 mL). The organic layer was dried ($Na_2SO_4$), filtered and concentrated *in vacuo* before purification by FCC (3:1 to 4:1 EtOAc: Hexanes) afforded thioester **3.29** (0.620 g, 59%) as a yellow oil. $R_f$ = 0.19 (3:1 EtOAc: Hexanes). $\delta_H$ (300 MHz; $CDCl_3$; 25°C) 0.91 (3H, s, $-CH_3$), 1.01 (3H, s, $-CH_3$), 1.22 (3H, t, *J* = 7.3 Hz, $-CH_3$), 2.79 (2H, t, *J* = 6.0 Hz, $-CH_2-$), 2.85 (2H, q, *J* = 7.2 Hz, $-CH_2-$), 3.49 (2H, d, *J* = 3.5 Hz, $-CH_2-$), 3.54-3.63 (2H, m, $-CH_2-$), 4.01 (1H, s, -CH-) and 7.12 (1H, br s, -NH-). O<u>H</u> protons not observed. $^1$H NMR data are consistent with those previously reported [72].

*(R)-N-(3-Hydrazinyl-3-oxopropyl)-2,4-dihydroxy-3,3-dimethylbutanamide* (**3.30**)

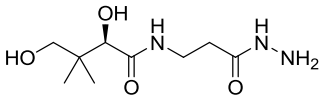

To a solution of thioester **3.29** (0.620 g, 2.35 mmol) in EtOH (24 mL) at rt was added 50-60% hydrazine hydrate (500 µL, 5.18 mmol). The reaction mixture was stirred at reflux overnight. The reaction mixture was cooled to rt and concentrated *in vacuo* to afford hydrazide **3.30** (510 mg, 93%) as a yellow oil which was subsequently used in the next step without any further purification. HRMS $[M+H]^+$ 234.1446 (Calculated $[C_9H_{20}N_3O_4]^+$ = 234.1454).

*(R,E)-N-(3-(2-Hexylidenehydrazinyl)-3-oxopropyl)-2,4-dihydroxy-3,3-dimethylbutanamide* (**3.32**)

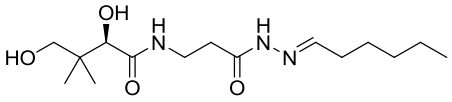

To a solution of hydrazide **3.30** (350 mg, 1.50 mmol) in anhydrous EtOH (15 mL) at rt under an inert atmosphere was added hexanal (**3.31**) (185 µL, 1.50 mmol). The reaction mixture was stirred at reflux for 48h. The reaction mixture was cooled to rt and concentrated *in vacuo* before purification by FCC (5% to 10% MeOH in DCM) afforded imine **3.32** (367 mg, 77%) as a yellow oil. $R_f$ = 0.24 (10% MeOH in DCM). $\delta_H$ (300 MHz; $CDCl_3$; 25°C) 0.91 (6H, s, $-(CH_3)_2$), 0.99 (3H, s, $-CH_3$), 1.25-1.39 (6H, m, $-(CH_2)_3-$), 1.44-1.57 (2H, m, $-CH_2-$), 2.83 (2H, t, *J* = 6.5 Hz, $-CH_2-$), 3.47 (2H, s, $-CH_2-$), 3.58-3.64 (2H, m, $-CH_2-$), 3.99 (1H, s, -CH-), 7.16 (1H, t, *J* = 5.3 Hz, -CH-), 7.34 (1H, br t, *J* = 6.0 Hz, -NH-) and 7.42 (1H, br t, *J* = 5.7 Hz, -NH-). O<u>H</u> protons not observed. $\delta_C$ (75 MHz; $CDCl_3$; 25°C) 13.9, 20.4, 21.5, 22.4, 25.9, 26.2, 31.4, 34.4, 39.3, 53.4, 70.9, 77.4, 148.8, 173.2 and 173.9. HRMS $[M+H]^+$ 316.2239 (Calculated $[C_{15}H_{30}N_3O_4]^+$ = 316.2236).

*N-Hexyl pantothenhydrazide* (**3.33**)

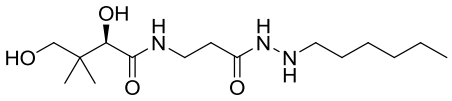

To a solution of imine **3.32** (145 mg, 0.460 mmol) in MeOH (3 mL) and DCM (2 mL) at rt was added $NaBH_3CN$ (34.7 mg, 0.552 mmol). The reaction mixture was acidified to pH 3 by the addition of 3 M aqueous HCl and the resulting solution was stirred at rt for 0.5h. Subsequently, the reaction mixture was acidified to pH 1 and the reaction mixture was stirred for an additional 5h at rt. The reaction was quenched by the addition of sat. aqueous $NaHCO_3$ (5 mL) and the resulting solution was filtered and concentrated *in vacuo*. The resulting crude residue was re-dissolved in EtOAc (40 mL) and the organic layer was washed with $H_2O$ (2 × 15 mL) and sat. aqueous NaCl (2 × 15 mL). The organic layer was dried ($Na_2SO_4$), filtered and concentrated *in vacuo* before purification by FCC (10:1:1:2 EtOAc: MeOH: $H_2O$: $CH_3CN$) afforded hydrazide **3.33** (39.4 mg, 27%) as a yellow oil. $R_f$ = 0.28 (FCC conditions). $\delta_H$ (300 MHz; $CDCl_3$; 25°C) 0.85 (3H, apparent t, *J* = 6.7 Hz, $-CH_3$), 0.91 (3H, s, $-CH_3$), 0.98 (3H, s, $-CH_3$), 1.27-1.35 (6H, m, $-(CH_2)_3-$), 1.41-1.52 (2H, m, $-CH_2-$), 2.39 (2H, t, *J* = 5.6 Hz, $-CH_2-$), 2.76 (2H, t, *J* = 7.3 Hz, $-CH_2-$), 3.47 (2H, s, $-CH_2-$), 3.51-3.63 (2H, m, $-CH_2-$), 3.98 (1H, s, -CH-), 7.42 (1H, br t, *J* = 6.0 Hz, -NH-) and 8.21 (1H, br s, -NH-). OH protons not observed. $\delta_C$ (75 MHz; $CDCl_3$; 25°C) 14.0, 20.6, 21.3, 22.6, 26.7, 27.8, 29.7, 31.7, 35.3, 39.3, 52.3, 70.6, 77.1, 170.4 and 174.1. HRMS $[M+H]^+$ 318.2385 (Calculated $[C_{15}H_{32}N_3O_4]^+$ = 318.2393).

*Benzyl 3-(heptylamino)-3-thioxopropylcarbamate* (**3.34**)

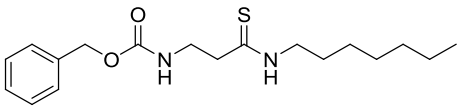

To a solution of amide **3.15** (400 mg, 1.25 mmol) in anhydrous toluene (20 mL) at rt under an inert atmosphere was added Lawesson's reagent (554 mg, 1.37 mmol). The reaction mixture was stirred at reflux overnight. The reaction mixture was cooled to rt, diluted with EtOAc (50 mL) and washed with 10% aqueous NaOH (3 × 15 mL) and sat. aqueous NaCl (1 × 20 mL). The organic layer was dried ($MgSO_4$), filtered and concentrated *in vacuo* before purification by FCC (1% to 2% MeOH in DCM) afforded thioamide **3.34** (282 mg, 67%) as a yellow solid. $R_f$ = 0.18 (2% MeOH in DCM). $\delta_H$ (300 MHz; $CDCl_3$; 25°C) 0.86 (3H, t, *J* = 6.6 Hz, $-CH_3$), 1.24-1.36 (8H, m, $-(CH_2)_4-$), 1.57 (2H, s, $-CH_2-$), 1.55-1.66 (2H, m, $-CH_2-$), 3.80 (2H, t, *J* = 6.0 Hz, $-CH_2-$), 3.57-3.65 (2H, m, $-CH_2-$), 5.09 (2H, s, $-CH_2-$), 5.34 (1H, br s, -NH-), 7.31-7.39 (5H, m, arom) and 7.43 (1H, br s, -NH-). $\delta_C$ (75 MHz; $CDCl_3$; 25°C) 14.0, 22.6, 26.9, 27.9, 28.9, 31.7, 41.0, 45.9, 46.2, 66.8, 128.0, 128.2, 128.5, 136.4, 156.6 and 201.6. HRMS $[M+H]^+$ 337.1945 (Calculated $[C_{18}H_{29}N_2O_2S]^+$ = 337.1950).

*3-Amino-N-heptylpropanethioamide hydrochloride salt* (**3.35**)

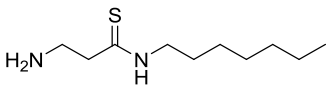

To a solution of carbamate **3.34** (280 mg, 0.832 mmol) in MeOH (6 mL) was added concentrated HCl (6 mL) and the resulting solution was stirred at reflux overnight. The reaction mixture was cooled to rt and quenched by the addition of $H_2O$ (20 mL). The aqueous solution was extracted with DCM (2 × 15 mL) after which the aqueous phase was lyophilized to yield the HCl salt of amine **3.35** (210 mg, >100%) as a white powder which was subsequently used in the next step without any further purification.

*N-Heptyl pantothenthioamide* (**3.36**)

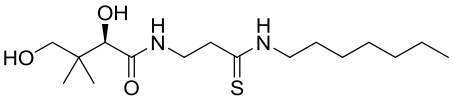

$Et_3N$ (361 µL, 2.59 mmol) and (*R*)-(-)-pantolactone **3.3** (338 mg, 2.59 mmol) were added to a solution of amine **3.35** (210 mg, 1.04 mmol) in EtOH (10 mL) and the resulting solution was stirred at reflux for 48h. The reaction mixture was cooled to rt and the solvent was removed *in vacuo*. The crude residue was purified by FCC (10% MeOH in DCM) to afford amide **3.36** (23.6 mg, 7%) as a yellow oil. $R_f$ = 0.32 (FCC conditions). $\delta_H$ (300 MHz; $CDCl_3$; 25°C) 0.86 (3H, apparent t, *J* = 7.0 Hz, -$CH_3$), 1.02 (3H, s, -$CH_3$), 1.04 (3H, s, -$CH_3$), 1.24-1.34 (8H, m, -$(CH_2)_4$-), 1.50 (2H, t, *J* = 7.0 Hz, -$CH_2$-), 2.54 (2H, t, *J* = 6.2 Hz, -$CH_2$-), 3.21-3.35 (2H, m, -$CH_2$-), 3.47-3.61 (4H, m, -$(CH_2)_2$-), 4.02 (1H, d, *J* = 4.1 Hz, -CH-), 6.70 (1H, br s, -NH-) and 7.17 (1H, br s, -NH-). O<u>H</u> protons not observed. $\delta_C$ (75 MHz; $CDCl_3$; 25°C) 14.3, 21.5, 21.8, 22.8, 27.1, 29.1, 29.8, 31.9, 39.6, 52.1, 61.1, 71.4, 76.6, 172.6 and 207.2. HRMS $[M-H]^-$ 331.2071 (Calculated $[C_{16}H_{31}N_2O_3S]^-$ = 331.2055).

*N-Carbobenzoxy taurine sodium salt* (**3.39**)

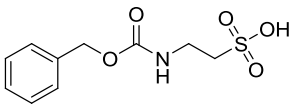

To a solution of taurine (**3.37**) (4.00 g, 32.0 mmol) in 1 M aqueous NaOH (32 mL) at rt was added a solution of Cbz chloride (**3.38**) (7.00 mL, 48.0 mmol) in dioxane (42 mL). To this was added another portion of 1 M aqueous NaOH (48 mL) and the reaction mixture was stirred for 1h at rt. The aqueous solution was extracted with EtOAc (2 × 125 mL) and the aqueous layer was concentrated *in vacuo*, followed by sequential co-evaporation with toluene (1 × 100 mL), EtOH (1 × 100 mL), and DCM (3 × 100 mL). The resulting crude product was lyophilized to yield taurine sodium salt **3.39** as a white powder. The crude product was subsequently used in the next step without any further purification.

*N-Carbobenzoxy tauryl fluoride* (**3.41**)

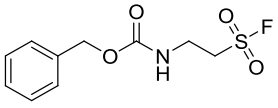

To a slurry of sulfonic acid **3.39** (500 mg, 1.78 mmol) in anhydrous DCM (20 mL) at 0°C under an inert atmosphere was added a solution of

(diethylamino)sulphur trifluoride (DAST, **3.40**) (585 µL, 4.45 mmol) in DCM (5 mL). The reaction mixture was stirred for 2h at 0°C and concentrated *in vacuo* before purification by FCC (1:1 to 3:1 DCM: Hexanes) afforded tauryl fluoride **3.41** (370 mg, 80%) as a yellow powder. $R_f$ = 0.78 (10% MeOH in DCM). $\delta_H$ (300 MHz; $CDCl_3$; 25°C) 3.62 (2H, q, *J* = 5.6 Hz, -$CH_2$-), 3.74 (2H, q, *J* = 5.9 Hz, -$CH_2$-), 5.13 (2H, s, -$CH_2$-), 5.31 (1H, br s, -NH-) and 7.33-7.38 (5H, m, arom.). $\delta_C$ (75 MHz; $CDCl_3$; 25°C) 35.7, 50.8, 67.4, 128.2, 128.4, 128.6, 135.8 and 156.1. $\delta_F$ (282 MHz; $CDCl_3$; 25°C) 56.8. HRMS $[M+H]^+$ 262.0538 (Calculated $[C_{10}H_{13}FNO_4S]^+$ = 262.0549).

*N-Carbobenzoxy N'-heptyltauramide* (**3.42**)

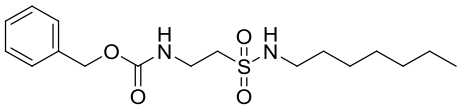

Heptylamine (**3.6**) (1.05 mL, 7.10 mmol) was added to a solution of tauryl fluoride **3.41** (370 mg, 1.42 mmol) in anhydrous DCM (5 mL) under an inert atmosphere, followed by stirring for 20h at 50°C. The reaction mixture was cooled to rt and quenched by the addition of 10% aqueous HCl (20 mL). The aqueous solution was extracted with DCM (2 × 15 mL) and the combined organic extracts were dried ($MgSO_4$), filtered and concentrated *in vacuo*. Purification by FCC (10% MeOH in DCM) yielded tauramide **3.42** (420 mg, 83%) as a yellow-orange powder. $R_f$ = 0.66 (FCC conditions). $\delta_H$ (300 MHz; $CDCl_3$; 25°C) 0.86 (3H, t, *J* = 6.7 Hz, -$CH_3$), 1.26-1.30 (8H, m, -$(CH_2)_4$-), 1.52-1.57 (2H, m, -$CH_2$-), 3.05 (2H, q, *J* = 6.7 Hz, -$CH_2$-), 3.18 (2H, t, *J* = 5.6 Hz, -$CH_2$-), 3.64-3.70 (2H, m, -$CH_2$-), 4.39 (1H, br s, -NH-), 5.11 (2H, s, -$CH_2$-), 5.41 (1H, br s, -NH-) and 7.31-7.37 (5H, m, arom.). $\delta_C$ (75 MHz; $CDCl_3$; 25°C) 14.1, 22.6, 26.5, 28.8, 30.3, 31.7, 36.1, 43.4, 52.1, 67.0, 128.1, 128.2, 128.6, 136.2 and 156.4. HRMS $[M+H]^+$ 357.1838 (Calculated $[C_{17}H_{29}N_2O_4S]^+$ = 357.1848).

*N-Heptyltauramide hydrochloride salt* (**3.43**)

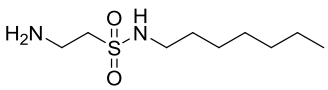

To a solution of carbamate **3.42** (420 mg, 1.81 mmol) in MeOH (8 mL) was added concentrated HCl (8 mL) and the resulting solution was stirred at reflux overnight. The reaction mixture was cooled to rt and quenched by the addition of $H_2O$ (20 mL). The aqueous solution was extracted with DCM (2 × 15 mL) after which the aqueous phase was lyophilized to yield the HCl salt of amine **3.43** (250 mg, 82%) as a white powder, which was subsequently used in the next step without any further purification. HRMS $[M+H]^+$ 223.1474 (Calculated $[C_9H_{23}N_2O_2S]^+$ = 223.1480).

*N-Heptyl pantoyltauramide* (**3.44**)

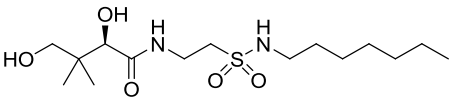

$Et_3N$ (337 µL, 2.42 mmol) and (*R*)-(-)-pantolactone **3.3** (315 mg, 2.42 mmol) were added to a solution of amine **3.43** (250

mg, 0.966 mmol) in EtOH (8 mL) and the resulting solution was stirred for 7h at reflux. The reaction mixture was cooled to rt and the solvent was removed *in vacuo*. The crude residue was purified by FCC (5% to 10% MeOH in DCM) before purification by SPE (Supelco 500 mg (3 mL) DSC-$NH_2$ column, conditioned the column with DCM, washed the sorbent with diethyl ether and eluted the product with $CH_3CN$) afforded amide **3.44** (59.8 mg, 18%) as a white oil. $R_f$ = 0.11 (10% MeOH in DCM). $\delta_H$ (400 MHz; $CDCl_3$; 25°C) 0.86 (3H, t, *J* = 7.0 Hz, -$CH_3$), 0.96 (3H, s, -$CH_3$), 1.03 (3H, s, -$CH_3$), 1.25-1.36 (8H, m, -$(CH_2)_4$-), 1.52-1.60 (2H, m, -$CH_2$-), 3.07 (2H, q, *J* = 6.7 Hz, -$CH_2$-), 3.19-3.24 (2H, m, -$CH_2$-), 3.52 (2H, s, -$CH_2$-), 3.72-3.80 (2H, m, -$CH_2$-), 4.03 (1H, s, -CH-), 4.93 (1H, br t, *J* = 5.9 Hz, -NH-) and 7.4 (1H, br s, -NH-). OH protons not observed. $\delta_C$ (100 MHz; $CDCl_3$; 25°C) 14.3, 20.9, 21.6, 22.8, 26.7, 29.0, 30.5, 31.9, 34.2, 39.5, 43.6, 51.7, 71.4, 78.4 and 173.8. HRMS $[M+H]^+$ 353.2102 (Calculated $[C_{15}H_{33}N_2O_5S]^+$ = 353.2110).

*3-Amino-N-heptylpropanamide* (**3.45**)

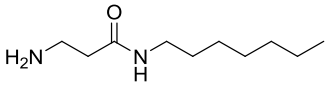

To a solution of carbamate **3.15** (1.46 g, 4.56 mmol) in MeOH (50 mL) at rt was added 10% Pd/C (194 mg, 1.82 mmol). The reaction atmosphere was filled with $H_2$ gas and the reaction mixture was stirred overnight at rt. The reaction mixture was filtered and concentrated *in vacuo* to give amine **3.45** (820 mg, 96%) as a white solid. $R_f$ = product on baseline (10% MeOH in DCM). $\delta_H$ (400 MHz; $CDCl_3$; 25°C) 0.85 (3H, t, *J* = 7.0 Hz, -$CH_3$), 1.25-1.32 (8H, m, -$(CH_2)_4$-), 1.44-1.53 (2H, m, -$CH_2$-), 1.96 (2H, br s, -$NH_2$), 2.30 (2H, t, *J* = 5.9 Hz, -$CH_2$-), 2.99 (2H, t, *J* = 5.9 Hz, -$CH_2$-), 3.19 (2H, q, *J* = 7.0 Hz, -$CH_2$-) and 6.95 (1H, br s, -NH-). $\delta_C$ (100 MHz; $CDCl_3$; 25°C) 14.2, 22.8, 27.1, 29.1, 29.7, 31.9, 38.0, 38.2, 39.6 and 172.3. HRMS $[M+H]^+$ 187.1807 (Calculated $[C_{10}H_{23}N_2O]^+$ = 187.1810).

*3,3-Dimethyl-2-oxo-butyric acid* (**3.46**)

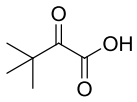

To a solution of NaOH (8.00 g, 200 mmol) and $KMnO_4$ (12.2 g, 77.2 mmol) in $H_2O$ (196 mL) at 0°C was added a solution of pinacolone (**3.47**) (10 mL, 83.4 mmol) in $H_2O$ (160 mL). The reaction mixture was stirred for 1h at 0°C and an additional 2h at rt. The reaction mixture was filtered through a pad of Celite, acidified to pH 2 with concentrated $H_2SO_4$, and the aqueous layer was extracted with diethyl ether (3 × 40 mL). The combined organic extracts were dried ($Na_2SO_4$), filtered and concentrated *in vacuo*. Bulb-to-bulb distillation (110°C, 27.5 mmHg) gave carboxylic acid **3.46** (3.99 g, 77%) as a clear oil. $\delta_H$ (300 MHz; $CDCl_3$; 25°C) 1.32 (9H, s, -$CH_3$). OH proton not observed. $^1$H NMR data are consistent with those previously reported [55].

*3,3-Dimethyl-2-oxo-N-(3-oxo-3-(heptylamino)propyl)butanamide* (**3.48**)

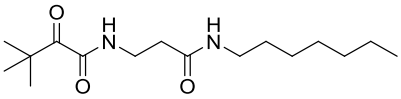

DIPEA (674 µL, 3.87 mmol) was added drop-wise over 5 min to a solution of heptylamine (**3.6**) (700 mg, 3.76 mmol) in DCM (30 mL) at 0°C under an inert atmosphere. HOBt (127 mg, 0.939 mmol), carboxylic acid **3.46** (537 mg, 4.13 mmol) and EDC hydrochloride (583 mg, 3.76 mmol) were then added consecutively and the reaction mixture was stirred overnight at rt. The reaction was quenched by the addition of 3 M aqueous HCl (25 mL) and the organic layer was washed with 3 M aqueous HCl (1 × 25 mL) and sat. aqueous $NaHCO_3$ (1 × 25 mL). The organic layer was dried ($Na_2SO_4$), filtered and concentrated *in vacuo* before purification by FCC (2:1 EtOAc: Hexanes) afforded amide **3.48** (251 mg, 22%) as a white powder. $R_f$ = 0.31 (FCC conditions). $\delta_H$ (600 MHz; $CDCl_3$; 25°C) 0.85 (3H, t, *J* = 6.7 Hz, $-CH_3$), 1.23-1.30 (8H, m, $-(CH_2)_4-$), 1.31 (9H, s, $-(CH_3)_3$), 1.43-1.52 (2H, m, $-CH_2-$), 2.40 (2H, t, *J* = 6.2 Hz, $-CH_2-$), 3.20 (2H, q, *J* = 7.0 Hz, $-CH_2-$), 3.53 (2H, q, *J* = 6.2 Hz, $-CH_2-$), 5.58 (1H, br s, -NH-) and 7.48 (1H, br s, -NH-). $\delta_C$ (150 MHz; $CDCl_3$; 25°C) 16.7, 25.2, 25.2, 28.9, 28.9, 29.5, 29.5, 31.5, 32.2, 34.3, 37.8, 38.0, 42.3, 163.0, 173.2 and 205.7. HRMS $[M+H]^+$ 299.2332 (Calculated $[C_{16}H_{31}N_2O_3]^+$ = 299.2335).

*(R/S)-4'-Deoxy N-heptyl-pantothenamide* (**3.49**)

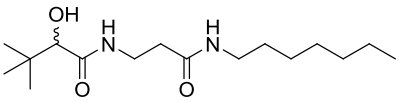

To a solution of ketoamide **3.48** (200 mg, 0.670 mmol) in anhydrous MeOH (30 mL) at 0°C under an inert atmosphere was added $NaBH_4$ (38.0 mg, 1.01 mmol) in small portions. The reaction mixture was stirred for 1h at 0°C, and left to stir overnight at rt. The reaction was quenched by the addition of sat. aqueous ammonium chloride ($NH_4Cl$) (10 mL) and the MeOH was removed *in vacuo*. The aqueous solution was extracted with EtOAc (3 × 20 mL) and the combined organic extracts were dried ($Na_2SO_4$), filtered and concentrated *in vacuo* to yield hydroxyl **3.49** (158 mg, 78%) as a white powder. $R_f$ = 0.51 (10% MeOH in DCM). $\delta_H$ (400 MHz; $CDCl_3$; 25°C) 0.85 (3H, t, *J* = 6.7 Hz, $-CH_3$), 0.97 (9H, s, $-(CH_3)_3$), 1.23-1.35 (8H, m, $-(CH_2)_4-$), 1.45-1.53 (2H, m, $-CH_2-$), 2.39 (2H, t, *J* = 6.0 Hz, $-CH_2-$), 3.19 (2H, q, *J* = 7.0 Hz, $-CH_2-$), 3.55 (2H, q, *J* = 6.5 Hz, $-CH_2-$), 3.65 (1H, s, -CH-), 5.70 (1H, br s, -NH-) and 6.87 (1H, br s, -NH-). O<u>H</u> proton not observed. $\delta_C$ (100 MHz; $CDCl_3$; 25°C) 14.3, 22.8, 26.1, 26.1, 26.1, 27.1, 29.1, 29.8, 31.9, 35.2, 35.5, 35.9, 39.9, 79.6, 171.4 and 173.0. HRMS $[M+H]^+$ 301.2497 (Calculated $[C_{16}H_{33}N_2O_3]^+$ = 301.2491).

*(R)-2,4-Bis(tert-butyldimethylsilyloxy)-N-(3-(heptylamino)-3-oxopropyl)-3,3-dimethylbutanamide* (**3.50**)

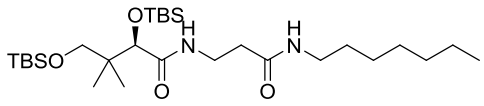

To a solution of 1,3-diol **3.10** (810 mg, 2.56 mmol) in anhydrous DMF (10 mL) at rt was added imidazole (1.04

g, 15.3 mmol) and TBS chloride (2.31 g, 15.3 mmol). The reaction mixture was stirred overnight at rt. The reaction was quenched by the addition of $H_2O$ (50 mL) and the aqueous layer was extracted with EtOAc (3 × 50 mL). The combined organic extracts were washed with sat. aqueous NaCl (2 × 15 mL) and the organic layer was dried ($Na_2SO_4$), filtered and concentrated *in vacuo* before purification by FCC (1:2 EtOAc: Hexanes) afforded **3.50** (1.16 g, 83%) as a yellow oil. $R_f$ = 0.38 (FCC conditions). $\delta_H$ (400 MHz; $CDCl_3$; 25°C) 0.01 (3H, s, $-CH_3$), 0.02 (3H, s, $-CH_3$), 0.04 (3H, s, $-CH_3$), 0.07 (3H, s, $-CH_3$), 0.84 (3H, s, $-CH_3$), 0.85-0.88 (3H, m, $-CH_3$), 0.89 (9H, s, $-(CH_3)_3$), 0.93 (9H, s, $-(CH_3)_3$), 1.23-1.33 (8H, m, $-(CH_2)_4-$), 1.43-1.52 (2H, m, $-CH_2-$), 2.38 (2H, t, *J* = 5.6 Hz, $-CH_2-$), 3.17-3.25 (2H, m, $-CH_2-$), 3.32 (1H, d, *J* = 9.4 Hz, $-CH_2-$), 3.39 (1H, d, *J* = 9.7 Hz, $-CH_2-$), 3.51 (2H, q, *J* = 6.2 Hz, $-CH_2-$), 4.00 (1H, s, -CH-), 5.79 (1H, br t, *J* = 5.0 Hz, -NH-) and 6.81 (1H, br t, *J* = 6.5 Hz, -NH-). $\delta_C$ (100 MHz; $CDCl_3$; 25°C) -9.98, -9.92, -9.80, -9.67, 13.8, 16.4, 16.5, 18.0, 21.2, 21.3, 21.4, 21.4, 21.5, 22.3, 24.4, 25.0, 27.2, 30.3, 30.4, 31.5, 35.1, 35.1, 35.6, 36.0, 64.3, 73.7, 166.1 and 168.4. HRMS $[M+H]^+$ 545.4164 (Calculated $[C_{28}H_{61}N_2O_4Si_2]^+$ = 545.4170).

*(R)-2-(Tert-butyldimethylsilyloxy)-N-(3-(heptylamino)-3-oxopropyl)-4-hydroxy-3,3-dimethylbutan-amide* (**3.51**)

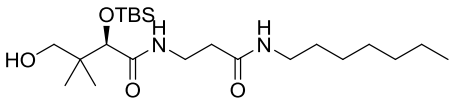


To a solution of **3.50** (1.05 g, 1.94 mmol) in anhydrous MeOH (20 mL) at 0°C under an inert atmosphere was added PPTS (510 mg, 2.03 mmol) in small portions. The reaction mixture was allowed to slowly warm up to rt and left to stir overnight at rt. The reaction mixture was concentrated *in vacuo* before purification by FCC (2:1 EtOAc: Hexanes) gave **3.51** (722 mg, 86%) as a yellow oil. $R_f$ = 0.35 (FCC conditions). $\delta_H$ (300 MHz; $CDCl_3$; 25°C) 0.01 (3H, s, $-CH_3$), 0.09 (3H, s, $-CH_3$), 0.78 (3H, s, $-CH_3$), 0.85 (3H, t, *J* = 7.0 Hz, $-CH_3$), 0.94 (9H, s, $-(CH_3)_3$), 1.00 (3H, s, $-CH_3$), 1.24-1.33 (8H, m, $-(CH_2)_4-$), 1.42-1.52 (2H, m, $-CH_2-$), 2.37-2.42 (2H, m, $-CH_2-$), 3.18-3.25 (2H, m, $-CH_2-$), 3.35-3.47 (2H, m, $-CH_2-$), 3.54-3.61 (2H, m, $-CH_2-$), 3.98 (1H, s, -CH-), 5.68 (1H, br s, -NH-) and 7.05 (1H, br t, *J* = 5.9 Hz, -NH-). O<u>H</u> proton not observed. $\delta_C$ (75 MHz; $CDCl_3$; 25°C) -5.25, -5.10, 14.1, 18.0, 18.8, 22.6, 23.7, 25.8, 25.8, 25.8, 26.9, 28.9, 29.6, 31.7, 34.9, 35.6, 39.7, 40.6, 70.3, 78.3, 170.5 and 174.0. HRMS $[M+H]^+$ 431.3301 (Calculated $[C_{22}H_{47}N_2O_4Si]^+$ = 431.3305).

*(R)-2-(Tert-butyldimethylsilyloxy)-N-(3-(heptylamino)-3-oxopropyl)-3,3-dimethyl-4-oxobutanamide* (**3.52**)

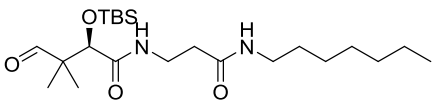


A solution of **3.51** (700 mg, 1.63 mmol) in anhydrous DCM (20 mL) was added dropwise to a solution of Dess-Martin periodinane (759 mg, 1.79 mmol) in anhydrous DCM (30 mL)

at rt under an inert atmosphere. The reaction mixture was stirred for 0.5h at rt before a 1:1 mixture of sat. aqueous sodium thiosulfate ($Na_2S_2O_3$) (30 mL) and sat. aqueous $NaHCO_3$ (30 mL) was added to the reaction mixture. The resulting mixture was extracted with DCM (5 × 20 mL). The combined organic extracts were washed with sat. $NaHCO_3$ (2 × 20 mL) and the organic layer was dried ($Na_2SO_4$), filtered and concentrated *in vacuo* before purification by FCC (1:1 to 2:1 EtOAc: Hexanes) afforded aldehyde **3.52** (670 mg, 96%) as a yellow oil. $R_f$ = 0.26 (FCC conditions). $\delta_H$ (400 MHz; $CDCl_3$; 25°C) 0.09 (3H, d, *J* = 5.0 Hz, -$CH_3$), 0.16 (3H, d, *J* = 1.5 Hz, -$CH_3$), 0.85 (3H, d, *J* = 6.6 Hz, -$CH_3$), 0.91 (9H, d, *J* = 1.2 Hz, -$(CH_3)_3$), 0.95 (3H, s, -$CH_3$), 1.08 (3H, s, -$CH_3$), 1.23-1.34 (8H, m, -$(CH_2)_4$-), 1.42-1.53 (2H, m, -$CH_2$-), 2.35-2.49 (1H, m, -$CH_2$-), 2.65-2.75 (1H, m, -$CH_2$-), 3.17-3.25 (2H, m, -$CH_2$-), 3.51-3.63 (2H, m, -$CH_2$-), 4.22 (1H, s, -CH-), 5.93 (1H, br s, -NH-), 7.03 (1H, br t, *J* = 5.9 Hz, -NH-) and 9.57 (1H, s, -CH-). $\delta_C$ (100 MHz; $CDCl_3$; 25°C) -4.10, -4.00, 14.3, 15.1, 18.5, 20.5, 22.8, 25.9, 26.0, 27.1, 29.1, 29.5, 29.5, 31.9, 40.0, 40.0, 43.3, 78.4, 87.7, 172.5, 173.5 and 175.1. HRMS $[M+H]^+$ 429.3168 (Calculated $[C_{22}H_{45}N_2O_4Si]^+$ = 429.3149).

*(R/S)-4'-Amino-N-heptyl pantothenamide* (**3.56**)

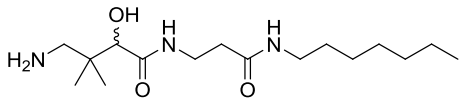

To a solution of carbamate **3.71** (150 mg, 0.334 mmol) (synthesis described on page 145) in MeOH (10 mL) at rt was added 10% Pd/C (14.3 mg, 0.134 mmol). The reaction atmosphere was filled with $H_2$ gas and the reaction mixture was stirred overnight at rt. The reaction mixture was filtered and concentrated *in vacuo* to give amine **3.56** (93.5 mg, 89%) as a white solid. $R_f$ = product on baseline (6:1 EtOAc: Hexanes). $\delta_H$ (600 MHz; $CDCl_3$; 25°C) 0.86 (3H, t, *J* = 7.0 Hz, -$CH_3$), 0.94 (3H, s, -$CH_3$), 1.03 (3H, s, -$CH_3$), 1.23-1.32 (10H, m, -$(CH_2)_4$- and -$NH_2$), 1.45-1.51 (2H, m, -$CH_2$-), 2.40 (2H, m, -$CH_2$-), 2.76-2.81 (2H, m, -$CH_2$-), 3.16-3.25 (2H, m, -$CH_2$-), 3.49-3.60 (2H, m, -$CH_2$-), 4.03 (1H, m, -CH-), 6.10 (1H, br s, -NH-) and 7.54 (1H, br s, -NH-). O<u>H</u> proton not observed. $\delta_C$ (150 MHz; $CDCl_3$; 25°C) 16.7, 22.2, 22.2, 25.2, 26.4, 29.5, 31.6, 32.1, 34.3, 37.7, 39.0, 42.3, 55.5, 83.3, 173.6 and 175.8. HRMS $[M+H]^+$ 316.2599 (Calculated $[C_{16}H_{34}N_3O_3]^+$ = 316.2600).

*Benzyl pantothenate* (**3.58**)

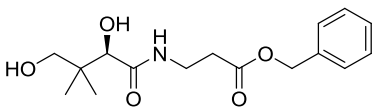

To a solution of sodium pantothenate (2.00 g, 8.30 mmol) in anhydrous DMF (30 mL) at rt under an inert atmosphere was added benzyl bromide (**3.57**) (988 µL, 8.30 mmol). The reaction mixture was stirred at 70°C overnight. The reaction mixture was cooled to rt and concentrated *in vacuo*. The resulting crude residue was re-dissolved in EtOAc (150 mL) and the organic layer was washed with sat. aqueous NaCl (3 × 40 mL). The organic layer was dried ($Na_2SO_4$), filtered and concentrated *in vacuo* before purification by FCC (2:1 to 4:1 EtOAc: Hexanes) afforded ester **3.58**

(1.89 g, 74%) as a yellow oil. $R_f$ = 0.26 (3:1 EtOAc: Hexanes). $\delta_H$ (300 MHz; $CDCl_3$; 25°C) 0.88 (3H, s, -$CH_3$), 1.00 (3H, s, -$CH_3$), 2.60 (2H, t, *J* = 6.0 Hz, -$CH_2$-), 3.45 (2H, t, *J* = 5.4 Hz, -$CH_2$-), 3.54-3.62 (2H, m, -$CH_2$-), 3.97 (1H, d, *J* = 5.0 Hz, -CH-), 5.14 (2H, s, -$CH_2$-), 7.12 (1H, br s, -NH-) and 7.33-7.40 (5H, m, arom). OH protons not observed. $^1$H NMR data are consistent with those previously reported [57].

*(R)-Benzyl 3-(2,4-bis(tert-butyldimethylsilyloxy)-3,3-dimethylbutanamido)propanoate* (**3.59**)

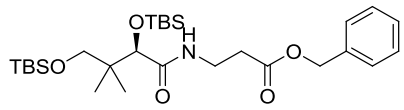


To a solution of 1,3-diol **3.58** (1.89 g, 6.11 mmol) in anhydrous DMF (30 mL) at rt was added imidazole (2.50 g, 36.7 mmol) and TBS chloride (5.53 g, 36.7 mmol). The reaction mixture was stirred overnight at rt. The reaction was quenched by the addition of $H_2O$ (60 mL) and the aqueous layer was extracted with EtOAc (3 × 70 mL). The combined organic extracts were washed with sat. aqueous NaCl (2 × 25 mL) and the organic layer was dried ($Na_2SO_4$), filtered and concentrated *in vacuo* before partial purification by FCC (1:3 EtOAc: Hexanes) afforded **3.59** (3.30 g, > 100%) as a yellow oil, which was subsequently used in the next step without any further purification. $R_f$ = 0.32 (FCC conditions).

*(R)-Benzyl 3-(2-(tert-butyldimethylsilyloxy)-4-hydroxy-3,3-dimethylbutanamido)propanoate* (**3.60**)

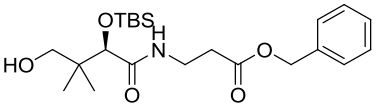


To a solution of **3.59** (2.60 g, 4.85 mmol) in anhydrous MeOH (50 mL) at 0°C under an inert atmosphere was added PPTS (1.28 g, 5.09 mmol) in small portions. The reaction mixture was allowed to slowly warm up to rt and left to stir overnight at rt. The reaction mixture was concentrated *in vacuo* before purification by FCC (1:1 EtOAc: Hexanes) afforded hydroxyl **3.60** (1.61 g, 78%) as a yellow oil. $R_f$ = 0.37 (FCC conditions). $\delta_H$ (300 MHz; $CDCl_3$; 25°C) 0.01 (3H, s, -$CH_3$), 0.09 (3H, s, -$CH_3$), 0.75 (3H, s, -$CH_3$), 0.94 (9H, s, -$CH_3$)$_3$), 0.99 (3H, s, -$CH_3$), 2.58 (2H, t, *J* = 4.4 Hz, -$CH_2$-), 3.33-3.42 (2H, m, -$CH_2$-), 3.55 (2H, q, *J* = 6.2 Hz, -$CH_2$-), 4.00 (1H, s, -CH-), 5.13 (2H, s, -$CH_2$-), 6.96 (1H, br s, -NH-) and 7.32-7.39 (5H, m, arom). OH proton not observed. $\delta_C$ (75 MHz; $CDCl_3$; 25°C) -5.32, -5.20, 19.0, 19.0, 23.2, 25.7, 25.7, 25.7, 34.0, 34.3, 40.4, 66.6, 69.8, 76.8, 126.8, 128.3, 128.4, 135.5, 171.9 and 173.5. HRMS $[M+H]^+$ 424.2509 (Calculated $[C_{22}H_{38}NO_5Si]^+$ = 424.2519).

*(R)-Benzyl 3-(2-(tert-butyldimethylsilyloxy)-3,3-dimethyl-4-oxobutanamido)propanoate* (**3.61**)

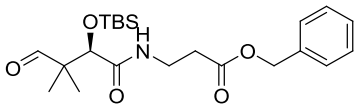


A solution of hydroxyl **3.60** (1.51 g, 3.57 mmol) in anhydrous DCM (40 mL) was added dropwise to a solution of Dess-Martin periodinane (1.66 g, 3.92 mmol) in anhydrous DCM (50 mL) at rt under an inert atmosphere. The reaction mixture was stirred for 0.5h at rt before a 1:1 mixture of

sat. aqueous $Na_2S_2O_3$ (70 mL) and sat. aqueous $NaHCO_3$ (70 mL) was added to the reaction mixture. The resulting mixture was extracted with DCM (5 × 30 mL). The combined organic extracts were washed with sat. aqueous $NaHCO_3$ (2 × 30 mL) and sat. aqueous NaCl (1 × 30 mL). The organic layer was dried ($Na_2SO_4$), filtered and concentrated *in vacuo* before purification by FCC (1:1 EtOAc: Hexanes) afforded aldehyde **3.62** (1.46 g, 97%) as a yellow to orange oil. $R_f$ = 0.63 (FCC conditions). $\delta_H$ (300 MHz; $CDCl_3$; 25°C) 0.01 (3H, s, -$CH_3$), 0.11 (3H, s, -$CH_3$), 0.94 (9H, s, -$(CH_3)_3$), 0.98 (3H, s, -$CH_3$), 1.04 (3H, s, -$CH_3$), 2.55 (2H, t, *J* = 5.9 Hz, -$CH_2$-), 3.52 (2H, q, *J* = 6.2 Hz, -$CH_2$-), 4.23 (1H, s, -CH-), 5.12 (2H, s, -$CH_2$-), 6.91 (1H, br s, -NH-), 7.32-7.39 (5H, m, arom) and 9.56 (1H, s, -CH-). $\delta_C$ (75 MHz; $CDCl_3$; 25°C) -5.27, -4.51, 16.0, 18.2, 25.6, 25.7, 25.7, 33.0, 36.3, 37.7, 42.6, 66.7, 89.3, 128.4, 128.5, 128.6, 135.5, 172.2, 173.3 and 174.4. HRMS $[M+H]^+$ 422.2342 (Calculated $[C_{22}H_{36}NO_5Si]^+$ = 422.2363).

*Potassium phthalimide* (**3.67**)

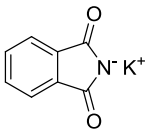

To a solution of phthalimide (4.41 g, 30.0 mmol) in anhydrous EtOH (20 mL) at rt under an inert atmosphere was added a solution of KOH (4.21 g, 75.0 mmol) in anhydrous MeOH (20 mL). The reaction mixture was stirred for 1h at rt. The reaction mixture was filtered and the filter cake was washed with EtOH (3 x 10 mL) to afford potassium phthalimide **3.67** (4.57 g, 82%) as a white solid, which was subsequently used in the next step without any further purification.

*4-(1,3-Dioxoisoindolin-2-yl)-2-hydroxy-3,3-dimethylbutanoic acid* (**3.68**)

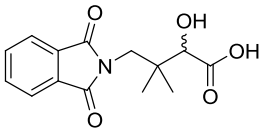

Potassium phthalimide (**3.67**) (5.00 g, 27.0 mmol) was added in small portions to (*R*)-(-)-pantolactone **3.3** (10.5 g, 81.0 mmol) heated to 140°C. The reaction mixture was stirred for an additional 0.5h at 250°C. The resulting homogeneous reaction mixture was cooled to rt, before purification by FCC (5:1:1:1 EtOAc: MeOH: $H_2O$: $CH_3CN$) afforded **3.68** (6.46 g, 86%) as a pale yellow solid. $R_f$ = 0.30 (FCC conditions). $\delta_H$ (300 MHz; $CDCl_3$; 25°C) 1.07 (3H, s, -$CH_3$), 1.22 (3H, s, -$CH_3$), 3.94 (1H, d, *J* = 9.9 Hz, -$CH_2$-), 4.02 (1H, d, *J* = 9.1 Hz, -$CH_2$-), 4.23 (1H, s, -CH-), 7.73-7.79 (2H, m, arom) and 7.81-7.91 (2H, m, arom). O<u>H</u> protons not observed. $^1$H NMR data are consistent with those previously reported [62].

*4-Amino-2-hydroxy-3,3-dimethylbutanoic acid* (**3.69**)

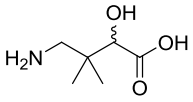

To a refluxing solution of **3.68** (6.00 g, 21.6 mmol) in EtOH (45 mL) was added 50-60% hydrazine hydrate (2.51 mL, 51.7 mmol). The reaction mixture was stirred at reflux for an additional 3h. The reaction mixture was cooled to rt and

70% aqueous acetic acid (60 mL) was added. The resulting solution was filtered through a pad of Celite to remove the precipitate and the filtrate was almost concentrated to dryness *in vacuo*. The crude residue was diluted with chloroform and the resulting precipitate upon standing was filtered and washed with chloroform (2 × 20 mL) to afford amine **3.69** (1.82 g, 57%) as a white powder. $\delta_H$ (300 MHz; $D_2O$; 25°C) 1.01 (3H, s, -$CH_3$), 1.08 (3H, s, -$CH_3$), 2.99 (2H, s, -$CH_2$-) and 3.85 (1H, s, -CH-). O<u>H</u> and N<u>H</u>$_2$ protons not observed. $^1$H NMR data are consistent with those previously reported [62].

*4-(Benzyloxycarbonylamino)-2-hydroxy-3,3-dimethylbutanoic acid* (**3.70**)

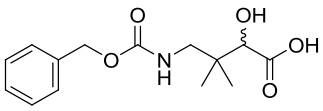

To a solution of amine **3.69** (900 mg, 6.12 mmol) and NaOH (500 mg, 12.5 mmol) in $H_2O$ (20 mL) at 0 to 5°C was added CbzCl (**3.38**) (961 µL, 6.73 mmol) dropwise over 1h. The reaction mixture was stirred for an additional 3h at 0 to 5°C. The aqueous layer was washed with diethyl ether (3 × 20 mL) and subsequently lyophilized to afford carbamate **3.70** (1.60 g, 93%) as a white solid. $\delta_H$ (300 MHz; $CDCl_3$; 25°C) 0.80 (6H, s, -$(CH_3)_2$), 2.66-3.32 (2H, m, -$CH_2$-), 3.65 (1H, s, -CH-), 4.96 (2H, s, -$CH_2$-) 5.63 (1H, br s, -NH-) and 7.15-7.42 (5H, m, arom). O<u>H</u> protons not observed. $^1$H NMR data are consistent with those previously reported [62].

*Benzyl 4-(3-(heptylamino)-3-oxopropylamino)-3-hydroxy-2,2-dimethyl-4-oxobutylcarbamate* (**3.71**)

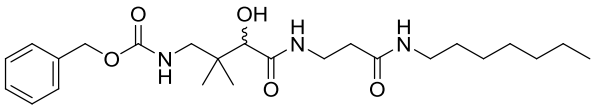

DIPEA (145 µL, 0.832 mmol) was added dropwise over 5 min to a solution of amine **3.45** (152 mg, 0.808 mmol) in DCM (12 mL) at 0°C under an inert atmosphere. HOBt (30.9 mg, 0.202 mmol), carboxylic acid **3.70** (250 mg, 0.889 mmol) and EDC hydrochloride (155 mg, 0.808 mmol) were then added consecutively and the reaction mixture was stirred overnight at rt. The reaction mixture was concentrated *in vacuo* before purification by FCC (6:1 EtOAc: Hexanes) afforded amide **3.71** (181 mg, 50%) as a yellow oil. $R_f$ = 0.21 (FCC conditions). $\delta_H$ (600 MHz; $CDCl_3$; 25°C) 0.86-0.89 (6H, m, -$(CH_3)_2$), 1.01 (3H, s, -$CH_3$), 1.21-1.31 (8H, m, -$(CH_2)_4$-), 1.43-1.48 (2H, m, -$CH_2$-), 2.38 (2H, t, *J* = 6.2 Hz, -$CH_2$-), 2.75 (1H, dd, *J* = 5.8, 8.8 Hz, -$CH_2$-), 3.18 (2H, q, *J* = 6.4 Hz, -$CH_2$-), 3.37-3.41 (1H, m, -$CH_2$-), 3.52 (2H, q, *J* = 5.9 Hz, -$CH_2$-), 3.78 (1H, s, -CH-), 5.06 (2H, m, -$CH_2$-), 5.40 (1H, br t, *J* = 6.4 Hz, -NH-), 5.99 (1H, br s, -NH-), 7.30-7.37 (5H, m, arom) and 7.45 (1H, br t, *J* = 5.6 Hz, -NH-). O<u>H</u> proton not observed. $\delta_C$ (150 MHz; $CDCl_3$; 25°C) 14.8, 16.7, 16.7, 23.1, 25.2, 29.5, 31.6, 32.1, 34.3, 37.9, 38.8, 42.0, 42.3, 69.8, 77.4, 130.7, 130.9, 131.2, 138.7, 160.7, 173.6 and 175.4. HRMS $[M+H]^+$ 450.2956 (Calculated $[C_{24}H_{40}N_3O_5]^+$ = 450.2968).

*N-Heptyl pantothenamide 4'-O,O-dibenzylphosphate* (**3.73**)

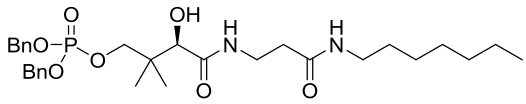

Dibenzyl chlorophosphate (**3.72**) was prepared *in situ* by reacting *N*-chloro-succinimide (304 mg, 2.28 mmol) and dibenzylphosphite (598 mg, 2.28 mmol) in anhydrous toluene (4 mL) under an inert atmosphere for 2h at rt. The reaction mixture was filtered to remove the succinimide. To a solution of hydroxyl **3.10** (240 mg, 0.758 mmol) in anhydrous pyridine (4.50 mL) at -40°C under an inert atmosphere was added dibenzyl chlorophosphate (**3.72**) drop-wise with stirring. The reaction mixture was stirred for an additional 2h at -40°C and the mixture was placed in the -20°C freezer overnight. The reaction mixture was allowed to warm to rt and was subsequently quenched with $H_2O$ (3 mL) and concentrated *in vacuo*. The resulting crude residue was re-dissolved in EtOAc (30 mL) and the organic layer was washed with 1 M aqueous $H_2SO_4$ (2 × 10 mL), 1 M aqueous $NaHCO_3$ (2 × 10 mL) and sat. aqueous $Na_2SO_4$ (1 × 10 mL). The organic layer was dried ($Na_2SO_4$), filtered and concentrated *in vacuo* before purification by FCC (10% MeOH in DCM) afforded **3.73** (150 mg, 34%) as a yellow solid. $R_f$ = 0.13 (FCC conditions). $\delta_H$ (400 MHz; $CDCl_3$; 25°C) 0.81 (3H, s, -$CH_3$), 0.85 (3H, t, *J* = 7.0 Hz, -$CH_3$), 1.05 (3H, s, -$CH_3$), 1.22-1.31 (8H, m, -$(CH_2)_4$-), 1.43-1.50 (2H, m, -$CH_2$-), 2.38 (2H, t, *J* = 5.8 Hz, -$CH_2$-), 3.17 (2H, q, *J* = 7.0 Hz, -$CH_2$-), 3.52-3.60 (3H, m, -$(CH_2)_2$-), 3.87 (1H, s, -CH-), 3.98-4.04 (1H, m, -$CH_2$-), 5.03 (2H, d, *J* = 8.6 Hz, -$CH_2$-), 5.04 (2H, d, *J* = 8.6 Hz, -$CH_2$-), 6.14 (1H, br s, -NH-), 7.27 (1H, br t, *J* = 7.8 Hz, -NH-) and 7.31-7.39 (10H, m, arom). O<u>H</u> proton not observed. $\delta_C$ (100 MHz; $CDCl_3$; 25°C) 14.3, 18.9, 21.4, 22.8, 27.1, 29.2, 29.7, 31.9, 35.6, 36.3, 39.7, 39.9, 69.9, 69.9, 70.0, 73.8, 128.2, 128.9, 135.7, 135.8, 171.2 and 172.6. $\delta_P$ (161 MHz; $CDCl_3$; 25°C) 0.87. HRMS $[M+H]^+$ 577.3055 (Calculated $[C_{30}H_{46}N_2O_7P]^+$ = 577.3043).

*4'-Phospho-N-heptyl pantothenamide* (**3.74**)

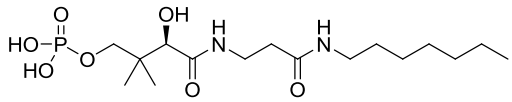

To a solution of **3.73** (130 mg, 0.225 mmol) in MeOH (9 mL) and $H_2O$ (1 mL) at rt was added 10% Pd/C (34.3 mg, 0.322 mmol). The reaction atmosphere was filled with $H_2$ gas and the reaction mixture was stirred overnight at rt. The reaction mixture was filtered and concentrated *in vacuo* to give **3.74** (87.5 mg, 98%) as a clear oil. $R_f$ = 0.07 (10% MeOH in DCM). $\delta_H$ (300 MHz; $D_2O$; 25°C) 0.78 (3H, t, *J* = 6.2 Hz, -$CH_3$), 0.85 (3H, s, -$CH_3$), 0.93 (3H, s, -$CH_3$), 1.14-1.30 (8H, m, -$(CH_2)_4$-), 1.37-1.48 (2H, m, -$CH_2$-), 2.43 (2H, t, *J* = 5.9 Hz, -$CH_2$-), 3.08 (2H, t, *J* = 6.5 Hz, -$CH_2$-), 3.38-3.54 (2H, m, -$CH_2$-), 3.61 (1H, m, -$CH_2$-), 3.82 (1H, m, -$CH_2$-) and 3.98 (1H, s, -CH-). O<u>H</u> protons not observed. $\delta_C$ (150 MHz; $D_2O$; 25°C) 14.3, 19.4, 21.3, 22.9, 27.2, 29.2, 29.3, 32.1, 36.0, 39.0, 39.1, 40.2, 72.5, 74.8, 173.8 and 175.3. $\delta_P$ (161 MHz; $CDCl_3$; 25°C) 0.63. HRMS $[M+H]^+$ 397.2102 (Calculated $[C_{16}H_{34}N_2O_7P]^+$ = 397.2104).

## 3.8.3 Characterization of the N7-Pan analogues

### 3.8.3.1 Bacterial growth inhibition studies of the N7-Pan analogues in minimal media

The $MIC_{80}$s of the N7-Pan analogues against *S. aureus* RN4220 were determined by microbroth dilution in 96-well microtiter flat-bottomed plates and turbidimetric analysis at $OD_{600}$. The *S. aureus* RN4220 strain was a kind gift from Prof L.M.T. Dicks at the Department of Microbiology, Stellenbosch University. The inhibition of *S. aureus* RN4220 by the N7-Pan analogues were tested in minimal media appropriate for *S. aureus* which contained 40.24 mM KCl, 162.6 mM NaCl, 5.274 mM $MgSO_4 \cdot 7H_2O$, 30.27 mM $(NH_4)_2SO_4$, 0.1129 mM $CaCl_2$, 1.029 mM $KH_2PO_4$, 0.02158 mM $FeSO_4 \cdot 7H_2O$, 0.04483 mM $MnSO_4 \cdot 4H_2O$, 0.03123 mM citric acid, 99.88 mM Tris-HCl, 27.75 mM glucose, 0.8003 mM L-arginine, 1.015 mM L-proline, 1.936 mM L-glutamic acid, 1.513 mM L-valine,1.484 mM L-threonine, 1.019 mM L-phenylalanine, 1.326 mM L-leucine, 0.7757 mM L-cysteine, 0.4093 µM biotin, 6.649 µM thiamin and 16.25 µM nicotinic acid [65]. The inhibition was determined by concentration-response analysis. Starter cultures of *S. aureus* RN4220 in 1% tryptone were inoculated with four separate colonies grown on Luria Bertani (LB) agar plates. The starter culture was grown to mid-log phase and then diluted 10-fold into the minimal media. A 10 µl aliquot of the diluted cell suspension was used to inoculate each well of the 96-well flat-bottomed plate containing 100 µl of minimal medium supplemented with the specific N7-Pan analogue of interest. The final concentrations of the N7-Pan analogues varied in the range 0.0977–200 µM depending on the potency of the N7-Pan analogue. The plates were incubated at 37°C for 24h before the cell densities were measured ($OD_{600}$). The extent of growth in each well was determined by normalizing the $OD_{600}$ values relative to those of the negative control (containing no N7-Pan analogue), which was taken as 100% bacterial cell growth. Each compound was tested in either two or three independent experiments, each performed triplicate.

### 3.8.3.2 Bacterial growth inhibition studies of the N7-Pan analogues in tryptone broth

The $MIC_{80}$s of the N7-Pan analogues against *S. aureus* RN4220 were determined by microbroth dilution in 96-well microtiter flat-bottomed plates and turbidimetric analysis at $OD_{600}$. Starter cultures of *S. aureus* RN4220 in 1% tryptone broth were inoculated with four separate colonies grown on LB agar plates. The starter culture was grown to mid-log phase and then diluted 10 000-fold into the same medium. A 10 µl aliquot of the diluted cell suspension was used to inoculate each well of the 96-well flat-bottomed plate containing 100 µl of 1% tryptone broth supplemented with the specific N7-Pan analogue of interest. The final concentrations of the N7-Pan analogues varied in the range 1.56–200 µM depending on the potency of the N7-Pan analogue. The plates were incubated at 37°C for 20h before the cell densities were measured ($OD_{600}$). The extent of growth in each well was determined by normalizing the $OD_{600}$ values relative to those of the

negative control (containing no N7-Pan analogue), which was taken as 100% bacterial cell growth. Each compound was tested in either two or three independent experiments, each performed triplicate.

#### 3.8.3.3 Construction of *Sa*PanK-II, protein expression and purification

The pET28a-*Sa coaA* construct containing the gene sequence of *Sa*PanK-II was available in our laboratory. Protein was produced in LB media (500 mL), supplemented with 30 mg/L kanamycin, and inoculated with plasmid containing *E. coli* BL21*(DE3) starter culture. The culture was grown until mid-log phase was reached and induced with a final concentration of 0.5 mM IPTG and grown further at 37°C overnight. The $His_6$-tagged protein was loaded to a 1.0 mL Amersham Biosciences HiTrap™ Chelating HP column (GE Healthcare) preloaded with $Ni^{2+}$ with binding buffer (20 mM Tris-HCl, pH 7.9, 500 mM NaCl, 50 mM imidazole, 0.05% $NaN_3$). After a wash step (85% binding buffer, 15% elution buffer) to remove any non-specifically bound proteins from the column, the target protein was eluted by stepwise increasing the concentration of imidazole in the elution buffer (20 mM Tris-HCl, pH 7.9, 500 mM NaCl, 500 mM imidazole, 0.05% $NaN_3$). The fractions containing the most protein was pooled and buffer exchanged using the HiTrap™ Desalting column (GE Healthcare) into buffer exchange buffer (25 mM Tris-HCl, pH 8.0, 5.0 mM magnesium chloride ($MgCl_2$), 5.0% glycerol). The protein concentrations were determined using Bradford in comparison to bovine serum albumin (BSA) standards from Biorad.

#### 3.8.3.4 PanK steady state kinetic analysis

Pantothenate kinase activity was determined using a continuous spectrophotometric assay that coupled the production of ADP to the consumption of NADH, monitored by the decrease in absorbance at 340 nm, as described previously [74]. An extinction coefficient of 6220 $M^{-1}.cm^{-1}$ was used for NADH.

Each 300 µL reaction mixture contained 50 mM Tris-HCl (pH 7.6), 10 mM $MgCl_2$, 20 mM potassium chloride (KCl), 1.5 mM ATP, 0.5 mM NADH, 0.5 mM PEP, 3 units PK, 3 units LDH and 1.5 µg *Sa*PanK-II. The concentration ranges are indicated in the legends and axis labels of the figures described the results of the respective experiments. The reaction was initiated by the addition of substrate (or mixtures of substrates and inhibitors) and was monitored for 5 min at 25°C. PK and LDH used in kinetic assays were from Roche (Basel, Switzerland).

#### 3.8.3.5 Data and statistical analysis

Using the raw kinetic data initial velocities were calculated for each substrate concentration (or substrate mixture, or substrate/inhibitor mixture) by linear regression of the readings made in the

50 second period after the initial 10 seconds (i.e. the period from 10 to 60 seconds after the reaction was started). For each experiment the three readings made for each data point was averaged and plotted with the standard deviation to give the respective kinetic profile. Kinetic parameters reported in Table 3.2 were determined for each experiment by fitting the appropriate equation to the data; the reported values are the average values of the parameters determined from all the individual independent experiments, and are given with errors that indicate the range/2 or SEM as appropriate.

## 3.9 References

1. Virga, K. G., Zhang, Y. M., Leonardi, R., Ivey, R. A., Hevener, K., Park, H. W., Jackowski, S., Rock, C. O. and Lee, R. E., Structure-activity relationships and enzyme inhibition of pantothenamide-type pantothenate kinase inhibitors. *Bioorganic & Medicinal Chemistry*, 2006**. 14** (4), 1007-1020.
2. Otto, M., Basis of virulence in community-associated methicillin-resistant *Staphylococcus aureus*. *Annual Review of Microbiology*, 2010**. 64**, 143-162.
3. Spellberg, B., Blaser, M., Guidos, R. J., Boucher, H. W., Bradley, J. S., Eisenstein, B. I., Gerding, D., Lynfield, R., Reller, L. B., Rex, J., Schwartz, D., Septimus, E., Tenover, F. C. and Gilbert, D. N., Combating antimicrobial resistance: Policy recommendations to save lives. *Clinical Infectious Diseases* 2011**. 52 Suppl 5**, S397-428.
4. Guillemot, D., Antibiotic use in humans and bacterial resistance. *Microbiology*, 1999**. 2** (5), 494-498.
5. Jeljaszewicz, J., Mlynarczyk, G. and Mlynarczyk, A., Antibiotic resistance in Gram-positive cocci. *International Journal of Antimicrobial Agents*, 2000**. 16** (4), 473-478.
6. Spry, C., Kirk, K. and Saliba, K. J., Coenzyme A biosynthesis: An antimicrobial drug target. *FEMS Microbiology Reviews*, 2008**. 32** (1), 56-106.
7. Leonardi, R., Chohnan, S., Zhang, Y. M., Virga, K. G., Lee, R. E., Rock, C. O. and Jackowski, S., A pantothenate kinase from *Staphylococcus aureus* refractory to feedback regulation by coenzyme A. *Journal of Biological Chemistry*, 2005**. 280** (5), 3314-3322.
8. Choudhry, A. E., Mandichak, T. L., Broskey, J. P., Egolf, R. W., Kinsland, C., Begley, T. P., Seefeld, M. A., Ku, T. W., Brown, J. R., Zalacain, M. and Ratnam, K., Inhibitors of pantothenate kinase: Novel antibiotics for staphylococcal Infections. *Antimicrobial Agents & Chemotherapy*, 2003**. 47** (6), 2051-2055.
9. Hong, B. S., Yun, M. K., Zhang, Y. M., Chohnan, S., Rock, C. O., White, S. W., Jackowski, S., Park, H. W. and Leonardi, R., Prokaryotic type II and type III pantothenate kinases: The same monomer fold creates dimers with distinct catalytic properties. *Structure*, 2006**. 14** (8), 1251-1261.
10. Thomas, J. and Cronan, J. E., Antibacterial activity of *N*-pentylpantothenamide is due to inhibition of coenzyme A synthesis. *Antimicrobial Agents & Chemotherapy*, 2010**. 54** (3), 1374-1377.
11. Jackowski, S. and Rock, C. O., Turnover of the 4'-phosphopantetheine prosthetic group of acyl carrier protein. *Journal of Biological Chemistry* 1984**. 259** (3), 1891-1895.
12. de Villiers, M., Barnard, L., Koekemoer, L., Snoep, J. L. and Strauss, E., Variation in pantothenate kinase type determines the pantothenamide mode of action and impacts on coenzyme A salvage biosynthesis. *FEBS Journal*, 2014**. 281** (20), 4731-4753.

13. Zeeuwen, P. L. J. M., Jansen, P. A. M., Schalkwijk, J., Rutjes, F. P. J. T., Ritzen, B. and Hermkens, P. H. H. Pantothenic acid derivatives and their use in the treatment of microbial infections (OCR). WO 2011/152720 A1, 8 December 2011.
14. Van Diepen, J. A., Jansen, P. A., Ballak, D. B., Hijmans, A., Hooiveld, G. J., Rommelaere, S., Galland, F., Naquet, P., Rutjes, F. P., Mensink, R. P., Schrauwen, P., Tack, C. J., Netea, M. G., Kersten, S., Schalkwijk, J. and Stienstra, R., PPAR-alpha dependent regulation of Vanin-1 mediates hepatic lipid metabolism. *Journal of Hepatology*, 2014**. 61** (2), 366-372.
15. Pitari, G., Malergue, F., Martin, F., Philippe, J. M., Massucci, M. T., Chabret, C., Maras, B., Dupre, S., Naquet, P. and Galland, F., Pantetheinase activity of membrane-bound Vanin-1: Lack of free cysteamine in tissues of Vanin-1 deficient mice. *FEBS Letters*, 2000**. 483** (2-3), 149-154.
16. Maras, B., Barra, D., Dupre, S. and Pitari, G., Is pantetheinase the actual identity of mouse and human Vanin-1 proteins? *FEBS Letters*, 1999**. 461** (3), 149-152.
17. Kaskow, B. J., Proffitt, J. M., Blangero, J., Moses, E. K. and Abraham, L. J., Diverse biological activities of the vascular non-inflammatory molecules - The Vanin pantetheinases. *Biochemical & Biophysical Research Communications*, 2012**. 417** (2), 653-658.
18. Min-Oo, G., Ayi, K., Bongfen, S. E., Tam, M., Radovanovic, I., Gauthier, S., Santiago, H., Rothfuchs, A. G., Roffe, E., Sher, A., Mullick, A., Fortin, A., Stevenson, M. M., Kain, K. C. and Gros, P., Cysteamine, the natural metabolite of pantetheinase, shows specific activity against *Plasmodium*. *Experimental Parasitology*, 2010**. 125** (4), 315-324.
19. Wittwer, C. T., Burkhard, D., Ririe, K., Rasmussen, R., Brown, J., Wyse, B. W. and Hansen, R. G., Purification and properties of a pantetheine-hydrolyzing enzyme from pig kidney. *Journal of Biological Chemistry*, 1983**. 253** (16), 9733-9738.
20. de Villiers, M., Macuamule, C., Spry, C., Hyun, Y. M., Strauss, E. and Saliba, K. J., Structural modification of pantothenamides counteracts degradation by pantetheinase and improves antiplasmodial activity. *ACS Medicinal Chemistry Letters*, 2013**. 4** (8), 784-789.
21. Haj-Yahya, M., Eltarteer, N., Ohayon, S., Shema, E., Kotler, E., Oren, M. and Brik, A., *N*-methylation of isopeptide bond as a strategy to resist deubiquitinases. *Angewandte Chemie, International Edition*, 2012**. 51** (46), 11535-11539.
22. Kumar, D., Judge, V., Narang, R., Sangwan, S., De Clercq, E., Balzarini, J. and Narasimhan, B., Benzylidene/2-chlorobenzylidene hydrazides: Synthesis, antimicrobial activity, QSAR studies and antiviral evaluation. *European Journal of Medicinal Chemistry*, 2010**. 45** (7), 2806-2816.
23. Kloss, F., Lincke, T. and Hertweck, C., Highly efficient total synthesis of the clostridium-derived anti-MRSA antibiotic closthioamide. *European Journal of Organic Chemistry*, 2011**.** (8), 1429-1431.

24. Banala, S. and Sussmuth, R. D., Thioamides in nature: In search of secondary metabolites in anaerobic microorganisms. *ChemBioChem*, 2010**. 11** (10), 1335-1337.
25. De Luca, L. and Giacomelli, G., An easy microwave-assisted synthesis of sulfonamides directly from sulfonic acids. *Journal of Biological Chemistry*, 2008**. 73** (10), 3967-3969.
26. Bahrami, K., Khodaei, M. M. and Soheilizad, M., Direct conversion of thiols and disulfides into sulfonamides. *Tetrahedron Letters*, 2010**. 51** (37), 4843-4846.
27. Chantarasriwong, O., Jang, D. O. and Chavasiri, W., A practical and efficient method for the preparation of sulfonamides utilizing $Cl_3CCN/PPh_3$. *Tetrahedron Letters*, 2006**. 47** (42), 7489-7492.
28. O'Shea, R. and Moser, H. E., Physicochemical properties of antibacterial compounds - Implications for drug discovery. *Journal of Medicinal Chemistry*, 2008**. 51** (10), 2871-2878.
29. Lipinski, C. A., Lombardo, F., Dominy, B. W. and Feeney, P. J., Experimental and computational approaches to estimate solubility and permeability in drug discovery and development settings. *Advanced Drug Delivery Reviews*, 1997**. 23** (1-3), 3-25.
30. Doak, B. C., Over, B., Giordanetto, F. and Kihlberg, J., Oral druggable space beyond the rule of 5: Insights from drugs and clinical candidates. *Chemistry & Biology*, 2014**. 21** (9), 1115-1142.
31. Dearden, J. C., Partitioning and lipophilicity in quantitative structure-activity relationships. *Environmental Health Perspectives*, 1985**. 61**, 203-228.
32. Andryukov, K. V. and Korkodinova, L. M., Calculating the constants of lipophilicity in aqueous and gaseous phases and their relationship to the structure of derivatives of *N*-alkyl substituted anthranilic acid. *Russian Journal of Physical Chemistry A*, 2014**. 88** (8), 1371-1374.
33. Mannhold, R. and Dross, K., Calculation procedures for molecular lipophilicity: A comparitive study. *Quantitative Structure-Activity Relationships*, 1996**. 15** (5), 403-409.
34. Viswanadhan, V. N., Ghose, A. K., Revankar, G. R. and Robins, R. K., Atomic physicochemical parameters for three dimensional structure directed quantitative structure-activity relationships. 4. Additional parameters for hydrophobic and dispersive interactions and their application for an automated superposition of certain naturally occurring nucleoside antibiotics. *Journal of Chemical Information & Computer Sciences*, 1989**. 29** (3), 163-172.
35. Bloch, D. E., Review of PHYSPROP Database (Version 1.0). *Journal of Chemical Information & Computer Sciences*, 1995**. 35** (2), 328-329.
36. Klopman, G., Li, J.-Y., Wang, S. and Dimayuga, M., Computer automated Log*P* calculations based on an extended group contribution approach. *Journal of Chemical Information & Computer Sciences*, 1994**. 34** (4), 752-781.

37. Nagy, P. I., Competing intramolecular vs. intermolecular hydrogen bonds in solution. *International Journal of Molecular Sciences*, 2014**. 15** (11), 19562-19633.
38. Alvim-Gaston, M., Grese, T., Mahoui, A., Palkowitz, A. D., Pineiro-Nunez, M. and Watson, I., Open innovation drug discovery (OIDD): A potential path to novel therapeutic chemical space. *Current Topics in Medicinal Chemistry*, 2014**. 14** (3), 294-303.
39. Jana, C. Synthesis and evaluation of pantothenic acid analogues as potential inhibitors of malaria parasites and bacteria. MSc, University of Stellenbosch, 2011.
40. Shioiri, T., Ninomiya, K. and Yamada, S., Diphenylphosphoryl azide. A new convenient reagent for a modified Curtius reaction and for peptide synthesis. *Journal of the American Chemical Society*, 1972**. 94** (17), 6203-6205.
41. Xia, Q., Liu, X., Zhang, Y., Chen, C. and Chen, W., Copper-catalyzed *N*-methylation of amides and O-methylation of carboxylic acids by using peroxides as the methylating reagents. *Organic Letters*, 2013**. 15** (13), 3326-3329.
42. Van der Westhuyzen, R. Synthesis and evaluation of inhibitors targeting coenzyme A biosynthesis and metabolism in *Staphylococcus aureus*. PhD, University of Stellenbosch, 2010.
43. Jablonski, J. J., Basu, D., Engel, D. A. and Geysen, H. M., Design, synthesis, and evaluation of novel small molecule inhibitors of the influenza virus protein NS1. *Bioorganic & Medicinal Chemistry* 2012**. 20** (1), 487-497.
44. Salvatore, R. N., Nagle, A. S. and Jung, K. W., Cesium effect: High chemoselectivity in direct *N*-alkylation of amines. *Journal of Organic Chemistry*, 2002**. 67** (3), 674-683.
45. Salvatore, R. N., Nagle, A. S., Schmidt, S. E. and Jung, K. W., Cesium hydroxide promoted chemoselective *N*-alkylation for the generally efficient synthesis of secondary amines. *Organic Letters*, 1999**. 1** (12), 1893-1896.
46. Van Wyk, M. and Strauss, E., Development of a method for the parallel synthesis and purification of *N*-substituted pantothenamides, known inhibitors of coenzyme A biosynthesis and utilization. *Organic & Biomolecular Chemistry*, 2008**. 6** (23), 4348-4355.
47. Sugie, Y., Dekker, K. A., Hirai, H., Ichiba, T., Ishiguro, M., Shiomi, Y., Sugiura, A., Brennan, L., Duignan, J., Huang, L. H., Sutcliffe, J. and Kojima, Y., CJ-15,801, a novel antibiotic from a fungus, *Seimatosporium sp*. *The Journal of Antibiotics*, 2001**. 54** (12), 1060-1065.
48. Tanoury, G. J., Chen, M., Dong, Y., Forslund, R. E. and Magdziak, D., Development of a novel Pd-catalyzed *N*-acyl vinylogous carbamate synthesis for the key intermediate of ICE inhibitor VX-765. *Organic Letters*, 2008**. 10** (2), 185-188.
49. Zhang, Z., Breslav, M., Grimm, J., Guan, K., Huang, A., Liu, F., Maryanoff, C. A., Palmer, D., Patel, M., Qian, Y., Shaw, C., Sorgi, K., Stefanick, S. and Xu, D., A new procedure for preparation of carboxylic acid hydrazides. *Journal of Organic Chemistry*, 2002**. 67** (26), 9471-9474.

50. Andreini, M., Felten, A.-S., Thien, H.-T. T., Taillefumier, C., Pellegrini-Moïse, N. and Chapleur, Y., Synthesis of new C-glycosyl aza-β3-amino acids building blocks. *Tetrahedron Letters*, 2012**. 53** (22), 2702-2705.
51. Carey, F. A. and Sundberg, R. J., Advanced Organic Chemistry: Part B: Reaction and synthesis. Fourth ed.; *Kluwer Academic Publishers*: New York, Boston, Dordrecht, London, Moscow, 2002.
52. Varma, R. S. and Kumar, D., Microwave-accelerated solvent-free synthesis of thioketones, thiolactones, thioamides, thionoesters, and thioflavonoids. *Organic Letters*, 1999**. 1** (5), 697-700.
53. Kuehne, M. E., Cowen, S. D., Xu, F. and Borman, L. S., Syntheses of 5a'-*homo*-vinblastine and congeners designed to establish structural determinants for isolation of atropisomers. *Journal of Organic Chemistry*, 2001**. 66** (16), 5303-5316.
54. Otani, Y., Hori, T., Kawahata, M., Yamaguchi, K. and Ohwada, T., Secondary structure of homo-thiopeptides based on a bridged β-proline analogue: Preferred formation of extended strand structures with *trans*-thioamide bonds. *Tetrahedron*, 2012**. 68** (23), 4418-4428.
55. Tuck, K. L., Saldanha, S. A., Birch, L. M., Smith, A. G. and Abell, C., The design and synthesis of inhibitors of pantothenate synthetase. *Organic & Biomolecular Chemistry* 2006**. 4** (19), 3598-3610.
56. Yan, X., Akinnusi, T. O., Larsen, A. T. and Auclair, K., Synthesis of 4'-aminopantetheine and derivatives to probe aminoglycoside *N*-6'-acetyltransferase. *Organic & Biomolecular Chemistry*, 2011**. 9** (5), 1538-1546.
57. Strauss, E., Kinsland, C., Ge, Y., McLafferty, F. W. and Begley, T. P., Phosphopantothenoylcysteine synthetase from *Escherichia coli*. Identification and characterization of the last unidentified coenzyme A biosynthetic enzyme in bacteria. *Journal of Biological Chemistry*, 2001**. 276** (17), 13513-13516.
58. Dangerfield, E. M., Plunkett, C. H., Win-Mason, A. L., Stocker, B. L. and Timmer, M. S., Protecting-group-free synthesis of amines: Synthesis of primary amines from aldehydes via reductive amination. *Journal of Organic Chemistry*, 2010**. 75** (16), 5470-5477.
59. Miriyala, B., Bhattacharyya, S. and Williamson, J. S., Chemoselective reductive alkylation of ammonia with carbonyl compounds: Synthesis of primary and symmetrical secondary amines. *Tetrahedron*, 2004**. 60** (7), 1463-1471.
60. De Kimpe, N., De Smaele, D., Hofkens, A., Dejaegher, Y. and Kesteleyn, B., Synthesis of 3-alkenylamines, 4-alkenylamines and 3-allenylamines via a transamination procedure. *Tetrahedron*, 1997**. 53** (31), 10803-10816.
61. Kopelevich, V. M., Bulanova, L. N. and Gunar, V. I., Synthesis of 4'-amino-4'-deoxy analog of pantothenic acid. *Tetrahedron Letters*, 1979**. 20** (40), 3893-3894.

62. Kopelevich, V. M., Bulanova, L. N. and Gunar, V. I., Analogs of D(+)-pantothenic acid. VI. Synthesis of D-, L-, and DL-4'-amino-4'-deoxypantothenic acid. *Chemistry of Natural Compounds*, 1982**. 18** (2), 215-219.
63. Wang, X., Ye, Y., Zhang, S., Feng, J., Xu, Y., Zhang, Y. and Wang, J., Copper-catalyzed C($sp^3$)-C($sp^3$) bond formation using a hypervalent iodine reagent: An efficient allylic trifluoromethylation. *Journal of the American Chemical Society*, 2011**. 133** (41), 16410-16413.
64. Strauss, E. and Begley, T. P., The antibiotic activity of N-pentylpantothenamide results from its conversion to ethyldethia-coenzyme a, a coenzyme a antimetabolite. *J. Biol. Chem.*, 2002**. 277** (50), 48205-48209.
65. Rudin, L., Sjöström, J.-E., Lindberg, M. and Philipson, L., Factors affecting competence for transformation in *Staphylococcus aureus*. *Journal of Bacteriology* 1974**. 188** (1), 155-164.
66. Jackowski, S. and Rock, C. O., Metabolism of 4'-phosphopantetheine in *Escherichia coli*. *Journal of Bacteriology*, 1984**. 158** (1), 115-120.
67. Macuamule, C. J. Coenzyme A biosynthesis and utilization in *Plasmodium falciparum*: Drug targets for antimalarial chemotherapy. PhD, University of Stellenbosch, 2013.
68. Mottaghi, K., Hong, B., Tempel, W. And Park, H. Unpublished crystal structure data (4M7X), 1.42Å. RCSB protein database (PDB). www.pdb.org (accessed 2 July 2015).
69. Macuamule, C. J., Tjhin, E. T., Jana, C. E., Barnard, L., Koekemoer, L., de Villiers, M., Saliba, K. J. and Strauss, E., A pantetheinase-resistant pantothenamide with potent, on-target, and selective antiplasmodial activity. *Antimicrobial Agents & Chemotherapy*, 2015**. 59** (6), 3666-3668.
70. Koekemoer, L. Characterization of prokaryotic pantothenate kinase enzymes and the development of type-specific inhibitors. PhD, University of Stellenbosch, 2011.
71. Van Wyk, M. A study of *N*-substituted pantothenamides, antimicrobials acting on coenzyme A biosynthesis and utilization. PhD, University of Stellenbosch, 2009.
72. Van Wyk, M. and Strauss, E., One-pot preparation of coenzyme A analogues *via* an improved chemo-enzymatic synthesis of pre-CoA thioester synthons. *Chemical Communications*, 2007**.** (4), 398-400.
73. Aquino, F., Pauling, H., Walther, W., Plattner, D. A. and Bonrath, W., A convenient dehydration procedure for the synthesis of enantiomerically pure cyanohydrins. *Synthesis*, 2000**.** (5), 731-737.
74. Strauss, E. and Begley, T. P., The antibiotic activity of *N*-pentylpantothenamide results from its conversion to ethyldethia-coenzyme A, a coenzyme A antimetabolite. *Journal of Biological Chemistry*, 2002**. 277** (50), 48205-48209.

*Chapter 4*

# Developing *P. falciparum* Inhibitors That Are Resistant to Pantetheinase-Mediated Degradation

## 4.1 Introduction

Malaria continues to present a major health challenge, specifically in resource limited countries [1]. Nearly one half of the world's population is at risk of contracting malaria, with children less than 5 years and pregnant woman being most susceptible of contracting the disease [2]. Despite decades of intensive efforts to control malaria, this disease still causes millions of clinical cases each year, with the WHO estimating that in 2013 ~584 000 people died from malaria worldwide, the majority of which lived in Africa [2-3]. There are five species of *Plasmodium* that are infectious to humans, namely *Plasmodium vivax*, *Plasmodium malariae*, *Plasmodium ovale*, *Plasmodium knowlesi* and *Plasmodium falciparum*, with the latter being the most virulent and primarily responsible for malaria-related deaths, although *P. vivax* also contributes significantly to the overall morbidity [1, 4-5].

*P. falciparum* has shown repeatedly that it has a substantial capability to develop antibiotic resistance to antimalarial drugs by means of evolutionary adaptation [6]. Consequently, the efficacy of the current available antimalarials is imperiled by the emergence of drug resistant strains of this parasite. The development of extensive resistance has already resulted in a considerable decrease in the efficacy of standard antimalarial drugs, including chloroquine, mefloquine, atabrine and pyrimethamine-sulfadoxine [3, 7]. Additionally, the development of resistance against the present generation drug, artemisinin and its derivatives, have also been observed. This has resulted in a resurgence of malaria and it is now even more imperative to develop new antimalarial drugs with novel mechanisms of action and/or different chemical origin to successfully counteract the development of antibiotic resistance [3].

### 4.1.1 Transmission and life cycle of the malaria parasite

Malaria is transmitted to humans by female *Anopheles* mosquitoes during a blood meal by injecting the human with parasites called sporozoites and completes its life cycle in two hosts; mosquito and human [4-5]. These sporozoites move to the liver where it invades hepatocytes, in which it grows and multiplies until it ruptures the hepatocyte and releases merozoites (daughter parasites) into the blood stream (Figure 4.1). Subsequently, the merozoites invade erythrocytes (red blood cells) and undergo asexual multiplication to form trophozoites followed by maturation into schizonts, with each schizont forming roughly 30 new merozoites. After the completion of this 48h cycle, the

erythrocyte will rupture to release the newly formed merozoites into the blood stream and each merozoite has the potential to infect a new erythrocyte and reinitiate the life cycle.

Additionally, during the asexual blood stage some of the intraerythrocytic parasites develop into male and female gametocytes; these are taken up by an uninfected *Anopheles* mosquito into the gut during a blood meal where they mature to form male and female gametes. The fertilized zygote develops into either an ookinete or an oocyst and finally into sporozoites that move to the salivary glands of the mosquito ready to be injected into a new human host [4].

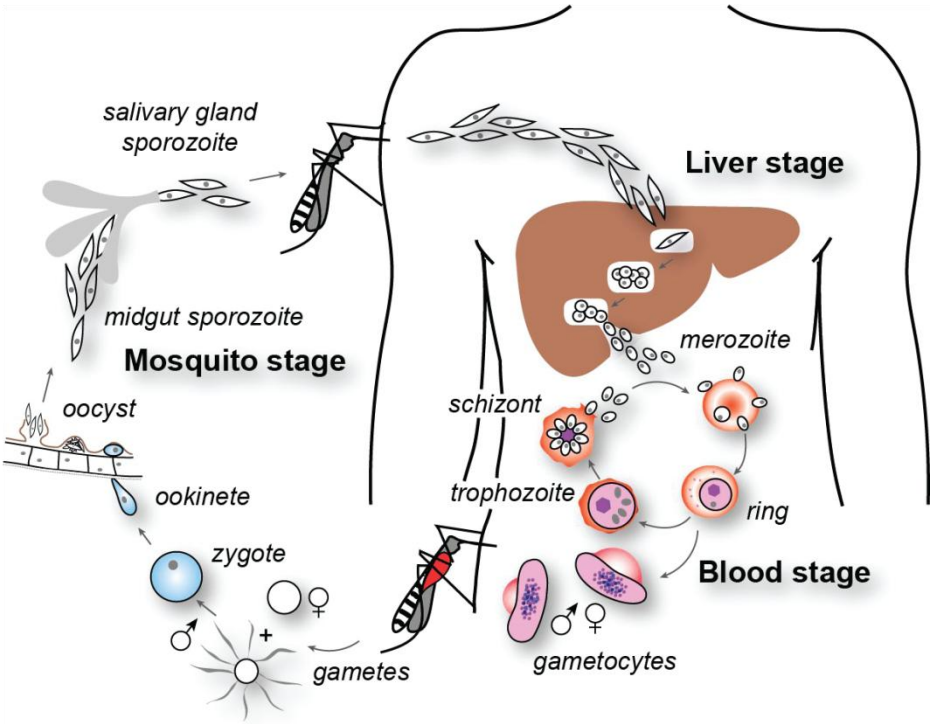


**Figure 4.1. The life cycle of *P. falciparum* in the human host and the mosquito. Reproduced from ref [4].**

### 4.1.2 Pantothenamides as potential small molecule inhibitors of the malaria parasite

In Chapter 1 the CoA biosynthetic pathway was discussed in detail as a potential target for antimalarial drug development. Originally it was thought that pantothenamides are poor inhibitors of the CoA biosynthetic pathway and CoA-utilizing enzymes in *P. falciparum* since most of the examples tested for inhibition of the proliferation of the 3D7 strain of the parasite by de Villiers *et al*. [8], as well as Spry *et al*. [9], had $IC_{50}$s >200 µM. The best hit, *N*-phenethyl pantothenamide (**4.1**, *N*-PE-PanAm) (boxed in Figure 4.2), showing antiplasmodial activity with an $IC_{50}$ of 53 ± 11 µM [10].

However, in 2011 Jansen *et al*. [11] discovered that this loss of antiplasmodial activity is due to pantetheinase enzymes present in the serum used to grow the parasites. When they tested N5-Pan against *P. falciparum* in the presence of an inhibitor of pantetheinase activity, its antimalarial potency ($IC_{90}$) was increased by a factor of 200 compared to N5-Pan alone [11]. Consequently, de Villiers *et al*. [8] retested the pantothenamides as inhibitors of the *P. falciparum* parasite in aged media (i.e. media in which the pantetheinases present in the commonly used serum substitute Albumax were inactivated through pre-incubation at 37°C) [8]. Under these conditions, the potency of the pantothenamides tested was similarly enhanced. Even pantothenamides that previously showed no inhibition in freshly prepared media (i.e. with the pantetheinase activity intact), displayed inhibition of parasite growth at sub-micromolar concentrations in aged (pre-incubated) media [8]. These findings indicated that pantothenamides have significant potential as antiplasmodial agents if their degradation by pantetheinases can be prevented, circumvented or resisted in some manner.

## 4.2 Study design and strategy

Given this background, we decided to also include *P. falciparum* into our study of the biological activity of pantetheinase-resistant pantothenamides. Previously, de Villiers *et al*. [8] established that the degradation of pantothenamides by pantetheinase can be prevented by the modification of their structures (discussed in detail in Chapter 1). This study demonstrated that the displacement of the scissile amide bond in pantothenamides (by forming either α-pantothenamides or homo-pantothenamides) lead to an increased potency against *P. falciparum* parasites in fresh medium compared to the normal pantothenamides. Additionally, the α- and homo-pantothenamides were also more resistant to pantetheinase degradation compared to the normal pantothenamides when treated with recombinant human pantetheinase [8]. Consequently, we decided to expand the strategy used for the discovery of pantetheinase-resistant pantothenamides active against *S. aureus* as described in Chapter 3 and to synthesize the same set of analogues with added steric bulk, bioisostere replacement and 4'-hydroxyl derivatization, but with an amide substituent that showed optimum activity against *P. falciparum*.

From a previous study by Spry *et al*. [9] *N*-PE-PanAm **4.1** was identified as the most potent analogue of those tested against the *P. falciparum* parasite with an $IC_{50}$ of 53 ± 11 µM in fresh medium and an $IC_{50}$ of 20 ± 2 nM (a value similar to that observed for chloroquine) in aged medium. Consequently, we set out to synthesize the same analogues that were synthesized as described in Chapter 3, but with the heptyl group as the amide substituent replaced with a phenethyl group. We expected that these nine *N*-PE-PanAm analogues should show increased resistance to pantetheinase-mediated degradation (Figure 4.2).

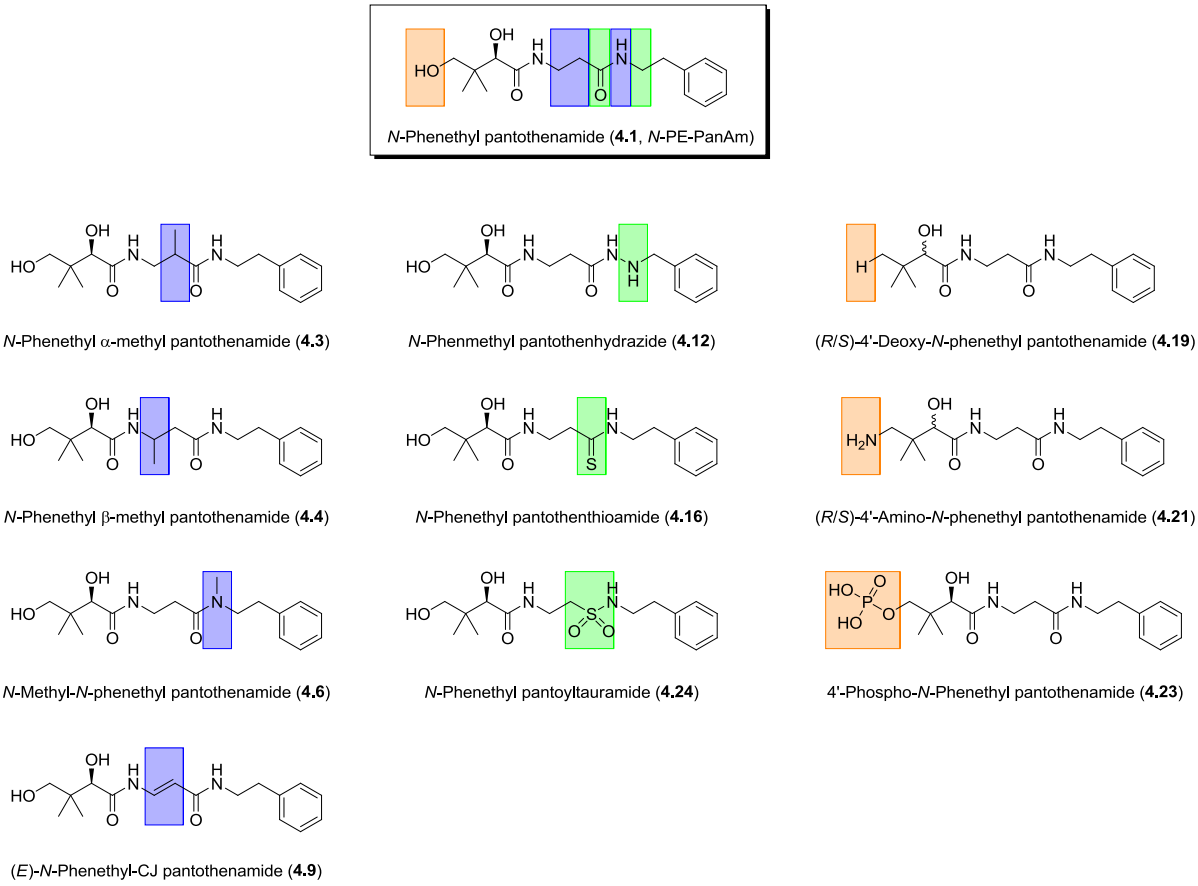


**Figure 4.2. *N*-Phenethyl pantothenamide analogues that should withstand pantetheinase-mediated hydrolysis. In these analogues the scissile amide bond of *N*-phenethyl pantothenamide 4.1 is protected by either increasing the steric bulk surrounding it though the addition of a methyl group, by replacement with bioisosteres or by removing or replacing its 4'-hydroxyl group. The modifications relative to the parent compound are highlighted in each case, with orange indicating the modifications to be made to the 4'-hydroxyl, green indicating the modifications to be made to the scissile amide bond, and blue indicating the modifications to be made through the addition of steric bulk.**

We did not include the sulfonamide bioisostere in this study, since *N*-phenethyl pantoyltauramide (**4.24**, *N*-PE-pantoyltauramide) was synthesized previously in our laboratory by Mr. Collins Jana during his MSc study [12] and was tested for its antiplasmodial activity in fresh and aged media by Dr. Cristiano Macuamule during his PhD study [13]. This particular analogue exhibited inhibition of the proliferation of *P. falciparum* 3D7 strain with an $IC_{50}$ of 35 ± 2 µM and 42 ± 0.4 µM in fresh and aged media, respectively. This indicated that *N*-PE-pantoyltauramide **4.24** was indeed resistant to pantetheinase-mediated degradation, but that the structural modification came at a significant cost in potency.

## 4.3 Physicochemical properties of the proposed *N*-Phenethyl pantothenamide analogues

Before we synthesized the analogues of *N*-PE-PanAm **4.1** we first determined their physicochemical properties (as was done for the N7-Pan analogues) by looking at their adherence to Lipinski's rules of 5, as well as at their extended *in silico* characterized properties. All of the analogues were found to obey at least three of the four Lipinski rules (Table 4.1): in all cases their molecular weights fall within the limit of ≤ 500 g.mol$^{-1}$, and all of the compounds fall within the limits for the number of H-bond acceptors (≤ 10) and donors (≤ 5). However, *N*-benzyl pantothenhydrazide (**4.12**, *N*-Bn-PanHy), (*R*/*S*)-4'-amino-*N*-phenethyl pantothenamide (**4.21**, (*R*/*S*)-4'-amino-*N*-PE-PanAm) and 4'-phospho-*N*-phenethyl pantothenamide (**4.23**, 4'-Phospho-*N*-PE-PanAm) fall outside the limit of ≤ 5 and ≥ 0 for their lipophilicity (cLog*P*), indicating that these analogues are not lipophilic enough and considered too hydrophilic to be a suitable drug candidate.

Looking at the additional *in silico* characterized properties, only 4'-phospho-*N*-PE-PanAm **4.23** have a higher PSA than the preferred ≤ 140 Å, while none of the *N*-PE-PanAm analogues exceed the optimal NRotB (≤ 10-20). For most of the analogues the partition coefficient is equal to the distribution coefficient since they do not contain ionizable groups. It is only 4'-phospho-*N*-PE-PanAm **4.23** and (*R*/*S*)-4'-amino-*N*-PE-PanAm **4.21** that are able to ionize due to the modifications at the 4'-position; unfortunately their Log$D_{7.4}$ values, as in the case with their cLog*P* values, fall outside the limits of the suggested Log$D_{7.4}$ values. Compared to the N7-Pan analogues, all of the *N*-PE-PanAm analogues have a lower percentage of F*sp*$^3$ carbons with most of them having 50-65.5% of F*sp*$^3$ carbons, except for (*E*)-*N*-phenethyl CJ-pantothenamide (*E*)-**4.9**, (*E*)-*N*-PE-CJ-PanAm) which has 41.2% F*sp*$^3$ carbons.

In summary, the proposed *N*-PE-PanAm analogues adhere to most of Lipinski's rules of 5 properties, as well as to most of the other *in silico* characterized properties. We therefore expected that these compounds should be orally bioavailable if they translate into potent inhibitors of parasite proliferation.

**Table 4.1. Physicochemical properties of the *N*-phenethyl pantothenamide analogues[a]. The values indicated in red fall outside the proposed limits.**

| Molecule | M/W (g.mol$^{-1}$) | cLog*P* | H-bond acceptors | H-bond donors | PSA (Å$^2$) | NRotBs | Log$D_{7.4}$ | Fs$p^3$ |
|---|---|---|---|---|---|---|---|---|
| 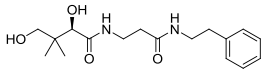 | 322.40 | 0.07 | 4 | 4 | 98.66 | 9 | 0.07 | 0.529 |
| 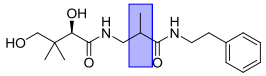 | 336.43 | 0.62 | 4 | 4 | 98.66 | 9 | 0.62 | 0.556 |
| 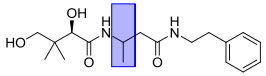 | 336.43 | 0.49 | 4 | 4 | 98.66 | 9 | 0.49 | 0.556 |
| 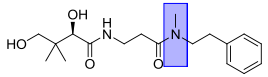 | 336.43 | 0.30 | 4 | 3 | 89.87 | 9 | 0.30 | 0.556 |
| 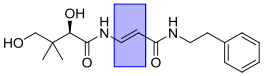 | 320.38 | 0.29 | 4 | 4 | 98.66 | 8 | 0.29 | 0.412 |
| 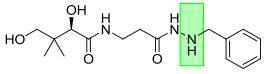 | 329.39 | -0.51 | 5 | 5 | 110.7 | 9 | -0.51 | 0.500 |
| 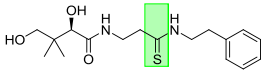 | 338.46 | 0.96 | 3 | 4 | 81.6 | 9 | 0.96 | 0.529 |
| 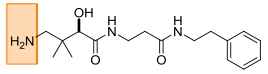 | 321.41 | -0.03 | 4 | 4 | 104.5 | 9 | -1.93 | 0.529 |
| 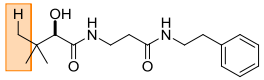 | 320.43 | 1.80 | 3 | 3 | 78.4 | 9 | 1.80 | 0.529 |
| 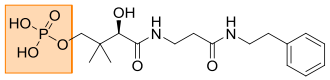 | 402.38 | -0.05 | 6 | 5 | 145.2 | 11 | -3.10 | 0.529 |

[a] Values of cLog*P* and Log$D_{7.4}$ were calculated with calculator plugins in the program MarvinSketch 6.0.6, 2013 from ChemAxon (Budapest, Hungary). cLog*P* and Log$D_{7.4}$ values were set at default: calculations used equal weights of VG, KLOP, and PHYS methods and electrolyte concentrations ($Na^+$,$K^+$ and $Cl^-$) set to 0.1 mol.dm$^{-3}$ [14-16]. We did not consider automerization in our calculations. PSA was calculated with the same program, but excluded sulfur and phosphorus atoms from the calculations. NRotB, H-bond donors and H-bond acceptors were calculated using the same program. The values that fall outside the limits of the physicochemical properties are indicated in red.

## 4.4 Synthesis of pantetheinase-resistant *N*-phenethyl pantothenamide analogues

The synthetic preparation of the nine *N*-PE-PanAm analogues was based on the synthetic routes that were developed as described in Chapter 3. Consequently, the synthesis of each analogue will not be discussed in detail here. Instead, a brief overview of the results obtained for each synthetic route will be provided. We first focused on the analogues that have steric bulk introduced in close proximity to the amide bond which is vulnerable to pantetheinase degradation, followed by the preparation of the analogues with bioisostere replacements. Lastly, we prepared the analogues where the 4'-hydroxyl group was removed or replaced to prevent substrate recognition.

### 4.4.1 Introducing steric bulk to *N*-phenethyl pantothenamide

#### 4.4.1.1 α-Methyl-*N*-phenethyl pantothenamide (4.3) and β-methyl-*N*-phenethyl pantothenamide (4.4)

The synthetic route for the preparation of α-methyl-*N*-phenethyl pantothenamide (**4.3**, α-Me-*N*-PE-PanAm) and β-methyl-*N*-phenethyl pantothenamide (**4.4**, β-Me-*N*-PE-PanAm) consisted of a two-step linear synthesis and included a condensation and coupling reaction (Scheme 4.1). Carboxylic acid **3.4** and **3.5** were prepared as discussed previously in Chapter 3 by condensation of the respective acids with (*R*)-(-)-pantolactone **3.3**. A DPPA-mediated coupling was used for the final amide bond formation in step 2. As such, a solution of carboxylic acid **3.4** or **3.5** and phenethylamine (**4.2**) in DMF was treated with DPPA and $Et_3N$. Subsequent purification by FCC gave amide **4.3** (when carboxylic acid **3.4** was coupled) as a yellow oil in 52% yield. Unfortunately, only a 30% yield was obtained for amide **4.4** (white solid) (when carboxylic acid **3.5** was coupled) after purification. DPPA-mediated coupling reactions require strictly anhydrous conditions to achieve successful amide bond formation [17]. Given that carboxylic acid **3.5** is very hygroscopic, the low yield obtained for amide **4.4** could be attributed to some moisture entering the reaction mixtures by association with this reagent. Additionally, the low yield could also be due to a possible competing coupling reaction at the unprotected 4'-hydroxyl position.

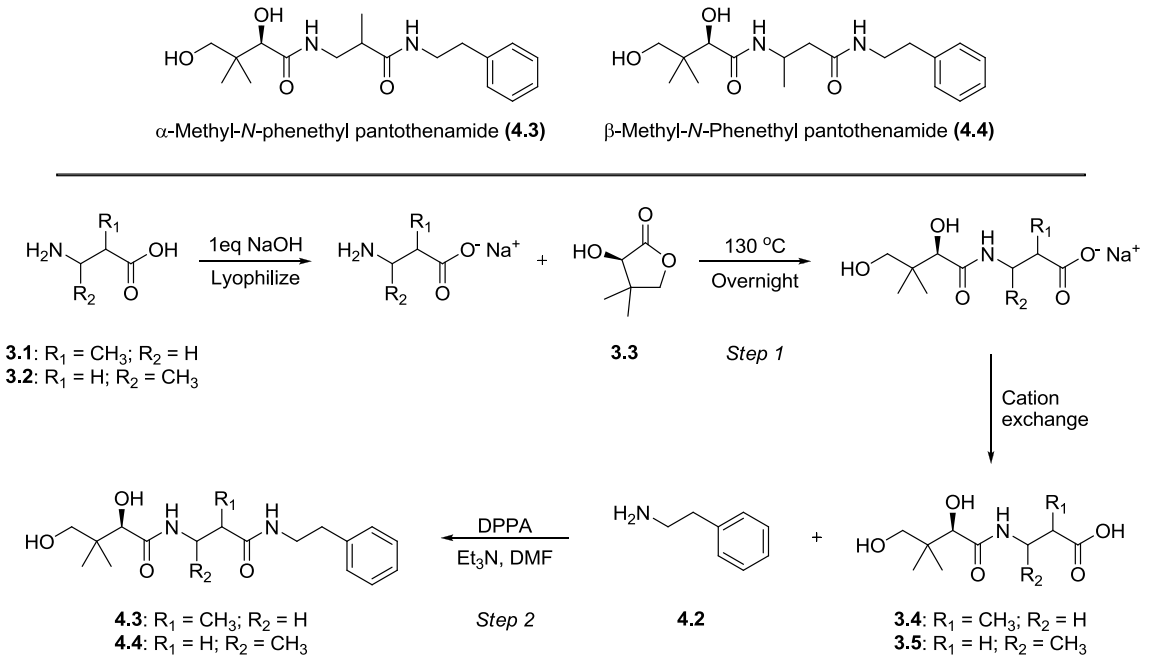


**Scheme 4.1. Synthetic route for the preparation of α-methyl-*N*-phenethyl pantothenamide (4.3) and β-methyl-*N*-phenethyl pantothenamide (4.4). 4.3 was prepared from (*R*/*S*)-3-amino-isobutyric acid 3.1 in two steps, while 4.4 was prepared from (*R*/*S*)-3-aminobutyric acid 3.2 in two steps.**

### 4.4.1.2 *N*-Methyl *N*-phenethyl pantothenamide (4.6)

The synthesis of *N*-methyl-*N*-phenethyl pantothenamide (**4.6**, *N*-Me-*N*-PE-PanAm) was based on a linear two-step synthesis that included an activation of the carboxylic acid and an aminolysis step (Scheme 4.2). Acid **3.9** was converted into the active thioester **3.20** in the first step by treating acid **3.9** with thiophenol (**3.19**), DEPC and $Et_3N$ in DMF. In the final step, thioester **3.20** was reacted with *N*-methyl phenethylamine (**4.5**) to give target amide **4.6** via aminolysis. Subsequent purification by FCC gave the product as a yellow oil in an excellent 82% yield.

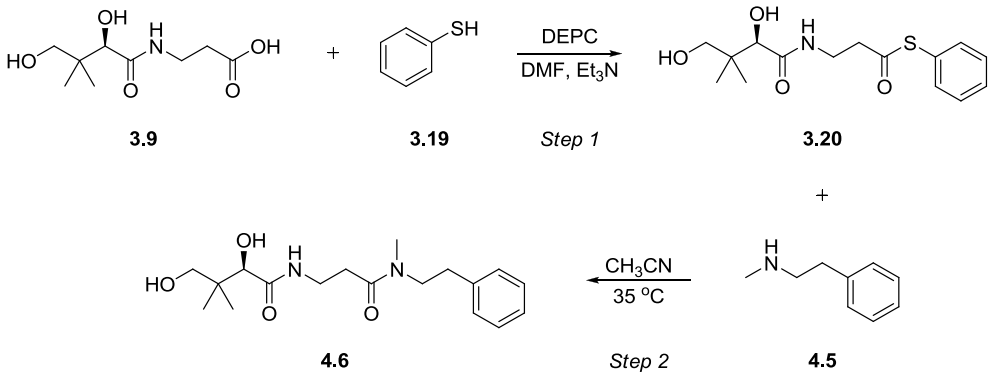


**Scheme 4.2. Synthetic route for the preparation of *N*-methyl-*N*-phenethyl pantothenamide (4.6) from pantothenic acid 3.9 using a two-step linear method that was developed by van Wyk and Strauss [18].**

### 4.4.1.3 (*E*)-*N*-Phenethyl CJ-pantothenamide ((*E*)-4.9)

The synthetic route for the synthesis of (*E*)-*N*-PE-CJ-PanAm (**4.9**) consisted of a six-step synthesis that entailed the preparation of two fragments which was subsequently coupled using a Pd-catalyzed reaction to introduce the enamide moiety (Scheme 4.3). Fragment 1 (amide **3.22**) was prepared as discussed previously in Chapter 3 by aminolysis of (*R*)-(-)-pantolactone **3.3**, followed by protection of the 2,4-diol **3.21** as the acetonide.

In step 1 of the synthesis of the second fragment, bromo acid **3.24** was prepared by refluxing propiolic acid (**3.23**) in 48% aqueous HBr and subsequent filtration of the precipitate upon cooling on an ice bath. In the second step, bromo acid **3.24** was successfully coupled to phenethylamine (**4.2**) using a standard DIC- and DMAP-mediated coupling procedure performed in DCM, before purification by FCC afforded acrylamide **4.7** as pale yellow solid in a moderate 45% yield.

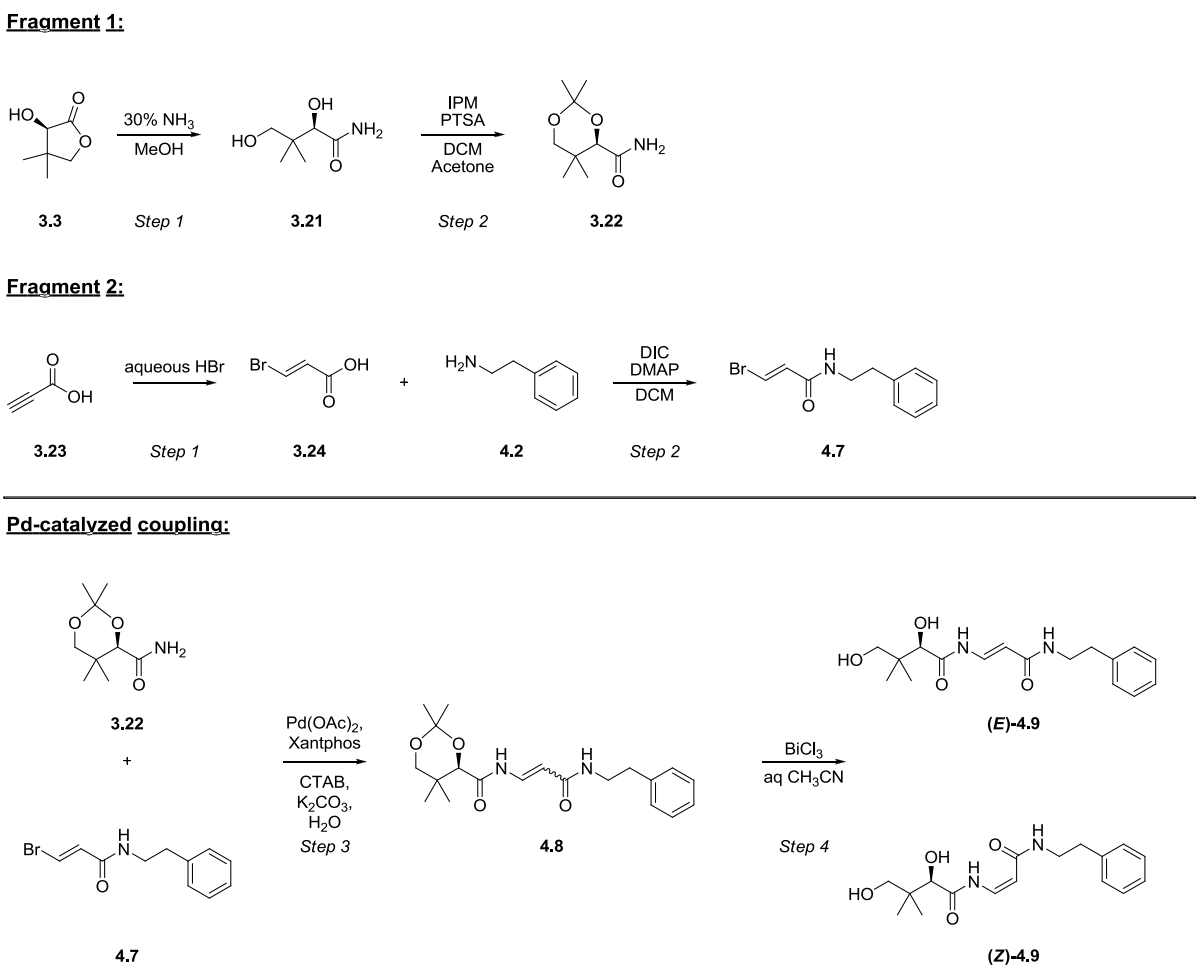


**Scheme 4.3. Synthetic route for the preparation of (*E*)-*N*-phenethyl CJ-pantothenamide ((*E*)-4.9) from (*R*)-(-)-pantolactone 3.3 and propiolic acid 3.23 using a six-step method that was developed by van der Westhuyzen [19].**

A Pd-catalyzed reaction was used to introduce the enamide moiety in step 3 [19]. Bromo acrylamide **3.25** (fragment 2) and amide **3.22** (fragment 1) were coupled in toluene using $Pd(OAc)_2$, Xantphos and CTAB to facilitate the enamide bond formation, with $K_2CO_3$ being added to neutralize the HBr formed during the course of the reaction. Subsequent purification by FCC (to separate the *E*- and *Z*-isomers) afforded enamide (*E*)-**4.8** and (*Z*)-**4.8** in 34% and 6%, respectively, with an *E:Z* ratio of 6:1. TLC analysis showed multiple side products, which could explain the low yield for the Pd-catalyzed coupling. In the final step, the acetonide protecting group was successfully removed with $BiCl_3$ in aqueous $CH_3CN$, before purification by FCC afforded (*E*)-**4.9** as a white solid in 13% yield and (*Z*)-**4.9** as a yellow oil in 46% yield, respectively. The absolute stereochemistry of the *E*- and *Z*-isomers was confirmed with $^1$H NMR spectroscopic analysis – the vinylic proton shifts as well as the *J*-couplings were consistent with those previously reported by Van der Westhuyzen [19].

## 4.4.2 Bioisostere replacement of the scissile amide in *N*-phenethyl pantothenamide

### 4.4.2.1 *N*-Benzyl pantothenhydrazide (4.12)

The synthetic route for the synthesis of *N*-Bn-PanHy **4.12** consisted of a four-step linear synthesis that included a thioesterification, as well as a reductive amination step (Scheme 4.4). Hydrazide **3.30** was prepared as discussed previously in Chapter 3 by thioesterification of acid **3.9** with ethanethiol (**3.28**), followed by hydrazinolysis of thioester **3.29**. Steps 3 and 4 entailed a metal hydride-mediated reductive amination of hydrazide **3.30**. As such, hydrazide **3.30** was reacted with benzaldehyde (**4.10**) in EtOH by stirring at reflux for 48h. After purification by FCC, imine **4.11** was obtained in a satisfactory 72% yield. In the final step, imine **4.11** was subjected to a $NaBH_3CN$-mediated reduction before purification by FCC afforded hydrazide **4.12** as a yellow oil, but unfortunately with only a 7% yield in the final step. TLC analysis showed that the reaction did not proceed to completion; consequently, a very low yield was obtained for the final step.

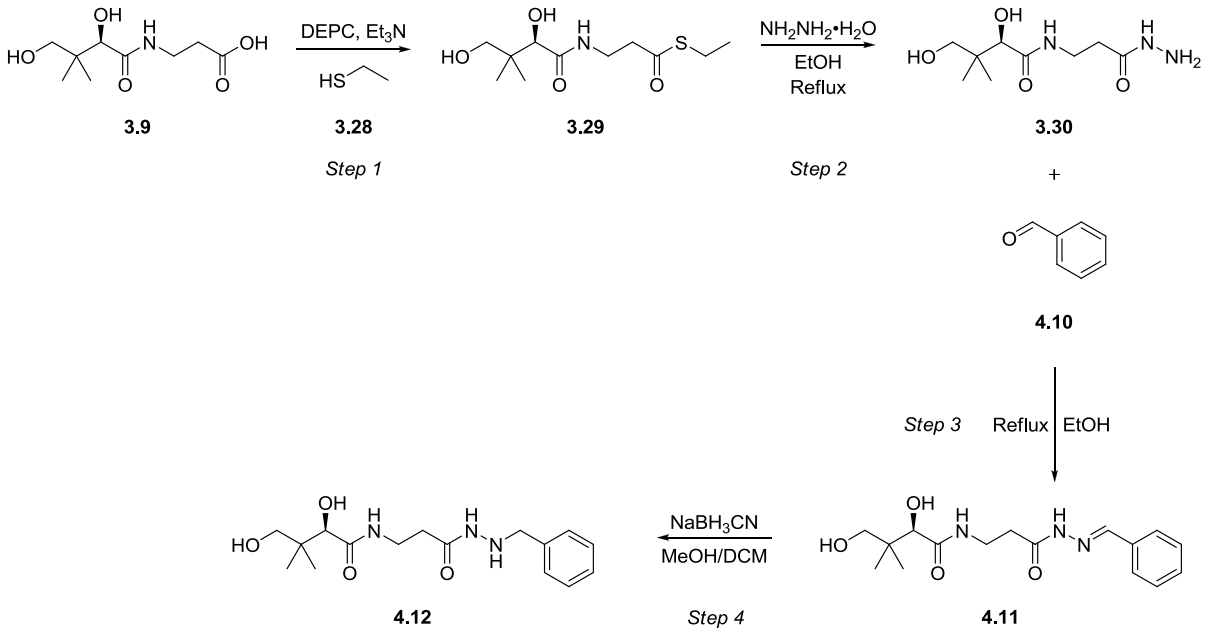


**Scheme 4.4. Synthetic route for the preparation of *N*-benzyl pantothenhydrazide (4.12) from pantothenic acid 3.9 in four steps.**

### 4.4.2.2 *N*-Phenethyl pantothenthioamide (4.16)

The synthetic route for the synthesis of *N*-phenethyl pantothenthioamide (**4.16**, *N*-PE-pantothenthioamide) consisted of a four-step linear synthesis that included a thionation and a condensation reaction (Scheme 4.5). In step 1, a solution of Cbz-β-alanine (**3.14**) and phenethylamine (**4.2**) in DMF was treated with DEPC and $Et_3N$ to facilitate the amide bond formation. The side-products and unreacted amine were removed through an aqueous work-up, which proved to be adequate to obtain amide **4.13** as a pure white powder in an excellent 99% yield. The second step of the synthesis entailed the thionation of the scissile amide bond. As such, amide **4.13** was treated with Lawesson's reagent in toluene and the reaction mixture was stirred at reflux overnight. Subsequent purification by FCC afforded thioamide **4.14** as a light yellow powder in moderate yield (51%). The third step of the synthesis entailed the deprotection of carbamate **4.14** by refluxing overnight in a 1:1 solution of MeOH and concentrated HCl. The crude amine **4.15** was lyophilized to afford the HCl salt of amine **4.15** as a white powder, which was subsequently used in the next step without any further purification.

The final step of the synthesis involved an amide bond formation between amine **4.15** HCl salt and (*R*)-(-)-pantolactone **3.3** in the presence of $Et_3N$ to facilitate the amide bond formation. During the synthesis of N7-pantothenthioamide **3.36** a very low yield was obtained (7%) in the final step. Consequently, in the final step of the preparation of *N*-PE-pantothenthioamide **4.16** the amount of $Et_3N$ in the reaction was increased from 2.5 equiv. to 5 equiv. to account for the HCl salt in the

reaction. Hence, amine **4.15** HCl salt was condensed with (*R*)-(-)-pantolactone **3.3** in the presence of $Et_3N$ by stirring for 48h at reflux in EtOH. Subsequent purification by FCC afforded amide **4.16** as a yellow oil. Although the yield was still low (30%), the increase in the amount of $Et_3N$ did increase the yield by three-fold.

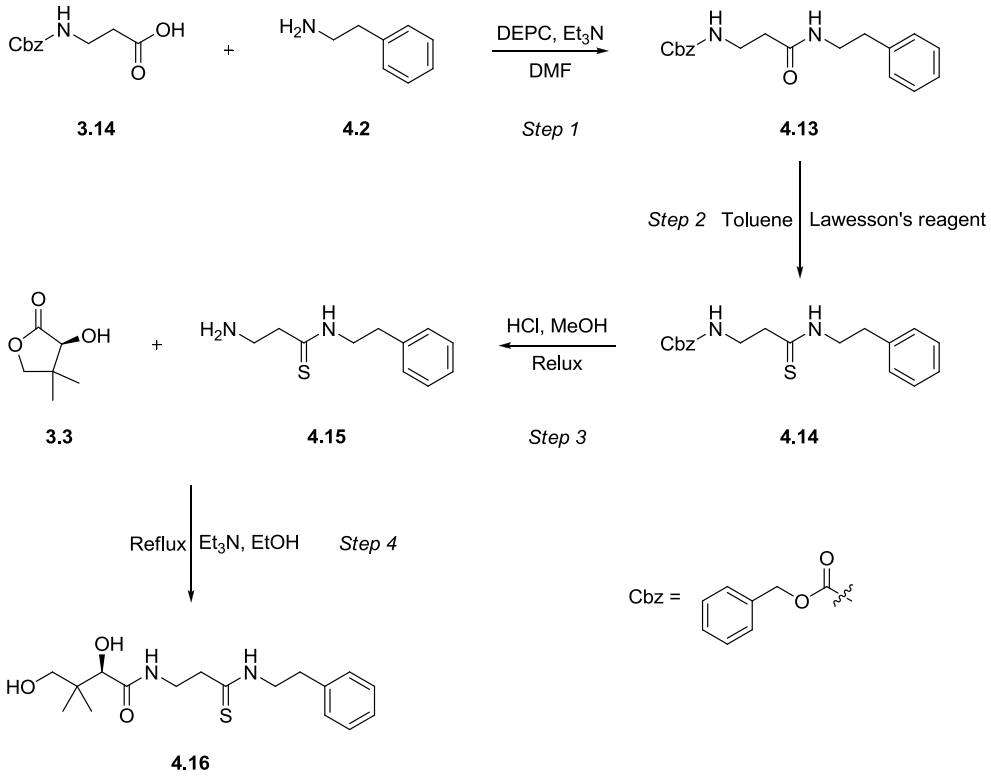


**Scheme 4.5. Synthetic route for the preparation of *N*-phenethyl pantothenthioamide (4.16) from Cbz-β-alanine (3.14) in a four-step synthesis.**

## 4.4.3 Removal of the 4'-OH group from *N*-phenethyl pantothenamide

### 4.4.3.1 (*R*/*S*)-4'-Deoxy-*N*-phenethyl pantothenamide (4.19)

(*R*/*S*)-4'-Deoxy-*N*-phenethyl pantothenamide (**4.19**, (*R*/*S*)-4'-deoxy-*N*-PE-PanAm) was synthesized through a four-step linear synthesis that included a coupling reaction and a $NaBH_4$-mediated reduction (Scheme 4.6). Amide **4.13** was synthesized via a DEPC-mediated coupling in step 1 as previously described for the synthesis of *N*-PE-pantothenthioamide **4.16** (Scheme 4.5). The second step of the synthesis entailed the deprotection of carbamate **4.13** with $H_2$ in the presence of 10% Pd/C to yield amine **4.17** as a pure pale yellow solid upon filtration in an excellent 98% yield; the purity was confirmed with $^1$H NMR spectroscopic analysis. In step 3, an EDC coupling was used to facilitate the final amide bond formation. As such, amine **4.17** and acid **3.46** (synthesized via the oxidation of ketone **3.47** by $KMnO_4$) were treated with EDC hydrochloride,

DIPEA and HOBt in DCM at 0°C and stirred overnight at rt. Subsequent purification by FCC afforded amide **4.18** as a white powder in 20% yield. This low yield is attributed to the low purity of carboxylic acid **3.46** since it degrades over time and it was not used immediately after its preparation. In the final step ketone **4.18** was reduced with $NaBH_4$, with hydroxyl **4.19** being obtained as a white solid in an excellent yield (94%) after an aqueous work-up.

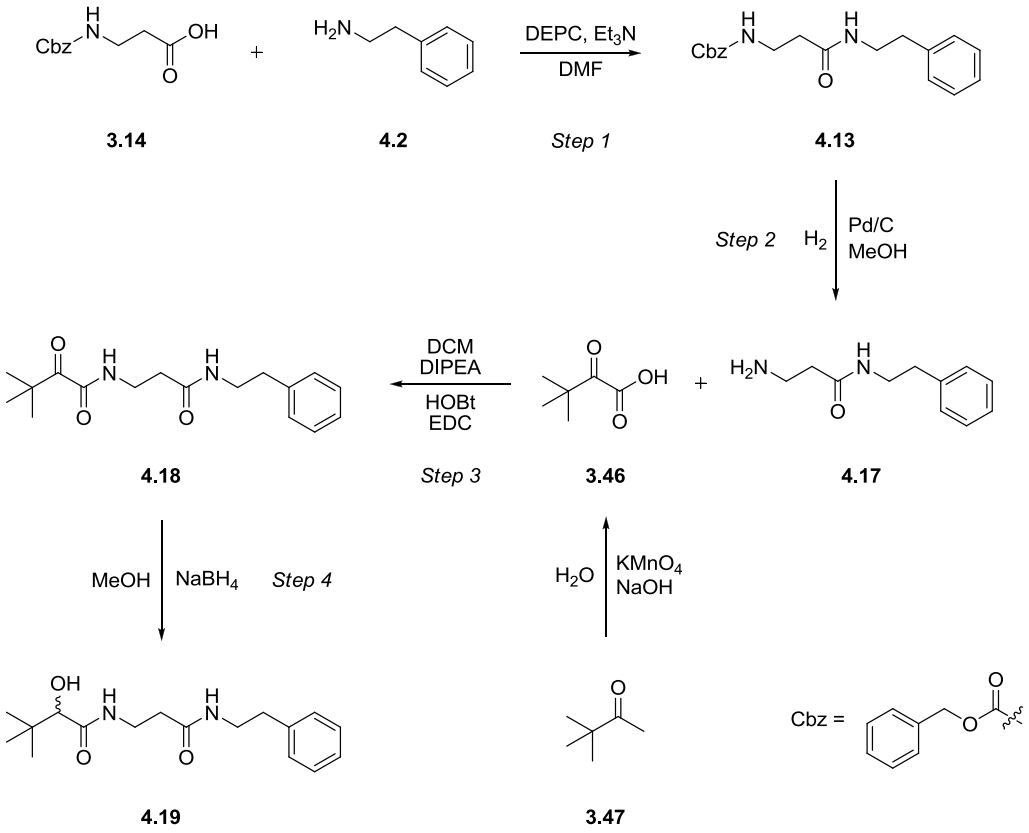


**Scheme 4.6. Synthetic route for the preparation of (*R*/*S*)-4'-deoxy-*N*-phenethyl pantothenamide (4.19) from Cbz-β-alanine (3.14) through a four-step linear synthesis developed in the manuscript described in Chapter 2 [20].**

### 4.4.3.2 (*R*/*S*)-4'-Amino-*N*-phenethyl pantothenamide (4.21)

The synthetic route for the synthesis of (*R*/*S*)-4-amino-*N*-PE-PanAm (**4.21**) consisted of a five-step linear synthesis which included a condensation and coupling reaction (Scheme 4.7). Carbamate **3.70** was synthesized in steps 1 to 3 (as previously described in Chapter 3) via a Gabriel-type synthesis to afford amine **3.69**, which was subsequently protected with Cbz chloride (**3.38**) in aqueous NaOH to give carbamate **3.70** as a white powder in an excellent 93% yield.

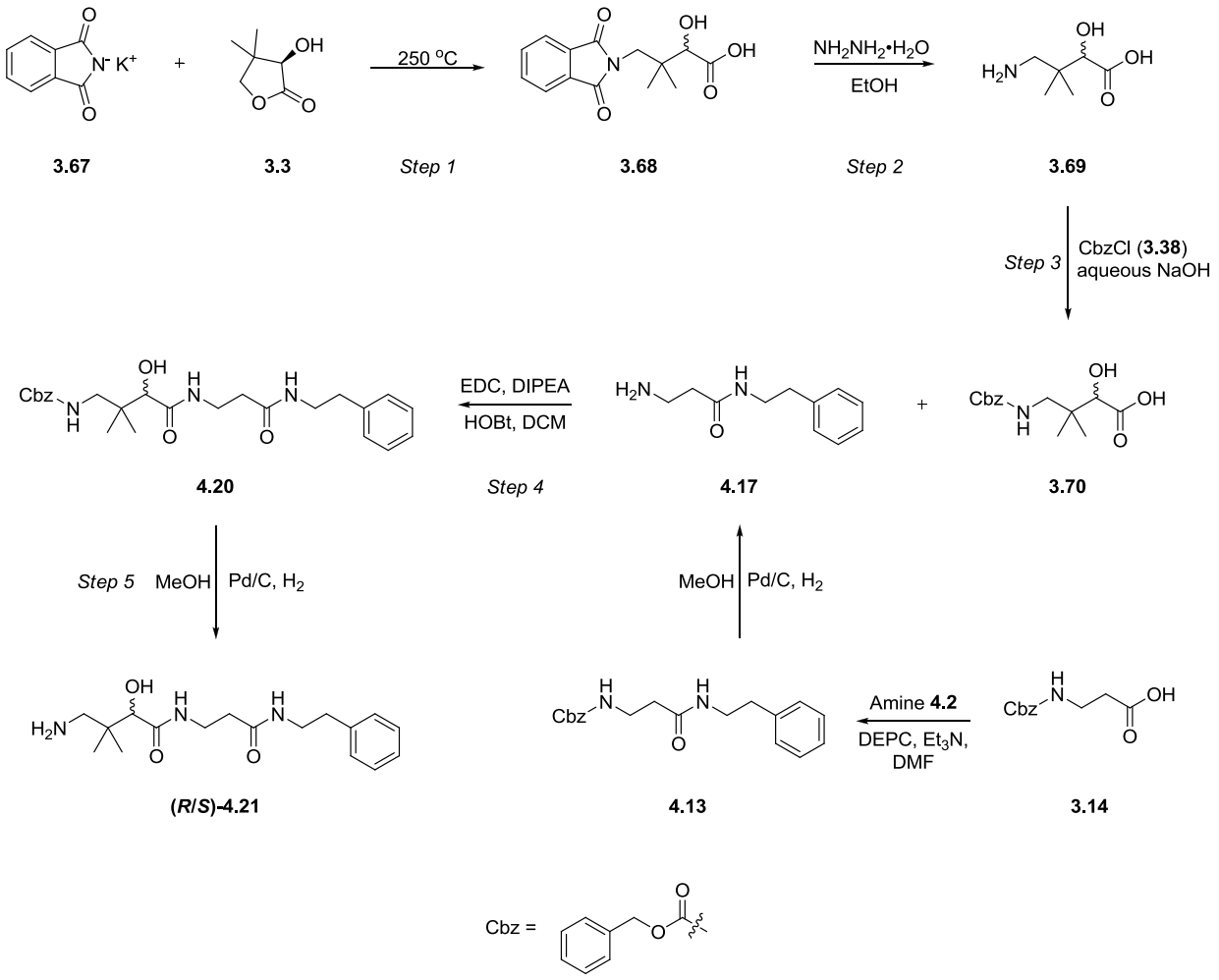


**Scheme 4.7. Synthetic route for the preparation of (*R*)-4'-amino-*N*-phenethyl pantothenamide (4.21) using phthalimide to introduce the 4'-amine. A method adapted from Kopelevich *et al*. [21] and de Villiers *et al*. [20] were used.**

In step 4, an EDC coupling was used to facilitate the amide bond formation. As such, acid **3.70** and amine **4.17** (synthesized by coupling Cbz-β-alanine (**3.14**) and phenethylamine (**4.2**) in the presence of DEPC and $Et_3N$, followed by subsequent deprotection of the carbamate **4.13** with 10% Pd/C and $H_2$) were treated with EDC hydrochloride, DIPEA and HOBt in DCM at 0°C and stirred overnight at rt. Subsequent purification by FCC afforded amide **4.20** as a yellow oil in 37% yield. The final step of the synthesis involved the deprotection of carbamate **4.20** by treatment with $H_2$ in the presence of 10% Pd/C to yield target compound (*R*/*S*)-**4.21** as yellow oil in a good yield (78%) upon filtration. The purity of (*R*/*S*)-**4.21** was confirmed by NMR spectroscopic analysis.

### 4.4.3.3 4'-Phospho-*N*-phenethyl pantothenamide (4.23)

The synthetic route for the preparation of 4'-phospho-*N*-PE-PanAm (**4.23**) comprised of a three-step linear synthesis that included a phosphorylation and deprotection step (Scheme 4.8). In the

first step calcium pantothenate was exchanged to free acid **3.9** using Amberlite IR120 resin and was subsequently coupled to phenethylamine (**4.2**) using DEPC in the presence of $Et_3N$ to facilitate the amide bond formation. The side products and unreacted amine were removed through an aqueous work-up, giving amide **4.1** which was subsequently used in the next step without any further purification. In the second step, the 4'-hydroxyl of **4.1** was phosphorylated with dibenzyl-chlorophosphate **3.72** (prepared *in situ* by reacting dibenzylphosphite and *N*-chlorosuccinimide in toluene for 2h, followed by filtration of the succinimide) in pyridine at -40°C, before purification by FCC afforded **4.22** as a yellow oil in a 28% yield. The final step of the synthesis entailed the deprotection of **4.22** and the benzyl protecting groups were successfully removed with $H_2$ in the presence of 10% Pd/C to yield target compound **4.23** as a clear oil in an excellent 99% yield upon filtration; the purity of **4.23** was confirmed by NMR spectroscopic analysis.

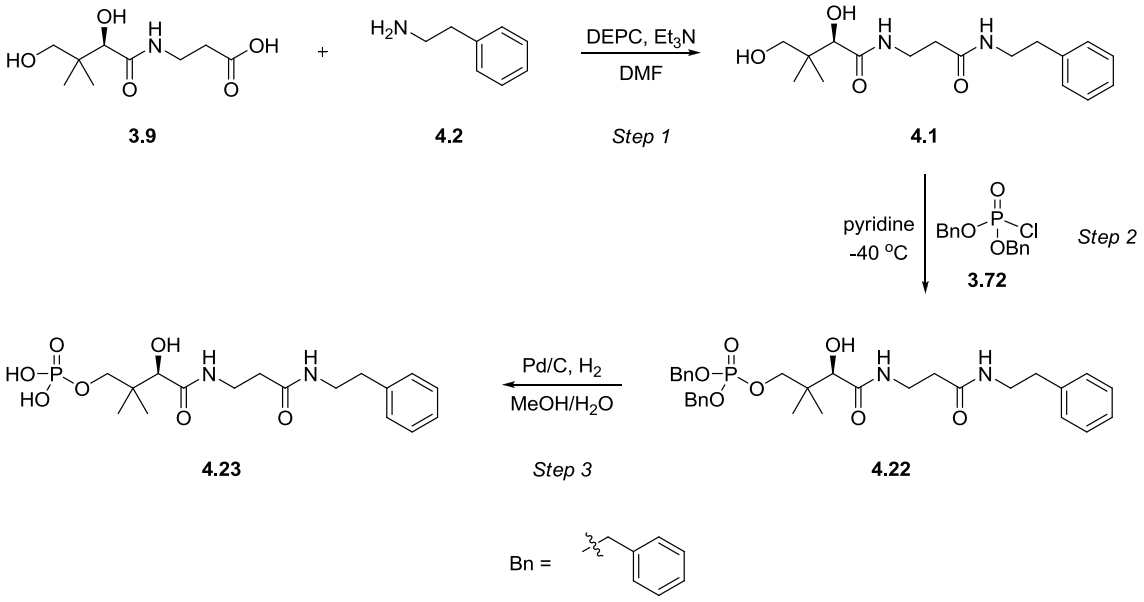


3.9 4.2 4.1 3.72 4.23 4.22

**Scheme 4.8. Synthetic route for the preparation of 4'-phospho-*N*-phenethyl pantothenamide (4.23) from pantothenic acid 3.9 using a method developed by Strauss *et al*. *[22]*.**

## 4.5 Determination of the antiplasmodial activity of the *N*-phenethyl-pantothenamide analogues against *P. falciparum*

The next objective was to evaluate whether the nine *N*-PE-PanAm analogues prepared above retained their potency towards *P. falciparum* compared to the parent compound *N*-PE-PanAm **4.1**. Ideally, it would also have been good to test whether these *N*-PE-PanAm analogues act as substrates or as inhibitors of *Pf*PanK and to determine their mode of action using the same experimental design that were used for *Sa*PanK-II in Chapter 3. However, thus far no one has successfully overexpressed and purified soluble PanK enzyme from the organism or a

heterologous expression system, even though PanK activity has been observed in lysates for years [5]. Consequently, these *N*-PE-PanAm analogues were only tested against the *P. falciparum* parasite.

The potency of these compounds were evaluated by testing them against *P. falciparum* in fresh medium (i.e. with active pantetheinase activity) as well as aged medium (i.e. medium in which the pantetheinases present in the commonly used serum substitute Albumax were deactivated through pre-incubation at 37°C). We decided to first test whether these analogues show antiplasmodial activity. Consequently, if antiplasmodial activity is observed in fresh and aged medium, the stability of the *N*-PE-PanAm analogues towards pantetheinase-mediated degradation will be confirmed by incubation with recombinant pantetheinase (human VNN1). Three of the nine *N*-PE-PanAm analogues were tested by Dr. Cristiano Macuamule during his PhD study [13] in our laboratory and the remaining six *N*-PE-PanAm analogues were sent to Dr. Kevin Saliba's laboratory at The Australian National University, Canberra, Australia. The results of these tests are still outstanding and will therefore not be discussed here.

### 4.5.1 Biological testing of the methylated and deoxy *N*-PE-PanAm analogues

Three of the nine *N*-PE-PanAm analogues, namely α-Me-*N*-PE-PanAm **4.3**, β-Me-*N*-PE-PanAm **4.4** and (*R*/*S*)-4'-deoxy-*N*-PE-PanAm **4.19** were tested by Dr. Macuamule against *P. falciparum*. α-Me-*N*-PE-PanAm **4.3** showed excellent antiplasmodial activity against the chloroquine-sensitive strain *P. falciparum* 3D7 (chloroquine $IC_{50}$ = 11 ± 1 nM) in aged medium, with an $IC_{50}$ of 29 ± 2 nM, a value which is only slightly higher than that of *N*-PE-PanAm **4.1** (20 ± 2 nM) in the same medium. Furthermore, in fresh medium, α-Me-*N*-PE-PanAm **4.3** showed exceptional antiplasmodial activity with an $IC_{50}$ of 52 ± 6 nM, compared to *N*-PE-PanAm **4.1** ($IC_{50}$ ~ 6200 nM). α-Me-*N*-PE-PanAm **4.3** is thus more than 100-fold more potent in fresh medium compared to *N*-PE-PanAm **4.1**. This illustrates that α-Me-*N*-PE-PanAm **4.3** is resistant to degradation by pantetheinase; this stability was further confirmed by incubation with recombinant pantetheinase (human VNN1) for 24 h. α-Me-*N*-PE-PanAm **4.3** showed only a 26% ± 2% hydrolysis compared to the 96% ± 9% observed for *N*-PE-PanAm **4.1**. These results were published as part of an article in Antimicrobial Agents and Chemotherapy [2]; the manuscript is attached as an addendum.

β-Me-*N*-PE-PanAm **4.4** was tested in a similar manner. It showed increased antiplasmodial activity compared to *N*-PE-PanAm **4.1** in fresh medium with an $IC_{50}$ of 14 ± 1 µM. β-Me-*N*-PE-PanAm **4.4** also showed increased stability when incubated with recombinant pantetheinase, which correlates well with the limited degradation observed for α-Me-*N*-PE-PanAm **4.3**. However, compared to α-Me-*N*-PE-PanAm **4.3**, its antiplasmodial potency is roughly 1000-fold lower. This indicates that the placement of the methyl group is an important consideration for target selectivity.

The final compound that was tested, (*R*/*S*)-4'-deoxy-*N*-PE-PanAm **4.19** did not act as an inhibitor, given that even at 200 µM the *P. falciparum* growth was still more than 50%. This suggests that *Pf*PanK is predisposed to binding pantothenamides that act as alternative substrates, and therefore serves to metabolically activate the pantothenamides to exert an inhibitory effect by being converted into antimetabolites of CoA, thus targeting processes downstream. This result is currently being incorporated into another manuscript that will be submitted for publication in a peer reviewed journal.

## 4.6 Conclusion

Nine *N*-PE-PanAm analogues were successfully synthesized using various organic synthesis methods and all of the compounds were fully characterized synthetically. The methylated *N*-PE-PanAm analogues showed stability towards degradation by pantetheinase. The antiplasmodial activity of α-Me-*N*-PE-PanAm **4.3** was 1000-fold higher than what we observed for β-Me-*N*-PE-PanAm **4.4**, which indicates that the placement of the methyl group targets selectivity in *P. falciparum*. In Chapter 3 we saw that the structural modifications to N7-Pan resulted in a loss of target specificity towards *Sa*PanK-II. Therefore, it will be important to determine whether the *N*-PE-PanAm analogues are still on target.

## 4.7 Experimental section

### 4.7.1 Material and methods

The *N*-PE-PanAm analogues were dissolved in DMSO to yield stock solutions at a concentration of 50-200 mM. General chemicals and reagents were purchased from Sigma-Aldrich, Merck Chemicals (Darmstadt, Germany) or Acros Organics (ThermoFisher, Fair Lawn, NJ, USA) and were of the highest purity. Solvents used for reactions were CHROMASOLV HPLC grade solvents from Sigma-Aldrich, while the hexanes, DCM and EtOAc used for purification were purchased from Merck Chemicals. Dry DMF was prepared by shaking up over KOH, distilled under reduced pressure and a nitrogen atmosphere, and finally stored over 4 Å molecular sieves in the dark. Dry DCM was distilled from $CaH_2$ under a nitrogen atmosphere while dry THF was distilled from sodium under a nitrogen atmosphere.

All $^{1}H$ and $^{13}C$ NMR spectra were obtained using a 300 MHz Varian VNMRS (75 MHz for $^{13}C$), 400 MHz Varian Unity Inova (100 MHz for $^{13}C$) or 600 MHz Varian Unity Inova (150 MHz for $^{13}C$) instruments at CAF of the University of Stellenbosch. All chemical shifts (δ) were recorded using the residual solvent peak and reported in p.p.m. All HRMS were performed on a Waters API Q-TOF Ultima spectrometer (Waters, Milford, MA, USA) at the Mass Spectrometry unit of CAF.

## 4.7.2 Synthetic preparation of the *N*-phenethyl pantothenamide analogues

*α-Methyl-N-Phenethyl pantothenamide* (**4.3**) *(mixture of diastereomers)*

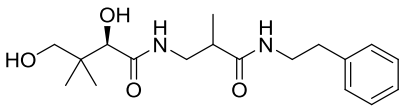

Phenethylamine (**4.2**) (163 µL, 1.29 mmol) and DPPA (278 µL, 1.29 mmol) were added to a solution of carboxylic acid **3.4** (250 mg, 1.07 mmol) in anhydrous DMF (4 mL) at rt under an inert atmosphere. After cooling the mixture to 0°C, $Et_3N$ (180 µL, 1.29 mmol) was added. The reaction mixture was stirred for an additional 2h at 0°C and left to stir overnight at rt. DMF was removed *in vacuo* and Amberlite IR400 ($OH^-$-form) resin was added (2.50 g). The reaction mixture was filtered and lyophilized before purification by FCC (10% MeOH in DCM) afforded amide **4.3** (188 mg, 52%) as a yellow oil. $R_f$ = 0.24 (FCC conditions). $\delta_H$ (600 MHz; $CDCl_3$; 25°C) 0.90 (3H, s, $-CH_3$, diastereomer A), 0.91 (3H, s, $-CH_3$, diastereomer B), 0.99 (3H, s, $-CH_3$, diastereomer A), 1.00 (3H, s, $-CH_3$, diastereomer B), 1.10 (3H, d, *J* = 7.1 Hz, $-CH_3$), 2.47-2.59 (1H, m, -CH-), 2.80 (2H, t, *J* = 7.1 Hz, $-CH_2$-), 3.28-3.38 (2H, m, $-CH_2$-), 3.42-3.49 (2H, m, $-CH_2$-), 3.51-3.58 (2H, m, $-CH_2$-), 3.98 (1H, apparent t, *J* = 5.1 Hz, -CH-, both diastereomers), 5.98 (1H, br s, -NH-), 7.17 (2H, d, *J* = 7.4 Hz, arom), 7.22 (1H, d, *J* = 7.3 Hz, arom), 7.25 (1H, br s, -NH-) and 7.30 (2H, dd, *J* = 7.3, 7.4 Hz, arom). O<u>H</u> protons not observed. $\delta_C$ (150 MHz; $CDCl_3$; 25°C) 15.7, 20.4, 20.4, 35.5, 40.6, 40.7, 42.1, 48.7, 70.8, 77.5, 126.6, 128.6, 128.7, 138.7, 173.7, and 175.0. (HRMS) $[M+H]^+$ 337.2124 (Calculated $[C_{18}H_{29}N_2O_4]^+$ = 337.2127).

*β-Methyl-N-Phenethyl pantothenamide* (**4.4**) *(mixture of diastereomers)*

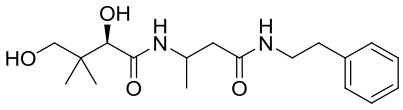

Phenethylamine (**4.2**) (590 µL, 4.68 mmol) and DPPA (1.01 mL, 4.68 mmol) were added to a solution of carboxylic acid **3.5** (910 mg, 3.90 mmol) in anhydrous DMF (6 mL) at rt under an inert atmosphere. After cooling the mixture to 0°C, $Et_3N$ (653 µL, 4.68 mmol) was added. The reaction mixture was stirred for an additional 2h at 0°C and left to stir overnight at rt. DMF was removed *in vacuo* and Amberlite IR400 ($OH^-$-form) resin was added (2.50 g). The reaction mixture was filtered and lyophilized before purification by FCC (10% MeOH in DCM) afforded amide **4.4** (398 mg, 30%) as a white solid. $R_f$ = 0.28 (FCC conditions). $\delta_H$ (300 MHz; $CDCl_3$; 25°C) 0.78 (3H, s, $-CH_3$, diastereomer A), 0.79 (3H, s, $-CH_3$, diastereomer B), 0.80 (3H, s, $-CH_3$, diastereomer A), 0.81 (3H, s, $-CH_3$, diastereomer B), 0.99 (3H, d, *J* = 6.2 Hz, $-CH_3$), 2.12-2.21 (1H, m, $-CH_2$-), 2.25-2.32 (1H, m, $-CH_2$-), 2.67 (2H, t, *J* = 7.6 Hz, $-CH_2$-), 3.15-3.23 (2H, m, $-CH_2$-), 3.25-3.33 (2H, m, $-CH_2$-), 3.66-3.69 (1H, m, -CH-), 4.06-4.17 (1H, m, -CH-, diastereomer A), 4.47-4.51 (1H, m, -CH-, diastereomer A), 7.19 (3H, m, arom), 7.26-7.31 (2H, m, arom), 7.61 (1H, d, *J* = 8.2 Hz, -NH-) and 7.96 (1H, q, *J* = 5.9, 12.3 Hz, -NH-). O<u>H</u> protons not observed. $\delta_C$ (75 MHz; $CDCl_3$; 25°C) 20.5, 20.8, 21.4, 35.6,

39.5, 41.7, 42.1, 42.2, 68.5, 75.4, 126.5, 128.8, 129.0, 139.9, 170.6 and 172.4. (HRMS) $[M+H]^+$ 337.2133 (Calculated $[C_{18}H_{29}N_2O_4]^+$ = 337.2127).

*N-Methyl-N-phenethyl pantothenamide* (**4.6**)

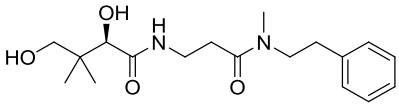

To a solution of thioester **3.20** (200 mg, 0.642 mmol) in $CH_3CN$ (7 mL) at rt was added *N*-methyl phenethylamine (**4.5**) (112 µL, 0.770 mmol). The reaction mixture was stirred overnight at 35°C. The reaction mixture was concentrated *in vacuo* before purification by FCC (5% MeOH in DCM) afforded amide **4.6** (178 mg, 82%) as a yellow oil. $R_f$ = 0.16 (FCC conditions). $\delta_H$ (600 MHz; $CDCl_3$; 25°C) 0.89 (3H, d, *J* = 14.6 Hz, -$CH_3$), 1.00 (3H, d, *J* = 9.4 Hz, -$CH_3$), 2.23 (1H, t, *J* = 5.9 Hz, -$CH_2$-), 2.51 (1H, t, *J* = 5.6 Hz, -$CH_2$-), 2.80-2.85 (2H, m, -$CH_2$-), 2.86 (3H, d, *J* = 24.9 Hz, -$CH_3$), 3.36-3.45 (1H, m, -$CH_2$-), 3.45-3.46 (1H, s, -$CH_2$-), 3.48-3.50 (2H, m, -$CH_2$-), 3.53-3.63 (2H, m, -$CH_2$-), 3.97 (1H, dd, *J* = 2.6, 8.2 Hz, -CH-), 7.13-7.32 (5H, m, arom) and 7.39 (1H, br t, -NH-). OH protons not observed. $\delta_C$ (150 MHz; $CDCl_3$; 25°C) 24.2, 24.2, 34.9, 35.8, 36.3, 38.6, 52.6, 54.2, 73.6, 80.1, 129.1, 131.2, 131.4, 141.4, 174.4 and 179.5. (HRMS) $[M+H]^+$ 337.2124 (Calculated $[C_{18}H_{29}N_2O_4]^+$ = 337.2127).

*(E)-3-Bromo-N-phenethylacrylamide* (**4.7**)

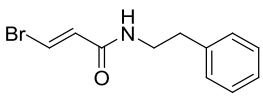

Phenethylamine (**4.2**) (1.00 mL, 7.95 mmol) and DMAP (130 mg, 1.06 mmol) were added to a solution of bromo acid **3.24** (800 mg, 5.30 mmol) in anhydrous DCM (15 mL) at rt under an inert atmosphere. The reaction mixture was cooled to 0°C before DIC (903 µL, 5.83 mmol) was added dropwise. The reaction mixture was warmed to rt and left to stir overnight. The reaction mixture was filtered through a pad of Celite and the solvent was removed *in vacuo*. The resulting crude residue was re-dissolved in EtOAc (50 mL) and the organic layer was washed with sat. aqueous $NaHCO_3$ (2 × 20 mL) and sat. aqueous NaCl (2 × 10 mL). The organic layer was dried ($Na_2SO_4$), filtered and concentrated *in vacuo* before purification by FCC (1:2 EtOAc: Hexanes) which afforded amide **4.7** (606 mg, 45%) as a pale yellow solid. $R_f$ = 0.32 (FCC conditions). $\delta_H$ (600 MHz; $CDCl_3$; 25°C) 2.83 (2H, t, *J* = 7.0 Hz, -$CH_2$-), 3.55 (2H, q, *J* = 7.0 Hz, -$CH_2$-), 5.77 (1H, br s, -NH-), 6.42 (1H, d, *J* = 13.5 Hz, -CH-), 7.18 (2H, d, *J* = 7.0 Hz, arom), 7.23 (1H, d, *J* = 7.0 Hz, arom), 7.30 (2H, t, *J* = 7.6 Hz, arom) and 7.14 (1H, d, *J* = 13.5 Hz, -CH-). $\delta_C$ (150 MHz; $CDCl_3$; 25°C) 38.0, 43.3, 125.4, 129.3, 131.4, 133.4, 141.2 and 166.2. (HRMS) $[M+H]^+$ 254.0174 (Calculated $[C_{11}H_{13}Br^{79}NO]^+$ = 254.0181) and $[M+H]^+$ 256.0164 (Calculated $[C_{11}H_{13}Br^{81}NO]^+$ = 256.0181).

*(R)-2,2,5,5-Tetramethyl-N-(3-oxo-3-(phenethylamino)prop-1-enyl)-1,3-dioxane-4-carboxamide* (**4.8**)

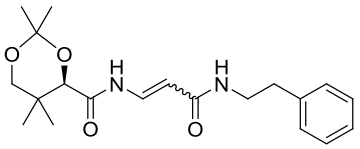

To an oven dried Schlenk tube were added $Pd(OAc)_2$ (53.0 mg, 0.236 mmol), Xantphos (205 mg, 0.354 mmol), $K_2CO_3$ (652 mg, 4.72 mmol), CTAB (172 mg, 0.472 mmol), amide **3.22** (450 mg, 2.36 mmol), bromide **4.7** (660 mg, 2.60 mmol) and anhydrous toluene (5.90 mL) at rt under an inert atmosphere. The reaction mixture was degassed by three alternating nitrogen/vacuum cycles until no further gas evolution was observed. The reaction mixture was stirred for 1h at 55°C after which $H_2O$ (128 µL, 7.11 mmol) was added and the reaction mixture was stirred for an additional 4h at 55°C. The resulting reaction mixture was cooled to rt, diluted with EtOAc (50 mL) and the organic layer was washed with $H_2O$ (2 × 15 mL). The organic layer was dried ($Na_2SO_4$), filtered and concentrated *in vacuo* before purification by FCC (1:1 EtOAc: Hexanes) afforded (*E*)- and (*Z*)-amide **4.8** in a combined yield of 40% as a yellow solids (*E*:*Z* ratio of 6:1).

(*E*)-amide **4.8**. $R_f$ = 0.16 (FCC conditions). $\delta_H$ (600 MHz; $CDCl_3$; 25°C) 0.99 (3H, s, $-CH_3$), 1.04 (3H, s, $-CH_3$), 1.44 (3H, s, $-CH_3$), 1.49 (3H, s, $-CH_3$), 2.82 (2H, t, *J* = 7.0 Hz, $-CH_2-$), 3.29 (1H, d, *J* = 11.7 Hz, $-CH_2-$), 3.58 (2H, q, *J* = 6.5 Hz, $-CH_2-$), 3.69 (1H, d, *J* = 11.7 Hz, $-CH_2-$), 4.17 (1H, s, -CH-), 5.49 (1H, br t, *J* = 5.3 Hz, -NH-), 5.73 (1H, d, *J* = 14.1 Hz, -CH-), 7.18-7.27 (3H, m, arom), 7.29 (2H, t, *J* = 7.6 Hz, arom), 7.76 (1H, dd, *J* = 10.8, 13.8 Hz, -CH-) and 8.26 (1H, br d, *J* = 11.1 Hz, -NH-). $\delta_C$ (150 MHz; $CDCl_3$; 25°C) 21.3, 21.4, 23.7, 24.5, 36.0, 38.3, 43.2, 73.9, 102.1, 108.7, 129.1, 130.7, 131.3, 131.4, 135.5, 141.6, 168.7 and 170.7. (HRMS) $[M+H]^+$ 361.2126 (Calculated $[C_{20}H_{29}N_2O_4]^+$ = 361.2127).

(*Z*)-amide **4.8**. $R_f$ = 0.54 (FCC conditions). $\delta_H$ (400 MHz; $CDCl_3$; 25°C) 1.05 (6H, s, $-(CH_3)_2$), 1.46 (3H, s, $-CH_3$), 1.62 (3H, s, $-CH_3$), 2.81 (2H, t, *J* = 7.03 Hz, $-CH_2-$), 3.30 (1H, d, *J* = 11.7 Hz, $-CH_2-$), 3.54-3.62 (2H, m, $-CH_2-$), 3.70 (1H, d, *J* = 10.9 Hz, $-CH_2-$), 4.19 (1H, s, -CH-), 4.93 (1H, d, *J* = 9.4 Hz, -CH-), 5.54 (1H, br t, *J* = 5.5 Hz, -NH-), 7.18-7.34 (6H, m, arom and -CH-) and 11.7 (1H, br d, *J* = 10.9 Hz, -NH-). $\delta_C$ (100 MHz; $CDCl_3$; 25°C) 18.9, 19.3, 22.2, 29.6, 29.6, 33.5, 35.9, 40.4, 71.6, 99.5, 100.8, 126.8, 128.8, 128.9, 133.5, 139.0, 168.0 and 169.1. (HRMS) $[M+H]^+$ 361.2122 (Calculated $[C_{20}H_{29}N_2O_4]^+$ = 361.2127).

*(E)-N-Phenethyl CJ-pantothenamide* (**(*E*)-4.9**)

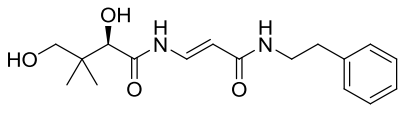

To a solution of acetonide (*E*)-**4.8** (270 mg, 0.749 mmol) in $CH_3CN$ (6.2 mL) at rt were added $H_2O$ (270 µL, 15.0 mmol) and $BiCl_3$ (47.3 mg, 0.150 mmol). The reaction mixture was stirred overnight at rt. The reaction mixture was filtered through a pad of Celite and the solvent was

removed *in vacuo*. The resulting crude residue was re-dissolved in EtOAc (20 mL) and the organic layer was washed with sat. aqueous $NaHCO_3$ (2 × 10 mL). The aqueous layer was extracted with EtOAc (1 × 10 mL) and the combined organic layers were dried ($Na_2SO_4$), filtered and concentrated *in vacuo* before purification by FCC (100% EtOAc) afforded hydroxyl (*E*)-**4.9** (31.2 mg, 13%) as a white solid. $R_f$ = 0.28 (FCC conditions). $\delta_H$ (300 MHz; DMSO-$d_6$; 25°C) 0.80 (3H, s, -$CH_3$), 0.83 (3H, s, -$CH_3$), 2.70 (2H, t, *J* = 7.3 Hz, -$CH_2$-), 3.14 (1H, dd, *J* = 5.3, 10.0 Hz, -$CH_2$-), 3.29 (2H, t, *J* = 5.6 Hz, -$CH_2$-), 3.86 (1H, d, *J* = 5.3 Hz, -CH-), 4.51 (1H, t, *J* = 5.6 Hz, -CH-) 5.84 (1H, d, *J* = 14.1 Hz, -CH-), 7.19-7.22 (3H, m, arom), 7.27-7.31 (2H, m, arom), 7.57 (1H, dd, *J* = 10.9, 13.8 Hz, -CH-), 7.90 (1H, br t, *J* = 5.6 Hz, -NH-) and 10.2 (1H, br d, *J* = 10.6 Hz, -NH-). O<u>H</u> protons not observed. $\delta_C$ (75 MHz; DMSO-$d_6$; 25°C) 20.4, 21.6, 35.7, 39.7, 40.8, 67.9, 75.4, 105.7, 126.5, 128.7, 129.1, 133.4, 140.1, 166.5 and 173.0. (HRMS) $[M+H]^+$ 321.1818 (Calculated $[C_{17}H_{25}N_2O_4]^+$ = 321.1814).

*(Z)-N-Phenethyl CJ-pantothenamide* (**(*Z*)-4.9**)

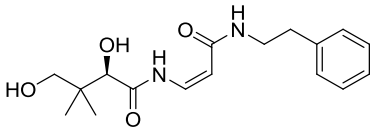

To a solution of acetonide (*Z*)-**4.8** (60.0 mg, 0.166 mmol) in $CH_3CN$ (1.5 mL) at rt were added $H_2O$ (59.9 µL, 3.33 mmol) and $BiCl_3$ (10.5 mg, 33.3 µmol). The reaction mixture was stirred overnight at rt. The reaction mixture was filtered through a pad of Celite and the solvent was removed *in vacuo*. The resulting crude residue was re-dissolved in EtOAc (15 mL) and the organic layer was washed with sat. aqueous $NaHCO_3$ (2 × 10 mL). The aqueous layer was extracted with EtOAc (1 × 10 mL) and the combined organic layers were dried ($Na_2SO_4$), filtered and concentrated *in vacuo* before purification by FCC (2:1 EtOAc: Hexanes) afforded hydroxyl (*Z*)-**4.9** (24.6 mg, 46%) as a yellow oil. $R_f$ = 0.30 (FCC conditions). $\delta_H$ (400 MHz; DMSO-$d_6$; 25°C) 0.77 (3H, s, -$CH_3$), 0.82 (3H, s, -$CH_3$), 2.70 (2H, t, *J* = 7.4 Hz, -$CH_2$-), 3.15 (1H, dd, *J* = 5.1, 10.5 Hz, -$CH_2$-), 3.29-3.37 (2H, m, -$CH_2$-), 3.85 (1H, d, *J* = 5.5 Hz, -CH-), 4.50 (1H, t, *J* = 5.3 Hz, -CH-) 5.88 (1H, d, *J* = 4.7 Hz, -CH-), 7.11 (1H, dd, *J* = 9.0, 11.3 Hz, -CH-), 7.16-7.21 (3H, m, arom), 7.26-7.29 (2H, m, arom), 8.09 (1H, br t, *J* = 5.9 Hz, -NH-) and 11.8 (1H, br d, *J* = 11.7 Hz, -NH-). O<u>H</u> protons not observed. $\delta_C$ (100 MHz; $CDCl_3$; 25°C) 20.6, 21.7, 35.9, 40.1, 40.8, 68.1, 75.2, 100.9, 126.8, 129.0, 129.3, 133.1, 140.1, 168.3 and 172.7. (HRMS) $[M+H]^+$ 321.1827 (Calculated $[C_{17}H_{25}N_2O_4]^+$ = 321.1814).

*(R,E)-N-(3-(2-Benzylidenehydrazinyl)-3-oxopropyl)-2,4-dihydroxy-3,3-dimethylbutanamide* (**4.11**)

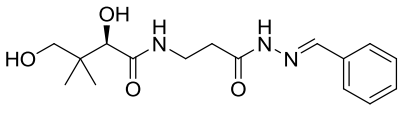

To a solution of hydrazide **3.30** (301 mg, 1.29 mmol) in anhydrous EtOH (15 mL) at rt under an inert atmosphere was added benzaldehyde (**4.10**) (197 µL, 1.94 mmol). The reaction mixture was stirred at reflux for 48h. The reaction mixture was cooled to rt and concentrated *in*

*vacuo* before purification by FCC (10% MeOH in DCM) afforded imine **4.11** (300 mg, 72%) as a yellow solid. $R_f$ = 0.38 (FCC conditions). $\delta_H$ (400 MHz; $CDCl_3$; 25°C) 0.91 (3H, s, -$CH_3$), 0.99 (3H, s, -$CH_3$), 2.99-3.04 (2H, m, -$CH_2$-), 3.48 (2H, s, -$CH_2$-), 3.62-3.72 (2H, m, -$CH_2$-), 4.01 (1H, s, -CH-), 7.38-7.43 (3H, m, arom), 7.45 (1H, br d, *J* = 7.8 Hz, -NH-), 7.62-7.64 (2H, m, arom), 7.82 (1H, s, -CH-) and 9.60 (1H, br s, -NH-). O<u>H</u> protons not observed. $\delta_C$ (100 MHz; $CDCl_3$; 25°C) 20.6, 21.7, 33.0, 34.6, 39.6, 71.2, 77.7, 127.5, 129.0, 130.6, 133.6, 144.9, 173.5 and 174.7. (HRMS) $[M+H]^+$ 322.1762 (Calculated $[C_{16}H_{24}N_3O_4]^+$ = 322.1767).

*N-Benzyl pantothenhydrazide* (**4.12**)

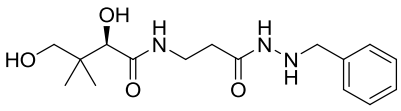

To a solution of imine **4.11** (280 mg, 0.871 mmol) in MeOH (6mL) and DCM (4 mL) at rt was added $NaBH_3CN$ (66.0 mg, 1.05 mmol). The reaction mixture was acidified to pH 3 by the addition of 3 M aqueous HCl and the resulting solution was stirred at rt for 0.5h. Subsequently, the reaction mixture was acidified to pH 1 and the reaction mixture was stirred for an additional 5h at rt. The reaction was quenched by the addition of sat. aqueous $NaHCO_3$ (10 mL) and the resulting solution was filtered and concentrated *in vacuo*. The resulting crude residue was re-dissolved in EtOAc (40 mL) and the organic layer was washed with $H_2O$ (2 × 20 mL) and sat. aqueous NaCl (2 × 20 mL). The organic layer was dried ($Na_2SO_4$), filtered and concentrated *in vacuo* before purification by FCC (10% MeOH in DCM) afforded hydrazide **4.12** (19.4 mg, 7%) as a yellow oil. $R_f$ = 0.34 (FCC conditions). $\delta_H$ (300 MHz; $CDCl_3$; 25°C) 0.88 (3H, s, -$CH_3$), 0.93 (3H, s, -$CH_3$), 2.31 (2H, t, *J* = 6.0 Hz, -$CH_2$-) 3.40 (2H, d, *J* = 4.4 Hz, -$CH_2$-), 3.38-3.52 (2H, m, -$CH_2$-), 3.91 (2H, s, -$CH_2$-), 3.93 (1H, s, -CH-), 7.25 (1H, br s, -NH-), 7.27-7.32 (5H, m, arom), 7.43 (1H, br t, *J* = 5.9 Hz, -NH-) and 8.32 (1H, br s, -NH-). O<u>H</u> protons not observed. $\delta_C$ (75 MHz; $CDCl_3$; 25°C) 20.6, 21.2, 33.9, 35.3, 39.3, 55.9, 70.4, 76.9, 127.7, 128.6, 128.9, 137.1, 170.8 and 174.2. (HRMS) $[M+H]^+$ 324.1924 (Calculated $[C_{16}H_{26}N_3O_4]^+$ = 324.1923).

*Benzyl 3-oxo-3-(phenethylamino)propylcarbamate* (**4.13**)

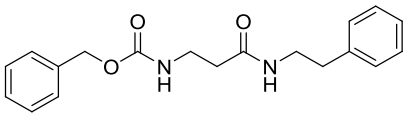

Phenethylamine (**4.2**) (621 µL, 4.93 mmol) and DEPC (748 µL, 4.93 mmol) were added to a solution of Cbz-β-alanine (**3.14**) (1.00 g, 4.48 mmol) in anhydrous DMF (7 mL) at rt under an inert atmosphere. The reaction mixture was cooled to 0°C before $Et_3N$ (1.31 mL, 9.41 mmol) was added. The reaction mixture was stirred for 2h at 0°C and left to stir overnight at rt. EtOAc (50 mL) was added and the organic layer was washed with 5% aqueous citric acid (3 × 10 mL), 1 M aqueous $NaHCO_3$ (2 × 10 mL) and sat. aqueous NaCl (1 × 10 mL). The organic layer was dried ($Na_2SO_4$), filtered and concentrated *in vacuo* to afford carbamate **4.13** (1.45 g, 99%) as a white

solid. $R_f$ = 0.30 (3:1 EtOAc: Hexanes). $\delta_H$ (300 MHz; $CDCl_3$; 25°C) 2.34 (2H, t, *J* = 5.9 Hz, -$CH_2$-), 2.78 (2H, t, *J* = 6.9 Hz, -$CH_2$-), 3.43 (2H, q, *J* = 6.2 Hz, -$CH_2$-), 3.48 (2H, q, *J* = 7.0 Hz, -$CH_2$-), 5.09 (2H, s, -$CH_2$-), 5.38 (1H, br s, -NH-), 5.52 (1H, br s, -NH-) and 7.16-7.36 (10H, m, arom). $\delta_C$ (75 MHz; $CDCl_3$; 25°C) 35.6, 36.0, 37.2, 40.6, 66.6, 126.6, 128.0, 128.5, 128.6, 136.6, 138.8, 156.6 and 171.3. (HRMS) $[M+H]^+$ 327.1705 (Calculated $[C_{19}H_{23}N_2O_3]^+$ = 327.1709).

*Benzyl 3-(phenethylamino)-3-thioxopropylcarbamate* (**4.14**)

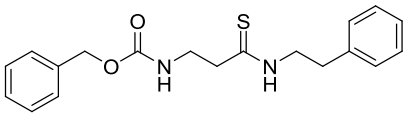

To a solution of amide **4.13** (1.00 g, 3.06 mmol) in anhydrous toluene (50 mL) at rt under an inert atmosphere was added Lawesson's reagent (1.36 g, 3.37 mmol). The reaction mixture was stirred at reflux overnight. The reaction mixture was cooled to rt, diluted with EtOAc (100 mL) and washed with 10% aqueous NaOH (3 × 30 mL) and sat. aqueous NaCl (1 × 40 mL). The organic layer was dried ($MgSO_4$), filtered and concentrated *in vacuo* before purification by FCC (2% MeOH in DCM) afforded thioamide **4.14** (531 mg, 51%) as a yellow solid. $R_f$ = 0.19 (FCC conditions). $\delta_H$ (600 MHz; $CDCl_3$; 25°C) 2.75 (2H, apparent t, *J* = 4.7 Hz, -$CH_2$-), 2.93 (2H, t, *J* = 7.0 Hz, -$CH_2$-), 3.58 (2H, q, *J* = 6.4, 12.3 Hz, -$CH_2$-), 3.89 (2H, q, *J* = 6.2 Hz, -$CH_2$-), 5.07 (2H, s, -$CH_2$-), 5.34 (1H, br s, -NH-), 7.17-7.25 (4H, m, arom), 7.29-7.37 (6H, m, arom) and 7.57 (1H, br s, -NH-). $\delta_C$ (150 MHz; $CDCl_3$; 25°C) 35.5, 39.0, 44.6, 49.4, 69.4, 129.1, 130.7, 131.0, 131.6, 139.0, 141.0, 153.7 and 204.8. (HRMS) $[M+H]^+$ 343.1480 (Calculated $[C_{19}H_{23}N_2O_2S]^+$ = 343.1480).

*3-Amino-N-phenethylpropanethioamide* (**4.15**)

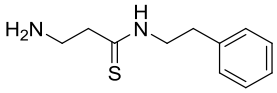

To a solution of carbamate **4.14** (520 mg, 1.52 mmol) in MeOH (11 mL) was added concentrated HCl (11 mL) and the resulting solution was stirred at reflux overnight. The reaction mixture was cooled to rt and quenched by the addition of $H_2O$ (35 mL). The aqueous solution was extracted with DCM (3 × 20 mL) after which the aqueous phase was lyophilized to yield the HCl salt of amine **4.15** (390 mg, >100%) as a white-yellow powder which was subsequently used in the next step without any further purification.

*N-Phenethyl pantothenthioamide* (**4.16**)

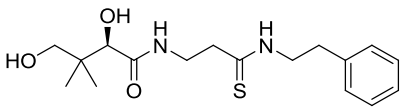

$Et_3N$ (886 µL, 6.36 mmol) and (*R*)-(-)-pantolactone **3.3** (414 mg, 3.18 mmol) were added to a solution of amine **4.15** (310 mg, 1.27 mmol) in EtOH (15 mL) and the resulting solution was stirred at reflux for 48h. The reaction mixture was cooled to rt and the solvent was removed *in vacuo*. The crude residue was purified by FCC (10% MeOH in DCM) to afford amide **4.16** (130 mg, 30%) as a yellow oil. $R_f$ = 0.51 (FCC conditions). $\delta_H$ (600 MHz; $CDCl_3$; 25°C) 0.85 (3H, s, -$CH_3$), 0.98 (3H, s,

-$CH_3$), 2.83 (2H, t, *J* = 7.3 Hz, -$CH_2$-), 3.42 (2H, d, *J* = 2.3 Hz, -$CH_2$-), 3.49-3.55 (4H, m, -$(CH_2)_2$-), 3.59-3.64 (2H, m, -$CH_2$-), 3.99 (1H, s, -CH-), 6.80 (1H, br s, -NH-), 7.02 (3H, t, *J* = 7.0 Hz, arom), 7.24 (1H, br s, -NH-) and 7.29 (2H, t, *J* =7.6 Hz, arom). OH protons not observed. $\delta_C$ (150 MHz; $CDCl_3$; 25°C) 22.6, 24.1, 38.3, 41.9, 42.7, 42.8, 47.5, 73.9, 80.3, 129.2, 131.2, 131.3, 141.2, 175.5 and 204.8. (HRMS) $[M+H]^+$ 339.1746 (Calculated $[C_{17}H_{27}N_2O_3S]^+$ = 339.1742).

*3-Amino-N-phenethylpropanamide* (**4.17**)

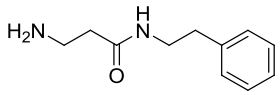

To a solution of carbamate **4.13** (950 mg, 2.91 mmol) in MeOH (50 mL) at rt was added 10% Pd/C (124 mg, 1.16 mmol). The reaction atmosphere was filled with $H_2$ gas and the reaction mixture was stirred overnight at rt. The reaction mixture was filtered and concentrated *in vacuo* to give amine **4.17** (550 mg, 98%) as a white-yellow solid. $R_f$ = product on baseline (10% MeOH in DCM). $\delta_H$ (600 MHz; $CDCl_3$; 25°C) 1.55 (2H, br s, -$NH_2$), 2.27 (2H, t, *J* = 6.0 Hz, -$CH_2$-), 2.80 (2H, t, *J* = 7.0 Hz, -$CH_2$-), 2.94 (2H, t, *J* = 6.0 Hz, -$CH_2$-), 3.49 (2H, q, *J* = 7.0 Hz, -$CH_2$-), 6.98 (1H, br s, -NH-), 7.19-7.24 (3H, m, arom) and 7.27-7.33 (2H, m, arom). $\delta_C$ (150 MHz; $CDCl_3$; 25°C) 38.3, 40.7, 41.0, 43.0, 129.0, 131.1, 131.4, 141.0 and 175.0 (HRMS) $[M+H]^+$ 193.1343 (Calculated $[C_{11}H_{17}N_2O]^+$ = 193.1341).

*3,3-Dimethyl-2-oxo-N-(3-oxo-3-(phenethylamino)propyl)pentanamide* (**4.18**)

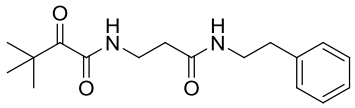

DIPEA (449 µL, 2.58 mmol) was added drop-wise over 5 min to a solution of amine **4.17** (480 mg, 2.50 mmol) in DCM (20 mL) at 0°C under an inert atmosphere. HOBt (59.3 mg, 0.439 mmol), carboxylic acid **3.46** (358 mg, 2.75 mmol) and EDC hydrochloride (480 mg, 2.50 mmol) were then added consecutively and the reaction mixture was stirred overnight at rt. The reaction was quenched by the addition of 3 M aqueous HCl (25 mL) and the organic layer was washed with 3 M aqueous HCl (1 × 25 mL) and sat. aqueous $NaHCO_3$ (1 × 25 mL). The organic layer was dried ($Na_2SO_4$), filtered and concentrated *in vacuo* before purification by FCC (2:1 EtOAc: Hexanes) afforded amide **4.18** (150 mg, 20%) as a white powder. $R_f$ = 0.35 (FCC conditions). $\delta_H$ (300 MHz; $CDCl_3$; 25°C) 1.32 (9H, s, -$(CH_3)_3$), 2.35 (2H, t, *J* = 6.0 Hz, -$CH_2$-), 2.79 (2H, t, *J* = 7.0 Hz, -$CH_2$-), 3.49-3.57 (4H, m, -$(CH_2)_2$-), 5.63 (1H, br s, -NH-), 7.15-7.26 (3H, m, arom), 7.28-7.33 (2H, m, arom) and 7.49 (1H, br s, -NH-). $\delta_C$ (100 MHz; $CDCl_3$; 25°C) 26.5, 35.3, 35.5, 35.8, 40.9, 43.1, 126.8, 128.8, 128.9, 138.9, 160.6, 171.0 and 203.3. (HRMS) $[M+H]^+$ 305.1874 (Calculated $[C_{17}H_{25}N_2O_3]^+$ = 305.1865).

*(R/S)-4'-Deoxy N-phenethyl pantothenamide* (**4.19**)

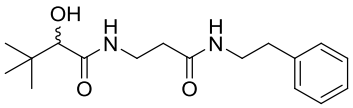

To a solution of ketoamide **4.18** (150 mg, 0.493 mmol) in anhydrous MeOH (10 mL) at 0°C under an inert atmosphere was added $NaBH_4$ (28.0 mg, 0.739 mmol) in small portions. The reaction mixture was stirred for 1h at 0°C, and left to stir overnight at rt. The reaction was quenched at 0°C by the addition of sat. aqueous $NH_4Cl$ (10 mL) and the MeOH was removed *in vacuo*. The aqueous solution was extracted with EtOAc (3 × 15 mL) and the combined organic extracts were dried ($Na_2SO_4$), filtered and concentrated *in vacuo* to yield hydroxyl **4.19** (143 mg, 94 %) as a white solid. $R_f$ = 0.35 (10% MeOH in DCM). $\delta_H$ (600 MHz; $CDCl_3$; 25°C) 0.98 (9H, s, -$(CH_3)_3$), 2.36 (2H, t, *J* = 6.0 Hz, -$CH_2$-), 2.80 (2H, t, *J* = 6.9 Hz, -$CH_2$-), 3.50-3.60 (4H, m, -$(CH_2)_2$-), 3.64 (1H, d, *J* = 5.3 Hz, -CH-), 5.63 (1H, br s, -NH-), 6.80 (1H, br s, -NH-), 7.18-7.25 (3H, m, arom) and 7.30-7.36 (2H, m, arom). O<u>H</u> proton not observed. $\delta_C$ (150 MHz; $CDCl_3$; 25°C) 28.6, 37.6, 37.8, 38.2, 38.2, 43.3, 82.1, 129.2, 131.2, 131.3, 141.2, 173.9 and 175.5. (HRMS) $[M+H]^+$ 307.2023 (Calculated $[C_{17}H_{27}N_2O_3]^+$ = 307.2022).

*Benzyl 3-hydroxy-2,2-dimethyl-4-oxo-4-(3-oxo-3-(phenethylamino)propylamino) butyl-carbamate* (**4.20**)

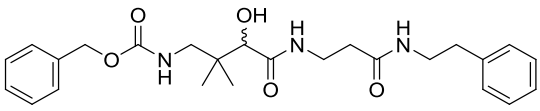

DIPEA (149 µL, 0.857 mmol) was added drop-wise over 5 min to a solution of amine **4.17** (160 mg, 0.832 mmol) in DCM (15 mL) at 0°C under an inert atmosphere. HOBt (31.9 mg, 0.208 mmol), carboxylic acid **3.70** (257 mg, 0.915 mmol) and EDC hydrochloride (175 mg, 0.915 mmol) were then added consecutively and the reaction mixture was stirred overnight at rt. The reaction mixture was concentrated *in vacuo* before purification by FCC (6:1 EtOAc: Hexanes) afforded amide **4.20** (140 mg, 37%) as a yellow oil. $R_f$ = 0.34 (FCC conditions). $\delta_H$ (300 MHz; $CDCl_3$; 25°C) 0.86 (3H, s, -$CH_3$), 1.03 (3H, s, -$CH_3$), 2.36 (2H, t, *J* = 5.6 Hz, -$CH_2$-), 2.78 (2H, t, *J* = 7.0 Hz, -$CH_2$-), 3.42-3.58 (4H, m, -$(CH_2)_2$-), 3.77 (1H, d, *J* = 5.0 Hz, -CH-), 5.09 (2H, d, *J* = 2.3 Hz, -$CH_2$-), 5.21 (1H, br t, *J* = 6.5 Hz, -NH-), 5.80 (1H, br t, *J* = 6.5 Hz, -NH-), 7.18-7.25 (3H, m, arom), 7.26-7.40 (7H, m, arom) and 7.42 (1H, br t, *J* = 6.6 Hz, -NH-). O<u>H</u> proton not observed. $\delta_C$ (75 MHz; $CDCl_3$; 25°C) 20.4, 21.9, 35.1, 35.6, 36.1, 39.4, 40.7, 49.6, 67.3, 74.6, 126.5, 128.1, 128.3, 128.5, 128.6, 128.7, 136.0, 138.7, 158.1, 171.0 and 172.6. (HRMS) $[M+H]^+$ 456.2511 (Calculated $[C_{25}H_{34}N_3O_5]^+$ = 456.2498).

*(R/S)-4'-Amino N-phenethyl pantothenamide* (**4.21**)

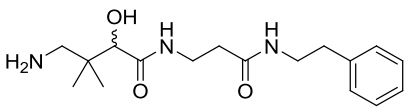

To a solution of carbamate **4.20** (120 mg, 0.263 mmol) in MeOH (10 mL) at rt was added 10% Pd/C (11.2 mg, 0.105 mmol). The

reaction atmosphere was filled with $H_2$ gas and the reaction mixture was stirred overnight at rt. The reaction mixture was filtered and concentrated *in vacuo* to give amine **4.21** (65.5 mg, 78%) as a yellow oil. $R_f$ = product on baseline (6:1 EtOAc: Hexanes). $\delta_H$ (600 MHz; $CDCl_3$; 25°C) 0.94 (3H, s, -$CH_3$), 1.03 (3H, s, -$CH_3$), 2.38 (2H, t, *J* = 6.2 Hz, -$CH_2$-), 2.78 (2H, s, -$CH_2$-), 2.79 (2H, apparent t, *J* = 6.9 Hz, -$CH_2$-), 3.18 (2H, br s, -$NH_2$), 3.41-3.59 (4H, m, -$(CH_2)_2$-), 4.03 (1H, s, -CH-), 6.08 (1H, br t, *J* = 5.4 Hz, -NH-), 7.18-7.25 (3H, m, arom), 7.28-7.34 (2H, m, arom) and 7.52 (1H, br t, *J* = 6.0 Hz, -NH-). O<u>H</u> proton not observed. $\delta_C$ (150 MHz; $CDCl_3$; 25°C) 22.2, 26.5, 37.6, 38.3, 38.9, 39.1, 43.3, 55.6, 83.3, 129.1, 131.2, 131.3, 141.4, 173.7 and 175.7. (HRMS) $[M+H]^+$ 322.2139 (Calculated $[C_{17}H_{28}N_3O_3]^+$ = 322.2131).

*N-Phenethyl pantothenamide 4'-O,O-dibenzylphosphate* (**4.22**)

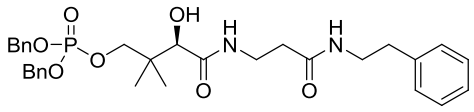

Dibenzyl chlorophosphate **3.72** was prepared *in situ* by reacting *N*-chlorosuccinimide (373 mg, 2.79 mmol) and dibenzylphosphite (732 mg, 2.79 mmol) in anhydrous toluene (4 mL) under an inert atmosphere for 2h at rt. The reaction mixture was filtered to remove the succinimide. To a solution of hydroxyl **4.1** (300 mg, 0.931 mmol) in anhydrous pyridine (5 mL) at -40°C under an inert atmosphere was added dibenzyl chlorophosphate **3.72** drop-wise with stirring. The reaction mixture was stirred for an additional 2h at -40°C and the mixture was placed in the -20°C freezer overnight. The reaction mixture was allowed to warm to rt and was subsequently quenched with $H_2O$ (3 mL) and concentrated *in vacuo*. The resulting crude residue was re-dissolved in EtOAc (40 mL) and the organic layer was washed with 1 M aqueous $H_2SO_4$ (2 × 10 mL), 1 M aqueous $NaHCO_3$ (2 × 10 mL) and sat. aqueous $Na_2SO_4$ (1 × 10 mL). The organic layer was dried ($Na_2SO_4$), filtered and concentrated *in vacuo* before purification by FCC (5% MeOH in DCM) afforded **4.22** (150 mg, 28%) as a yellow oil. $R_f$ = 0.11 (FCC conditions). $\delta_H$ (600 MHz; $CDCl_3$; 25°C) 0.80 (3H, s, -$CH_3$), 1.04 (3H, s, -$CH_3$), 2.34 (2H, t, *J* = 4.3 Hz, -$CH_2$-), 2.76 (2H, t, *J* = 7.2 Hz, -$CH_2$-), 3.44-3.52 (4H, m, -$(CH_2)_2$-), 3.55 (1H, dd, *J* = 7.6, 10.3 Hz, -$CH_2$-), 3.88 (1H, s, -CH-), 3.98 (1H, dd, *J* = 6.9, 9.5 Hz, -$CH_2$-), 5.03 (2H, d, *J* = 8.8 Hz, -$CH_2$-), 5.05 (2H, d, *J* = 8.2 Hz, -$CH_2$-), 6.16 (1H, br t, *J* = 5.6 Hz, -NH-), 7.02 (1H, br s, -NH-), 7.16-7.23 (5H, m, arom) and 7.28-7.38 (10H, m, arom). O<u>H</u> proton not observed. $\delta_C$ (150 MHz; $CDCl_3$; 25°C) 19.4, 21.9, 36.0, 36.3, 36.7, 40.1, 41.4, 70.4, 70.5, 74.2, 74.3, 120.9, 124.3, 127.2, 128.7, 129.3, 129.4, 136.0, 139.5, 171.8 and 173.2. $\delta_P$ (161.9 MHz; $CDCl_3$; 25°C) 0.79. (HRMS) $[M+H]^+$ 583.2575 (Calculated $[C_{31}H_{40}N_2O_7P]^+$ = 583.2573).

*4'-Phospho-N-phenethyl pantothenamide* (**4.23**)

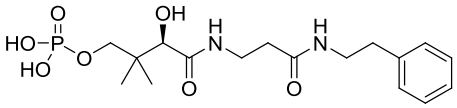

To a solution of **4.22** (120 mg, 0.206 mmol) in MeOH (9 mL) and $H_2O$ (1 mL) at rt was added 10% Pd/C (31.3 mg, 0.294 mmol). The reaction atmosphere was filled with $H_2$ gas and the reaction mixture was stirred overnight at rt. The reaction mixture was filtered and concentrated *in vacuo* to give hydroxyl **4.23** (82.3 mg, 99%) as a clear oil. $R_f$ = 0.06 (10% MeOH in DCM). $\delta_H$ (300 MHz; $D_2O$; 25°C) 0.76 (3H, s, -$CH_3$), 0.83 (3H, s, -$CH_3$), 2.26 (2H, t, *J* = 6.7 Hz, -$CH_2$-), 2.66 (2H, t, *J* = 6.7 Hz, -$CH_2$-), 3.25-3.37 (4H, m, -$(CH_2)_2$-), 3.48 (1H, dd, *J* = 5.0, 9.7 Hz, -$CH_2$-), 3.68 (1H, dd, *J* = 4.7, 10.0 Hz, -$CH_2$-), 3.87 (1H, s, -CH-), 7.14-7.18 (2H, m, arom) and 7.22-7.30 (3H, m, arom). O<u>H</u> protons not observed. $\delta_C$ (75 MHz; $D_2O$; 25°C) 19.2, 21.2, 35.1, 36.1, 38.9, 39.0, 41.2, 72.1, 75.0, 127.2, 129.3, 129.5, 139.8, 174.3 and 175.4. $\delta_P$ (161.9 MHz; $D_2O$; 25°C). (HRMS) $[M+H]^+$ 403.1625 (Calculated $[C_{17}H_{28}N_2O_7P]^+$ = 403.1634).

## 4.8 References

1. Flannery, E. L., Fidock, D. A. and Winzeler, E. A., Using genetic methods to define the targets of compounds with antimalarial activity. *Journal of Medicinal Chemistry*, 2013**. 56** (20), 7761-7771.
2. Macuamule, C. J., Tjhin, E. T., Jana, C. E., Barnard, L., Koekemoer, L., de Villiers, M., Saliba, K. J. and Strauss, E., A pantetheinase-resistant pantothenamide with potent, on-target, and selective antiplasmodial activity. *Antimicrobial Agents & Chemotherapy*, 2015**. 59** (6), 3666-3668.
3. Fletcher, S. and Avery, V. M., A novel approach for the discovery of chemically diverse anti-malarial compounds targeting the *Plasmodium falciparum* coenzyme A synthesis pathway. *Malaria Journal*, 2014**. 13**, 343.
4. Cowman, A. F., Berry, D. and Baum, J., The cellular and molecular basis for malaria parasite invasion of the human red blood cell. *The Journal of Cell Biology*, 2012**. 198** (6), 961-971.
5. Spry, C., Kirk, K. and Saliba, K. J., Coenzyme A biosynthesis: An antimicrobial drug target. *FEMS Microbiology Reviews*, 2008**. 32** (1), 56-106.
6. Miotto, O., Almagro-Garcia, J., Manske, M., Macinnis, B., Campino, S., Rockett, K. A., Amaratunga, C., Lim, P., Suon, S., Sreng, S., Anderson, J. M., Duong, S., Nguon, C., Chuor, C. M., Saunders, D., Se, Y., Lon, C., Fukuda, M. M., Amenga-Etego, L., Hodgson, A. V., Asoala, V., Imwong, M., Takala-Harrison, S., Nosten, F., Su, X. Z., Ringwald, P., Ariey, F., Dolecek, C., Hien, T. T., Boni, M. F., Thai, C. Q., Amambua-Ngwa, A., Conway, D. J., Djimde, A. A., Doumbo, O. K., Zongo, I., Ouedraogo, J. B., Alcock, D., Drury, E., Auburn, S., Koch, O., Sanders, M., Hubbart, C., Maslen, G., Ruano-Rubio, V., Jyothi, D., Miles, A., O'Brien, J., Gamble, C., Oyola, S. O., Rayner, J. C., Newbold, C. I., Berriman, M., Spencer, C. C., McVean, G., Day, N. P., White, N. J., Bethell, D., Dondorp, A. M., Plowe, C. V., Fairhurst, R. M. and Kwiatkowski, D. P., Multiple populations of artemisinin-resistant *Plasmodium falciparum* in Cambodia. *Nature Genetics*, 2013**. 45** (6), 648-655.
7. Prigge, S. T., He, X., Gerena, L., Waters, N. C. and Reynolds, K. A., The initiating steps of a type II fatty acid synthase in *Plasmodium falciparum* are catalyzed by *pf*ACP, *pf*MCAT, and *pf*KASIII. *Biochemistry*, 2003**. 42** (4), 1160-1169.
8. de Villiers, M., Macuamule, C., Spry, C., Hyun, Y. M., Strauss, E. and Saliba, K. J., Structural modification of pantothenamides counteracts degradation by pantetheinase and improves antiplasmodial activity. *ACS Medicinal Chemistry Letters*, 2013**. 4** (8), 784-789.
9. Spry, C., Macuamule, C., Lin, Z., Virga, K. G., Lee, R. E., Strauss, E. and Saliba, K. J., Pantothenamides are potent, on-target Inhibitors of *Plasmodium falciparum* growth when serum pantetheinase is inactivated. *PLoS One*, 2013**. 8** (2), e54974.

10. Van Wyk, M. A study of *N*-substituted pantothenamides, antimicrobials acting on coenzyme A biosynthesis and utilization. PhD, University of Stellenbosch, 2009.
11. Jansen, P. A. M., Schalkwijk, J., Rutjes, F. P. J. T., Sauer-wein, R. and Hermkens, P. H. H. Derivatives of pantothenic acid and their use for the treatment of malaria. WO2011152721A1, 8 December 2011.
12. Jana, C. Synthesis and evaluation of pantothenic acid analogues as potential inhibitors of malaria parasites and bacteria. MSc, University of Stellenbosch, 2011.
13. Macuamule, C. J. Coenzyme A biosynthesis and utilization in *Plasmodium falciparum*: Drug targets for antimalarial chemotherapy. PhD, University of Stellenbosch, 2013.
14. Viswanadhan, V. N., Ghose, A. K., Revankar, G. R. and Robins, R. K., Atomic physicochemical parameters for three dimensional structure directed quantitative structure-activity relationships. 4. Additional parameters for hydrophobic and dispersive interactions and their application for an automated superposition of certain naturally occurring nucleoside antibiotics. *Journal of Chemical Information & Computer Sciences*, 1989**. 29** (3), 163-172.
15. Klopman, G., Li, J.-Y., Wang, S. and Dimayuga, M., Computer automated Log*P* calculations based on an extended group contribution approach. *Journal of Chemical Information & Computer Sciences*, 1994**. 34** (4), 752-781.
16. Bloch, D. E., Review of PHYSPROP Database (Version 1.0). *Journal of Chemical Information & Computer Sciences*, 1995**. 35** (2), 328-329.
17. Shioiri, T., Ninomiya, K. and Yamada, S., Diphenylphosphoryl azide. A new convenient reagent for a modified Curtius reaction and for peptide synthesis. *Journal of the American Chemical Society*, 1972**. 94** (17), 6203-6205.
18. Van Wyk, M. and Strauss, E., One-pot preparation of coenzyme A analogues *via* an improved chemo-enzymatic synthesis of pre-CoA thioester synthons. *Chemical Communications*, 2007**.** (4), 398-400.
19. Van der Westhuyzen, R. Synthesis and evaluation of inhibitors targeting coenzyme A biosynthesis and metabolism in *Staphylococcus aureus*. PhD, University of Stellenbosch, 2010.
20. de Villiers, M., Barnard, L., Koekemoer, L., Snoep, J. L. and Strauss, E., Variation in pantothenate kinase type determines the pantothenamide mode of action and impacts on coenzyme A salvage biosynthesis. *FEBS Journal*, 2014**. 281** (20), 4731-4753.
21. Kopelevich, V. M., Bulanova, L. N. and Gunar, V. I., Analogs of D(+)-pantothenic acid. VI. Synthesis of D-, L-, and DL-4'-amino-4'-deoxypantothenic acid. *Chemistry of Natural Compounds*, 1982**. 18** (2), 215-219.
22. Strauss, E., Kinsland, C., Ge, Y., McLafferty, F. W. and Begley, T. P., Phosphopantothenoylcysteine synthetase from *Escherichia coli*. Identification and

characterization of the last unidentified coenzyme A biosynthetic enzyme in bacteria. *Journal of Biological Chemistry*, 2001**. 276** (17), 13513-13516.

*Chapter 5*

# Conclusion and Future Research Possibilities

In this study we addressed the following two main objectives:

*iii)* To elucidate the role of PanK in the mode of action of inhibitory pantothenamides in *S. aureus.*

iv) To develop inhibitors that are resistant to pantetheinase-mediated degradation while retaining good antimicrobial activity.

## 5.1 Summary of results achieved

### 5.2.1 Elucidating the role of PanK in the mode of action of inhibitory pantothenamides in *S. aureus*

Two mechanisms of action have been proposed for pantothenamide-mediated inhibition, with PanK playing a central role in both: 1) Inhibition based on the pantothenamides inhibiting PanK activity directly [Target 2 in Figure 31.6, Chapter 1], and 2) metabolic activation of the molecules by PanK (i.e. by them acting as alternative substrates of PanK), followed by their conversion to CoA antimetabolites for subsequent inhibition of the ACPs and/or other CoA-dependent processes [Targets 3 and 4 in Figure 1.6, Chapter 1].

The results presented in Chapter 2 confirmed that the mode of action of bacterial pantothenamide inhibition is determined by the PanK type of the targeted organism. The results with *E. coli*, which has a type-I PanK, demonstrates that pantothenamides exert their inhibitory activity by acting as alternative substrates for PanK-I, therefore PanK-I only serves to metabolically activate them. After phosphorylation by PanK, these compounds are converted to CoA antimetabolites which can inhibit a variety of CoA-dependent processes (Target 3, Figure 1.6, Chapter 1), and which cause the synthesis of inactive ACPs (Target 4, Figure 1.6, Chapter 1). These findings are in agreement with the conclusions of previous studies [1-4].

In *S. aureus*, which has an atypical PanK type-II, the situation is completely different. The results demonstrated that pantothenamides have a complex interaction with this organism's PanK enzyme, acting as substrates that stimulate its activity when present at low concentrations, but turning into uncompetitive inhibitors as their concentrations gradually increase. Furthermore, we demonstrated that a pantothenamide analogue that cannot act as a PanK substrate can still inhibit *S. aureus* growth. These results suggest that in *S. aureus* growth inhibition is as a result of at least two factors working in combination: 1) by the formation of inactive ACPs and CoA antimetabolites

(as was observed in a previous study [4]) [Target 3 and 4, Figure 1.6, Chapter 1] and 2) by the reduction of CoA levels through the inhibition of *Sa*PanK-II [Target 2, Figure 1.6, Chapter 1].

Furthermore, the kinetic model developed as part of the study predicts that pantothenamides (and PantSH) inhibit *Sa*PanK-II via an uncompetitive mechanism; this could imply that *Sa*PanK-II contains an allosteric binding site selective for the pantothenamides. However, only two *Sa*PanK-II structures have been deposited into Protein Data Bank to date, neither of which has pantothenic acid bound in the active site. These structures present no indication of the possible location of such an allosteric site. Furthermore, a more recently published structure (the ternary complex of the enzyme bound to a phosphorylated pantothenamide (N354-Pan) and ADP) shows that *Sa*PanK-II has distinct open and closed conformations, with the later preventing product release [5]. This discovery complicates the structural investigation to identify an allosteric site even further. Consequently, we cannot exclude the possibilty that alternative kinetic models could also provide accurate descriptions of our data; however, our kinetic model is the simplest one that gives an accurate description of the total data set while taking into account the current knowledge we have on *Sa*PanK-II.

Our finding that PantSH mirrors the same complex interaction with *Sa*PanK-II observed for the normal pantothenamides suggests that CoA biosynthesis in *S. aureus* is regulated through a unique mechanism. Previous studies showed that *Sa*PanK-II does not experience feedback inhibition by CoA or its thioesters, nor does regulation occur downstream of PanK in other CoA biosynthetic enzymes [4, 6-7]. The reason for this lack of feedback inhibition was thought to be because *S. aureus*, unlike other bacteria, does not rely on glutathione as its main redox buffer, but uses CoA instead and therefore needs high concentrations of this metabolite [8]. With these new findings we hypothesize that contrary to what was previously reported, CoA biosynthesis in *S. aureus* is indeed regulated at the PanK level, and that this regulation occurs by a unique mechanism by which low PantSH concentrations stimulate *Sa*PanK-II activity and high PantSH concentrations inhibit *Sa*PanK-II activity.

To conclude, in this part of the study two major discoveries were made: first, the mode of action of the pantothenamides in *S. aureus* was elucidated, and second, a unique mechanism by which CoA biosynthesis can be regulated in *S. aureus* was uncovered.

### 5.2.2 Developing antimicrobial pantothenamides that are resistant to pantetheinase-mediated degradation

In this part of the study we successfully synthesized ten N7-Pan analogues (Chapter 3) and nine *N*-PE-PanAm analogues (Chapter 4) using various synthetic organic methods, and fully characterized all of the compounds analytically. These analogues included methylations either on the α- or β-position relative to the scissile amide bond or the amide bond itself, three amide bioisosteres including sulfonamides, thioamides and hydrazides, an addition of a double bond in the β-alanine moiety as well as removal of the 4'-hydroxyl and its replacement with an amine and phosphate functional groups.

The ten N7-Pan analogues were fully characterized *in vitro* in regards to 1) their interaction with *Sa*PanK-II (using kinetic analysis) and 2) their potency as growth inhibitors of *S. aureus*. None of the analogues showed the same complex interaction with *Sa*PanK-II that was observed for N7-Pan **3.10**. Of the ten N7-Pan analogues tested, only (*R*/*S*)-4'-deoxy-N7-Pan **3.49** and 4'-phospho-N7-Pan **3.74** acted as inhibitors of *Sa*PanK-II. Inhibition by the latter was surprising, since this would imply inhibition of the enzyme by its product. Furthermore, 4'-phospho-N7-Pan **3.74** was the only N7-Pan analogue that showed inhibition in 1% tryptone medium, with an $MIC_{80}$ of ~25 µM. This was also highly unexpected, given that it is generally believed that phosphorylated molecules are too polar to enter cells unassisted [9]. It is therefore possible that *S. aureus* has a specific uptake mechanism for phosphorylated pantothenic acid analogues (most likely phospho-PantSH) but no reports on this have been made to date.

Unfortunately, the *Sa*PanK-II crystal structure with a pantothenamide bound only became available after we had already completed most of the experiments on the degradation-resistant pantothenamides. Having this structure to help guide the design strategy to achieve degradation resistance without losing selectivity (i.e. binding to PanK) may have prompted us not to pursue some of the structures. Nonetheless, using the structure we were able to rationalize why some of the N7-Pan analogues did not show inhibition of either *Sa*PanK-II or *S. aureus* RN4220. Figure 5.1 shows a graphical illustration of the H-bonding interactions of *Sa*PanK-II with 4'-phospho-N7-Pan **3.74** in the active site. Two amino acid residues (Arg113 and Thr172) form critical H-bonding interactions with the pantothenamides in the active site; unfortunately, many of these were lost or weakened with the structural modifications that were implemented. *N*-methyl-N7-Pan **3.11** lost a crucial H-bonding interaction with Thr172 when the NH of the scissile amide was methylated, while the H-bonding interaction with Arg113 was weakened when the carbonyl oxygen was replaced with a sulfur in N7-pantothenthioamide **3.36**.

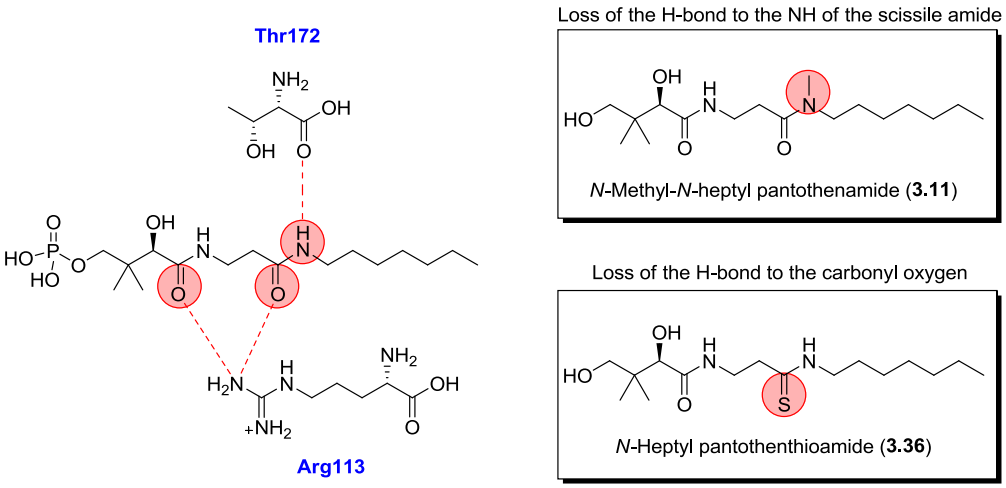


**Figure 5.1. Graphical illustration of the H-bonding interactions of *Sa*PanK-II with 4'-phospho-N7-Pan 3.74 in the active site. Arg113 forms H-bonding interactions with the two carbonyl oxygens of the amide bonds and Thr172 forms an H-bonding interaction with the NH of the scissile amide bond. Both, *N*-methyl-N7-Pan 3.11 and N7-pantothenthioamide 3.36 (in the black boxes) lost one of these interactions, respectively (indicated in the red circles).**

Of the nine *N*-PE-PanAm analogues that were successfully synthesized, only three analogues have been tested against *P. falciparum* thus far. α-Me-*N*-PE-PanAm **4.3** showed excellent antiplasmodial activity with an $IC_{50}$ comparable to that of chloroquine. β-Me-*N*-PE-PanAm **4.4** has a potency that is ~1000-fold lower than what we observe for α-Me-*N*-PE-PanAm **4.3**. This indicates that the placement of the methyl group is an important consideration for target selectivity. Additionally, (*R*/*S*)-4'-deoxy-*N*-PE-PanAm **4.19** did not act as an inhibitor of *P. falciparum*, suggesting that pantothenamides act as substrates for *Pf*PanK and subsequently targets processes downstream through the formation of CoA antimetabolites (Targets 3 and 4 in Figure 1.7, Chapter 1).

To conclude, in this part of the study a number of N7-Pan- and *N*-PE-PanAm analogues were successfully synthesized and characterized as inhibitors of *S. aureus* and *P. falciparum*, respectively. Although none of the N7-Pan analogues acted as good inhibitors of *S. aureus*, valuable information was obtained regarding the modifications that can and cannot be made to the pantothenamides to retain their potency. Lastly, we have obtained a promising result with one *N*-PE-PanAm analogue, α-Me-*N*-PE-PanAm **4.3**, which showed antiplasmodial activity with an $IC_{50}$ comparable to that of chloroquine. In light of the fact that the N7-Pan analogues were not good inhibitors of *S. aureus*, the remaining untested *N*-PE-PanAm analogues might not show good antiplasmodial activity either. However, their antiplasmodial activity remains to be determined.

## 5.2 Future research possibilities

### 5.3.1 Elucidating the role of PanK in the mode of action of inhibitory pantothenamides in *S. aureus*

The inhibition of *Sa*PanK-II and *S. aureus* by 4'-phospho-N7-Pan **3.74**—the product of the PanK-II catalyzed reaction—was highly unexpected. Consequently, additional experiments will have to be performed to help explain the inhibition observed. Future work will include kinetic assays with 4'-phospho-N7-Pan **3.74** to determine the type of inhibition of *Sa*PanK-II. Furthermore, we will also have to revisit the kinetic model developed as part of this study and determine whether it describes the data with the phosphorylated pantothenamides as well. Growth inhibition of *S. aureus* by the phosphorylated pantothenamides could also indicate that CoA antimetabolites are formed that inhibit targets other than PanK, such as fatty acid biosynthesis. However, previous studies have shown that some bacteria (especially some Gram-positives) have the ability to suppress fatty acid biosynthesis when exogenous fatty acids are present. This strict biochemical regulation of fatty acid biosynthesis by exogenous fatty acids means that these organisms are refractory to fatty acid biosynthesis inhibitors [10]. These implications will have to be considered for the development of antimicrobials that solely target fatty acid biosynthesis.

### 5.3.2 Developing antimicrobial pantothenamides that are resistant to pantetheinase-mediated degradation

It will be difficult to synthesize potent pantetheinase-resistant inhibitors for *S. aureus* because of the various H-bonding interactions that need to be retained; however, this could be achieved by selecting bioisosteres such as an imidazole, 1,2,4-triazole or a trifluoro-ethylamine that will retain the interactions (Figure 5.2). Future work will include synthesizing the N7-Pan analogues containing these three bioisosteres which can subsequently be characterized against *Sa*PanK-II kinetically and as *S. aureus* growth inhibitors.

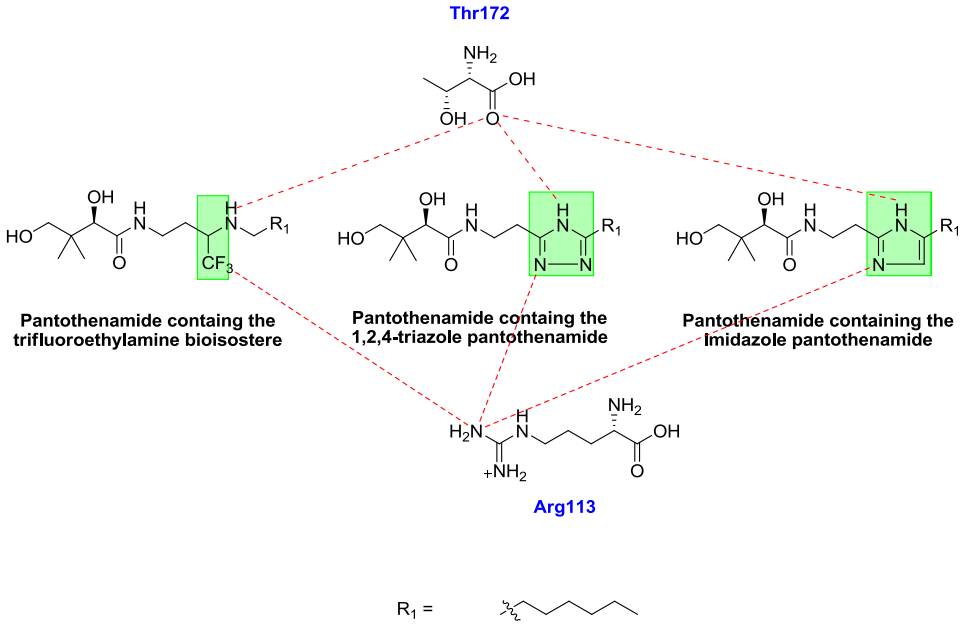


**Figure 5.2. Suggested pantothenamides that will retain the H-bonding interactions with Arg113 and Thr172. These bioisosters include a trifluoroethylamine, imidazole, and a 1,2,4-triazole.**

To date, only three of the nine *N*-PE-PanAm analogues synthesized in this study have been tested for inhibition of proliferation of *P. falciparum*. Consequently, six *N*-PE-PanAm analogues remain to be tested as part of future work, in addition to testing whether the analogues that do show antiplasmodial activity are pantetheinase resistant. Furthermore, based on its potent inhibition of *P. falciparum* blood-stage proliferation, α-Me-*N*-PE-PanAm **4.3** is an excellent lead compound for further development. However, in this study a mixture of diastereomers (i.e. correct stereochemistry of the pantoyl 2'-OH group, but both stereoisomers at the methyl-bearing centre) were used. Additionally, no data relating to the compound's pharmacokinetic properties (absorption, metabolism and excretion) or its toxicity are available at this stage. Therefore, future work will include synthesizing the two diastereomers of α-Me-*N*-PE-PanAm **4.3** and testing them separately in blood-stage proliferation assays to identify any differences in potency. The most potent isomer identified in this manner will be used to determine its pharmacokinetic properties as well as its toxicity *in vivo*. Moreover, substitutions with different functional groups can also be made on the *ortho*, *meta* or *para*-positions of the phenyl-ring to determine whether we can further increase the potency of α-Me-*N*-PE-PanAm **4.3**.

## 5.3 Final remarks

Although the CoA biosynthetic pathway has been under intense investigation for many years, it is evident that this pathway has a lot to offer in possible new antimicrobial and antimalarial strategies. The results of our study of the mode of action of the pantothenamides in *S. aureus* showed that these compounds exert their growth inhibitory effects at least partially by inhibiting PanK has contributed significantly to our knowledge in this regard. Furthermore, we identified a potent pantetheinase-resistant pantothenamide in this study through structural modifications of the pantothenamide scaffold; we hope that this study will encourage more investigation using this strategy.

## 5.4 References

1. Zhang, Y. M., Frank, M. W., Virga, K. G., Lee, R. E., Rock, C. O. and Jackowski, S., Acyl carrier protein is a cellular target for the antibacterial action of the pantothenamide class of pantothenate antimetabolites. *Journal of Biological Chemistry*, 2004**. 279**, 50969-50975.
2. Thomas, J. and Cronan, J. E., Antibacterial activity of *N*-pentylpantothenamide is due to inhibition of coenzyme A synthesis. *Antimicrobial Agents & Chemotherapy*, 2010**. 54** (3), 1374-1377.
3. Strauss, E. and Begley, T. P., The antibiotic activity of *N*-pentylpantothenamide results from its conversion to ethyldethia-coenzyme A, a coenzyme A antimetabolite. *Journal of Biological Chemistry*, 2002**. 277** (50), 48205-48209.
4. Leonardi, R., Chohnan, S., Zhang, Y. M., Virga, K. G., Lee, R. E., Rock, C. O. and Jackowski, S., A pantothenate kinase from *Staphylococcus aureus* refractory to feedback regulation by coenzyme A. *Journal of Biological Chemistry*, 2005**. 280** (5), 3314-3322.
5. Hughes, S. J., Antoshchenko, T., Kim, K. P., Smil, D. and Park, H. W., Structural characterization of a new *N*-substituted pantothenamide bound to pantothenate kinases from *Klebsiella pneumoniae* and *Staphylococcus aureus*. *Proteins*, 2014**. 82** (7), 1542-1548.
6. Spry, C., Kirk, K. and Saliba, K. J., Coenzyme A biosynthesis: An antimicrobial drug target. *FEMS Microbiology Reviews*, 2008**. 32** (1), 56-106.
7. Hong, B. S., Yun, M. K., Zhang, Y. M., Chohnan, S., Rock, C. O., White, S. W., Jackowski, S., Park, H. W. and Leonardi, R., Prokaryotic type II and type III pantothenate kinases: The same monomer fold creates dimers with distinct catalytic properties. *Structure*, 2006**. 14** (8), 1251-1261.
8. delCardayre, S. B., Stock, K. P., Newton, G. L., Fahey, R. C. and Davies, J. E., Coenzyme A disulfide reductase, the primary low molecular weight disulfide reductase from *Staphylococcus aureus*. Purification and characterization of the native enzyme. *Journal of Biological Chemistry*, 1998**. 273**, 5744-5751.
9. Jackowski, S. and Rock, C. O., Metabolism of 4'-phosphopantetheine in *Escherichia coli*. *Journal of Bacteriology*, 1984**. 158** (1), 115-120.
10. Yao, J. and Rock, C. O., How bacterial pathogens eat host lipids: Implications for the development of fatty acid synthesis therapeutics. *Journal of Biological Chemistry*, 2015**. 290** (10), 5940-5946.

*Addendum*

# A Pantetheinase-Resistant Pantothenamide with Potent, On-Target and Selective Antiplasmodial Activity

Cristiano J. Macuamule, Erick T. Tjhin, Collins E. Jana, **Leanne Barnard,** Lizbé Koekemoer, Marianne de Villiers, Kevin J. Saliba, and Erick Strauss.

*Antimicrobial Agents & Chemotherapy*

Vol. 59 (2015) pp. 3666–3668[2]

[2] Reproduced with permission from "Macuamule, C. J., Tjhin, E. T., Jana, C. E., Barnard, L., Koekemoer, L., de Villiers, M., Saliba, K. J. and Strauss, E. *Antimicrobial Agents & Chemotherapy*. 59 (2015) 3666–3668. DOI: 10.1128/AAC.04970-14". Copyright © 2015 by the American Society for Microbiology.

http://aac.asm.org/content/59/6/3666

AAC Journals.ASM.org

# A Pantetheinase-Resistant Pantothenamide with Potent, On-Target, and Selective Antiplasmodial Activity

**Cristiano J. Macuamule,[a] Erick T. Tjhin,[b] Collins E. Jana,[a] Leanne Barnard,[a] Lizbé Koekemoer,[a] Marianne de Villiers,[a] Kevin J. Saliba,[b,c] Erick Strauss[a]**

Department of Biochemistry, Stellenbosch University, Stellenbosch, South Africa[a]; Research School of Biology, College of Medicine, Biology, and Environment, The Australian National University, Canberra, ACT, Australia[b]; Medical School, College of Medicine, Biology, and Environment, The Australian National University, Canberra, ACT, Australia[c]

**Pantothenamides inhibit blood-stage *Plasmodium falciparum* with potencies (50% inhibitory concentration [$IC_{50}$], ~20 nM) similar to that of chloroquine. They target processes dependent on pantothenate, a precursor of the essential metabolic cofactor coenzyme A. However, their antiplasmodial activity is reduced due to degradation by serum pantetheinase. Minor modification of the pantothenamide structure led to the identification of α-methyl-*N*-phenethyl-pantothenamide, a pantothenamide resistant to degradation, with excellent antiplasmodial activity ($IC_{50}$, 52 ± 6 nM), target specificity, and low toxicity.**

One-half of the world's population (~3.4 billion people) is at risk of contracting malaria, with pregnant women and children <5 years of age being especially vulnerable. In 2013, the WHO estimated that malaria caused ~584,000 deaths globally, with the majority occurring in Africa (1). Although efforts to control and to eliminate malaria in the past 15 years have saved an estimated 3.3 million lives (1), drug-resistant parasites continue to emerge (2). This places the progress in the fight against the disease under pressure, especially since there is no effective vaccine against malaria (3). Several new drug targets have been identified in recent years (4); however, these targets now need to be exploited through the development of directed treatments.

We are interested in targeting the biosynthesis of the essential cofactor coenzyme A (CoA) from the water-soluble vitamin $B_5$ (pantothenate, compound 1 in Fig. 1) for antimalarial drug development (5, 6). It has been shown that extracellular pantothenate is essential for intracellular malaria parasites (7), which indicates that *Plasmodium falciparum* does not utilize exogenous CoA but must synthesize CoA *de novo* (8).

Pantothenate analogues interfere with the ability of *P. falciparum* to utilize the vitamin, with many analogues being characterized as growth inhibitors of the blood-stage parasites (9–11). Furthermore, a recent study showed that CoA biosynthesis can be targeted by a chemically diverse set of inhibitors that do not resemble pantothenate, the most potent of which had a 50% inhibitory concentration ($IC_{50}$; the concentration that inhibits parasite proliferation by 50%) of 120 nM against blood-stage parasites (12). These studies support pantothenate utilization (and therefore CoA biosynthesis and CoA-dependent processes) as an antiplasmodial target.

Recently we showed that *N*-substituted pantothenamides (PanAms), a specific class of pantothenate analogues, have excellent antiplasmodial activity. Among these, *N*-phenethyl-pantothenamide (*N*-PE-PanAm) (compound 2 in Fig. 1) exhibited an $IC_{50}$ of 20 nM (13); this potency is comparable to that of chloroquine (14, 15). In practice, however, the antiplasmodial activity of the PanAms is decreased since they are degraded by pantetheinase (13), a ubiquitous enzyme of the Vanin protein family that is present in serum (16, 17). Pantetheinase normally catalyzes the hydrolysis of pantetheine (a CoA-derived metabolite) to form pantothenate and cysteamine (18, 19), but it also acts on compounds with a wide range of variations in the cysteamine moiety, including the PanAms (Fig. 1) (13). In a previous study, we found that replacement of the β-alanine moiety of the PanAms with either glycine or γ-aminobutyric acid gave rise to pantetheinase-resistant variants, due to displacement of the scissile amide bond (20). Unfortunately, these structural modifications also reduced the potency of the resulting PanAms ($IC_{50}$ values of ≥1 μM), indicating that their target (or targets) requires the pantothenate core structure to be retained for optimal inhibition.

In light of this finding, we set out to develop a pantetheinase-resistant PanAm in which the β-alanine core was retained. This was achieved by adding a methyl group to the carbon adjacent to the amide carbonyl group, thereby increasing the steric bulk at this center. We predicted that this modification would reduce the rate of pantetheinase-mediated hydrolysis by limiting the access of the enzyme's cysteine nucleophile to the scissile amide bond. The methylated version of *N*-PE-PanAm, i.e., α-methyl-*N*-PE-PanAm (α-Me-*N*-PE-PanAm) (compound 3 in Fig. 1), was prepared by condensing D,L-3-amino-isobutyrate to pantolactone, followed by partial purification by cation-exchange chromatography. The product, α-methyl-D-pantothenate, was purified by flash column chromatography (FCC) before being coupled to *N*-phenethylamine using diphenylphosphoryl azide in the presence of triethylamine. After purification by FCC, α-Me-*N*-PE-PanAm was

**Received** 9 December 2014 **Returned for modification** 4 January 2015
**Accepted** 2 April 2015

**Accepted manuscript posted online** 6 April 2015

**Citation** Macuamule CJ, Tjhin ET, Jana CE, Barnard L, Koekemoer L, de Villiers M, Saliba KJ, Strauss E. 2015. A pantetheinase-resistant pantothenamide with potent, on-target, and selective antiplasmodial activity. Antimicrob Agents Chemother 59:3666–3668. doi:10.1128/AAC.04970-14.

Address correspondence to Erick Strauss, estrauss@sun.ac.za.

C.J.M. and E.T.T. contributed equally to this article.

Supplemental material for this article may be found at http://dx.doi.org/10.1128/AAC.04970-14.



doi:10.1128/AAC.04970-14

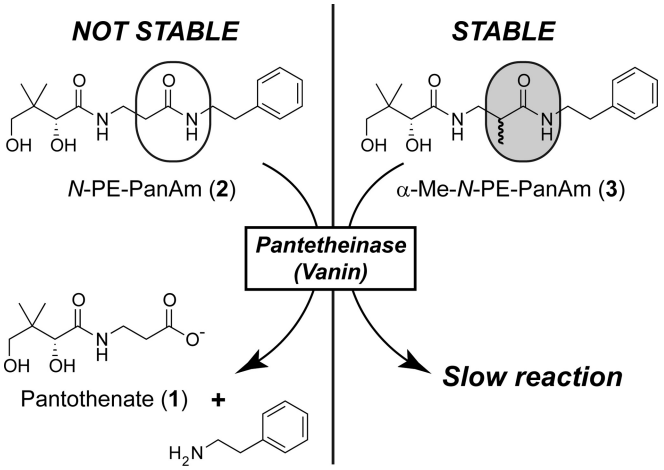


**FIG 1** (Left) Structure of *N*-PE-PanAm (compound 2), which can be degraded by pantetheinase (Vanin) to form pantothenate (compound 1) and phenethylamine. (Right) Structure of α-Me-*N*-PE-PanAm (compound 3), which shows limited degradation by pantetheinase. The vulnerable (scissile) amide bond is indicated by the oval on the left, while the shaded oval on the right shows how it is modified by introduction of the methyl group to increase stability.

obtained in a final overall yield of 45%, as a mixture of two epimers (see the supplemental material for more details).

The antiplasmodial activity of α-Me-*N*-PE-PanAm against the chloroquine-sensitive *P. falciparum* strain 3D7 (chloroquine $IC_{50}$, 11 ± 1 nM [mean ± standard error of the mean {SEM}]; $n = 3$) was determined in "aged medium" (i.e., medium in which pantetheinase had been inactivated by incubation at 37°C for 40 h), in a manner similar to that used previously for *N*-PE-PanAm (13, 20). Under these conditions, α-Me-*N*-PE-PanAm showed excellent antiplasmodial activity, with an $IC_{50}$ of 29 ± 2 nM (mean ± SEM; $n = 3$), a value that is only slightly greater than that of *N*-PE-PanAm (Fig. 2a). Furthermore, α-Me-*N*-PE-PanAm demonstrated exceptional resistance to degradation by pantetheinase, compared to *N*-PE-PanAm, as can be seen from its antiplasmodial activity in normal medium (i.e., with active pantetheinase), with an $IC_{50}$ of 52 ± 6 nM (mean ± SEM; $n = 3$) (Fig. 2a), compared to the *N*-PE-PanAm $IC_{50}$ of ~6,200 nM (13, 20). Performing the same test with a chloroquine-resistant strain (strain Dd2; chloroquine $IC_{50}$, 173 ± 5 nM [mean ± range/2]; $n = 2$) gave an $IC_{50}$ of 129 ± 4 nM (mean ± range/2; $n = 2$); based on currently available data, it is unclear whether this difference is related to chloroquine resistance or is merely a variation in strain sensitivity. More importantly, resistance to pantetheinase degradation did not come at a cost in target specificity, since addition of excess extracellular pantothenate (100 μM) to the medium antagonized the antiplasmodial activity of α-Me-*N*-PE-PanAm against the 3D7 strain ($IC_{50}$, 860 ± 102 nM [mean ± SEM]; $n = 3$; $P = 0.01$) (Fig. 2a).

To confirm the stability of α-Me-*N*-PE-PanAm, we also tested its *in vitro* degradation by recombinant pantetheinase (human VNN1) (Fig. 2b). This was done by incubating substrate (500 μM *N*-PE-PanAm or α-Me-*N*-PE-PanAm; 500 μM phenethylamine was used as a reference, i.e., equivalent to 100% product formation) in 100 mM HEPES (pH 7.6) containing 500 μM dithiothreitol (DTT) and 0.05 μg/μl bovine serum albumin (BSA), at 37°C. The reaction (in a final volume of 300 μl) was initiated by the addition of pantetheinase (1.6 μg/μl), and the mixture was incubated for 24 h. The amount of amine produced was determined by quenching 30 μl of the reaction mixture with 10 μl of *N*-ethylmaleimide (6 μM), followed by incubation (for 10 min at 37°C) with 2 mM fluorescamine in 517 mM borate (pH 9), in a final volume of 145 μl. Fluorescence was subsequently measured using a Thermo Varioskan multiplate spectrofluorimeter (excitation wavelength, 395 nm; emission wavelength, 485 nm). We were able to confirm that α-Me-*N*-PE-PanAm was more resistant to pantetheinase-mediated degradation than *N*-PE-PanAm, as it showed only 26% ± 2% (mean ± range/2; $n = 2$) hydrolysis (normalized to the control, which represented 100% phenethylamine formed) after 24 h, compared to 96% ± 9% (mean ± range/2; $n = 2$) for *N*-PE-PanAm under the same conditions.

The activity of α-Me-*N*-PE-PanAm was tested against a human cell line (human foreskin fibroblasts [HFF]) to determine its selectivity (21). The cells were exposed to α-Me-*N*-PE-PanAm

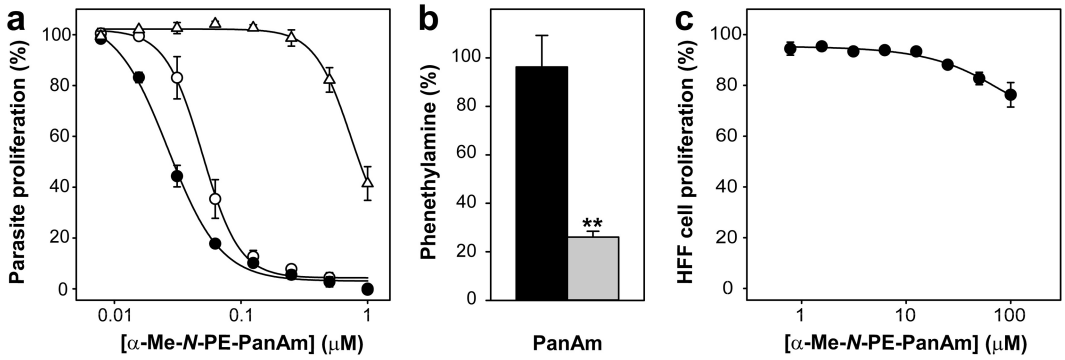


**FIG 2** (a) Inhibition of proliferation of *P. falciparum* parasites (chloroquine-sensitive strain 3D7) by α-Me-*N*-PE-PanAm. Parasites were cultured for 96 h in medium with (○) or without (●) pantetheinase activity; the inhibition was antagonized when the extracellular pantothenate concentration in the medium with pantetheinase was increased from the usual 1 μM to 100 μM (△), consistent with the compound being on target. Values represent the mean ± SEM of three independent experiments, each performed in triplicate. (b) Pantetheinase-mediated hydrolysis of *N*-PE-PanAm (black bar) and α-Me-*N*-PE-PanAm (gray bar) *in vitro* after treatment with recombinant human pantetheinase for 24 h. The amount of phenethylamine released was determined by derivatization with fluorescamine. Values represent the mean from two independent experiments, each performed in triplicate; the error bars represent range/2. **, $P < 0.001$, Student's *t* test. (c) HFF proliferation in the presence of α-Me-*N*-PE-PanAm after 96 h. Values represent the mean ± SEM of three independent experiments, each performed in triplicate.

(0.781 to 100 μM) for 4 days to reach confluence, and plates were stored at −80°C prior to exposure to SYBR Safe, as was done for the parasite experiments. We found that α-Me-*N*-PE-PanAm had limited cytotoxicity for HFF cells, with a selectivity index (SI) greater than 1,500 (Fig. 2c), rivalling the SI of chloroquine (~1,300) determined using a similar cell line (15).

With these promising findings, we unveil α-Me-*N*-PE-PanAm as the first pantothenate analogue with excellent potential as a new lead compound for antimalarial drug development, based on its potent inhibition of blood-stage parasites in the presence of serum pantetheinase, lack of activity against human cells, and desirable physicochemical characteristics (22) (see the supplemental material for details). Future work will focus on determining whether the two epimers show a difference in activity, performing tests on other stages of the parasite's life cycle, and determining the pharmacokinetic properties and *in vivo* efficacy of α-Me-*N*-PE-PanAm, to establish its long-term potential for development as an antimalarial.

## ACKNOWLEDGMENTS

Aspects of this work were supported by a grant from the South African Malaria Initiative to K.J.S. and E.S. Australia Awards Small Grants Scheme, an initiative of the Australian Government (to C.J.M.), made visits to the Australian National University possible and are gratefully acknowledged. C.J.M. was supported by a Canon Collins Trust Scholarship. E.T.T. was supported by an International Postgraduate Research Scholarship from the Australian government. C.E.J., L.B., and L.K. were supported by bursaries and fellowships from the National Research Foundation of South Africa. M.D.V. was supported by the National Research Foundation of South Africa as a Research Career Advancement Fellow.

We are grateful to the Canberra Branch of the Australian Red Cross Blood Service for the provision of red blood cells and the van Dooren laboratory at the Australian National University for providing the HFF cells.

## REFERENCES

1. **World Health Organization.** 2014. World malaria report 2014. World Health Organization, Geneva, Switzerland.
2. **Miotto O, Almagro-Garcia J, Manske M, Macinnis B, Campino S, Rockett KA, Amaratunga C, Lim P, Suon S, Sreng S, Anderson JM, Duong S, Nguon C, Chuor CM, Saunders D, Se Y, Lon C, Fukuda MM, Amenga-Etego L, Hodgson AV, Asoala V, Imwong M, Takala-Harrison S, Nosten F, Su XZ, Ringwald P, Ariey F, Dolecek C, Hien TT, Boni MF, Thai CQ, Amambua-Ngwa A, Conway DJ, Djimde AA, Doumbo OK, Zongo I, Ouedraogo JB, Alcock D, Drury E, Auburn S, Koch O, Sanders M, Hubbart C, Maslen G, Ruano-Rubio V, Jyothi D, Miles A, O'Brien J, Gamble C, Oyola SO, Rayner JC, Newbold CI, Berriman M, Spencer CC, McVean G, Day NP, White NJ, Bethell D, Dondorp AM, Plowe CV, Fairhurst RM, Kwiatkowski DP.** 2013. Multiple populations of artemisinin-resistant *Plasmodium falciparum* in Cambodia. Nat Genet **45:**648–655. http://dx.doi.org/10.1038/ng.2624.
3. **Olotu A, Fegan G, Wambua J, Nyangweso G, Awuondo KO, Leach A, Lievens M, Leboulleux D, Njuguna P, Peshu N, Marsh K, Bejon P.** 2013. Four-year efficacy of RTS,S/AS01E and its interaction with malaria exposure. N Engl J Med **368:**1111–1120. http://dx.doi.org/10.1056/NEJMoa1207564.
4. **Drinkwater N, McGowan S.** 2014. From crystal to compound: structure-based antimalarial drug discovery. Biochem J **461:**349–369. http://dx.doi.org/10.1042/BJ20140240.
5. **Spry C, van Schalkwyk DA, Strauss E, Saliba KJ.** 2010. Pantothenate utilization by *Plasmodium* as a target for antimalarial chemotherapy. Infect Disord Drug Targets **10:**200–216. http://dx.doi.org/10.2174/187152610791163390.
6. **Strauss E.** 2010. Coenzyme A biosynthesis and enzymology, p 351–410. *In* Mander L, Liu H-W (ed), Comprehensive natural products II: chemistry and biology, vol 7. Elsevier, Oxford, United Kingdom.
7. **Divo AA, Geary TG, Davis NL, Jensen JB.** 1985. Nutritional requirements of *Plasmodium falciparum* in culture. I. Exogenously supplied dialyzable components necessary for continuous growth. J Protozool **32:**59–64.
8. **Spry C, Kirk K, Saliba KJ.** 2008. Coenzyme A biosynthesis: an antimicrobial drug target. FEMS Microbiol Rev **32:**56–106. http://dx.doi.org/10.1111/j.1574-6976.2007.00093.x.
9. **Saliba K, Kirk K.** 2005. CJ-15,801, a fungal natural product, inhibits the intraerythrocytic stage of *Plasmodium falciparum* in vitro via an effect on pantothenic acid utilisation. Mol Biochem Parasitol **141:**129–131. http://dx.doi.org/10.1016/j.molbiopara.2005.02.003.
10. **Saliba KJ, Ferru I, Kirk K.** 2005. Provitamin $B_5$ (pantothenol) inhibits growth of the intraerythrocytic malaria parasite. Antimicrob Agents Chemother **49:**632–637. http://dx.doi.org/10.1128/AAC.49.2.632-637.2005.
11. **Spry C, Chai CL, Kirk K, Saliba KJ.** 2005. A class of pantothenic acid analogs inhibits *Plasmodium falciparum* pantothenate kinase and represses the proliferation of malaria parasites. Antimicrob Agents Chemother **49:**4649–4657. http://dx.doi.org/10.1128/AAC.49.11.4649-4657.2005.
12. **Fletcher S, Avery VM.** 2014. A novel approach for the discovery of chemically diverse anti-malarial compounds targeting the *Plasmodium falciparum* coenzyme A synthesis pathway. Malar J **13:**343. http://dx.doi.org/10.1186/1475-2875-13-343.
13. **Spry C, Macuamule C, Lin Z, Virga KG, Lee RE, Strauss E, Saliba KJ.** 2013. Pantothenamides are potent, on-target inhibitors of *Plasmodium falciparum* growth when serum pantetheinase is inactivated. PLoS One **8:**e54974. http://dx.doi.org/10.1371/journal.pone.0054974.
14. **van Schalkwyk DA, Chan XW, Misiano P, Gagliardi S, Farina C, Saliba KJ.** 2010. Inhibition of *Plasmodium falciparum* pH regulation by small molecule indole derivatives results in rapid parasite death. Biochem Pharmacol **79:**1291–1299. http://dx.doi.org/10.1016/j.bcp.2009.12.025.
15. **Sumanadasa SDM, Goodman CD, Lucke AJ, Skinner-Adams T, Sahama I, Haque A, Do TA, McFadden GI, Fairlie DP, Andrews KT.** 2012. Antimalarial activity of the anticancer histone deacetylase inhibitor SB939. Antimicrob Agents Chemother **56:**3849–3856. http://dx.doi.org/10.1128/AAC.00030-12.
16. **Kaskow BJ, Proffit JM, Blangero J, Moses EK, Abraham LJ.** 2012. Diverse biological activities of the vascular non-inflammatory molecules: the Vanin pantetheinases. Biochem Biophys Res Commun **417:**653–658. http://dx.doi.org/10.1016/j.bbrc.2011.11.099.
17. **Pace H, Brenner C.** 2001. The nitrilase superfamily: classification, structure and function. Genome Biol **2:**reviews0001.1–reviews0001.9. http://dx.doi.org/10.1186/gb-2001-2-1-reviews0001.
18. **Wittwer C, Wyse B, Hansen RG.** 1982. Assay of the enzymatic hydrolysis of pantetheine. Anal Biochem **122:**213–222. http://dx.doi.org/10.1016/0003-2697(82)90273-1.
19. **Wittwer CT, Burkhard D, Ririe K, Rasmussen R, Brown J, Wyse BW, Hansen RG.** 1983. Purification and properties of a pantetheine-hydrolyzing enzyme from pig kidney. J Biol Chem **258:**9733–9738.
20. **de Villiers M, Macuamule C, Spry C, Hyun Y-M, Strauss E, Saliba KJ.** 2013. Structural modification of pantothenamides counteracts degradation by pantetheinase and improves antiplasmodial activity. ACS Med Chem Lett **4:**784–789. http://dx.doi.org/10.1021/ml400180d.
21. **Hoegl A, Darabi H, Tran E, Awuah E, Kerdo ESC, Habib E, Saliba KJ, Auclair K.** 2014. Stereochemical modification of geminal dialkyl substituents on pantothenamides alters antimicrobial activity. Bioorg Med Chem Lett **24:**3274–3277. http://dx.doi.org/10.1016/j.bmcl.2014.06.013.
22. **Lipinski CA, Lombardo F, Dominy BW, Feeney PJ.** 2001. Experimental and computational approaches to estimate solubility and permeability in drug discovery and development settings. Adv Drug Deliv Rev **46:**3–26. http://dx.doi.org/10.1016/S0169-409X(00)00129-0.

# SUPPLEMENTAL MATERIAL

# A pantetheinase-resistant pantothenamide with potent, on-target and selective antiplasmodial activity

Cristiano J. Macuamule,[a] Erick T. Tjhin,[b] Collins E. Jana,[a] Leanne Barnard,[a] Lizbé Koekemoer,[a] Marianne de Villiers,[a] Kevin J. Saliba,[b,c] Erick Strauss[a#]

Department of Biochemistry, Stellenbosch University, Stellenbosch, South Africa[a]; Research School of Biology, The Australian National University, Canberra, ACT, Australia[b]; Medical School, College of Medicine, Biology and Environment, The Australian National University, Canberra, ACT, Australia[c]

#Address correspondence to Erick Strauss, estrauss@sun.ac.za.

C.J.M. and E.T.T. contributed equally to this work.

## MATERIALS

All materials used were as described before (1, 2).

## STATISTICAL ANALYSES

The statistical significance for the $IC_{50}$ values and the pantetheinase assay was determined using a two-tailed Student's t-test for paired samples.

## SYNTHESES

***α-Methyl pantothenic acid (mixture of epimers)***

D,L-3-Amino isobutyric acid (500 mg, 4.85 mmol) was dissolved in 1 M aqueous sodium hydroxide (4.80 mL, 4.85 mmol) and lyophilized, after which pantolactone (700 mg, 5.28 mmol) was added. The mixture was stirred under an inert atmosphere overnight at 130 °C. The resulting sticky oil was dissolved in water and loaded onto a prewashed Amberlite IR120 ($H^+$-form) ion exchange resin. The free acid was eluted with water and lyophilized before purification by flash column chromatography (5:2:1:1 ethyl acetate: methanol: water: acetonitrile) afforded the product (0.97 g, 86%) as a white powder. $R_f$ = 0.47. $\delta_H$ (400 MHz; $D_2O$; 25 °C) 0.76 (3H, s, $-CH_3$), 0.79 (3H, s, $-CH_3$), 1.01 (3H, d, *J* = 7.1 Hz, $-CH_3$), 2.47–2.59 (1H, m, -CH-), 3.21–3.25 (2H, m, $-CH_2$-), 3.26 (1H, d, *J* = 11.1 Hz, -CH-), 3.38 (1H, d, *J* = 11.1 Hz, -CH-), 3.85 (1H, s, -CH-, epimer A) and 3.86 (1H, s, -CH-, epimer B). $\delta_C$ (100 MHz; $D_2O$; 25 °C) 14.9, 19.8, 21.1, 39.2, 40.2, 40.3, 42.2, 42.3, 69.1, and 76.5; (MS-ESI) $[M+H]^+$ 234.14 (Calculated $[C_{10}H_{20}NO_5]^+$ = 234.13), $[M-H]^-$ 232.09 (Calculated $[C_{10}H_{18}NO_5]^-$ = 232.12).

***α-Me-N-PE-PanAm (mixture of epimers)***

Phenethylamine (163 µL, 1.29 mmol) and diphenylphosphoryl azide (278 µL, 1.29 mmol) were added to a solution of α-methyl pantothenic acid (250 mg, 1.07 mmol) in dimethylformamide (4 mL) at RT. After cooling the mixture to 0 °C, triethylamine (180 µL, 1.29 mmol) was added. The reaction mixture was stirred for an additional 2 h at 0 °C and left to stir overnight at RT. Dimethylformamide was removed *in vacuo* and Amberlite IR400 ($OH^-$-form) resin was added. The reaction mixture was filtered and lyophilized before purification by flash column chromatography (10% methanol/dichloromethane) afforded the target compound (188 mg, 52%) as a yellow oil. $R_f$ = 0.24. $\delta_H$ (600 MHz; $CDCl_3$; 25 °C) 0.90 (3H, s, $-CH_3$, epimer A), 0.91 (3H, s, $-CH_3$, epimer B), 0.99 (3H, s, $-CH_3$, epimer A), 1.00 (3H, s, $-CH_3$, epimer B), 1.10 (3H, d, *J* = 7.1 Hz, $-CH_3$), 2.47–2.59 (1H, m, -CH-), 2.80 (2H, t, *J* = 7.1 Hz, $-CH_2$-), 3.28–3.28 (2H, m, $-CH_2$-), 3.42–3.49 (2H, m, $-CH_2$-), 3.51–3.58 (2H, m, $-CH_2$-), 3.98 (1H, apparent t, *J* = 5.1 Hz, -CH-, both epimers), 5.98 (1H, br s, -NH-), 7.17 (2H, d, *J* = 7.4 Hz, arom), 7.22

(1H, d, $J$ = 7.3 Hz, arom), 7.25–7.27 (1H, br s, -NH-) and 7.30 (2H, dd, $J$ = 7.3, 7.4 Hz, arom). $\delta_C$ (150 MHz; $CDCl_3$; 25 °C) 15.7, 20.4, 20.4, 35.5, 40.6, 40.7, 42.1, 48.7, 70.8, 77.5, 126.6, 126.6, 128.7, 128.7, 128.7, 138.7, 173.7, and 175.0; (HRMS) $[M+H]^+$ 337.2124 (Calculated $[C_{18}H_{29}N_2O_4]^+$ = 337.2127).

## PHYSICOCHEMICAL PROPERTIES

***α-Me-N-PE-PanAm***

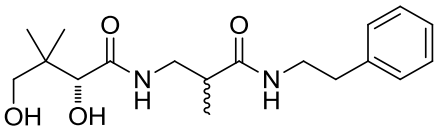


Molecular weight: 336.42 $g.mol^{-1}$

Calculated lipophilicity (ClogP): 0.62

Number of H-bond donors: 4

Number of H-bond acceptors: 2

Polar surface area (PSA): 98.66 $Å^2$ at pH = 7.40

Distribution (logD): 0.62 at pH = 7.40

Number of rotatable bonds (NRotB): 9

Fraction of $sp^3$ carbons ($Fsp^3$): 0.556

Values of ClogP, PSA, logD and NRotB were calculated with calculator plugins in the program MarvinSketch 6.0.6, 2013 from ChemAxon (Budapest, Hungary). Calculations used equal weights of VG, KLOP, and PHYS methods, and used electrolyte concentrations ($Na^+$, $K^+$ and $Cl^-$) set to 0.1 $mol.dm^{-3}$. Tautomerization were not considered in the calculations (see https://www.chemaxon.com/marvin-archive/5.11.3/marvin/help/calculations/partitioning.html).

## REFERENCES

1. **De Villiers M, Macuamule C, Spry C, Hyun Y-M, Strauss E, Saliba KJ.** 2013. Structural modification of pantothenamides counteracts degradation by pantetheinase and improves antiplasmodial activity. ACS Med. Chem Lett. **4:**784-789.
2. **Spry C, Macuamule C, Lin Z, Virga KG, Lee RE, Strauss E, Saliba KJ.** 2013. Pantothenamides are potent, on-target inhibitors of *Plasmodium falciparum* growth when serum pantetheinase is inactivated. PLoS One **8:**e54974.